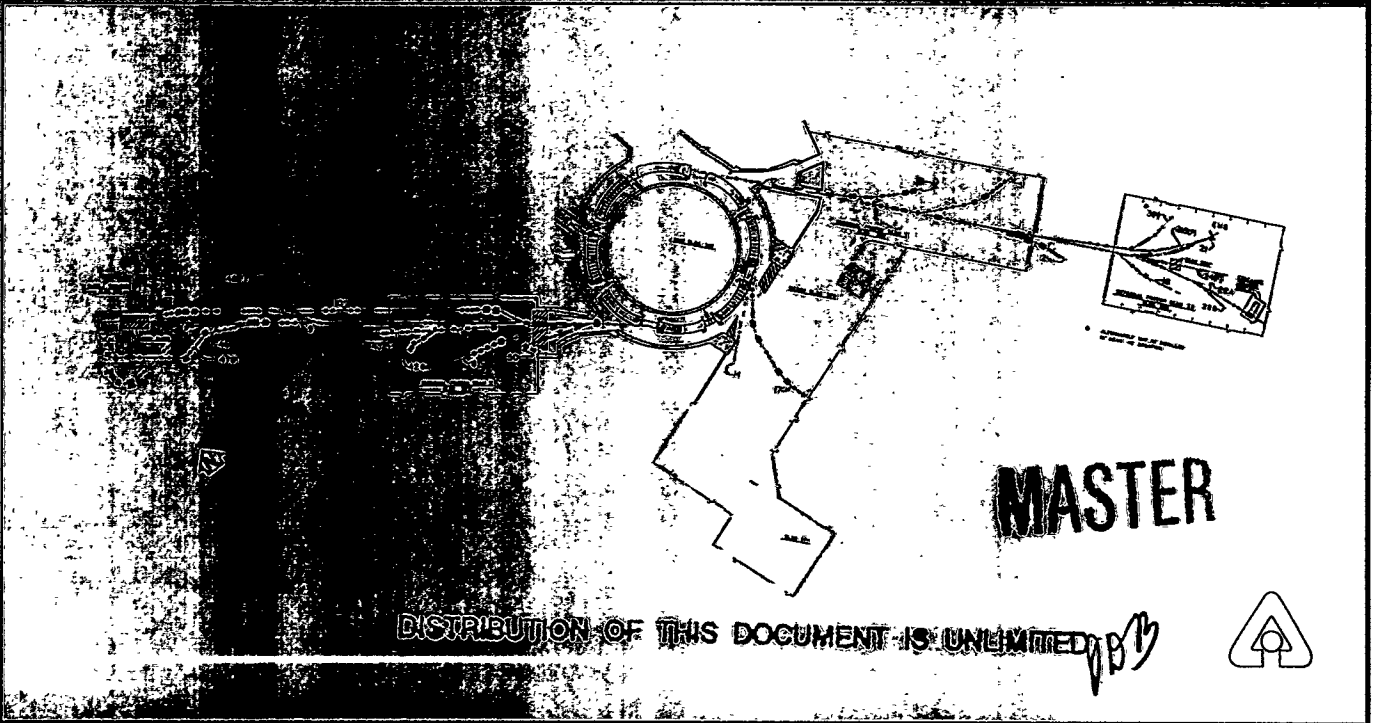


30th Anniversary ZGS

OSTI

Edited by Malcolm DeFoa

Held at Argonne National Laboratory
May 6, 1994



DISCLAIMER

This report was prepared as an account of work sponsored by an agency of the United States Government. Neither the United States Government nor any agency thereof, nor any of their employees, makes any warranty, express or implied, or assumes any legal liability or responsibility for the accuracy, completeness, or usefulness of any information, apparatus, product, or process disclosed, or represents that its use would not infringe privately owned rights. Reference herein to any specific commercial product, process, or service by trade name, trademark, manufacturer, or otherwise does not necessarily constitute or imply its endorsement, recommendation, or favoring by the United States Government or any agency thereof. The views and opinions of authors expressed herein do not necessarily state or reflect those of the United States Government or any agency thereof.

Pictured on Front Cover: Layout of ZGS beams in 1975.

ZGS Symposium
Argonne 1994

Organizing Committee

Yanlai Cho

Joanne S. Day

Malcolm Derrick

Thomas H. Fields

Donald R. Getz

Sandra A. Klepec

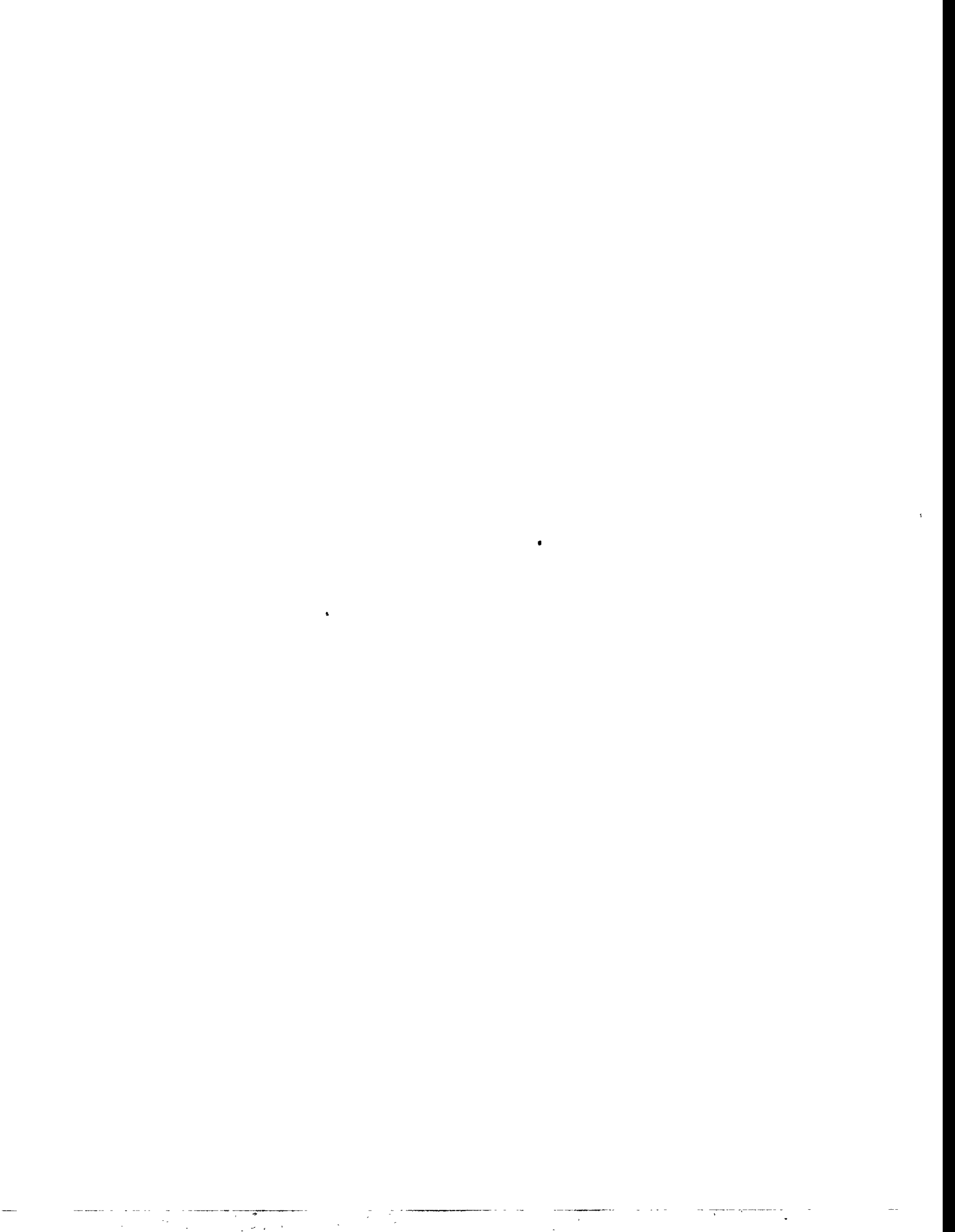
Martin J. Knott

David Manson

Ronald L. Martin

Beverly A. Marzec

Judith A. McGhee



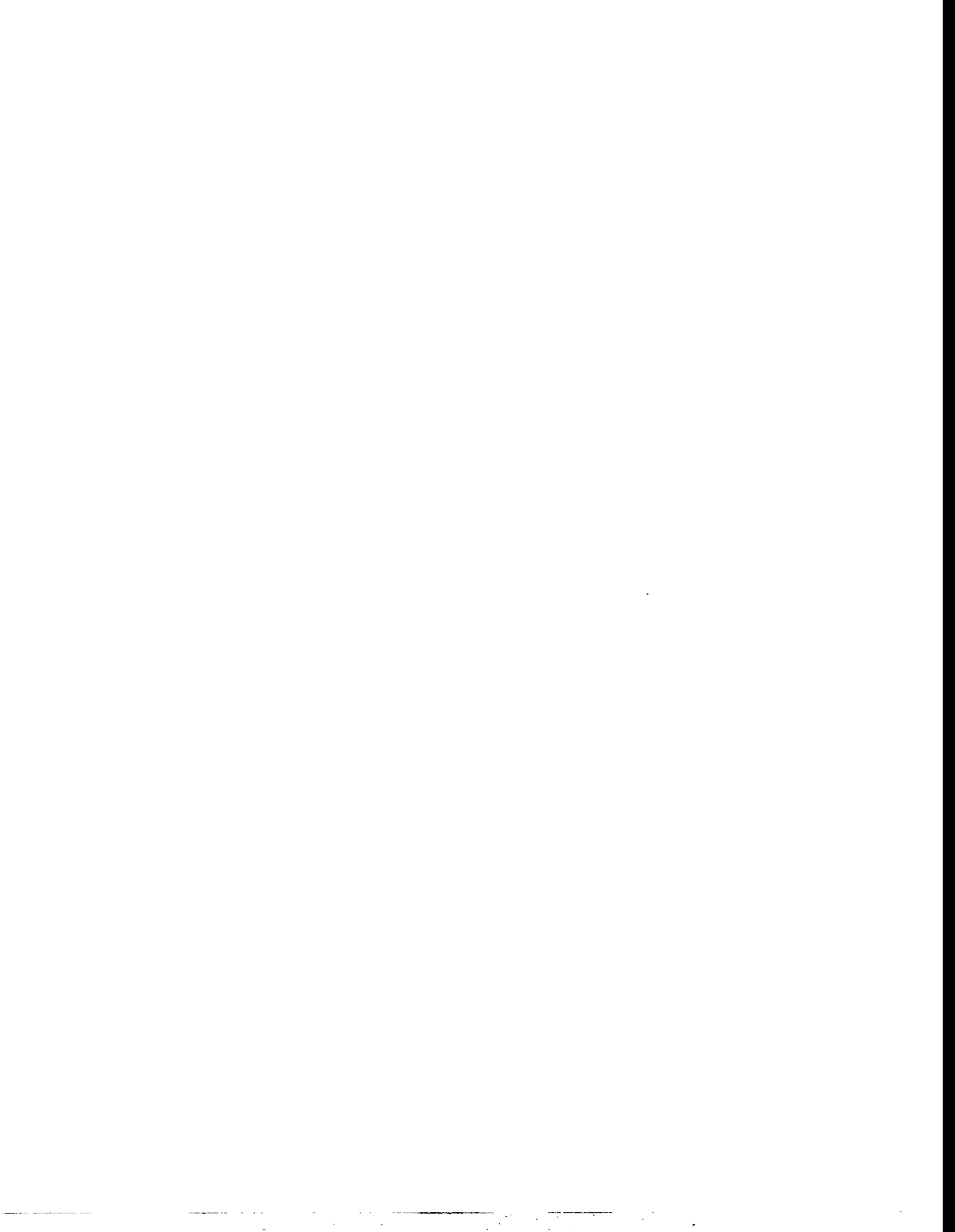
*Symposium on the 30th Anniversary
of the ZGS Startup*

*Talks on further developments in areas of
science and technology where ZGS people
made pioneering contributions.*

*Proceedings of a one-day symposium
held in the
High Energy Physics Division
of
Argonne National Laboratory*

May 6, 1994

Edited by M. Derrick



Forward

This book contains written versions of the talks given at the "Symposium to Mark the 30th Anniversary of the Startup of the ZGS". The Symposium was held at Argonne National Laboratory on May 6, 1994. These proceedings document a number of aspects of a big science facility and its impact on science, on technology, and on the continuing program of a major U.S. research institution.

The Zero Gradient Synchrotron (ZGS) was a 12.5 GeV weak focusing proton accelerator that operated at Argonne for fifteen years - from 1964 to 1979. It was a major user facility which led to new close links between the Laboratory and university groups: in the research program; in the choice of experiments to be carried out; in the design and construction of beams and detectors; and even in the Laboratory management. For Argonne, it marked a major move from being a Laboratory dominated by nuclear reactor development to one with a stronger basic research orientation.

The history of the ZGS and its physics research program was covered in a 1979 meeting, whose proceedings were published by the AIP - History of the ZGS (Argonne, 1979); edited by Joanne S. Day, Alan D. Krisch, and Lazarus G. Ratner. The present meeting covered the progress in accelerator science, in the applications of technology pioneered or developed by people working at the ZGS, as well as in physics research and detector construction.

At this time, when the future of the U.S. research programs in science is being questioned as a result of the ending of the Cold War and plans to balance the Federal budget, the specific place of the National Laboratories in the spectrum of research activities is under particular examination. This Symposium highlights one case history of a major science program that was completed more than a decade ago - so that the further developments of both the science and the technology can be seen in some perspective. The subsequent activities of the people who had worked in the ZGS program as well as the redeployment of the ZGS facilities were addressed in the talks of Joanne Day and Frank Brumwell.

If the National Laboratories are to thrive and continue to serve the needs of the Nation, some basic issues must be addressed on a continuing basis. For example, the work environment must be such as to attract outstanding people at all skill levels. How does an organization like Argonne cope with a major reduction in a program? How does it preserve the seed corn so that future crops may grow? Such questions are of particular importance when a science activity such as the ZGS program lasts for about half of a working lifetime. What new activities do the people engage in and how does the institution best manage the inevitable transitions when facilities and programs have best served their purposes?

Many of the decisions about new facilities in science are colored, or even determined, not only by objective scientific criteria but by what one might call an "Institutional Imperative," which is also often buttressed by political actions. This is particularly evident in the U.S. High Energy Physics program where the two major Laboratories are large single-purpose institutions.

In such a Laboratory, a decision to retire a large accelerator terminate can endanger the institution itself.

Multipurpose laboratories can be much more robust, as was illustrated in this Symposium. The termination of the ZGS program did not mean the end of Argonne as a Laboratory. In fact the capability in accelerator science and technology that was needed to run the ZGS program proved crucial in launching the Advanced Photon Source (APS), which is the successor to the ZGS as a major user-based science facility. The long and complicated transition between the end of the ZGS and the start of the APS was covered in the talk by Yang Cho.

Another program that grew even more directly out of the ZGS work is the spallation neutron source, Intense Pulsed Neutron Source (IPNS). This program was started using the ZGS itself and then inherited much of its hardware and buildings from the ZGS. With the recent cancellation of the reactor-based Advanced Neutron Source, proposed for Oak Ridge, the decisions to develop and implement the IPNS program, which maintained neutron scattering science in the U.S. these many years, looks particularly far-sighted. The history of these activities is covered in the talk of Jack Carpenter.

The final years of ZGS operation were devoted to experiments using a polarized, accelerated proton beam - the first such multi-GeV beam. Further progress in this technology is described by Alan Krisch, who was a leader in developing the ZGS facility. This program was another outstanding example of a productive collaboration between university and Laboratory scientists at the ZGS.

Other, more diverse, applications of accelerator science pioneered at the ZGS are discussed by Ron Martin. In retrospect, the DOE decision not to support a continuing program of accelerator R&D at Argonne after the ZGS closed was not a good one. The specific Argonne plan to continue work on the problems of polarized beams using a small storage ring is now being proposed, fifteen years later, for the Indiana University Cyclotron Facility. Polarized proton beams are planned for the RHIC collider at Brookhaven and are being seriously considered for the Fermilab Tevatron and the HERA collider at DESY.

The overall ZGS story also highlights a major weakness in the U.S. system for supporting accelerator research. Most U.S. accelerator R&D work has been supported by the HEP program, even though the applications are quite diverse. It will be necessary for other parts of the DOE, such as Basic Energy Science, to invest in accelerator science if future facilities are to be developed and built in a cost-effective way.

The ZGS program spawned several developments in technology, notably the pioneering work on superconducting magnets as is discussed in the presentation of Gale Pewitt. In the course of the remarkable development of the 4 Tesla magnet for the 25 cm helium bubble chamber, an understanding of the crucial parameters necessary to produce a working magnet was obtained. This advance was closely followed by the success of the 16-foot diameter superconducting magnet built for the 12-foot bubble chamber. So, in less than a decade, as a direct result of the Argonne work, superconducting magnets developed from a Laboratory

curiosity to become the technology of choice for both bubble chambers and colliding beam detectors.

Another remarkable example of a technology that grew out of a ZGS high energy physics experiment - the nonfocussing optical concentrator - is described by Earl Swallow.

The research program in high energy physics at Argonne has continued in a mode that brings the specific strengths of a Laboratory-based group (special and diverse technical strengths, long-term commitments, and staff flexibility) to collaborations involving both Laboratory and university groups. With the dominance of HEP research by large multipurpose detectors, mostly at colliding beam facilities, there is a clear place for such collaborations, as discussed by Brian Musgrave. Some of the developments in strong and weak interactions in the past 15 years are highlighted in other talks at the Symposium.

*Malcolm Derrick, Argonne, IL
February 1996*



Table of Contents

Welcome

A. Schriesheim, Director, Argonne National Laboratory

Introduction to Symposium

T. H. Fields, Argonne National Laboratory

Session I: Accelerator Science and Technology ***Chair: L. E. Price, Argonne National Laboratory***

Accelerator Developments since the ZGS by ZGS People

Y. Cho, Argonne National Laboratory

ZGS Roots of Superconductivity: People and Devices

E. G. Pewitt, Fermi National Accelerator Laboratory

Polarized Proton Beams since the ZGS

A. Krisch, University of Michigan

Session II: Diverse Applications ***Chair: J. Purcell (Advanced Cryo Magnetics, Inc.)***

Spallation Neutron Sources

J. Carpenter, Argonne National Laboratory

Some Non-HEP Applications Developed at the ZGS

R. L. Martin, Argonne National Laboratory

From Hyperons to Applied Optics: "Winston Cones" during and after the ZGS Era

E. Swallow, Elmhurst College

Session III: Physics and Detectors ***Chair: W. D. Walker (Duke University)***

The Quark Revolution and the ZGS - New Quark Physics since the ZGS

H. Lipkin, Weizmann Institute

Neutrino Physics in the HEP Division at Argonne: Past, Present, and Future

M. Derrick, Argonne National Laboratory

Visual Detectors since the ZGS

B. Musgrave, Argonne National Laboratory

U.S. HEP Accelerator Projects in the 1980's and 1990's
J. O'Fallon, U.S. Department of Energy

Session IV: Projects and People
Chair: A. Wattenberg (University of Illinois)

New Projects in the ZGS Buildings
F. Brumwell, Argonne National Laboratory

Activities of ZGS People in the 1980's and 1990's
J. S. Day, Argonne National Laboratory

Session V
Chair: M. Block (Northwestern)

Concluding Remarks
R. G. Sachs, University of Chicago

List of Attendees

Welcome

Alan Schriesheim, Director
Argonne National Laboratory

This is the third welcoming speech I have given this morning, so I guess I am partially responsible for the delay at the Visitor Reception Center. In any case, I am pleased to welcome you back to the Laboratory. All of you have been here before and, in fact, predate me.

The official history says that the ZGS program ended fifteen years ago, but I think that that view ought to be modified. Programs started in the ZGS time thrive today. The legacy of the accelerator work is alive at the Advanced Photon Source and the Intense Pulsed Neutron Source, both of which rely on people who trained and developed their skills at the ZGS. This is also true of projects, such as the Tevatron, which are located at other institutions. Some of the ZGS hardware also remains: the linac and booster and some special devices such as the superconducting dipole built for energy research. This, I am told, is still the world's largest.

Looking at the schedule of the talks, it is clear that beyond bricks and mortar the spirit of the ZGS lives on in each of you, as well as in many of your colleagues who could not be present today: the senior scientists who guided the program, the graduate students who did their thesis research here, and the program managers who threaded their way through the maze of conflicting demands that characterizes today's complicated world. Your spiritual and cultural legacy lives on at Argonne.

The ZGS gave the Laboratory not only an outstanding scientific and technical reputation, but proved our capability to manage a large scientific, user-oriented, project. It transformed the relationship between the Laboratory and the university community.

I was not here in that period, but I have read about the conflicts surrounding the start of the program. It seems that the university scientists trusted neither Argonne nor the University of Chicago. In older facilities at other labs, the builders enjoyed a feast and the others had to settle for the crumbs. That did not happen at the ZGS.

The program spawned a new National Laboratory paradigm. So much so that it also produced two Laboratory Directors, one of whom, Bob Sachs, is here today. I think that Bob will agree with me that more than any other single project, the ZGS was a defining event in the cooperative partnership between ANL and the university community. We have come a long way since then. Now the Laboratory rings with outreach activities, both with industry and with universities. It is an ever increasing part of our research, with projects both large and small,

including companies such as Dow, DuPont, and IBM. In fact, I just came from a meeting on the development of a new generation of vehicles.

The largest of our new facilities, the APS, is a major asset of the region and, indeed, of the nation. I invite you to take a tour. You will recognize the ZGS in it. I can say with confidence that Argonne is a better place today as a result of the ZGS program, and I appreciate your contributions. Have a good meeting!

Introduction

T. H. Fields
High Energy Physics Division
Argonne National Laboratory

Let me begin by adding a warm welcome from the Organizing Committee to that which we have just heard from Alan Schriesheim. All of the members of our Committee (listed on the title page) are pleased that so many of you have been able to attend this celebration of the 30th Anniversary of the Startup of the Zero Gradient Synchrotron.

The most recent ZGS Symposium took place in 1979 at the time of the ZGS shutdown. In the fifteen years since then, much change has taken place in the field of high energy physics, in the wider worlds of science and technology, and at Argonne. Of course, fifteen years is also a long time in anyone's life and career, so there are lots of individual stories to catch up on by now.

With such thoughts in mind, it occurred to some of us last fall that a celebration of the 30th anniversary of the ZGS startup was an idea whose time had come. I believe that Yang Cho was the person who initiated this idea, and soon we had recruited an organizing committee. We have not been deterred by the fact that the initial operation of the ZGS was in 1963, by now some 31(!) years ago.

Our Committee concluded that this Symposium should aim to focus sharply upon events which have occurred SINCE the shutdown of the ZGS fifteen years ago. Our two compelling reasons for this decision were: first, that the events and accomplishments associated with the ZGS up to 1979 are documented rather completely in the 1980 book 'History of the ZGS'. That book, published by the American Institute of Physics, includes talks given at the 1979 ZGS Symposium as well as other ZGS information and statistics.

The second reason is that the broader and longer term impacts of "big science" basic research are a subject of much present-day discussion and controversy. It should be interesting to a broader audience as well as to everyone in this auditorium to learn about the longer term impacts of the ZGS work and people in the fifteen years since the machine was shut down. Long term thinking is never easy and is not always in fashion. But hopefully, the talks at this Symposium will make it easier to visualize and appreciate that many kinds of longer term benefits which society receives from its investment in basic research programs like that at the ZGS.

Our Committee also decided that this reunion should consist of three components: first, a scientific and technical symposium as described above; second, an evening social event and banquet; and third, a series of tours (tomorrow) showing the present uses of the ZGS buildings and the status if the 7 GeV Advanced Photon Source storage ring and accelerator systems. We hope that this combination of activities will provide good opportunities for seeing both old and

recent accomplishments in a new perspective, and for sharing ideas and reminiscences with friends and colleagues.

* * * * *

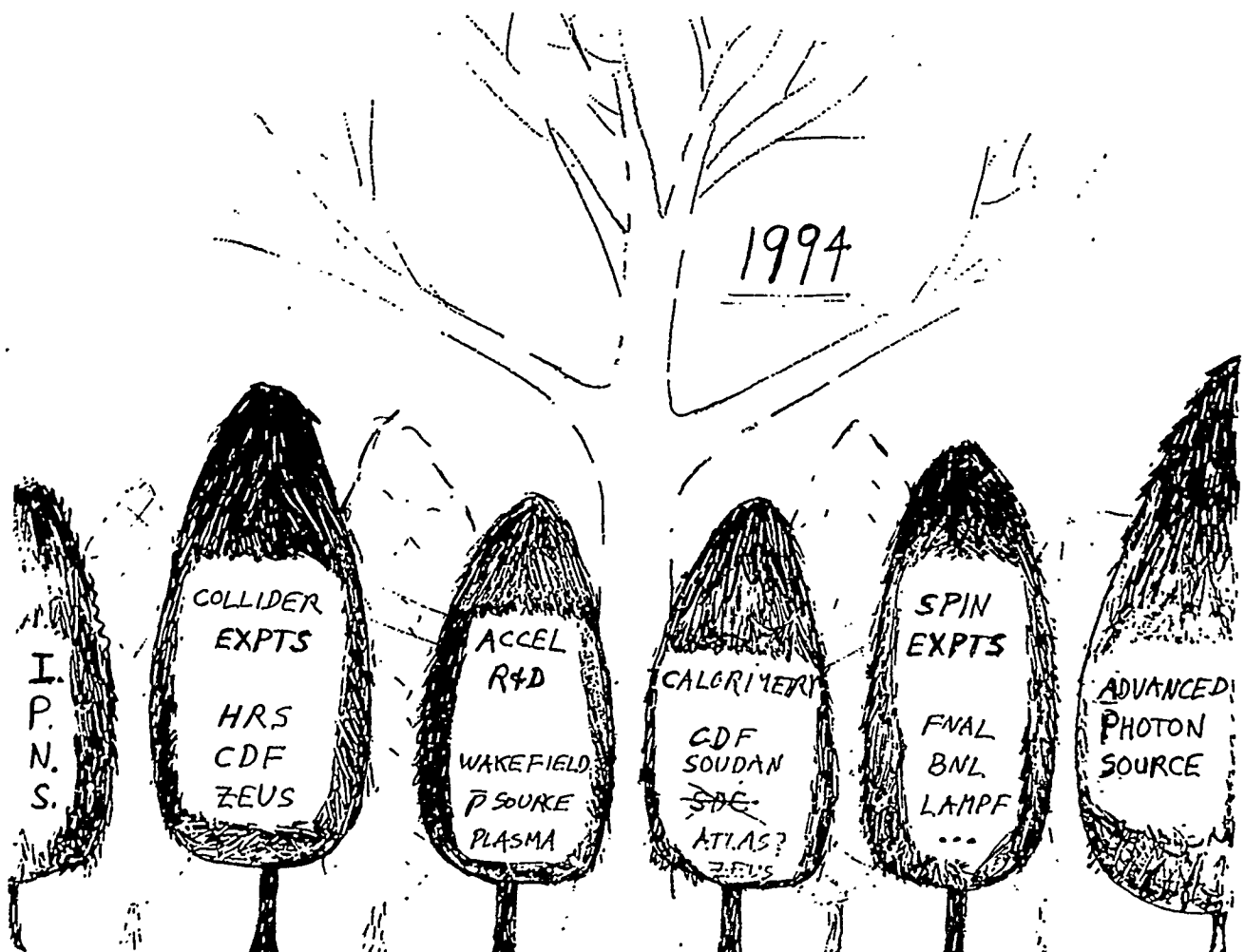
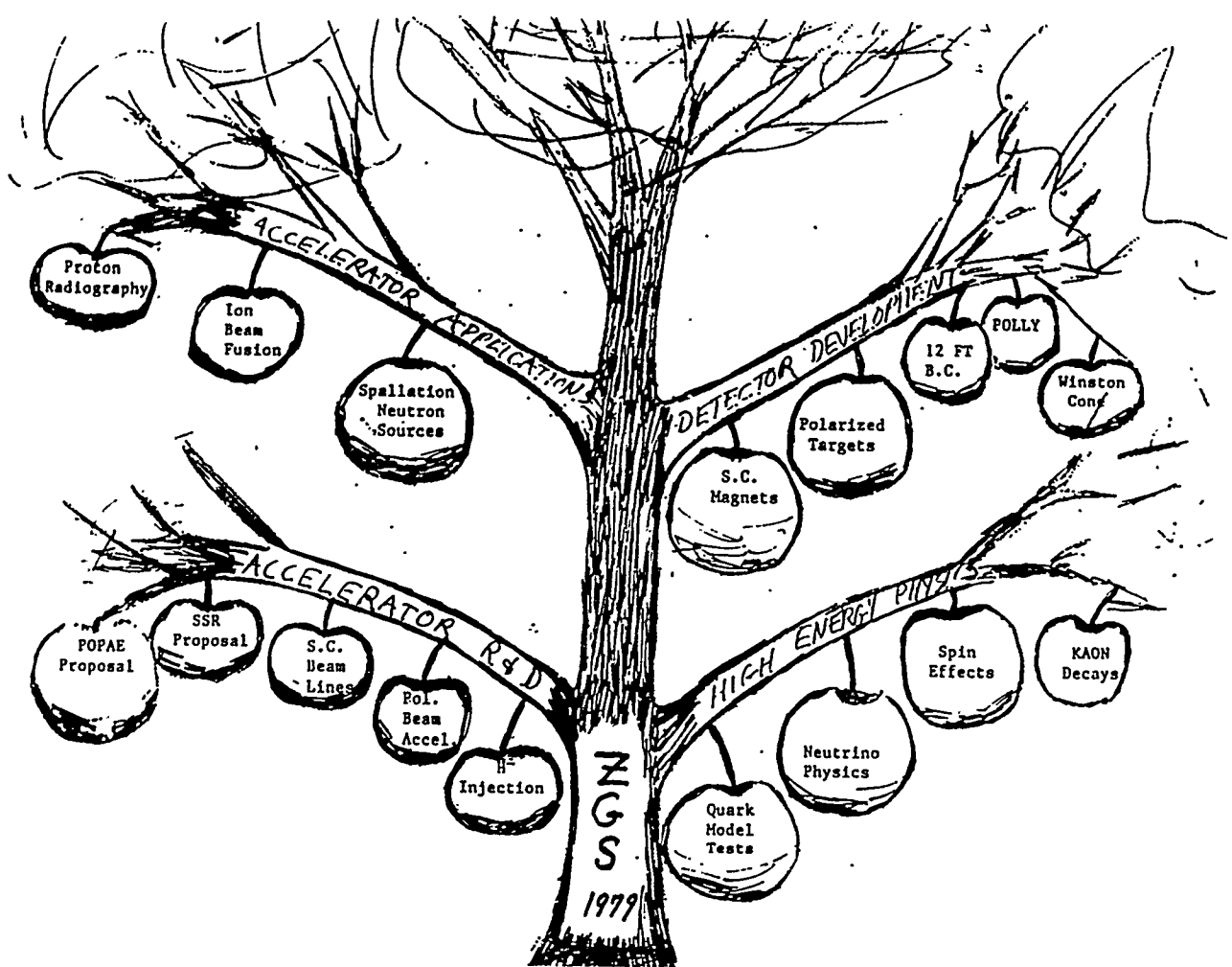
A few statistics about this event: we first sent out a questionnaire to about 400 people, and received a very enthusiastic response and many good suggestions. After the date and program were set, invitations were sent to our entire mailing list, by then some 680 people. There are 220 registered Symposium attendees, and about 320 persons will attend the banquet tonight.

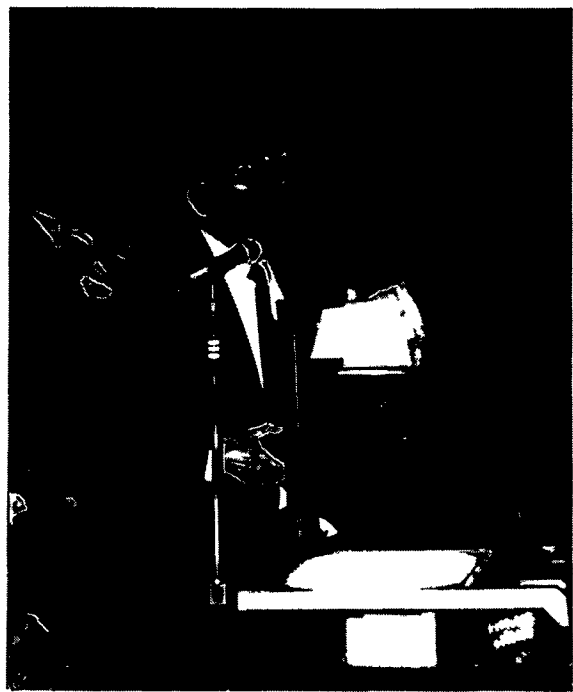
The registration form contained a section for describing your activities since 1979, and Sandra Klepec has put together an 87-page book containing all of the responses. Copies will be available later today.

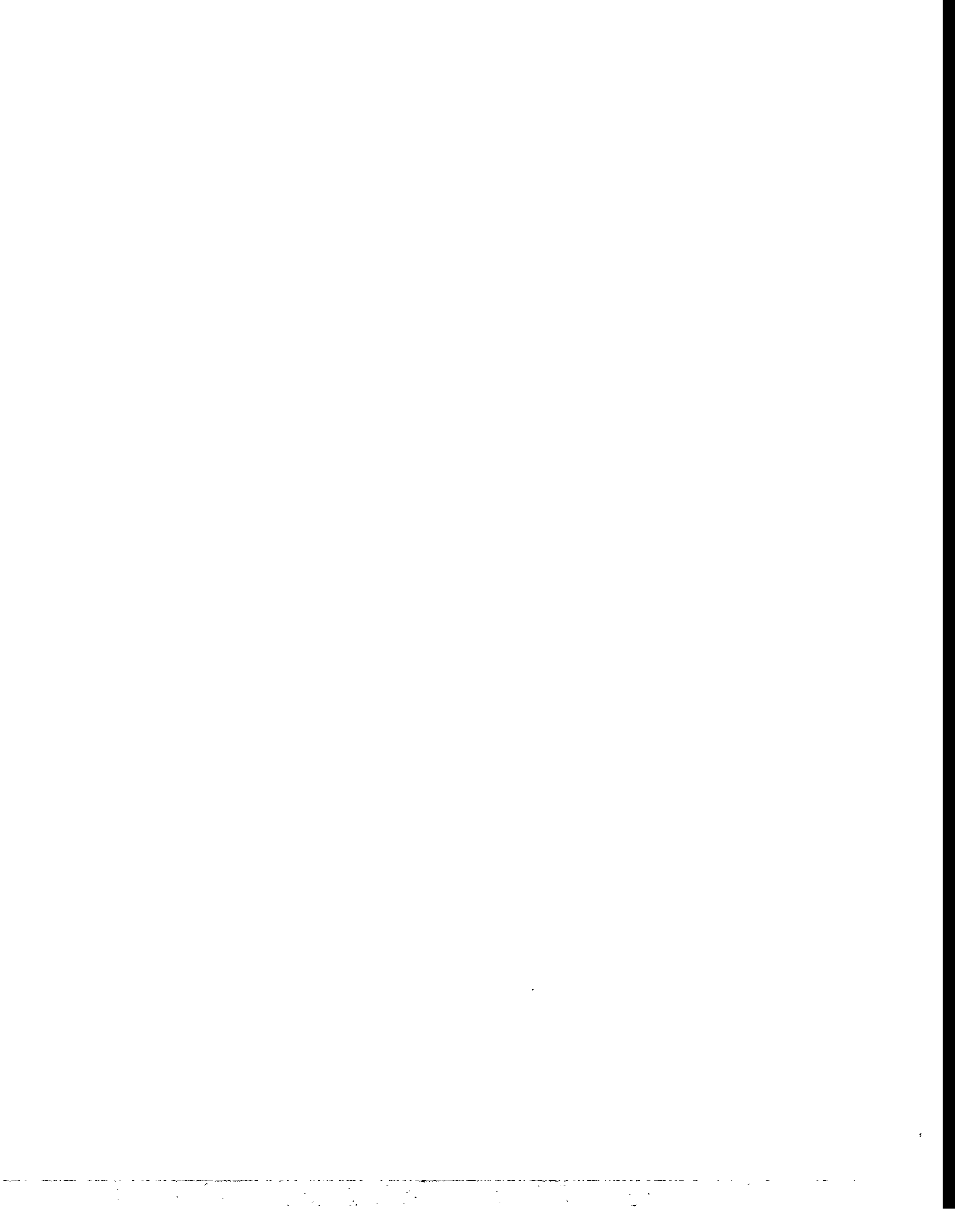
* * * * *

Some years ago, I saw a transparency which depicted that many pioneering nuclear reactors designed or built at Argonne as brightly colored apples on an impressive apple tree. That reactor development work is mostly history by now, and its future is quite uncertain - but of course it seems clear that big science and technology projects must now learn to cope with increasing uncertainty and survive it if they can. Sadly, the Super Collider did not survive, and neither may the Argonne reactor program.

Anyway, in the figure I have used a similar apple tree metaphor to depict many of the fruits of the ZGS program as they were described at the ZGS History Symposium in 1979 - a mature and bountiful ZGS tree indeed. The current state of affairs is shown in the lower part of the figure. The ZGS apple tree is barely visible, but its seeds have taken root and are now yielding a wonderful, diverse collection of valuable new trees. It shows that there is much to hear about and catch up on at this Symposium, so let's get started.







the Physics Division to work on a multi-GeV continuous beam electron microtron (GEM) the design work of which is described later. Crosbie, Khoe and Kustom returned to the HEP Division in 1984 to join the APS Project.

People returning from the ARF Division to HEP were Y. Cho, S. Kramer and J. Simpson who had started their careers in the HEP Division. Simpson and Kramer were members of P-bar Group working on the anti-proton project for Fermilab. After completion of the P-bar work, Simpson and his group have been carrying out very interesting work on new concepts of acceleration which is discussed later. Cho started the APS Project in 1983 from the HEP Division, as described in some detail below.

A large accelerator facility like the ZGS has a unique group of experts on electromagnetics and mechanical engineering to provide magnets and their supports, power supplies, vacuum chamber systems, etc. We had such a group under leadership of W. Praeg, and during the post-ZGS era, this group was called ET (Electromagnetic Technology) Group, and worked on various projects throughout the Laboratory including the GEM project. In 1984, this group joined the APS Project and become the key players in that activity.

Birth of the APS: Starting from the summer of 1983, I was on-loan to the University of Wisconsin-Madison to work on the university's synchrotron radiation source which was being commissioned but having difficulties meeting its performance goals. In November of that year, while in Madison, I obtained a copy of letter report from the Eisenberg-Knotek Committee being circulated amongst the synchrotron radiation community in the US. The Committee was chartered by the Office of Basic Energy Science of the US DOE to recommend priorities for the Nation's synchrotron radiation facilities. The Committee advocated that the first priority of the DOE synchrotron facility should be the construction of 6 GeV accelerator facility to produce very bright hard x-ray beams for materials research. With a copy of this letter report on hand, I requested Laboratory program development funds to support a group to design and construct a 6 GeV accelerator facility.

To that time, utilization of synchrotron radiation in research was not a strong point of the ANL program, but, in spite of this, the Laboratory management decided to give a chance to a group of people to compete with other proponents. The funding support for FY 1984 was some \$400K.

Former ZGS people who had returned to the HEP Division or participated from other ANL Divisions were: Y. Cho and S. Kramer from HEP Division, E. Crosbie, T. Khoe and R. Kustom from PHY Division, W. Praeg, S. Kim, M. Knott, D. McGhee, J. Moenich (who un-retired to work on the APS), K. Thompson, and R. Wehrle from ET Group, A. Rauchas from IPNS Division, R. Bouie from PFS Division, L. Genes and D. Hillis from EES Division. The initial members of the team who were not former ZGS staff were G. Mavrognes from CHM Division, and G. Shenoy, G. Knapp and J. Viccaro from MSD Division. It should be noted that the team enjoyed very strong support from Associate

Accelerator Developments Since the ZGS by ZGS People

Yanlai Cho
Argonne National Laboratory
Argonne, IL 60439

I. INTRODUCTION

The ZGS was a facility, as well as an organization, where people got together to pursue a common goal of doing exciting science of the day. In this note, we describe notable events related to accelerators and accelerator people since the closing of the ZGS program some 15 years ago. Many of the same ZGS people have been carrying out the state-of-the-art accelerator work around the Laboratory with the same dedication that characterized their work in the earlier days.

First we describe how the activities were re-organized after the closing of the ZGS, the migration of people, and the organizational evolution since that time. Doing this shows the similarity between the birth of the ZGS and the birth of the Advanced Photon Source (APS). Then, some of the accelerator work by the former ZGS people are described. These include: 1) Intense Pulsed Neutron Source (IPNS), 2) GeV Electron Microtron (GEM), 3) Wake Field Accelerator Test Facility, 4) Advanced Photon Source, and 5) IPNS Upgrade.

II. PEOPLE

We like to high-light the activities of the people since the closing of the ZGS. The people work in an organization, which we learn how to work together. So it may be worthwhile to review how the ZGS organization evolved starting from 1956, and how it stands today. There was an accelerator group under the leadership of J. J. Livingood in the Physics Division from 1954 to 1956. In 1956, this group became the Particle Accelerator Division (PAD) to work on what had become the ZGS. In 1958, an Associate Laboratory Directorship (ALD) for High Energy Physics was created and the High Energy Physics Division branched out from PAD in 1959. During the peak years of the ZGS(1967), PAD was further divided to an Accelerator Division (AD) and a High Energy Facilities Division (HEF). As the ZGS operations progressed into a mature phase, AD and HEF were combined again to form Accelerator Research Facilities Division (ARF) in 1973.

After closing the ZGS in September 1979, the ALD-HEP position was discontinued in 1980, and both ARF and HEP divisions were led by the ALD-Physical Research. In April 1982, the ARF Division was dissolved, and people were moved to other Divisions such as IPNS, Physics Division, HEP Division and ET (Electromagnetic Technology) Group.

The ZGS Operations Group under leadership of C. Potts and F. Brumwell became IPNS Operations Group. E. Crosbie, T. Khoe, R. Kustom, E. Colton and H. Takeda went to

Laboratory Director for Physical Research, K. Kliewer and from the HEP Division Director, T. Fields.

Although the team spent only a half of the budget in the first year, the second year (FY 85) budget was \$1M, and by the end of the second year the team had produced a Conceptual Design Report together with its supporting documentation including the cost and schedule estimates.

Hard work by this handful of people paid off handsomely. In 1986, DOE decided to build what was then called then 6 GeV synchrotron source at ANL. An Associate Laboratory Director-ship for the APS was created in 1987, and the APS Division branched out from HEP Division in 1988. The APS Division further branched to Accelerator Systems Division and an Experimental Facilities Division in 1991.

It is interesting to note that PHY Division gave birth to PAD and the ZGS, and one of the ZGS Division, (HEP Division) gave birth to APS Divisions.

III. MACHINES

The ZGS was a unique machine. Despite the normal wisdom that all separated function machines are of the strong focusing type, it was the first separate of function machines ever built and at the same time it was a weak focusing machine. It was the first machine to accelerate polarized protons to GeV range, and the first US machine to employ the H⁻ ion injection scheme in a routine way to enhance the transverse phase space. While doing all this frontier development, the ZGS organization raised and trained a large number of highly motivated and skilled scientists and engineers during its tenure of some 15 years. Following are some highlight of accelerator work performed by the former ZGS personnel after the closing.

III.1 IPNS Rapidly Cycling Synchrotron (RCS)

Some years before the closing of the ZGS, as a ZGS intensity improvement program, a 30 Hz RCS was built as a Booster to raise the ZGS injection energy from 50 MeV to 500 MeV. This machine had no opportunity to be used as the ZGS Booster because of closing of the ZGS before its completion. However, this 500 MeV fast cycling synchrotron has become the work horse of generating slow neutrons for condensed matter research both in neutron scattering to investigate the bulk material structure and in radiation damage by neutrons. Jack Carpenter's talk in this conference covers the details of how the IPNS program developed.

Figure III.1-1 shows the layout of the IPNS facility. The old 50 MeV linac designed and built as the ZGS injector linac which had a repetition period of 2 seconds now operates with repetition rate of 30 Hz. The 50 MeV beam turns around 180°, and heads for the RCS in Building 399 which is located under the bridge to the Center Building. The former EPB-II building houses the neutron generating target station.

The machine has been operating for 11 years and 9 billion pulses at the space charge limit of 3×10^{12} protons per pulse. It is the most reliable machine ever. Figure III.1-2 shows the IPNS accelerator system availability since 1981, and the figure shows that the recent years' availability varies between 94 and 96 %, a remarkable performance.

III.2. GEM (GeV Electron Microtron)

The GEM project was to design an accelerator complex to produce a cw electron beam of 4 GeV with a time averaged current greater than 100 μ A for the medium energy physics program of the U.S. The science at ANL is centered in the Physics Division. This study occurred during 1982-83. As noted earlier, at the termination of Accelerator Research Facilities Division, a group of accelerator people transferred to the Physics Division to work on the design. There was a competition for this project, that came from a newly formed Southeast Universities Research Association (SURA).

The SURA design of the accelerator system consisted of a full energy pulsed linac and a storage ring which stretches the pulse by extracting the beam slowly.

The ANL design utilized a microtron concept by re-circulating the beam 37 times through the accelerating sections. Figure III.2-1 shows a schematic layout of the GEM, which consisted of a 23 MeV injector linac, a 185 MeV booster microtron and a 4 GeV 6-sided microtron (Hexatron). The Hexatron consisted of 6 sector magnets and 3 linacs. A pair of the sector magnets were designed to separate the trajectory of each turn as shown in the figure.

The other important point of the ANL design was to use the ZGS buildings. The proposal was to house the Hexatron in the ring building; a monochromatic photon facility in the Meson Building, a high resolution spectrometer in the 30 inch bubble chamber building, and a medium resolution spectrometer facility in the EPB-I building. The proposed arrangement is shown in Figure III.2-2.

We lost the competition to SURA. A DOE review committee favored the pulse-stretcher ring concept over the microtron concept. However SURA abandoned the pulse stretcher ring concept, and they are in commissioning process of a 4-turn re-circulating accelerator. They also named their facility Continuous Electron Beam Accelerator Facility (CEBAF).

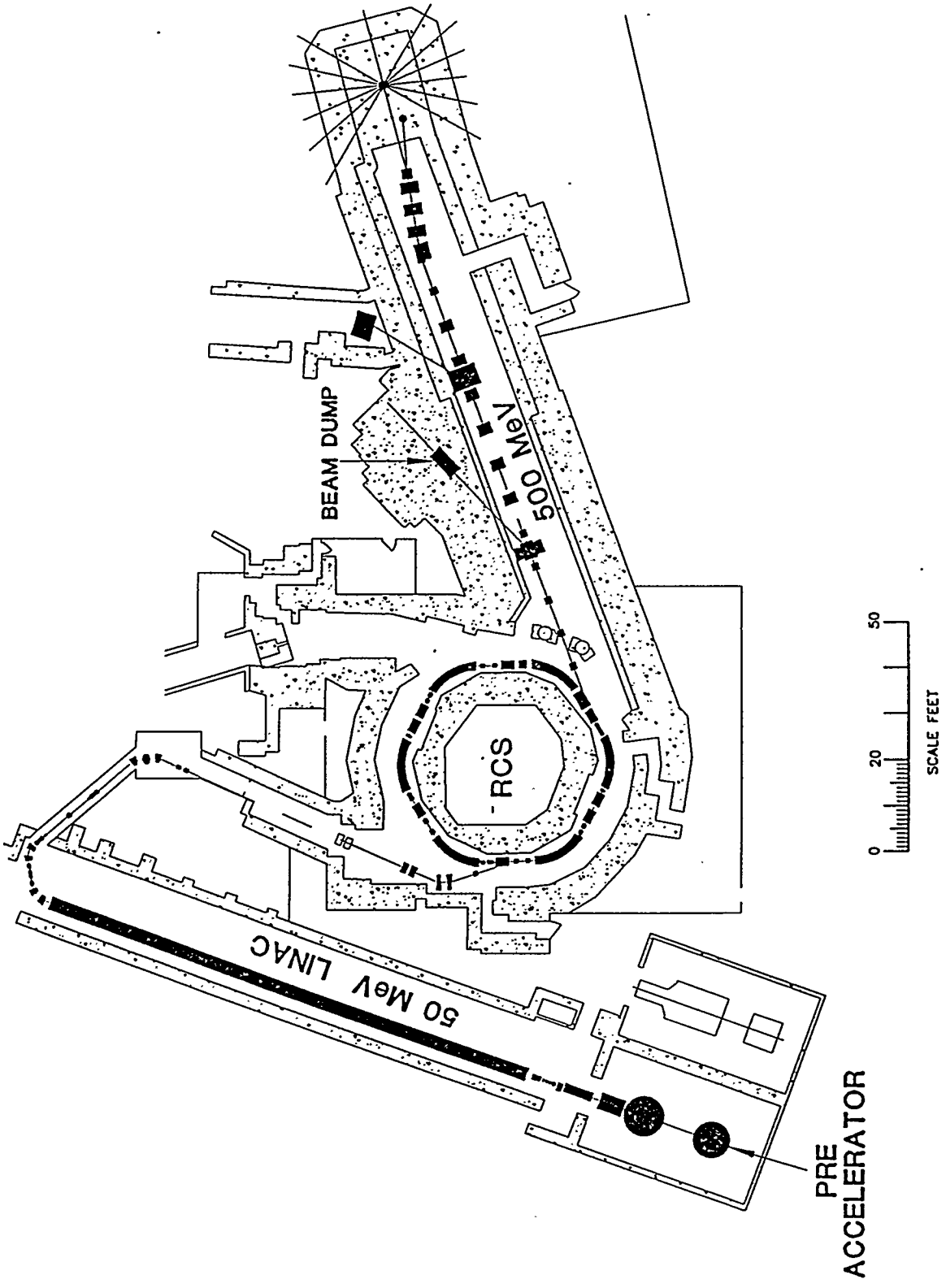


Figure III.1.1-1
IPNS Facility Layout

IPNS Accelerator System Availability

1981-1994

April 1994

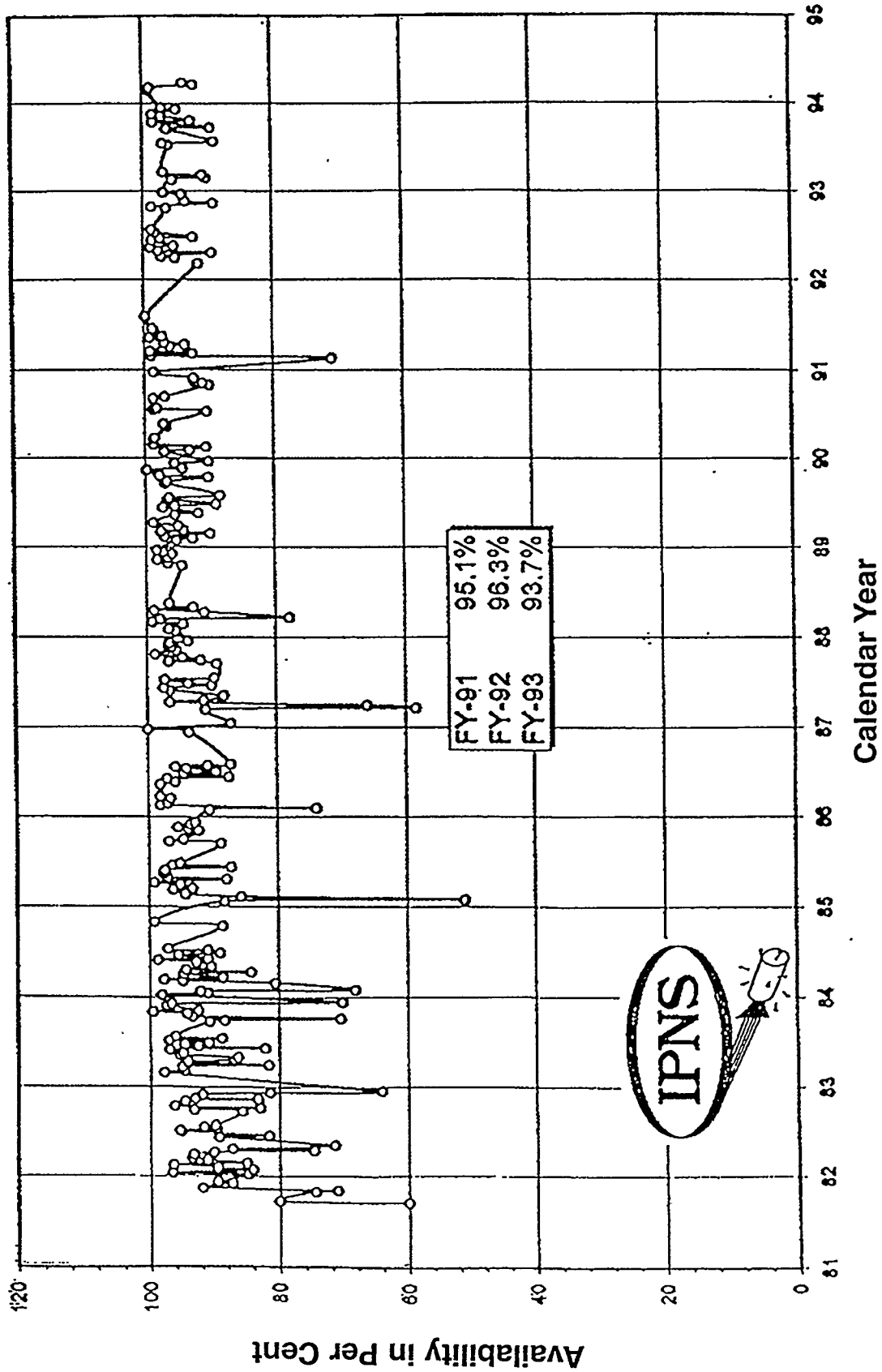
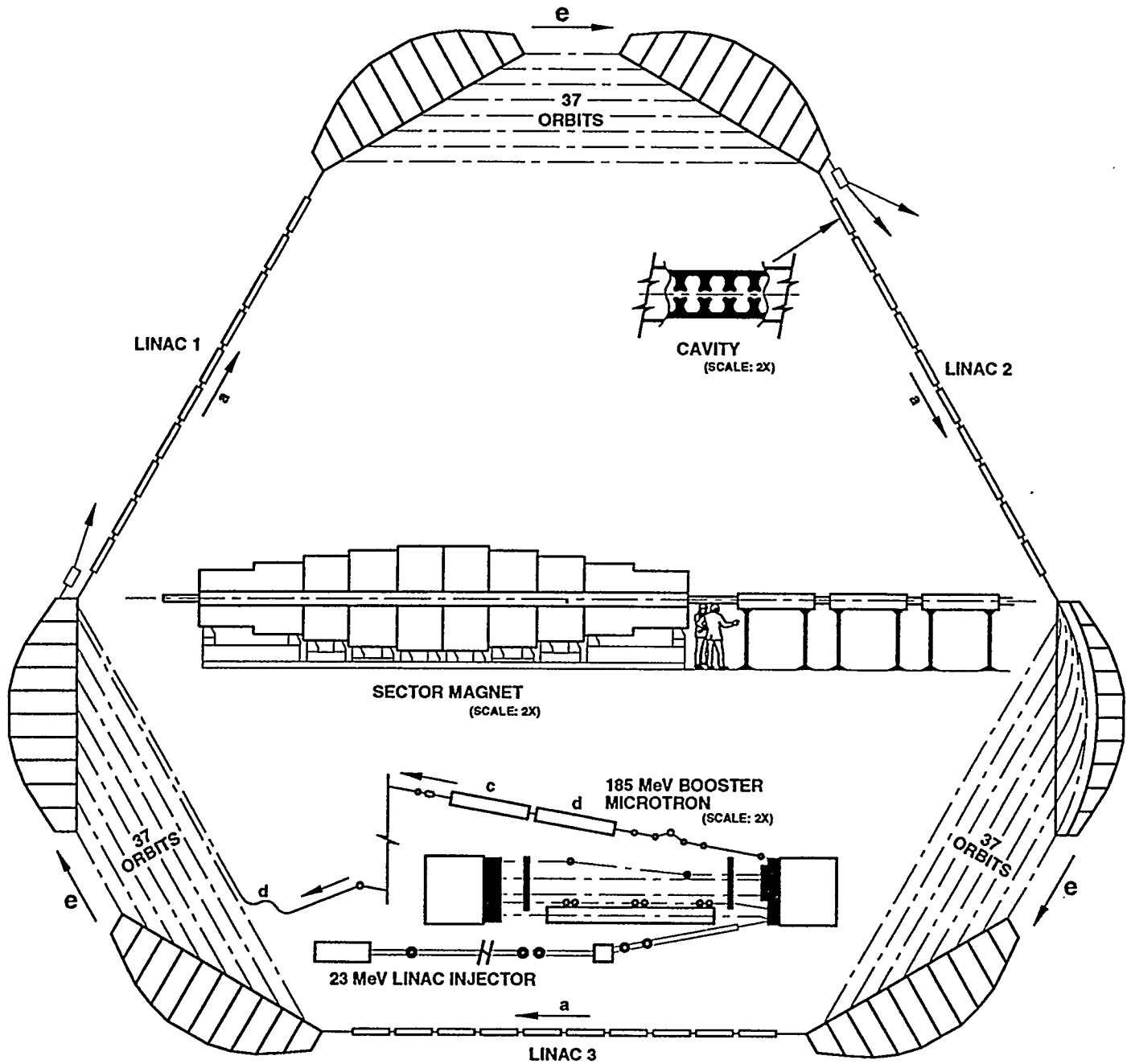


Figure III.1-2
IPNS Facility Availability



- a - LINAC STRAIGHT SECTION
- b - SUBHARMONIC rf CAVITY
- c - RF MATCHING CAVITY
- d - TRIPLE 80° DIPOLE SYSTEM
- e - DISPERSIVE STRAIGHT SECTION

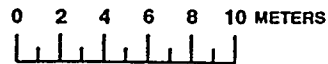


Figure III.2-1
Schematic Layout of GEM Hexatron

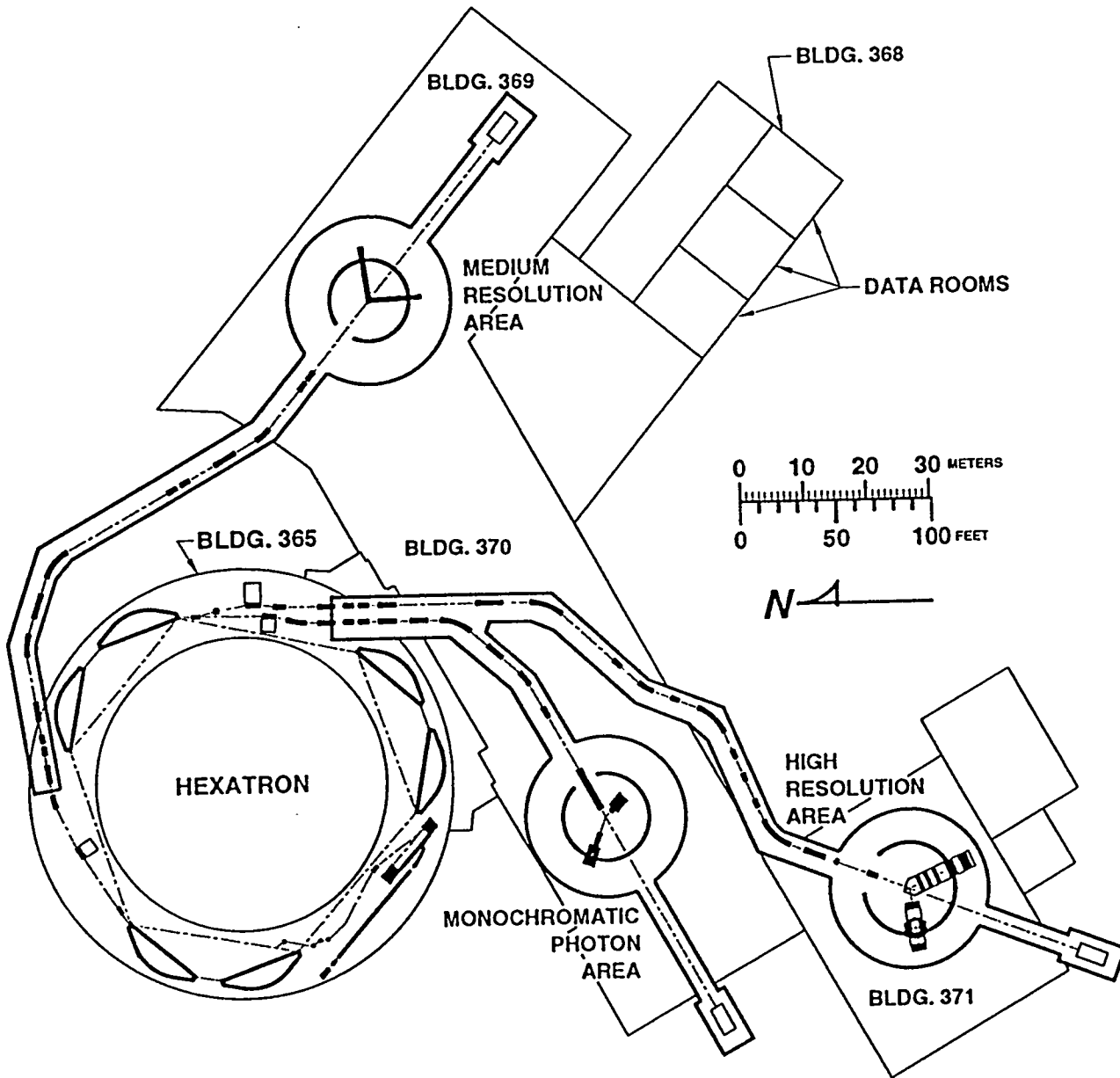


Figure III.2-2
 Hexatron and Experimental Facilities
 Layout Utilizing the ZGS Builings

III.3 Argonne Wake Field Accelerator (AWA)

Some of us are constructing and operating high energy accelerators for other scientific disciplines such as x-ray and neutron scattering, and some of us are trying to improve accelerator technology itself. For example, when the SLAC linac was built, the accelerating gradient was 8 MV/m for an electron linac. The present day electron linac has a typical gradient of 20 MV/m. For future multi-TeV linear colliders, higher energy gradients are essential. The AWA, under the leadership of Jim Simpson, is such a development of physics and technology, and is supported by the advanced technology section of DOE's Division of High Energy Physics.

The research addresses the wake field produced by a large charge and very short bunches of electrons. A typical example is 100 nC of electrons in 5 psec (rms.) bunches producing collinear wake fields in slow wave devices and plasmas.

The goals include development of high gradient in excess of 200 MV/m, and demonstration of acceleration of beam energy > 1 GeV in a less than 10 m long structure. The initial test will start in the coming summer.

III.4 Advanced Photon Source (APS)

III.4.1 Birth of APS

The official DOE name for the APS is 6-7 GeV Synchrotron Radiation Source, and following is a brief chronology of how it started.

In November 1983, a DOE committee (Eisenberger/Knotek) advocated construction of a 6-GeV synchrotron radiation source be number one priority for the US synchrotron radiation user community. With this background, I obtained Laboratory management support to start a group to design a 6-GeV synchrotron radiation facility.

In April 1984, a National Academy of Science panel (Seitz and Eastman) reviewed research facilities needs for material research and made priority recommendation to the Office of Science and Technology Policy. The first priority of the recommendation was that the nation should build a 6-GeV synchrotron radiation source. Such a source had been proposed by four institutions: ANL, BNL, Cornell University and Stanford University. The second priority was to build the Advanced Light Source (ALS) a (1-2 GeV Light Source) at Lawrence Berkeley Laboratory, the third as to build the Advanced Neutron Source (ANS) reactor proposed by Oak Ridge National Laboratory, and the fourth was a pulsed neutron source using an FFAG concept proposed by ANL.

During this period, we assembled the former ZGS people who had moved to other programs into the HEP Division to design and write a proposal. The initial budget was

\$174K in fiscal year 1984, and \$1M for FY 85 which came from Laboratory Director's program development funds.

In early October 1984, there was a meeting at Ames Laboratory, Ames, Iowa of accelerator builders and users to set the parameters of the 6-GeV synchrotron source. The parameters were an energy of 6 GeV, and a stored current of 100 mA as well as other details. The parameters are shown in Table II.4.2-1. Note that the parameter table includes a statement that positrons are to be used rather than electrons. This has to do with the fact that a stored electron beam attracts ions from residual gas ionized by the circulating beam which result degradation of the beam. The way to avoid such ion-trapping is to use positrons. Table II.4.2-1 also shows that the APS parameters which can be compared with the Ames parameters.

By August 1985, a complete concept of the facility was put together so that a bottoms-up cost estimate of the construction project could be commenced.

Table II.4.2-1

Ames and APS Parameters

<u>Parameters</u>	<u>Ames (1984)</u>	<u>APS(1987)</u>
Beam Energy	6 GeV	7 GeV
Beam Current	> 100 mA	300 mA
Beam Lifetime	> 10 h	> 10 h
Number of Bunches	1 - 40	1 - 60
Bunch Duration	10 - 100 ps	10 - 100 ps
Horizontal Emittance	< 7 10 ⁻⁹ m.rad	< 7 10 ⁻⁹ m.rad
Circumference	~ 800 m	1060 m
Number of Straight Sections	32	40
Straight Section Length (Standard)	6 m	6 m
Straight Section Vertical Aperture	8 mm	8 mm
Radiation Sources	Undulators, Wigglers, Bending Magnets	Undulators, Wigglers, Bending Magnets
Fundamental Undulator Energy (10 mm ID gap)	20 keV	20 keV (tunable)
Beam Particle	Positron	Positron
Injection Energy	Full Energy	Full Energy

A DOE Review Committee on Technical, Costs, Schedule and Management reviewed the design and construction planning of the facility in May 1986, and recommended to Laboratory management to initiate funding approval.

Soon after the review, the Director of Energy Research (DOE) made a general agreement between laboratory directors to spread large users facilities to several laboratories. The agreement was: 1 - 2 GeV Light Source to LBL, 6-GeV Synchrotron Radiation Source to ANL, RHIC (Relativistic Heavy Ion Collider) to BNL, and ANS (Advanced Neutron Source), which is a reactor based neutron source to ORNL.

What was called in 1986 the 6-GeV Synchrotron Radiation Source became the Advanced Photon Source (APS) in 1987, and the accelerator energy was changed from 6-GeV to 7-GeV in order to provide additional flexibility.

III.4.2 Scientific Capability of APS

A figure of merit of a facility can be measured either with beam energy or beam intensity. Since Roentgen discovered x-rays in 1895, beams of x-rays have been used for all kind of scientific and technological endeavors. Figure III.4.2-1 shows the historical development of the brilliance of x-rays since the advent of x-ray tube by Roentgen. The figure shows that during the first 60 years of x-ray history, brilliance of x-ray sources were around $10^7 \sim 10^8$ photons/sec $\text{mm}^2\text{mrad}^2(0.1\% \text{band width})$ coming from x-ray tubes. Utilization of electron synchrotrons in 1970s changed the brilliance to 10^{12} range, and this era is called the first generation synchrotron source. In this period synchrotron facilities belonged to the high energy physics program, and x-ray users used the facilities in a parasitic mode to the high energy experimental program. In late 70s, several dedicated facilities were built throughout the world, and these we call the second generation sources. These sources have brilliance of order of $10^{14} \sim 10^{15}$, and energies of the accelerators less than 3 GeV. The APS, a third generation source is produce brilliance of order of 10^{19} as shown in the figure.

In a technical jargon, "the APS facility is optimized to produce insertion device (ID) hard x-rays with brilliance better than 10^{19} ." Then a question is what kind of science one can do with four orders of magnitude brighter x-ray source. Simple extrapolation indicates that the new x-ray source will open new research capabilities. For example, the increase in brightness means one can use smaller samples to get a similar results as today's facility and/or one can reduce exposure time of the sample. This ability to use smaller samples and/or shorter exposure time opens up new areas of research. Analyses of the structure of proteins, virus, living cells, geological micro-crystals, x-ray motion pictures, and so on.

Figure III.4.2-2 shows the brilliance of various sources as a function of photon energy. This figure shows that the APS covers a wide range of x-ray energy from a few keV to 100 keV range with unprecedented brightness. Figure III.4.2-3 shows a schematic of an undulator constructed with permanent magnets arranged as shown. When positron beam passes through the device, the magnetic fields in the device causes the beam to undergo an undulating wave motion. Every time the beam changes its direction of motion it emits photons, and the photons from one wave make constructive interference with photons from another wave. This results in a discrete energy of photons emerging from the device

History of (8-keV) X-Ray Sources

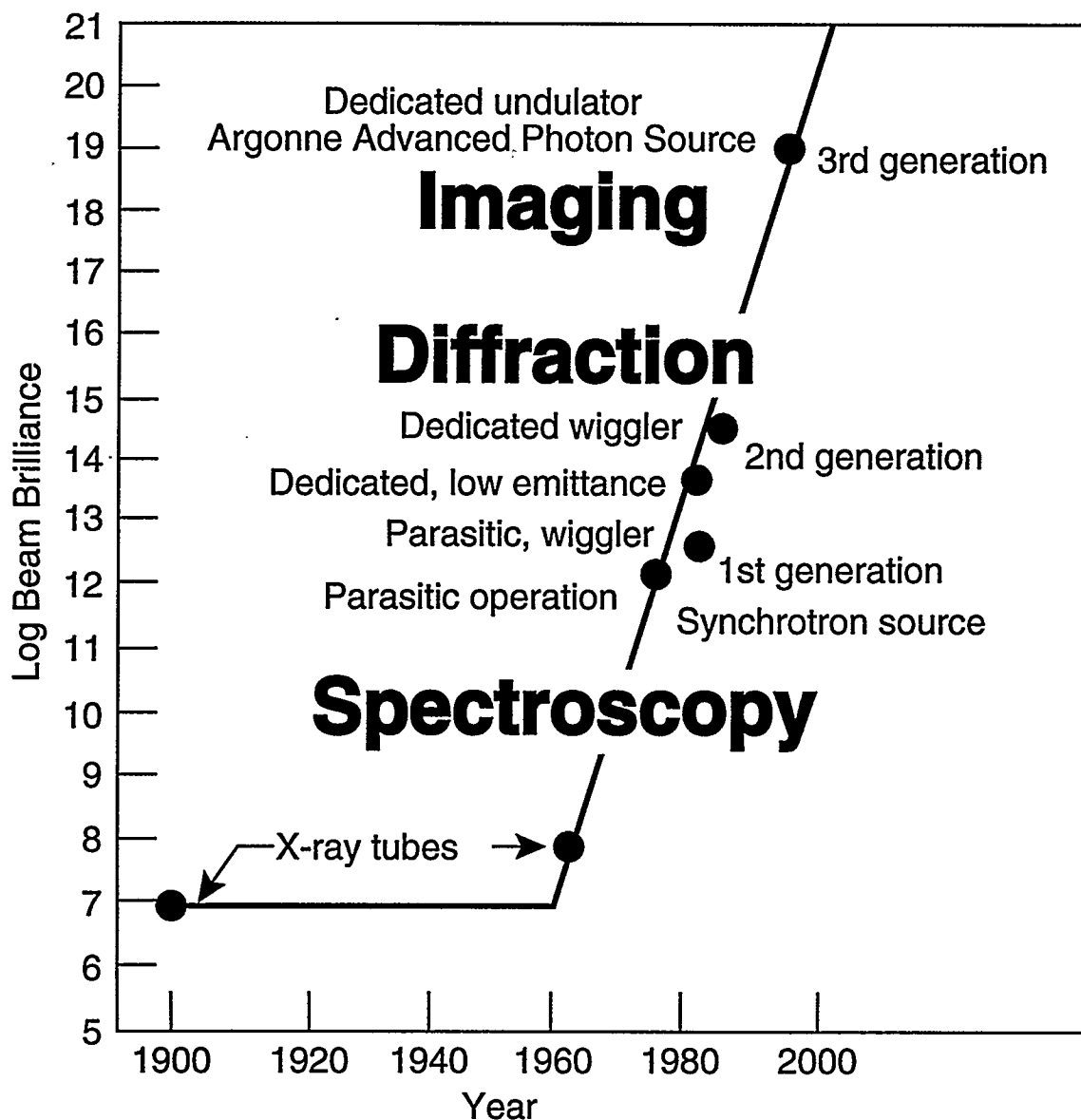


Figure III.4.2-1
History of x-ray Brilliance

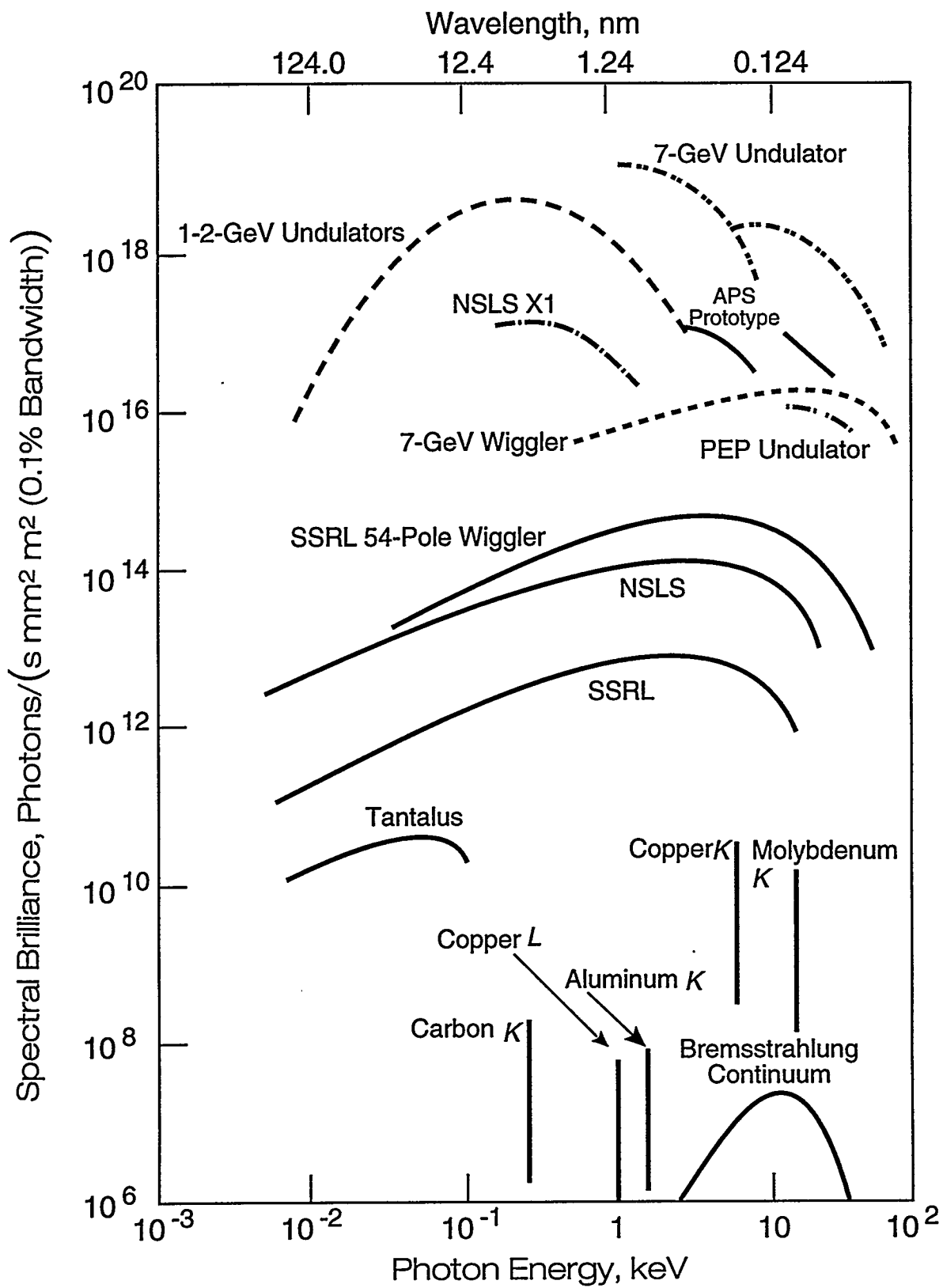


Figure III.4.2-2
Brilliance of Various Sources as a Function of Photon Energy

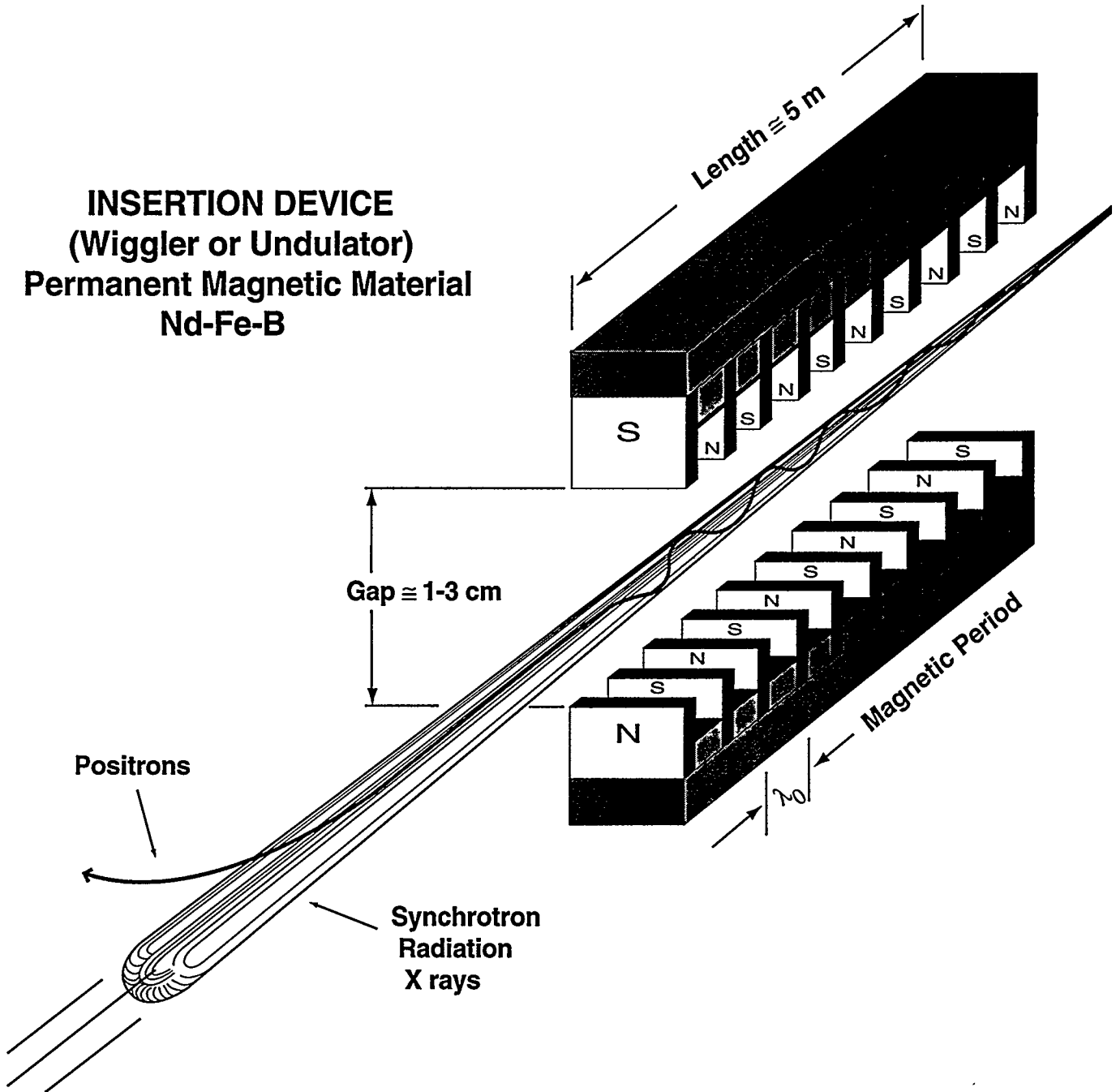


Figure III.4.2-3
Schematic of an Undulator

depending on the magnetic periodicity of the undulator and the field strength of the device. In another word, one can tune the photon energy by adjusting the gap height of the device which changes the magnetic field.

III.4.3 Accelerator Configuration

As noted in the Ames parameters, the accelerator system is to utilize positrons and a full energy injector. The original plan was to locate the APS near the ZGS complex to take advantages of existing utilities and infrastructure. However a detailed study showed that a better location could be the southwest corner of the laboratory boundary as shown in Figure III.4.3-1. This corner is called 400 Area in contrast to the 300 Area of the ZGS.

A detailed layout of 400 Area is shown in Figure III.4.3-2. A linac system consisting of an electron and a positron linac is house in Building 411. These are a 200 MeV electron linac capable of delivering 50 nC charges in 30 nsec pulse with a repetition rate of 60 Hz to a positron production target, followed by a 450 MeV positron linac.

The Positron Accumulator Ring (PAR) which accepts 24 positron linac pulses with 60 Hz rate, and lets the accumulated beam damp for 100 msec before ejecting the damped beam for injection to the booster synchrotron for every 1/2 sec. The PAR has a circumference of 30 m, and is housed in Building 412, which is called Injection Building.

The Booster synchrotron accelerates the 450 MeV positrons to 7 GeV with a repetition rate of 2 Hz.

The center piece of the facility is the storage ring. The ring and some 70 beamlines together with experimental setups are housed in Building 400 as shown Figure III.4.3-2. The circumference of the ring which consists of 40 sectors, grew to 1104 m during the detailed design process from the 1060 m noted in Table III.4.2-1. Each sector has 2 dipole, 10 quadrupole, and 7 sextupole magnets. Figure III.4.3-3 shows the magnetic lattice of one sector. Photon beam paths from ID and dipole magnet are also shown in the figure.

In order to facilitate passage of the photon beams emerging tangentially from the ring, we had to invent a suitable vacuum chamber geometry. The geometry of the chamber is called Bob Wehrle and John Moenich's FISH which is shown in Figure III.4.3-4. This geometry allows not only the photons to pass through without interception but also facilitates a continuous pumping along the circumference of the ring. The chamber system consists of a beam chamber and an and the ante-chamber where a distributed getter system is installed. Figure III.4.3-4 shows both the beam chamber and the ante-chamber. The photon beam passes through the narrow channel between two chambers.

The magnetic lattice of the storage ring also has to accommodate the passage of the extracted photon beam. To do this, Walter Praeg and Ken Thompson invented a

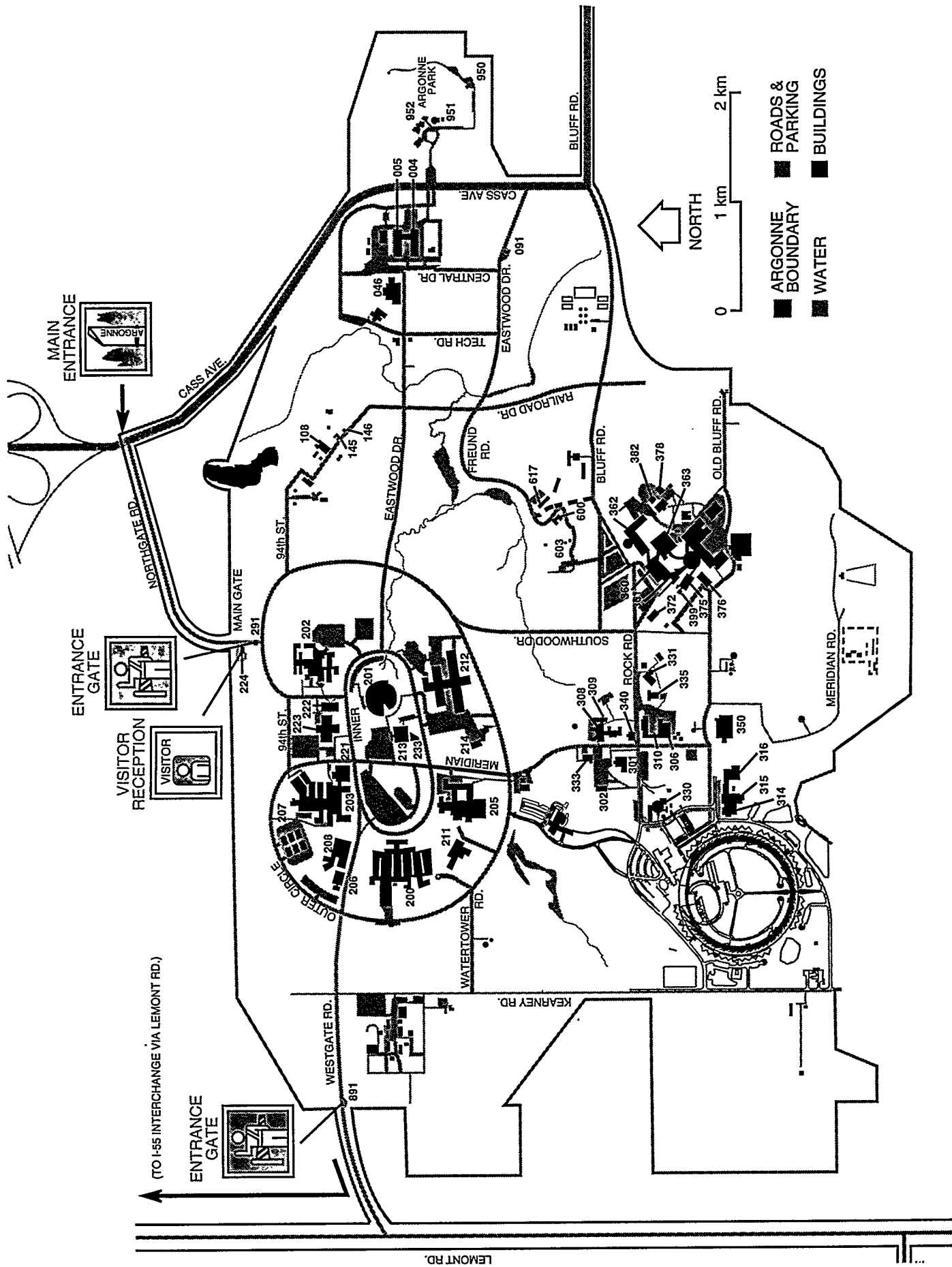


Figure III.4.3-1 ANL Site Drawing Showing the APS Site

Plan View of the Advanced Photon Source

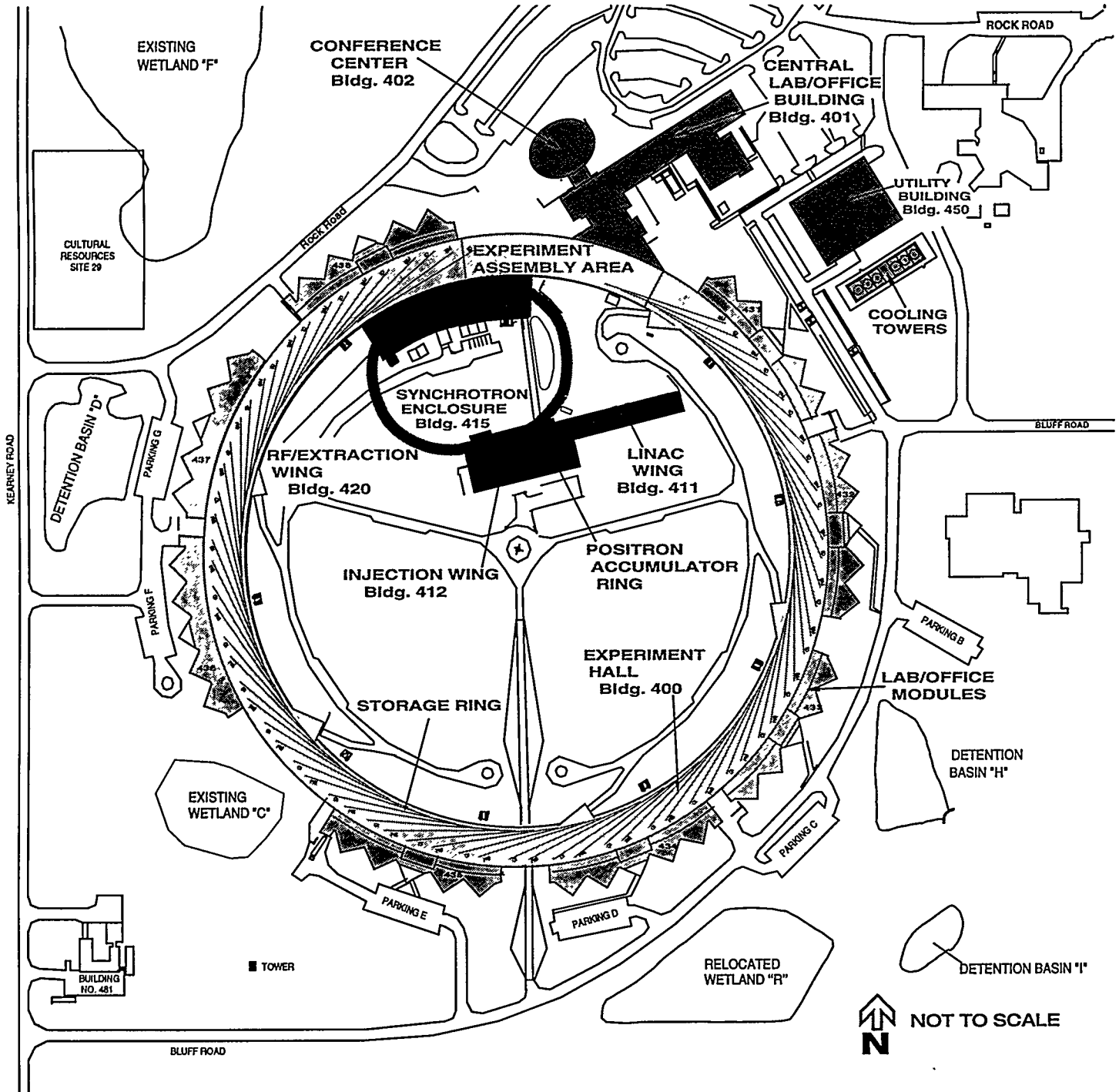


Figure III.4.3-2
Layout of 400 Area Showing the APS Buildings

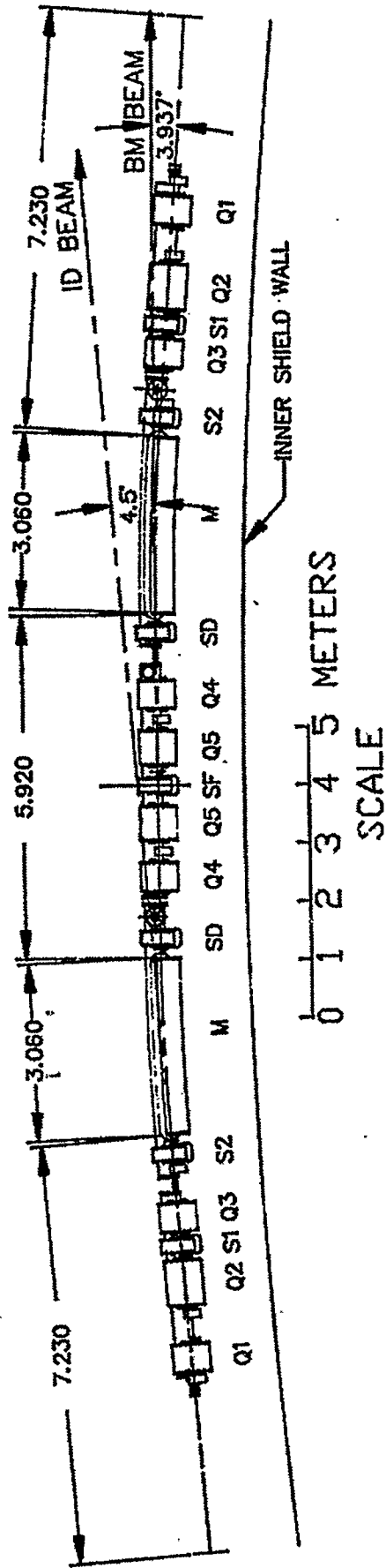


Figure III.4.3-3
Magnetic Lattice of a Sector

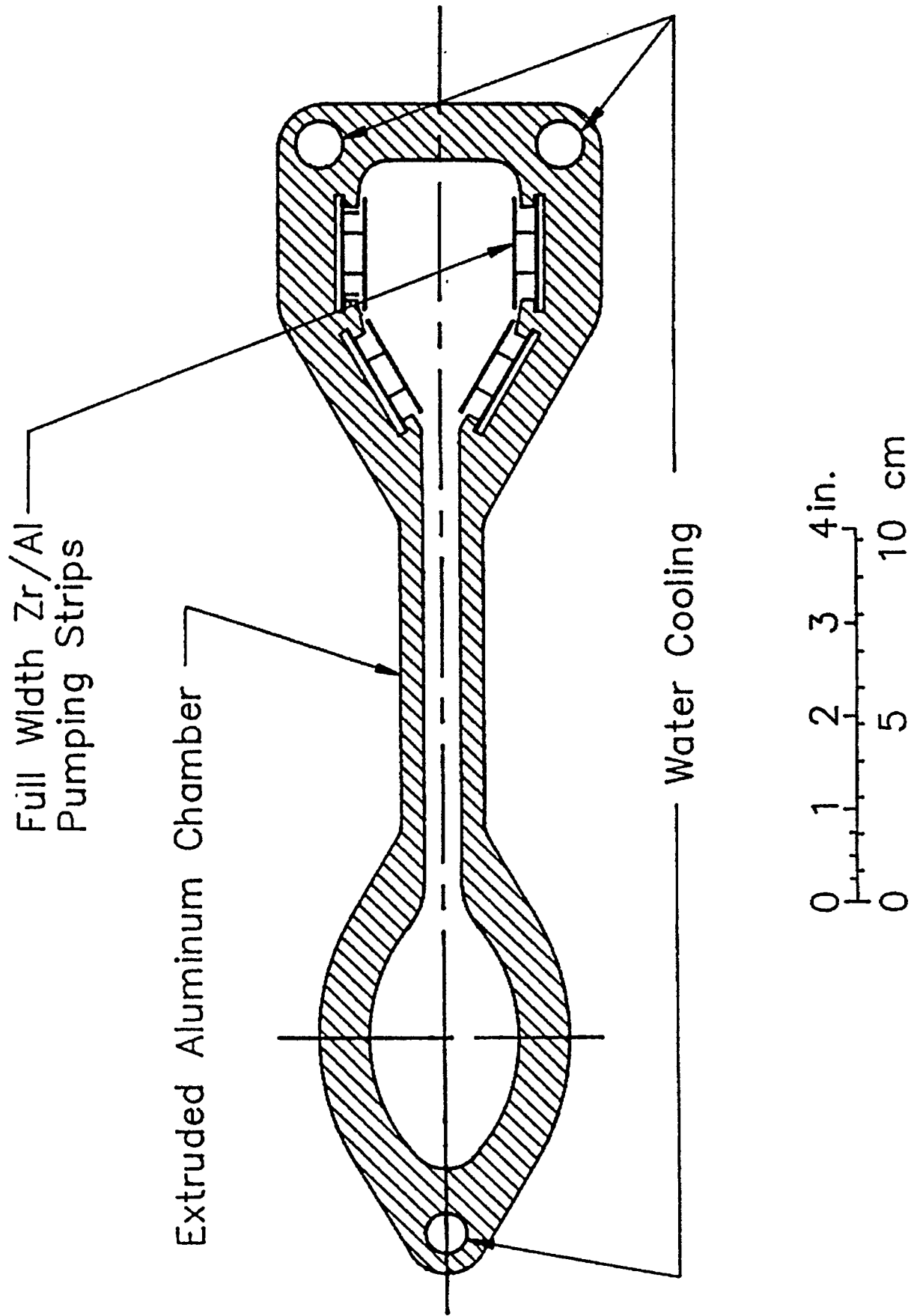


Figure III.4.3-4
Storage Ring Vacuum Chamber Cross Section
"FISH"

“FIGURE 8” quadrupole magnet, where two of four of the magnetic field return yokes were removed so that the magnetic field lines make a figure 8. This is shown in Figure III.4.3-5. This figure also shows how the fish-shaped vacuum chamber system fits into the magnet.

The accelerator system uses 6 of the 40 long-straight sections in the ring. The remaining 36 straight sections from 36 sectors are to be equipped for the users scientific program. The plan is that each sector will have one ID beam line and one dipole magnet beam line. Therefore there will be total of 68 beam lines. A layout of sectors, associated beam lines, and users office and laboratory modules are shown in Figure III.4.3-6. As shown in the figure, each sector will have 2 laboratory spaces, 8 offices and a conference room.

For the management of the scientific program, we use the CAT (Collaborating Access Team) concept. A consortium of users proposes a program of experiments to be performed. Once their scientific program is approved, the team obtains the funds for the beamlines and equipment. The CAT uses 75% of the beam time, and 25% goes for independent users.

So far we have approved programs for 20 sectors. The initial funds needed for the 20 sectors are some \$180M, and they have obtained some \$100M so far.

It is very interesting to note that we have heavy involvement by industry; AT&T, Dow Chemical, Du Pont, IBM, AMOCO and some 15 pharmaceutical companies to name a few.

The total project cost of the APS is \$892M, which includes the construction cost of \$467M, the pre-construction R&D and other start-up costs. It is anticipated that the annual operating cost to be about \$90M with the facility staff of some 350 personnel. Figure III.4.3-7 shows the construction milestone vs. cost.

Figure III.4.3-8 shows a picture of the APS site before the construction started seen from the weather tower. Figure III.4.3-9 shows the APS as of today.

III.5 IPNS Upgrade

As noted in Section III.4.1, the Seitz-Eastman Panel reviewed and recommended that the ANS, a reactor source at Oak Ridge be the third priority, and the 4th be a pulsed source. That was in 1984. Since that time activities of proponents of pulsed neutron sources were dormant until a group of Europeans started to organize a consortium of European Laboratories to advocate a 5 MW pulsed source called ESS (European Spallation Source) in 1991. I had actively participated in the birth of the ESS, and at the same time obtained small funds to form an ANL study group of a pulsed source.

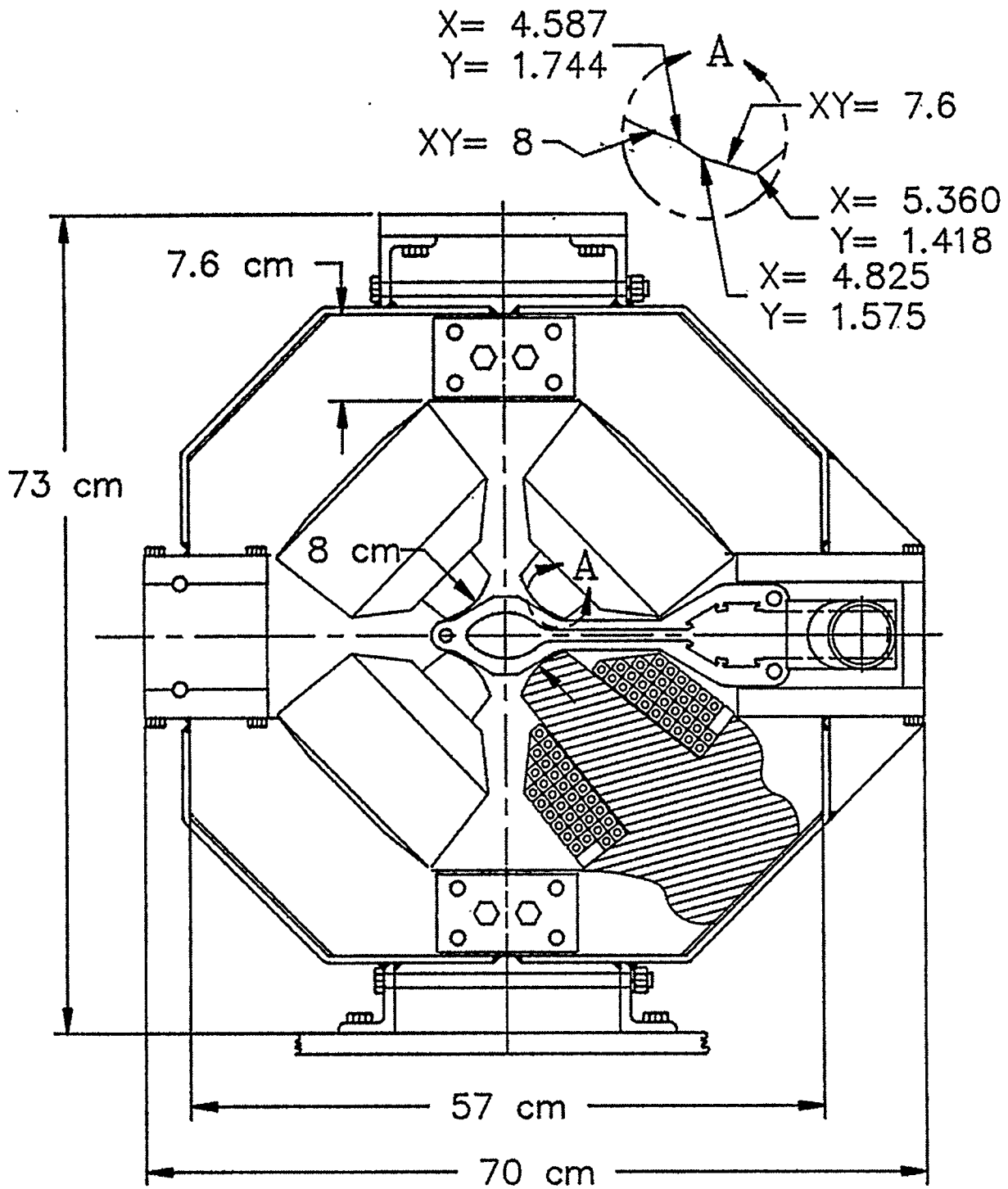


Figure III.4.3-5
 "Figure 8" Quadrupole Magnet

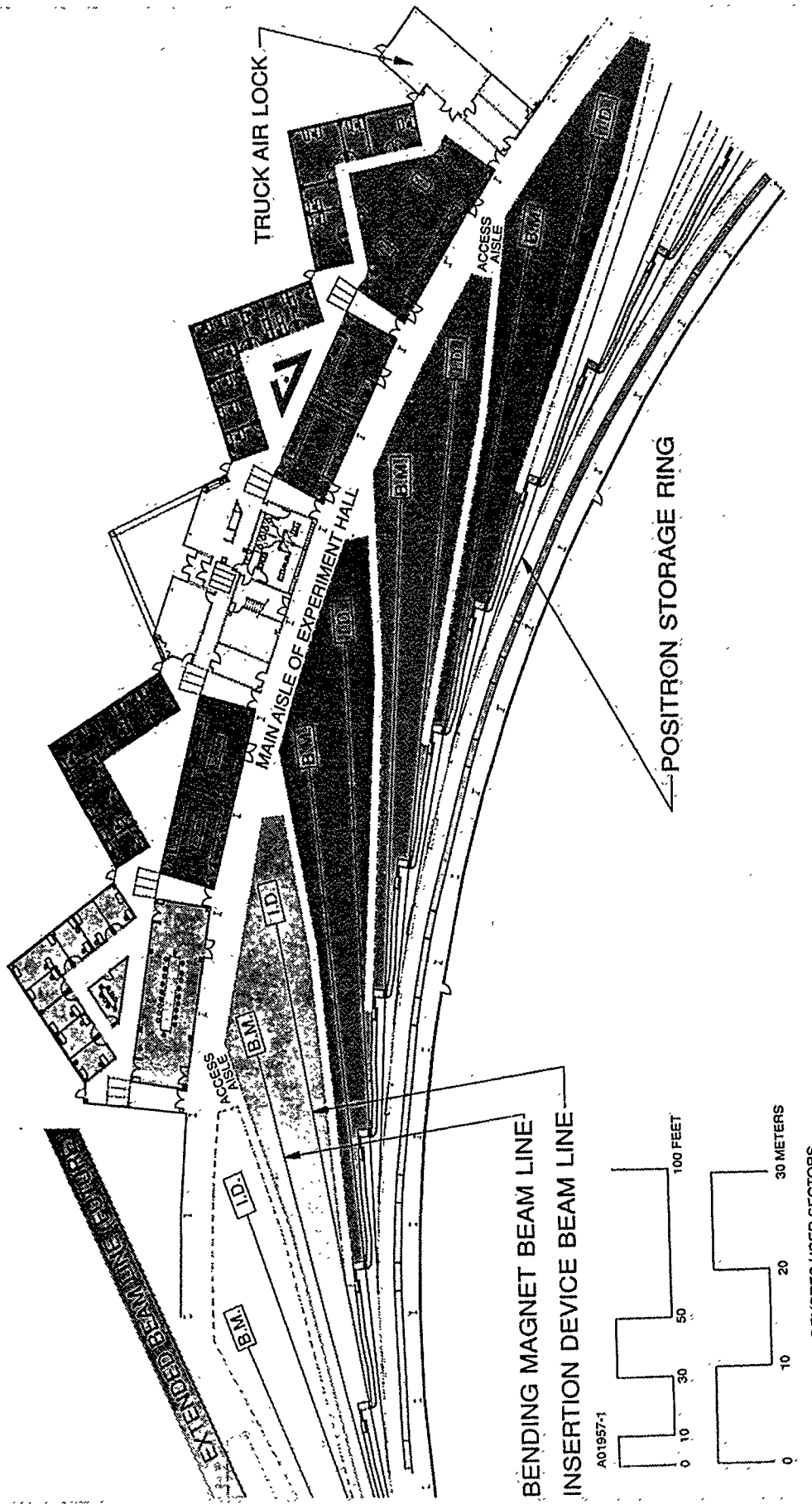


Figure III.4.3-6
 Experimental Area Layout Showing
 Users Laboratories and Offices Associated with a Sector

APS PROJECT MILESTONES VS. COST

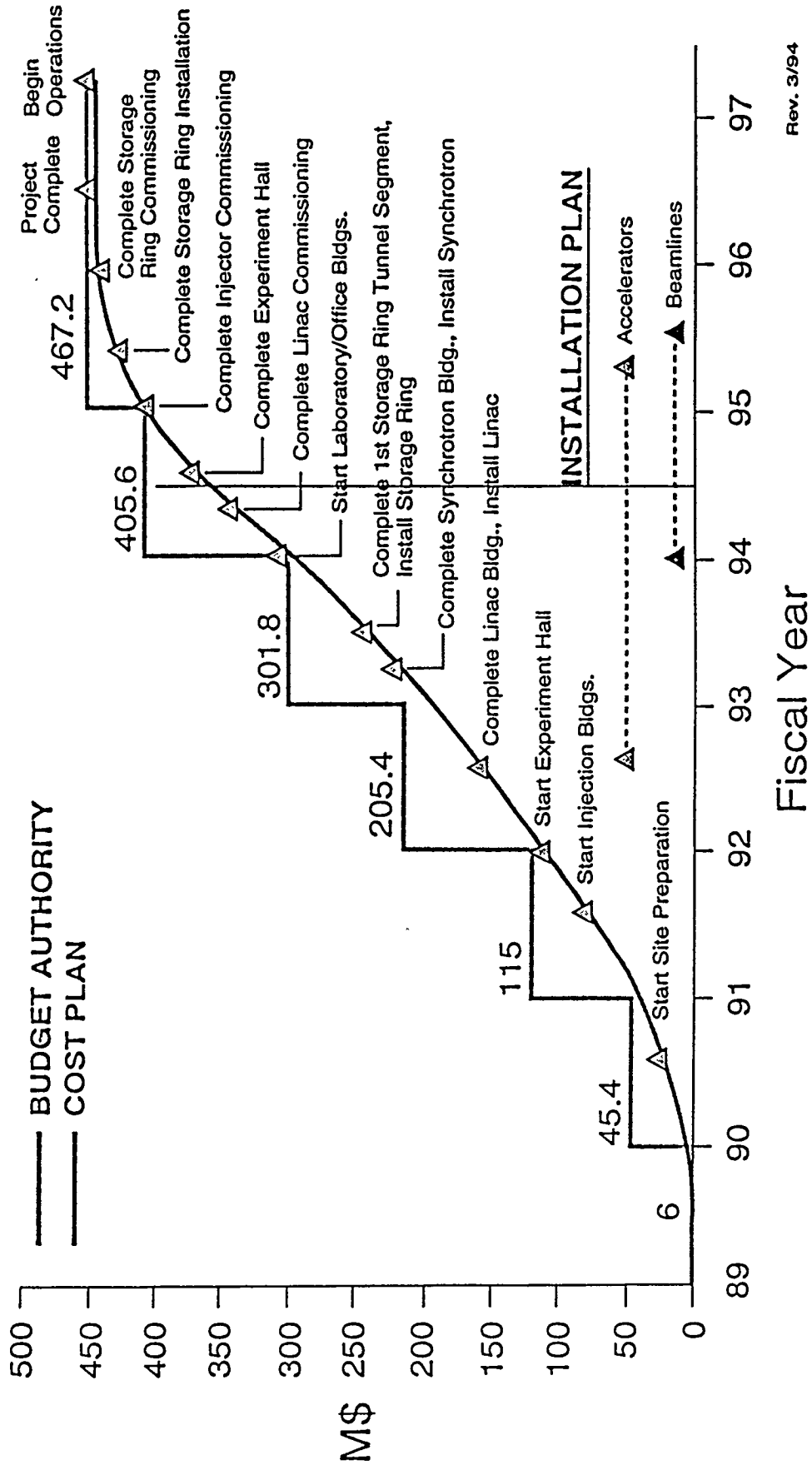


Figure III.4.3-7
 Construction Schedule Milestone vs. Cost



Figure III.4.3-8
APS Site Before Construction



March 23, 1994

Figure III.4.3-9
APS Site Today Showing Progress of Construction

In 1992, DOE Basic Energy Science Advisory Committee (BESAC) appointed a sub-panel (known as the Kohn Panel) to review the situation regarding neutron sources in the US. The Kohn Panel recommended that (1) the ANS, a reactor source in Oak Ridge continue as the number one priority, and (2) the US should pursue a 1 MW pulsed source as a complementary facility to the ANS, and there should be a competitive design effort for the 1 MW pulsed source.

In response to the Kohn Panel recommendation, groups from both ANL and Los Alamos National Lab. (LANL) are pursuing feasibility studies. LANL already has an 800 MeV proton linac which can deliver 1 mA beam current. LANL proposes to build an accumulator ring to compress the linac pulse length to the required 1 microsecond or less.

The ANL plan is to use the existing ZGS building and infrastructure to house and operate 1 MW synchrotron. The book value of the replacement cost of the ZGS complex is about \$150M ~ \$200M, so there is a potential of saving some \$150M.

A 2 GeV rapid cycling synchrotron operating at 30 Hz repetition rate is to be housed in the ZGS tunnel. The synchrotron delivers 10^{14} protons/pulse to make 0.5 mA time averaged current. There will be two neutron generating targets; one receiving the proton beam at 10 Hz rate and the other receiving at 30 Hz rate. The 10 Hz target station is to be placed in Building 369 (EPB-I), and the 30 Hz at Building 370 (Meson Building).

There will be a 400 MeV linac system for the injection into the RCS. The linac system consists of a negative hydrogen ion source, a 2 MeV radio-frequency quadrupole, a 70 MeV drift-tube linac, and a coupled cavity linac to make the beam 400 MeV.

Figure III.5-1 shown the layout of the facility. Note that Building 376 (ZGS MG set building) is to house the power supplies associated with the RCS, Building 371 (30 inch Hydrogen Bubble Chamber Building) is to support the 30 Hz target, and Building 367 (40 inch Hydrogen Bubble Chamber Building) is to support the 10 Hz target. Only new building construction needed for the upgrade is a new linac building (Building 394) and the low energy beam transport line.

Figure III.5-2 shows an aerial view of the ZGS Area with new linac buildings sketched in.

IV. SUMMARY

The ZGS as a facility and an organization provided us with an opportunity to learn, to grow, to mature and to contribute in a major way to the basic science facilities of the country. That is the legacy of the ZGS.

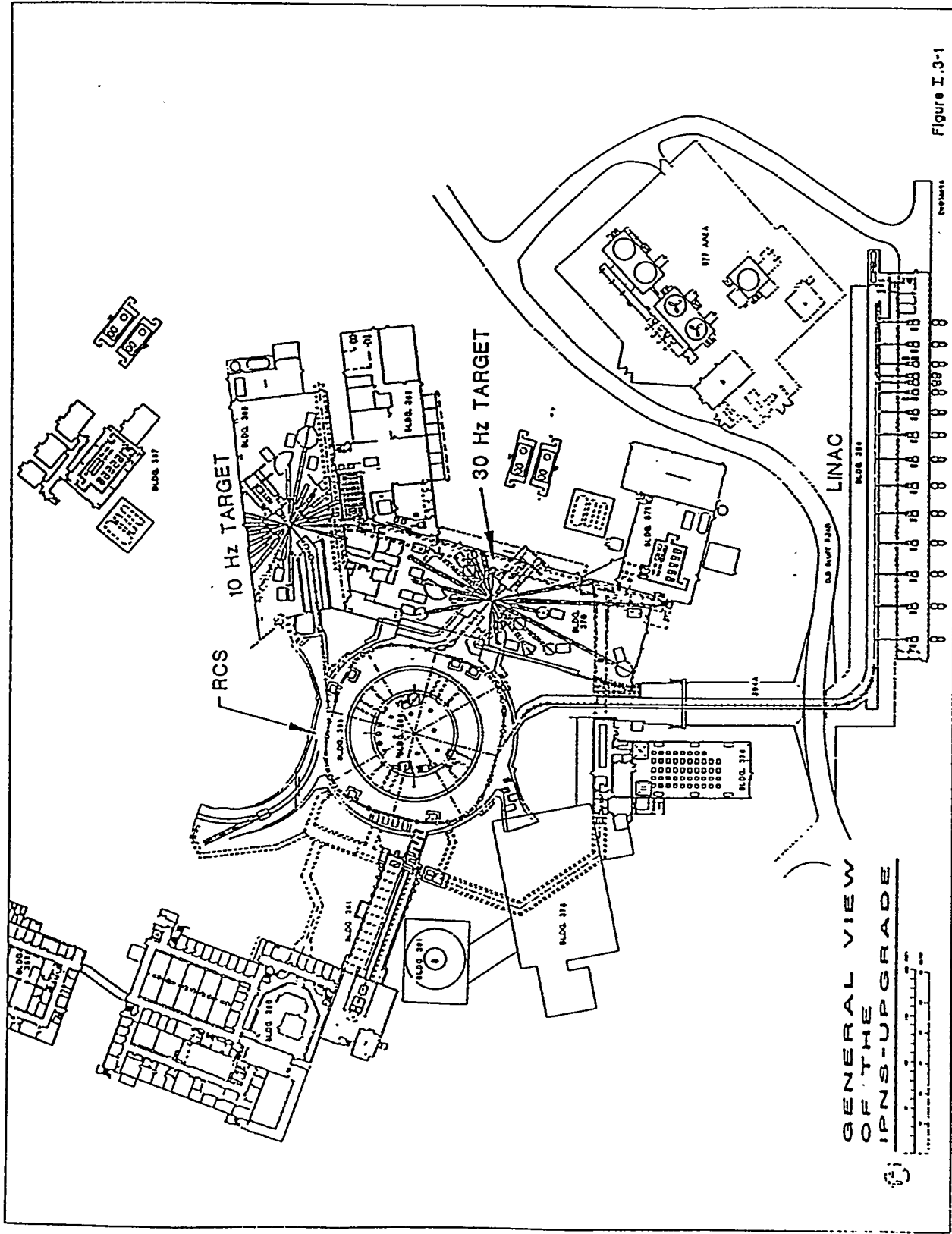


Figure I.3-1

Figure III.5-1
 IPNS Upgrade Layout
 Using ZGS Buildings

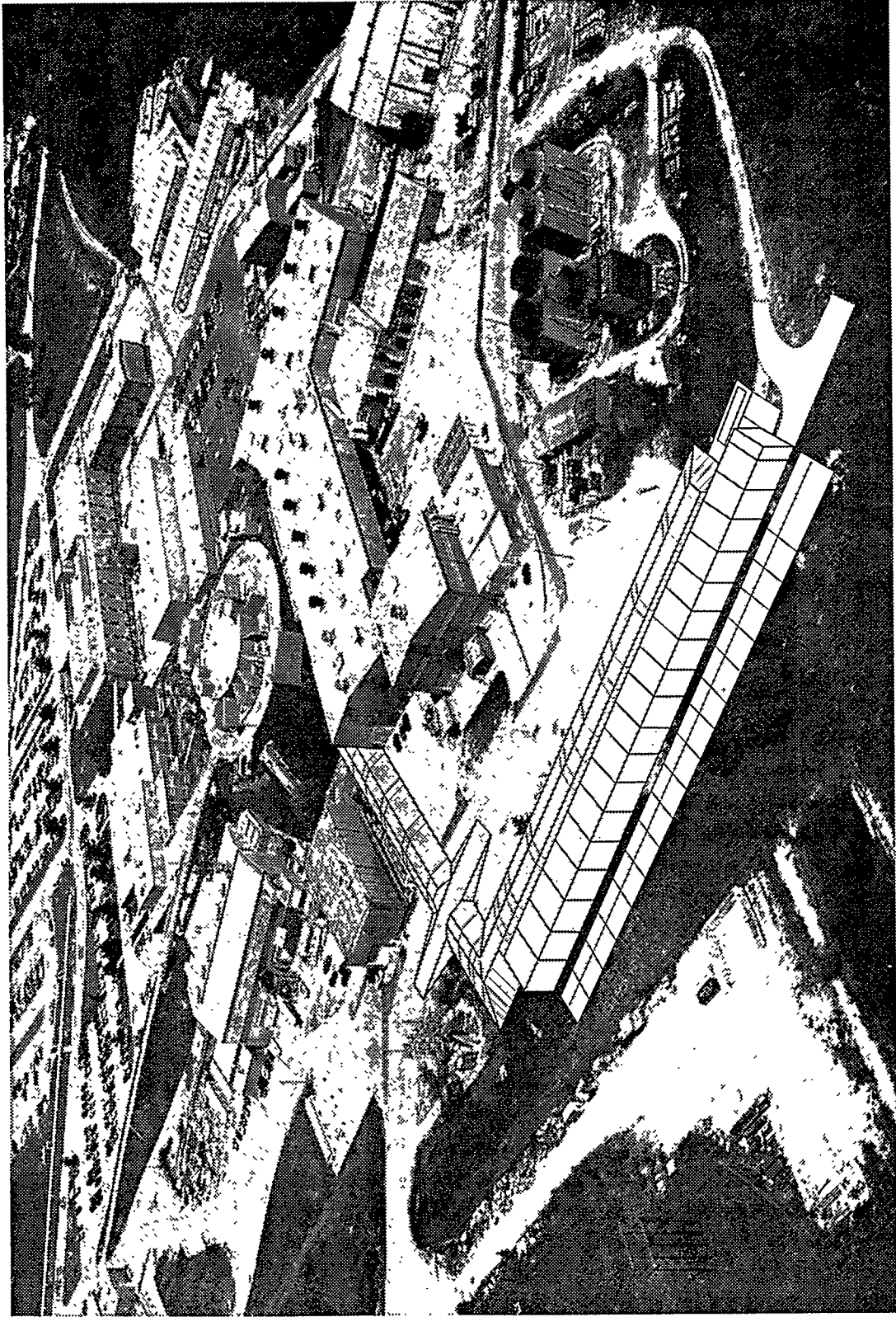


Figure III.5-2
Aerial View Of the ZGS Area with
New Linac Building Sketched in

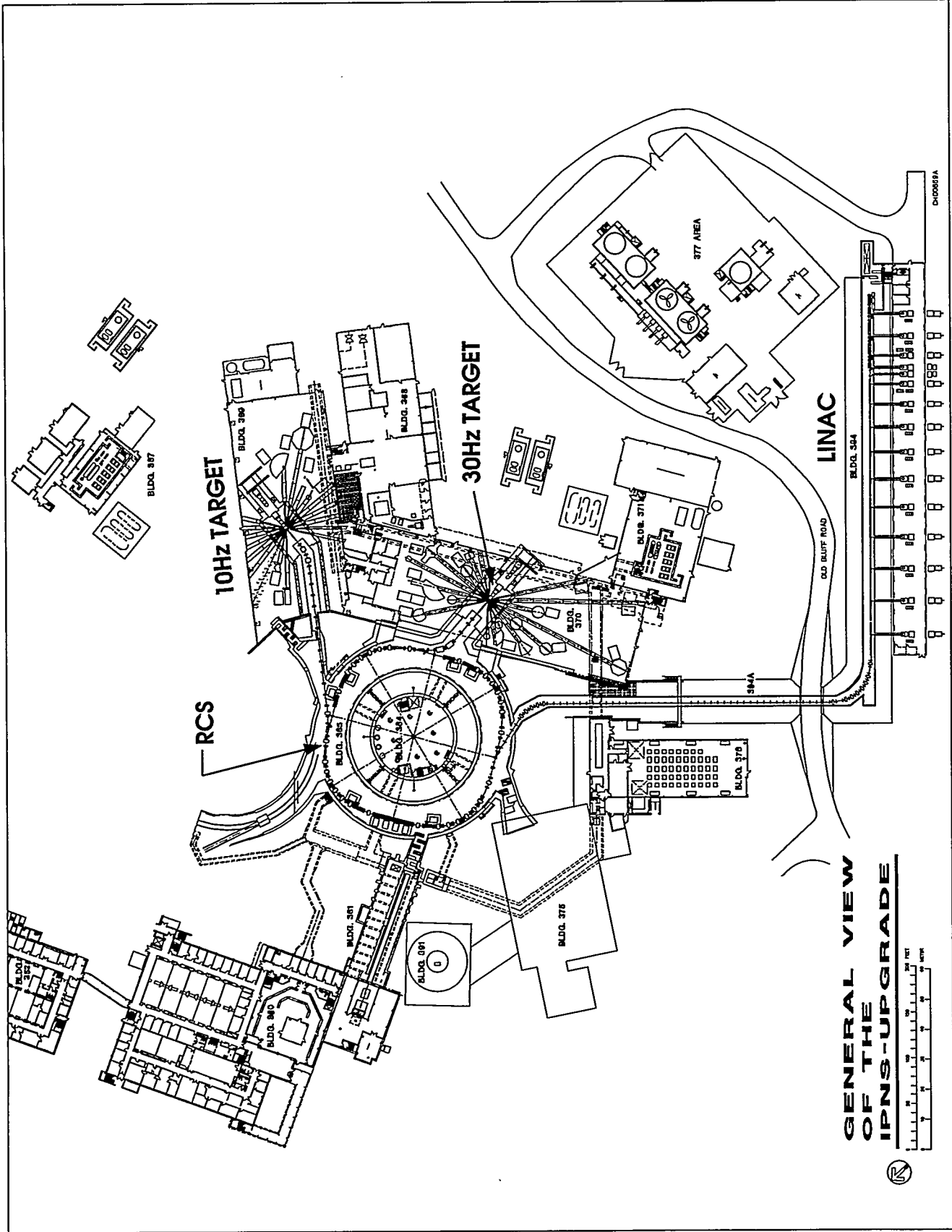
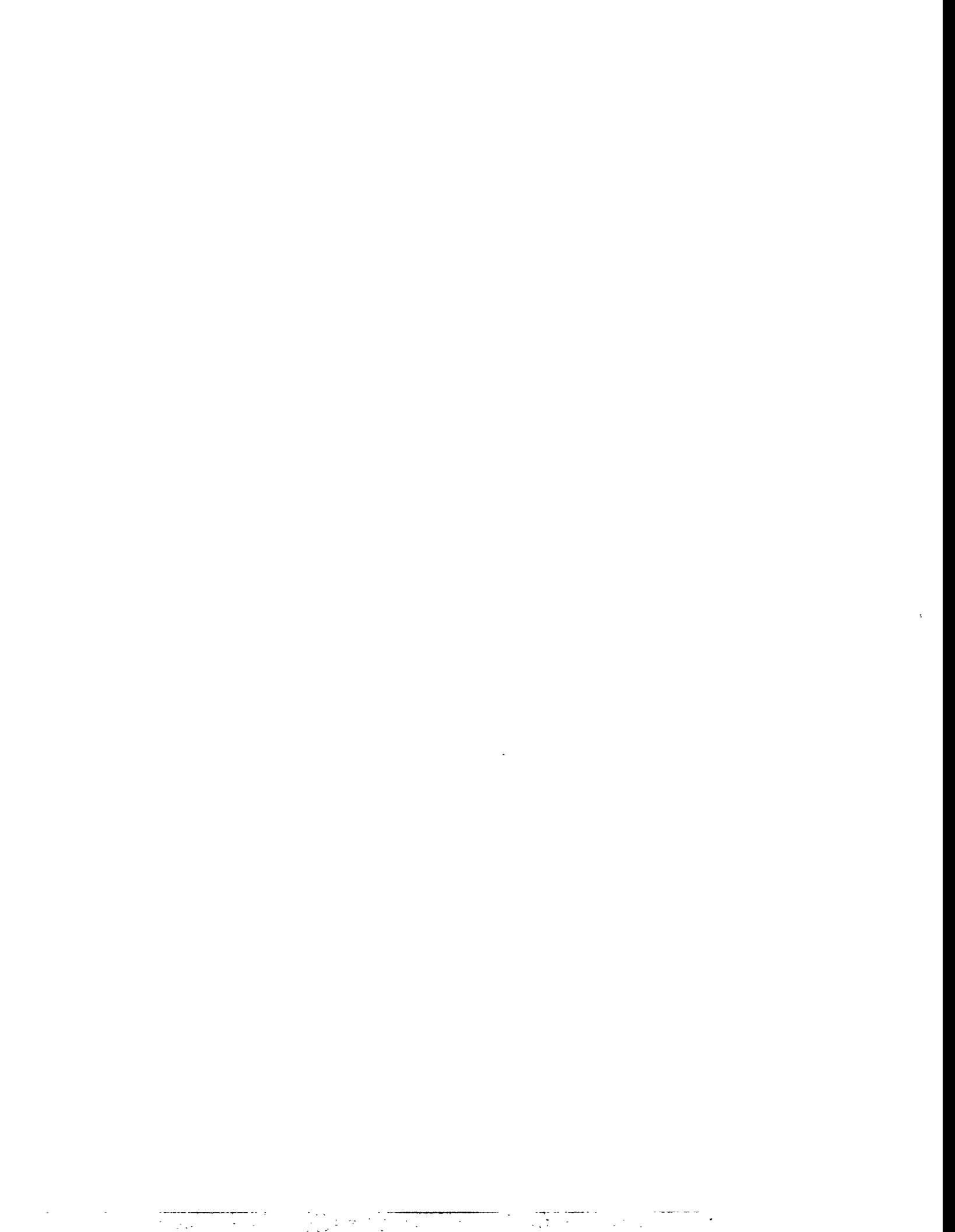
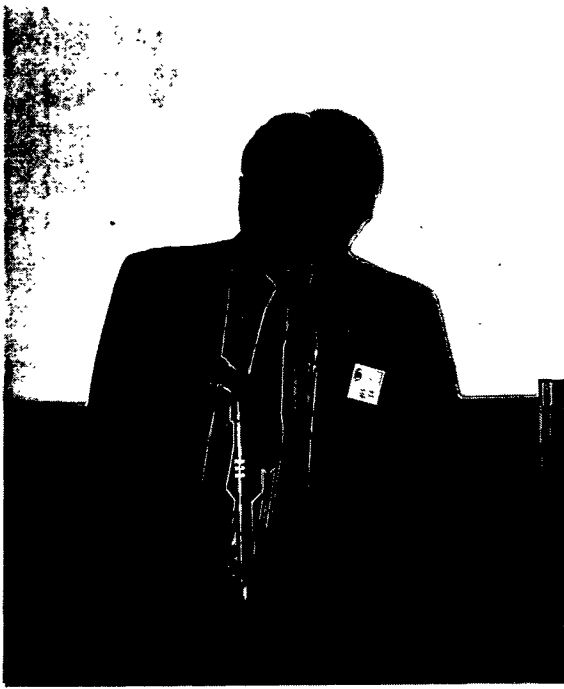


Figure III.5-1
 IPNS Upgrade Layout
 Using ZGS Buildings







superconducting coils. The operating costs strongly favored superconducting coils. The conventional coils required 10 MWatts of power. Note that the magnet run for the 10" Helium Bubble Chamber had occurred in March 1966. John Purcell put forth an excellent design for the superconducting coils for the 12' bubble chamber magnet. It appeared that, from a mechanical point of view, this new technology could be well engineered and was doable. We selected the superconducting alternative and proceeded to procure and fabricate the magnet. The design was 1.8 T, 1800 Amps with a stored energy of 80 MJ. We procured the conductor, 2.0" by .100" with 6 Niobium strands co-extruded with low resistance copper from Supercon. The president of Supercon, Jimmy Wong, provided an excellent conductor. The successful operation of this magnet was a dramatic demonstration of practicability of superconducting technology on a large scale.

It is interesting that the people at the Rutherford Lab questioned whether or not this magnet would operate successfully because the conductor was not twisted. They had done a great deal of work on persistent currents⁵ and since we had required the Niobium Titanium strands not to be twisted so that the rivets of the conductor splices would not interrupt superconductor, they expressed concern about the 12' magnet operation. A three foot diameter coil (no iron) of the 12' conductor was tested in liquid helium. The test demonstrated that it was unlikely that we would have a problem with persistent currents.

With the unsaturated iron yoke, the radial fields of this magnet were very small and no problem was experienced with longitudinal forces on the conductor. This was not the case for the 7' Hydrogen test facility magnet at Brookhaven or the BEBC magnet at CERN. During initial testing both of these magnets experienced conductor displacement resulting from longitudinal forces arising from radial magnetic field components. Additional conductor support was added in each case.

Alain Herve of SACLAY joined John Purcell and worked with him on the design and testing problems of this magnet. Figure #2 depicts the shells being added to half of the magnet coils that formed the helium container.

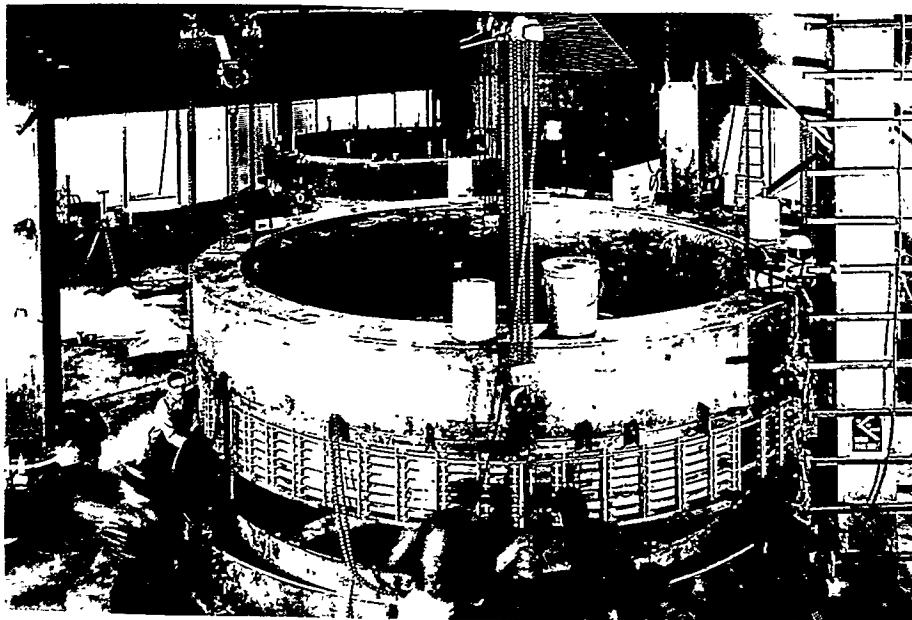


Figure 2 Helium vessels being fitted over the 12' Hydrogen Bubble Chamber coils in the high bay of 362.

⁵Peter Smith, private communication, and Superconducting Magnets, Martin N. Wilson (Clarendon Press, Oxford, 1983), p. 159.

Solenoid for Fermilab 15' Hydrogen Bubble Chamber - 1972

Bob Wilson asked John Purcell to build a magnet for a Fermilab bubble chamber and he wanted the most magnet he could get for \$2 M. It was planned that there would be no iron for this magnet. John designed a 14' I.D. magnet. The weight of the conductor was 55 tons, the stainless steel was 26 tons, the cryostat was 45 tons, for a total weight of 126 tons for the magnet. The conductor was 1.5" X .150" and contained 60 Niobium Titanium strands which were twisted and had a copper to superconducting ratio of 17:1. The central field was 3 T with a peak field at the coil of 5.1 T. The stored energy at full field was 400 MJ. The magnet was made of two coil sections that were separated 22". The compressive force between these coils was 11,250 tons. A snout on the bubble chamber extended across the gap between the magnet coils to get a hydrogen dimension of 15'. The startup and test of this magnet proceeded without any significant problems. Henri Desportes from SACLAY assisted in the design and fabrication of this magnet. Figure #3 shows the magnet assembled in the cryostat being rigged into the bubble chamber building at Fermilab.

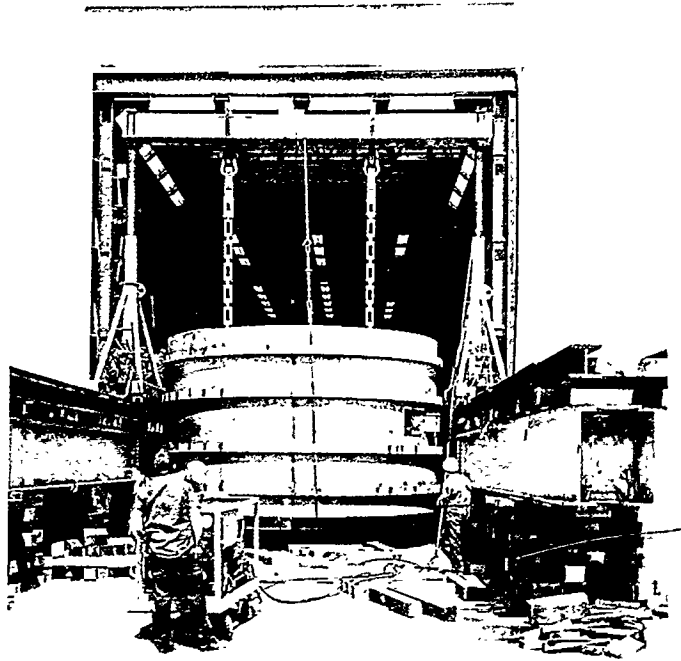


Figure 3 Fermilab 15' HBC magnet being moved into the bubble chamber building at Fermilab.

Polarized Proton Targets - 1972

Superconducting magnets for polarized proton targets offer much better access to the polarized target as well as much greater ease in achieving a useful volume with a highly uniform field. Two superconducting magnets were built at ZGS for polarized proton targets. Superconducting magnet #1 (SCM-1), a 2.5 T vertical dipole with an azimuthal aperture of approximately $4\pi/3$, was designed in 1970 by Henri Desportes. It was built by Argonne National Laboratory and Cryogenics Consultants, Inc., and was used at the ZGS from 1973 to 1979, and was used at LAMPF from 1980 to 1982.

SCM-2 was designed in 1973 by Henri Desportes and Bert Wang. It has a 2.5 T horizontal dipole field with azimuthal and polar apertures of approximately $4\pi/2$. A picture of this magnet coil is shown in Figure #4. This magnet was built by Argonne with the assistance of Meyer Tool and Manufacturing Co. It was used at the ZGS from 1976 to 1979, and then used at LAMPF from 1982 to 1985. It is presently providing fields in the Engineering Technology Division of Argonne for high temperature superconductor tests.

Superconducting Stretcher Ring (SSR) Proposal - 1974

Ron Martin conceived the idea of a DC storage ring for the ZGS tunnel in 1971. It would demonstrate the first use of super-conducting magnets for this purpose and would significantly add to the capabilities of the ZGS for high energy physics. It would double the intensity for the same power in that there would be no flat top and we would have a 100% beam available from the storage ring. The design was for 128 3 T, 190 amp dipoles and 64 quadrupoles. With discretionary money, ten 31" dipoles were built and five 16" quadrupoles. These magnets had cold iron yokes with the Lorentz forces being contained by aluminum bands around the coil windings. The integral field homogeneity was $\pm 0.1\%$ over a 3" diameter. During the tests of these magnets, the correlation between the warm field measurements and cold field measurements was used very successfully. These magnets were also placed in a proton beam. A diffuse beam did not quench the magnets, but it caused much greater helium boil-off. If the proton beam was focused on the coil windings, the magnets would quench.

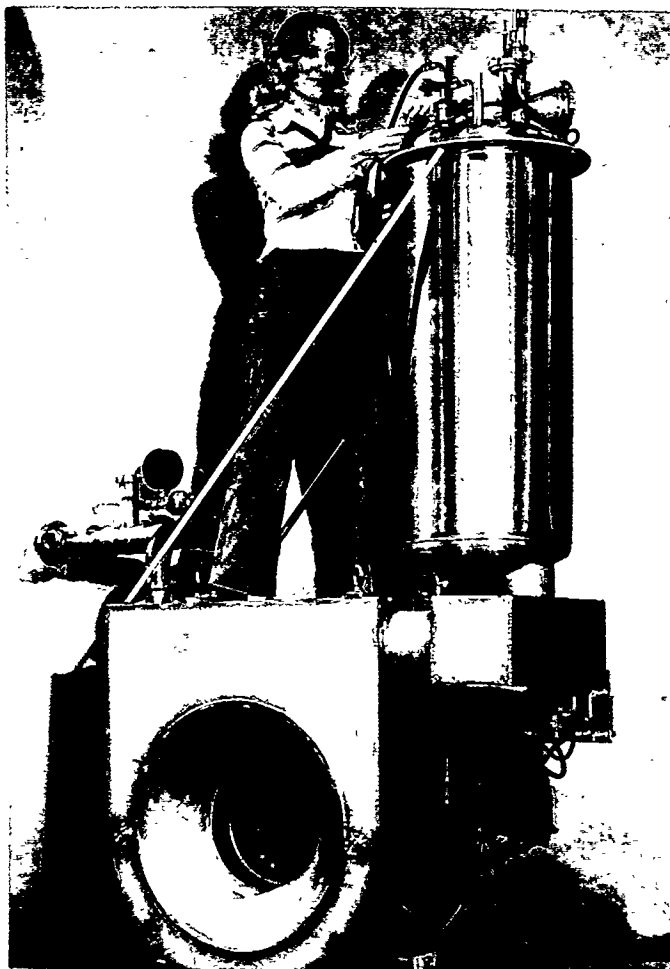


Figure 4 Polarized Proton Target, SCM-2, designed by Henri Desportes and Bert Wang

This proposal was turned down by the AEC although it was well thought out and would have provided a significant step toward demonstrating the feasibility of superconducting magnets for storage rings and superconducting accelerators. Figure #5 is a picture of a dipole/quadrupole/dipole section of the SSR.

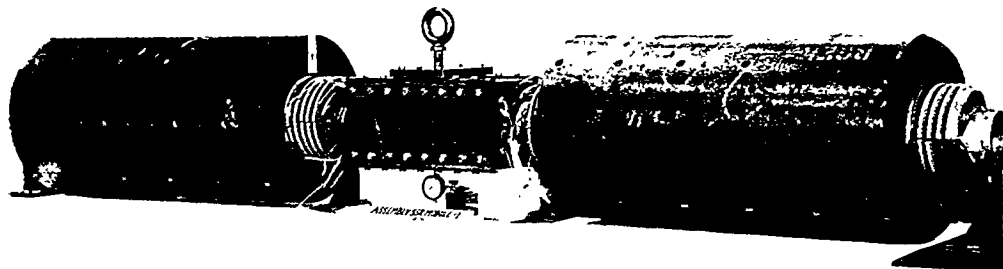


Figure 5 Dipole - Quadrupole - Dipole magnet section for the Superconducting Storage Ring.

Superconducting Beam Line at the ZGS - 1976-1978

Ten of the superconducting dipoles and two of the superconducting quadrupoles that were built for the SSR proposal were used in a superconducting beam line. The length of this beam line was 60 meters and was used for transporting 12 GeV/c polarized protons to the effective mass spectrometer in EPB-1. There were four cryostats, three of which contained three dipoles each, and one cryostat that contained one quad, a dipole, followed by another quad. The dipoles operated at 2.6 T over 91 centimeters at a current of 160 Amperes. The quadrupoles operated at .31 T per centimeter gradient over 41 centimeters with 190 Amperes. This beam line was the first one to be used in high energy physics accelerator operations.⁶ Its compact size permitted it to be installed along side an existing 6 GeV/c meson beam and provided excellent opportunities to obtain experience useful for future installations.

POPAE Proposal⁷ - 1976

A group lead by Bob Diebold proposed the construction of a 1000 GeV proton on proton colliding beam facility. The storage ring would be located on the Fermilab site. Each ring would have 570 dipoles with a field of 6 T and a length of 6.17m. The stored energy in each dipole would be 1.7 MJ. The ring would also contain 138 quadrupoles with a 1.2 T per centimeter field strength and 1.32 meter length. The inner diameter of the vacuum chamber would be 3 centimeters. Although this proposal was made jointly with Fermi National Accelerator Laboratory, they withdrew their support of the proposal.

A limited amount of laboratory work was done for this proposal. There was a 6" diameter dipole built for providing backing fields for coil tests. This work was done by Rich Smith, Larry Turner, Lyle Genens, Lloyd Hyman, Martin Foss, and John Purcell. Figure #6 is a picture of this backing field dipole being lowered into a dewar.



Figure 6 Don Jankowski and Fred Catania with an 8" bore backing field dipole for the test to support the POPAE proposal.

⁶J. Bywater, C. Brzegowy, J. Dvorak, R. Fuja, H. Ludwig, K. Mataya, R. Moffett, R. Neumann, S. Wang, J Purcell, IEEE Transactions on Magnetics, Vol. Mag-13, No. 1, January, 1977, p. 294.

⁷A 1000 GeV Proton-Proton Colliding Beam Facility (proposal document, 149 pages), FNAL and ANL (1976).

U-25 Bypass SC Magnet - 1975

Mike Petrick was instrumental in establishing a U.S. / Russian collaboration in Magnet Hydrodynamics (MHD) research. Agreement was reached that a 3 MW thermal bypass would be installed at the 25 MW thermal MHD test facility at the High Temperature Institute in Moscow. The Russians agreed to build an MHD channel and the U.S. would supply a superconducting magnet. The parameters of this magnet are given in Table I.

Table I
U-25 ByPass SC Magnet (1975 - 80) "Dipole" - Circular saddle

MHD Channel dia.	40 cm -> 60 cm
Field	4 T -> 5 T -> 3.2 T
Magnetic length	250 cm
Overall length	440 cm
Stored energy	34 MJ
Total weight	45 tons

This magnet was installed in July 1977 at the High Temperature Institute. There were approximately ten test runs over 2 1/2 years. The collaboration was terminated in the early part of 1980 when the U.S. ERDA suspended the cooperative program due to the Russian invasion of Afghanistan in December 1979. This was the first coupling of a large superconducting magnet with an operating channel. The power densities and flow interaction parameters have not been equaled to this day.

John Purcell chose the conductor and winding design for this dipole magnet and the real burden fell upon Bert Wang to complete the design and oversee the construction. It was the largest dipole in the world when it was built. The cryogenics were designed by Ralph Niemann. Figure #7 is a picture of the U-25 magnet being loaded into a C5A at O'Hare International Airport. The trucking task was contracted out. The low bidder supplied this truck with a driver for \$1.00. Note that the truck went to Moscow with the magnet on a non-stop flight with re-fueling in-flight. ZGS personnel operated this magnet for 2 1/2 years in Russia at considerable personal inconvenience.

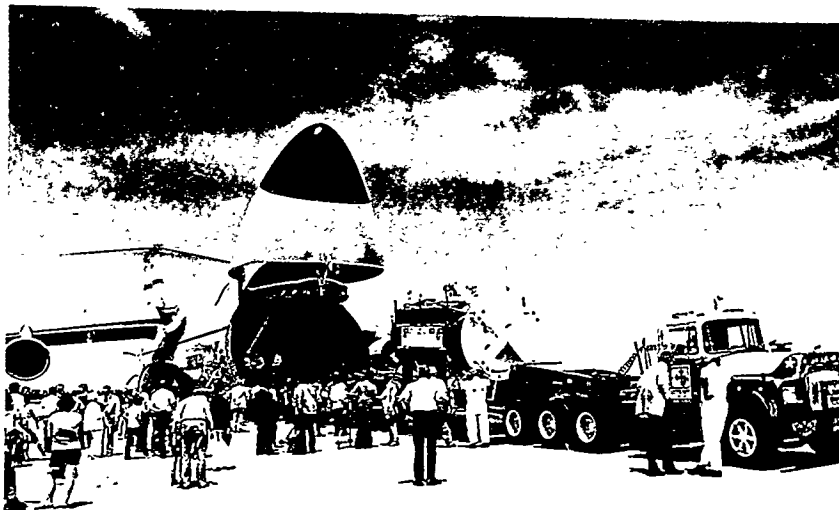


Figure 7 U-25 bypass magnet being loaded into a C5A at O'Hare International Airport in Chicago.

University of Tennessee Space Institute/Coal Fired Flow Facility Magnet (1979 - 1981)

Mike Petrick arranged with DOE for the ZGS magnet group to design and build an even larger dipole for the MHD program in the United States. The particulars of this dipole magnet are given in Table II.

Table II
UTSI/CFFF Dipole (1979 - 1981)

Circular saddle without Iron	
Coil winding bore	119 cm
Coil winding OD	226 cm
Coil length	488 cm
Peak field	6.9 T
Stored energy	210 MJ
Total weight	183 tons
Cost	\$9.8 M

At the time, there were two major MHD programs in the United States: one at the Coal-Fired Flow Facility (CFFF) in Butte, Montana, and the other at the University of Tennessee Space Institute (UTSI), Tullahoma, Tennessee. We started the program building a UTSI magnet; then, we were told we were building a CFFF magnet. After this magnet was built and tested, the Department of Energy decided not to ship the magnet to either program. While this design was started before the ZGS was shutdown, it was completed in 1981. It was also the world's largest dipole at the time of its completion.

In the late 1980's, the U.S. Navy (DARPA) funded a sea water MHD propulsion study at \$4.8 M. Dan Hill reconditioned the magnet system and brought it into operation. The test was concluded in 1992.

Figure #8 is a picture of the workers and cold mass of the UTSI/CFFF magnet showing the aluminum girders and tie bars designed by Warren Young of the University of Wisconsin.

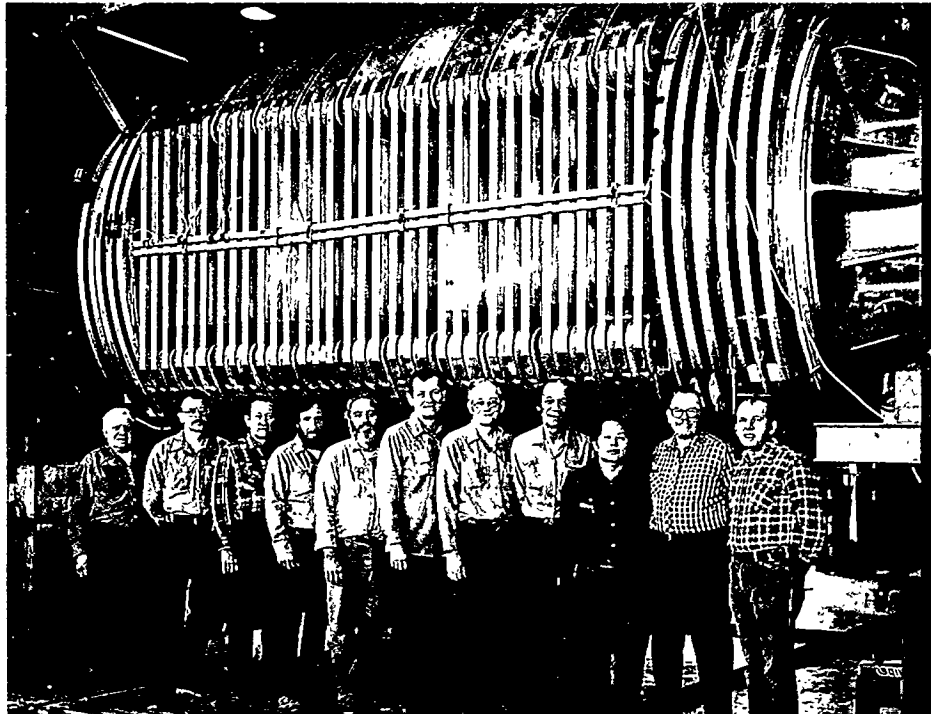


Figure 8 Bert Wang with colleagues in front of the UTSI/CFFF magnet.

Unfinished Business...

At the ZGS symposium in 1979, Tom Fields gave the final talk entitled, "History and Speculations." He divided his talk into finished and unfinished business. Superconductivity he characterized as unfinished business. He asked why, fourteen years after the helium bubble chamber run and ten years after the 12' operation that there was no superconducting accelerator. He answered his question by saying that this was, after all, an exceptional challenge that had been underestimated and also there was lack of funding for development. He also asked the more general question, "Will the technology of large systems of superconducting accelerator magnets begin to progress so that Isabelle and Tevatron achieve their design goals?" The answer to this question follows.

POST ZGS PERIOD - CONTRIBUTIONS BY ZGS PEOPLE

Superconducting Quads - 1981

Rich Smith took over the leadership of the super-conducting magnet group in 1979 while the design of the UTSI magnet was underway. In 1981, Rich led the design and construction of a 2.8 meter length superconducting quadrupole. This quadrupole was to be used in a polarized proton beam at Fermilab. Table III gives its parameters.

Table III
SC Quad (1981) - Polarized Proton Beam at Fermilab

Length	2.8 m
Bore	13 cm
Gradient	50 T/m
Iron Yoke ID/OD	30/50 cm
Conductor	NbTi
Cu:SC	1.8:1.0
Conductor Support	Epoxy Impregnation
Coil Support	Al Rings
	Al Bore Tube

This quadrupole reached design parameters. Figure #9 illustrates how they addressed the support of the conductors at the coil ends. Joe Cook of Applied Math assisted them in understanding this problem. Figure #10 is a picture of the .53 m prototype quadrupole magnet built for this project. The shrunk fit aluminum bands have been added; however, the cold iron has not been installed.



Figure 9 Coil end of the 2.8 m length and 13 cm bore superconducting quadrupole.

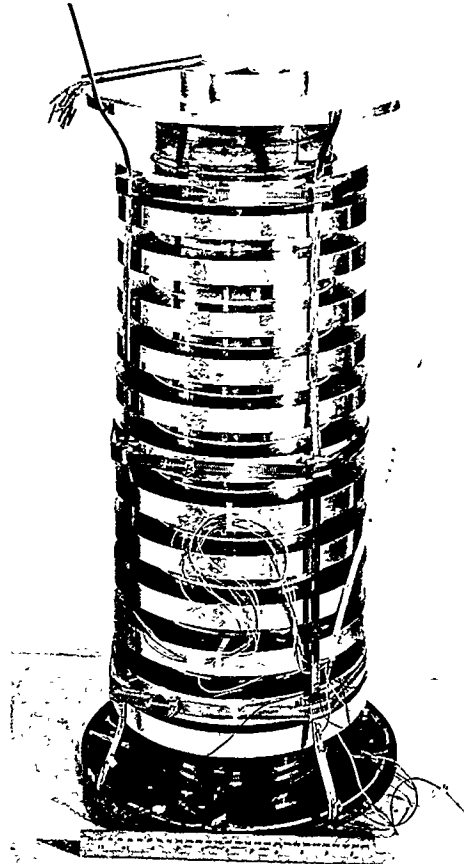


Figure 10 Prototype .53 m quadrupole with coil supports installed.

After the completion of this 2.8 meter magnet, Rich Smith and his group tested this magnet in a proton beam at Fermilab. This magnet is being used today in materials beneficiation studies at Argonne. Figure #11 is a picture of John Gonczy and a portion of the 2.8 meter quadrupole being assembled.

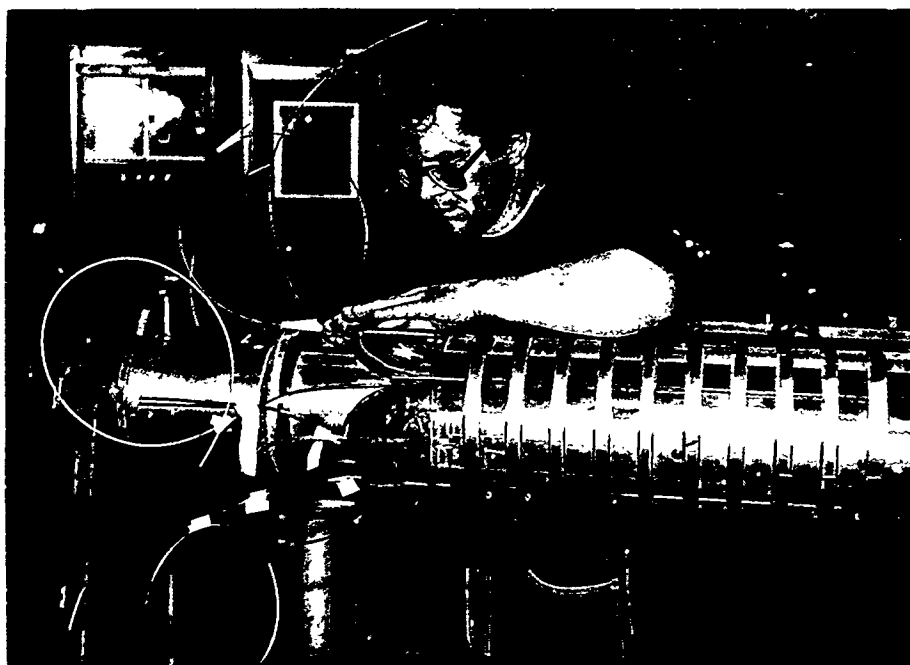


Figure 11 John Gonczy fabricating the 2.8 m superconducting quadrupole.

Superconducting Magnet Accelerators

While the Isabelle project was terminated in 1983, the Tevatron at Fermilab reached its first operational milestone in May 1983. The design incorporated stainless collars, helium permeable Rutherford cable with two $\cos \theta$ current shells, and warm iron. It is generally accepted that this extraordinary accomplishment was the result of the leadership of four individuals, one of whom, Richard Lundy, had a ZGS background. Richard Lundy was responsible for building more than 1,000 superconducting magnets needed for the Tevatron. He was awarded a Presidential medal in 1988 for his contribution.⁸

In 1992, HERA at DESY began operation. The quadrupole and dipole magnets were all supplied by industrial concerns. The dipoles had a 5 T field with cold iron and aluminum collars. It should be noted that Henri Desportes made quadrupole models at SACLAY before these were procured from industry.

The RHIC accelerator at Brookhaven is expected to come into operation in 1999. This design has a one shell current winding, operating with cold iron. The dipoles and quadrupoles will be furnished by Grumman. The first dipole was delivered in May, 1994.

As you all know, the SSC was canceled in 1993; however, pre-production dipoles for this accelerator were designed by a collaborative effort between Fermilab, Brookhaven, and the SSC Laboratory. Quadrupoles were designed and built by a collaboration between LBL and SSCL. Figure #12 is a cross section of the cold mass of the SSC 50mm Collider Dipole Magnet. In assembly, the collars

⁸The three non-ZGS related individuals were Alvin Tollestrup (the major contributor to the magnet design), Helen Edwards (responsible for the machine design), and Rich Orr (built the machine apart from the magnets). They were also each awarded a Presidential medal in 1988 for this outstanding work.

compress the coils and tapered keys are inserted while the superconductor is under considerable pressure. Note that there are strain gauges to measure the pre-stress in the inner and outer coils. This pre-stress is nominally 12 K psi. As the coil is energized, the Lorentz forces relieve this pre-stress.

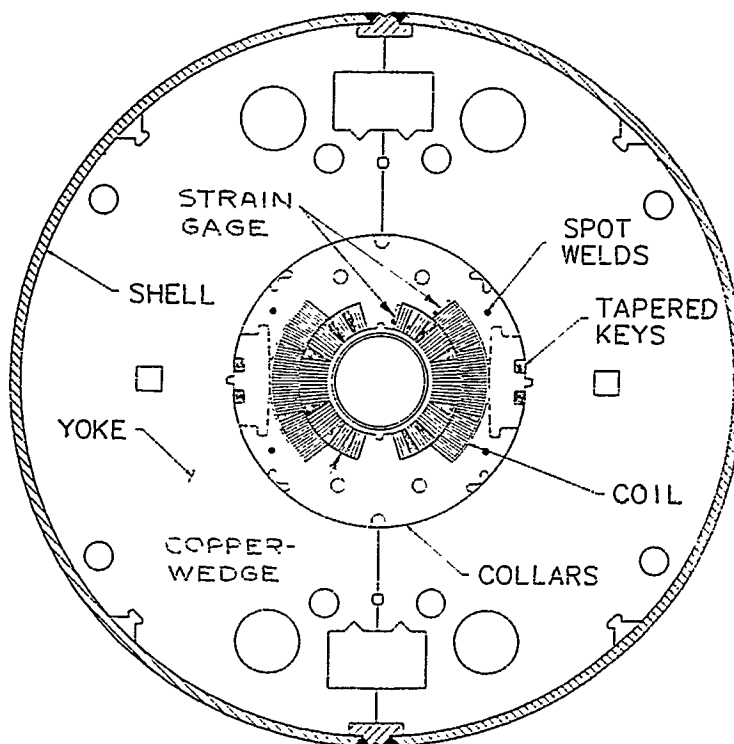


Figure 12 Cross section of the 50 mm SSC Collider Dipole Magnet (CDM).

Thirteen of these SSC dipoles were constructed at Fermilab. The technology of the assembly was transferred to General Dynamics in a two step process. First General Dynamics assisted in the assembly of two of these magnets, and then General Dynamics assembled seven of these dipoles. Five of these industrially assembled dipoles were operated at SSCL in a string test in August 1992, along with one quadrupole that was fabricated by LBL. Tom Dombeck was the person responsible for the string test operation. The successful operation of this string test was clearly the most outstanding technical milestone for the SSC Laboratory.

Ralph Niemann and John Gonczy contributed to the design of the SSC dipole cryostat and Gale Pewitt managed the Fermilab design and fabrication activities. Henri Desportes' group at SACLAY had been assigned the responsibility for fabricating the quadrupoles for the High Energy Booster of the SSC.

The Fiberglas parts used to support the superconducting cable at the ends were manufactured using design data supplied by Joe Cook of the Applied Math Division at Argonne. As stated earlier, Rich Smith had first interested him in this challenge. Figure #13 shows an outer coil as well as some graphics to illustrate the complexity of the surfaces needed on the Fiberglas parts to provide support for the superconducting cable.

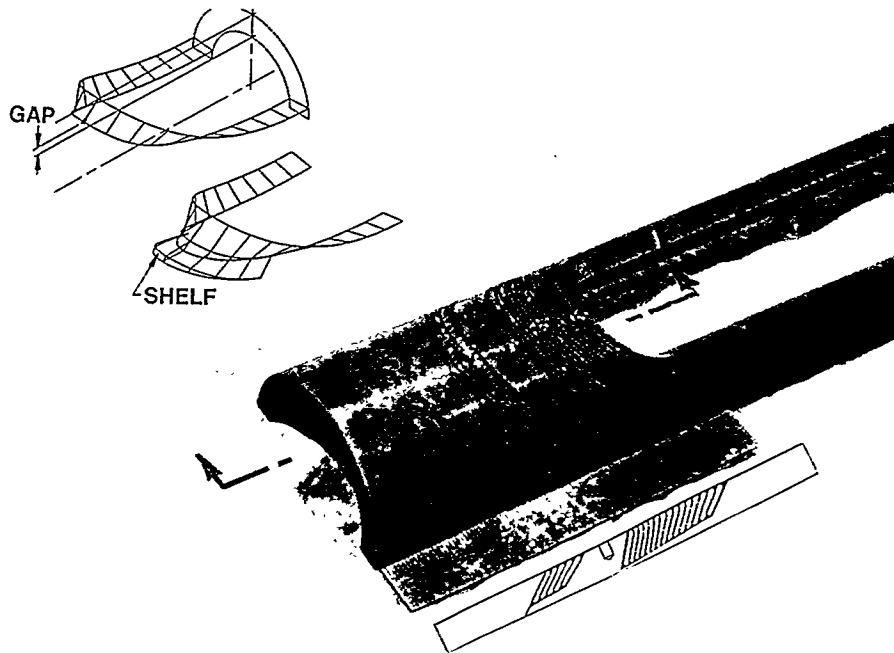


Figure 13 Outer coil return end of 50 mm Collider Dipole Magnet illustrating the complexity of conductor cable surface.

Figure #14 is a view from the crane in the Industrial Center Building at Fermilab of the fabrication of the 50mm Collider Dipole Magnets. There are five magnets in various stages of fabrication shown in the picture. The seventeen meter cold masses were assembled in this half of the building. The other half of the building was used for the assembly of the cold mass into the cryostat.

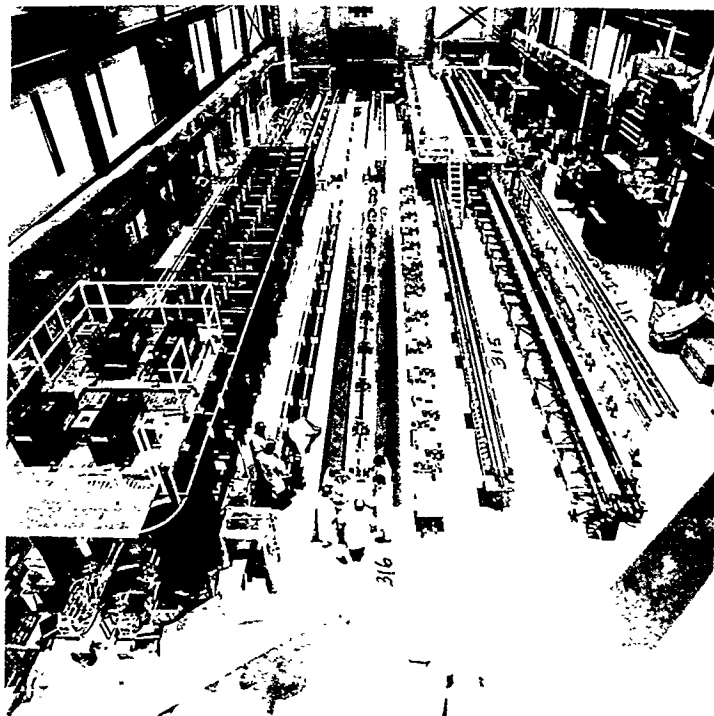


Figure 14 Cold mass assembly area of the 50 mm CDM in the Industrial Center Building at Fermilab.

Selected Superconducting Magnets for Detectors

Table IV presents six superconducting detector magnets. The information was taken from a review article by H. Desportes.⁹ Indirect cooling of the superconductor was first proposed in the design of the TPC detector. This eliminates the need for vessels to contain the helium cooling. It is replaced by pipes which provide conduction cooling to the superconductor. This gives a magnet which has a much smaller radiation length since a thick-walled helium pressure vessel is not required. This concept was applied to the CELLO magnet designed by Henri Desportes' group at SACLAY for operation at PETRA and DESY.

Table IV
Selected detectors with superconducting magnets

Project	TPC	CELLO	HRS	CDF	DELPHI	ALEPH
Location	PEP/ SLAC	DESY	PEP/ SLAC	FNAL	LEP/ CERN	LEP/ CERN
Manufacturer	LBL	SACLAY	ANL	Hitachi	RAL	SACLAY
Inner Bore (m)	2	1.5	4.45	2.86	5.2	4.96
Winding Length (m)	3.4	3.42	2.8	4.8	6.8	6.36
Stabilizer	Al	Al	Cu	Al	Al	Al
Field (T)	1.5	1.5	1.62	1.5	1.2	1.5
Stored Energy (MJ)	10.9	7	80	30	109	130
Radiation Length	.68 ♦	.5 ♦	X	.85 ♦	4 ♦♦	1.6 ♦♦○

- ♦ - Indirect Cooling - TPC
- ♦ - Internal Winding - TOPAZ / Tristan / KEK
- - Thermosyphon - ALEPH

The CDF magnet supplied by Hitachi for Fermilab incorporated this indirect cooling as well. The stability of this magnet is marginal as the magnet only operates in one polarity. It will quench at a current below the operating current if the polarity is reversed! The two detectors, the DELPHI and the ALEPH, at LEP utilize internal winding where the superconductor is wound on the inside of a cylinder which is used to support the hoop stress. This was first used in the TOPAZ magnet at Tristan at KEK. Henri Desportes' group added to the ALEPH magnet the thermosyphon. In this approach, a manifold of helium at the bottom of the detector supplies helium to vertical circumferential coils where the helium flow due to gravity supplies cooling to the superconductor.

The HRS detector at PEP and SLAC used the 12' bubble chamber magnet. After the bubble chamber was decommissioned, the magnet was modified at Argonne so that it would operate with a horizontal axis and was then transported cross country to SLAC. Figure #17 is a picture of a test of horizontal axis operation.

⁹H. Desportes, Proceedings 9th International Conference on Magnet Technology, Zurich, 1985, p. 149.

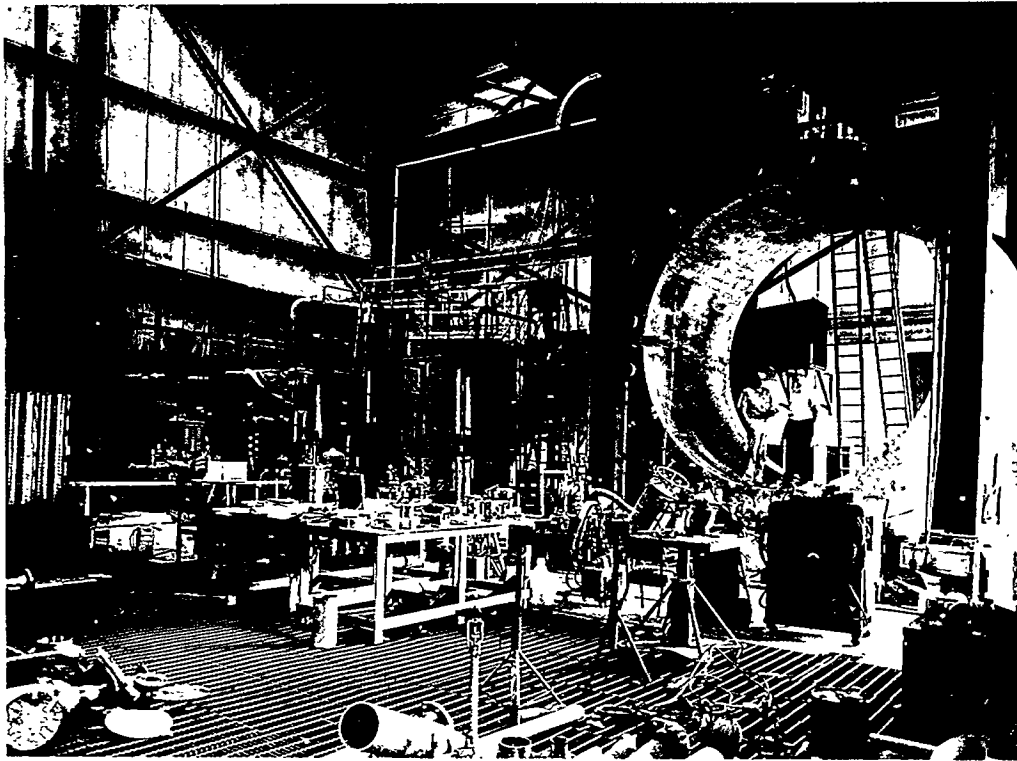


Figure 17 Malcolm Derrick and Klaus Yeager inside the rotated coils of the 12' Hydrogen Bubble Chamber during testing in 374.

Figure #18 pictures the HRS magnet ascending the Rocky Mountains on the way to California. One of the press clippings from this trip stated that there were a number of garage doors activated while this magnet was transported across Utah.



Figure 18 144 wheel truck transporting the 12' superconducting coils up the Rocky Mountains on the way to SLAC.

Superconductor Cost

Table V presents the cost vs. time for superconductor material. The price for the SSC conductor is the delivered price at the quantities used in the pre-production activities. According to Don Capone of the SSCL, for SSC production quantities it was expected that the price would drop by 50%. Note that the number of filaments for the 12' conductor was 6 and for the SSC inner cable was 7800.

Table V
Cost of conductor for
superconducting magnets vs. time

Application / Year	Conductor Dimen. / # of Filaments	Cu:SC Ratio	\$/KA-FT
12' HBC / 1967	2.0" X .100" / 6	20:1	\$ 1.00
15' HBC / 1970	1.5" X .150" / 60	17:1	\$ 1.12
Tevatron / 1980	.027" / 2000	1.8 : 1	\$ 0.95
1993			\$ 0.86
SSC / 1993	Inner .0318" D / 7800	1.3 : 1	\$ 0.69
	Outer .0255" D / 4200	1.8 : 1	\$ 0.63

From Table V, it can be seen that superconductor technology has gained on inflation during the past 25 years. Although the 12' conductor was the first co-extruded conductor, its price was quite competitive with later conductors.

Jimmy Wong of Supercon, who supplied the 12' Bubble Chamber conductor, credits the former Argonne business manager Herb Ross with playing a key role in the choice of the co-extruded superconductor for the 12' bubble chamber magnet. Herb Ross had previous experience in the fabrication of co-extruded nuclear reactor fuel. Jimmy Wong had previously worked at Wah Chang Corporation and the MIT Materials Lab.

Recently, Jimmy Wong has done some development work utilizing a "jelly roll" of Niobium sheet and Titanium sheet which is extruded and is estimated by Scanlan, et. al.¹⁰ to reduce the cost by 40%.

Fusion Magnet Development at the ZGS

- Baseball Magnet - 1965

A test magnet was wound at Argonne in 1965 by Charles Laverick and Clyde Taylor of LLNL. This baseball or "minimum B" magnet with the windings located as the seams are on a baseball is believed to be the first superconducting fusion magnet fabricated and tested¹¹.

¹⁰R. M. Scanlan, A. Lietzke, J. Royet, A. Wandesforde, C. E. Taylor, J. Wong, M. K. Rudziak, MT-13 Thirteenth International Conference on Magnet Technology, Victoria, British Columbia, Canada, 20-24 September, 1993.

¹¹C. E. Taylor, C. Laverick, Proceedings of the International Symposium on Magnet Technology (MT-1), Stanford, CA, 8-10 September 1965, p. 594.

- Pulse Superconducting Coils - 1979

S. H. Kim developed a program for Argonne in Fusion Energy for studying pulse superconducting coils. Ohmic heating coils are required for Tokomak operation with a 1 GJ energy storage with a charge rate of 9 T/s. Peak currents are on the order of 50 to 100 KAmps. S. H. Kim designed, built, and tested the first pulse superconducting magnets to model Tokomak ohmic heating coils. In 1979, Kim tested a 1.5 MJ pulse superconducting coil, with a peak field of 4.5 T, a current of 11 KA and 11 T/s charge rate. This magnet met its design goals and was awarded a 1979 IR100 Award. Figure #19 depicts S. H. Kim and the 1.5 MJ pulse superconducting coil.



Figure 19 S. H. Kim and the 1.5 MJ pulse superconducting coil.

In 1982, S. H. Kim and his group completed a 3.3 MJ pulse superconducting coil. This coil also had a current of 11 KA with a peak field of 6.5 T at a charge rate of 6 T/s and a loss rate of .24% of the stored energy per cycle. This testing, of course, required non-metallic cryostats. This magnet, too, was awarded an IR100 Award in 1982.

- Energy Transfer Coils and Circuits for Tokomak Operation - 1976

Figure #20 is a picture of two superconducting coils which were built by Rich Smith's group for Bob Kustom, et. al.¹² to study energy transfer for Tokomak Operations.

¹²Thyristor Networks for the Transfer of Energy Between Superconducting Coils, by Robert L. Kustom, (University of Wisconsin Press, Madison, WI, 1980).

- Safety and Stability - 1979

Larry Turner performed many studies on the safety and stability of superconducting magnets.¹³ He performed a "finite element" analysis of stability. He looked at the time varying heat balance on each element of a superconducting magnet using temperature dependent properties. He also studied the behavior of shorted turns in a superconducting magnet. In 1981 Larry Turner applied this analysis to the shorted turn in the G.E./G.D. large coil supplied to the Oak Ridge National Laboratory as part of the Large Coil Experiment. This \$100 M U.S. expenditure provided three coils which were "D" shaped, giving a field of 8 T. The three U.S. coils were provided by Oak Ridge National Laboratory, Westinghouse, and G.E./G.D. Three foreign coils were supplied by JAERI (Japan), Euratom (Europe), and TSI/ABB (Switzerland).

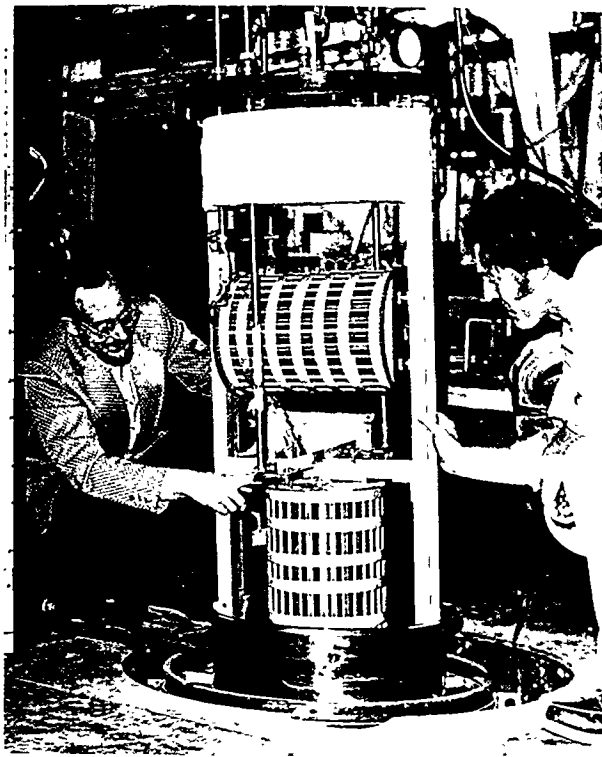


Figure 20 Rich Smith and Jim Hrusosky testing Kustom energy transfer test magnets.

MRI

The foremost practical application of superconducting magnets is in Magnet Resonance Imaging (MRI). The magnets used in this extremely useful and non-invasive medical technique are unquestionably a spin-off of development work done in high energy physics. One MRI magnet costs about \$1 M. According to Jimmy Wong, the materials business for MRI is approximately \$10 to 20 M per year. He also states that, of the \$1 M unit cost, only approximately \$20 K of this is for superconducting material. This gives a total magnet market value on an annual basis of anywhere from \$500 M to \$1 B for MRI units. According to Jimmy, this market is flat because of the health care costs scrutiny. Oxford (Siemens) and General Electric supply approximately 75% of this market. IGC, Toshiba, Mitsubishi, and others supply the rest of the market.

While John Purcell was at General Atomic (G.A.), they produced approximately 100 MRI units before selling this capability to Toshiba. Bert Wang formed his own company in 1984, Wang NMR, Inc. and has sold several MRI units.

The magnets for MRI require a very uniform field, 5 ppm over a 30 cm sphere. The field must have essentially no drift, < 1 ppm per hour. They also require low heat leak, approximately one tenth of a watt.

¹³L. Turner, Advances in Cryogenic Engineering, Vol. 31, p. 407, edited by R. Fast, (Plenum Press, New York, 1986).

Ore Separation

A patent for ore separation was awarded in the late 1960's to Pete Marston. Marston consulted on the 12' bubble chamber magnet. Marston's firm, Magnetic Engineering Associates (MEA), marketed several iron core conventional magnets for ore separation in the early 1970's. During this period, Magnetic Corporation of America (MCA), John Stekly president, also contributed to the development of ore separation technology.

At the ZGS, Rich Smith contracted industrial firms in regard to ore separation and designed a model SC ore separation magnet. Following his interaction, Eriez Magnetics in 1986 sold a superconducting magnet system to Huber Corporation for kaolin clay processing. The cryogenics for this magnet were designed by Cryogenic Consultants, Inc., Peter VanderArend, also a consultant for the 12' HBC. The magnets were built by John Purcell of General Atomic. Three systems were ultimately delivered. A significant fact is that Rich Smith served during this period on the Technical Advisory Board to Eriez Magnetics.

Recently, in 1992, Advanced Cryo Magnetics (ACMI), a firm in which John Purcell is an owner, has converted two separation magnets to superconductivity which were previously conventional iron yoke copper coil magnets. The number of ampere turns can be approximately doubled and the field can be raised from 2 T to 2.5 T. Figure #21 is a picture of these conversion coils manufactured by Advanced Cryo Magnetics.

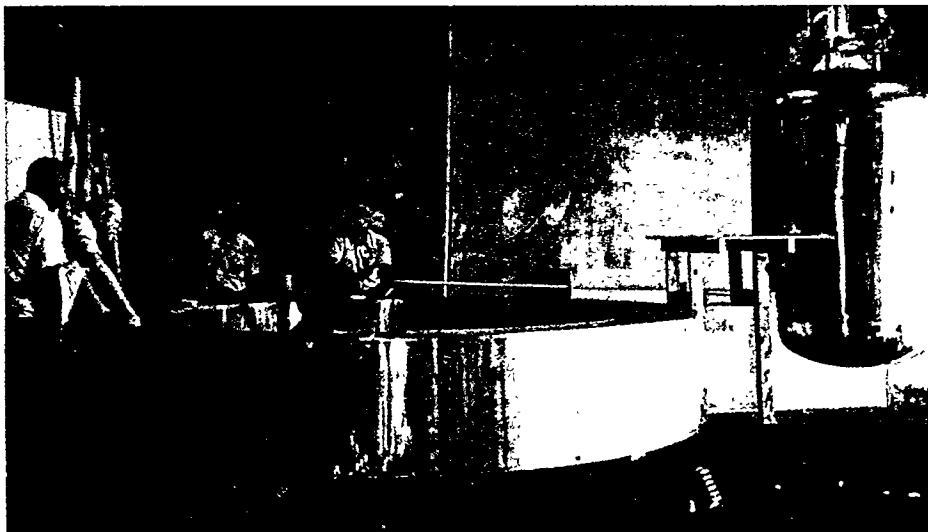


Figure 21 John Purcell, 2nd from the left, inspecting a superconducting coil manufactured by Advance Cryo Magnetics for ore separation.

There are approximately 30 ore separation magnets built and owned by 10 companies. Purified kaolin clay is worth approximately \$100 per ton, with total sales per year of approximately \$1 B.

In summary, Rich Smith and John Purcell have had a real impact on this industry.

Superconducting Magnet Energy Storage (SMES)

John Purcell, working for General Atomics, designed and constructed a 30 MJ superconducting magnet in 1981 to be used for power line stabilization.¹⁴ He did this in cooperation with John Rogers of the Bonneville Power Authority. John Purcell is also a consultant to Bechtel, one of the two firms which have developed studies for 20 MWatt hour, 400 MWatt engineering test model. Funding for this test model is highly uncertain.

A small company, Superconductivity, Inc. of Madison, WI, has marketed eight units of micro SMES's or Superconducting Storage Devices (SSD). There appears to be a small market for these devices. They have sold the majority of these items to the U.S. Air Force for momentary power line interruptions. The purpose of the SSD is to eliminate voltage drops and other momentary disturbances which might trip off industrial facilities in the paper, textile, metal or plastic industry. This is particularly true where the customer relies on sensitive electronically controlled digital equipment. The SSD units have a .3 KW hour energy rating with a power rating of 1 MWatt. Richard Lundy is the Chief Technical Officer of Superconductivity, Inc. Several other ZGS people have participated in the work of this firm. Ralph Niemann has designed 1.5 KAm high T_c leads, and R. Trendler and A. Visser served as consultants to this firm.

Babcock and Wilcox is supplying a .5 MW hour SSD with a power rating of 30 MWatts to the Anchorage Light and Power Company. R. Niemann, who has now returned to Argonne, is committed to supplying 16 KAm high T_c prototype leads for this unit in 1995.

Summary of Notable Accomplishments

Table VI provides a summary of accomplishments in applied superconductivity by Charles Laverick, John Purcell, Henri Desportes, and S. T. Wang. Table VII is a continuation of the accomplishments of other ZGS high achievers. Peter VanderArend and Pete Marston are two consultants who worked with the ZGS projects, particularly the 12 foot bubble chamber.

¹⁴J. R. Purcell, S. C. Burnett, R. I. Schermer, "Design and Fabrication of the Bonneville Power Admin. 30-MJ Storage Coil for Long-Distance Transmission Line Stabilization," Proc. Mech. Magnetic and Underground Energy Storage 1981 Annual Contractors' Rev., Conf-810833.

Table VI: Outstanding achievements of Charles Laverick, John Purcell, Henri Desportes, and Bert Wang to superconducting magnet technology.

Charles Laverick (at ANL '58 - '74)	H. Desportes (at ANL '69 - '71 & summer '72)	S. T. Wang (at ANL '72 - '79)
ANL: - 11" AVCO Magnet - 11" Cable Magnet - 7" Cable 6.7 T - Fusion "baseball" - Helium Supply Sr. "Wise" Man	SACLAY: - PPT '65 - Hera PPT '67 ANL: - PPT SCM-1 - FNAL 15' HBC magnet - PPT SCM-2	ANL: - PPT SCM-2 - SSR ring magnets - Proton spin magnet - U-25 MHD - 1.5 MJ Pulsed - UTSI MHD LLNL: - Yin Yang
John Purcell (at ANL '66 - '75)	SACLAY: - 13T, 5cm bore solenoid - 6 T dipole - 8T -> 12T lab solenoids - Misc. magnets: . Gyrotron . U Separation . Ion source . RMN spectrom. - PPT Magnets . Saturne exp. set of 4 solenoids . E-704 @ FNAL . U of Bonn . SMC @ CERN - Large Det. Mag. . EHS - CERN Rapid cycling BC . CELLO solenoid DESY . ALEPH solenoid CERN - LHC Detector . CMS & ATLAS	Wang NMR ('85-'94): 18 magnets: - MRI magnets - NMR magnets - Spin magnets - PPT - CEBAF magnets - Etc.
ANL: - 12' HBC - FNAL 15' HBC Magnet - SSR ring magnets - U-25 MHD magnet		
GA: 30 MJ - SMES - Many designs fusion - SMES design Bechtel - Absolute Ampere NBS - Magnets for gyrotron tubes - ~100 MRI magnets		
ACMI: - Homo polar brush - Testing magnet, NRL - Separation magnets - Kaolin clay		

**Table VII: Additional outstanding achievements
by other ZGS related personnel.**

R. Smith	L. Turner	S. Kim
- U-25	- 12'	- U-25
- POPAE	- U-25	- UTSI
- UTSI	- UTSI	- Pulsed Magnet
- 3' + 10' Quad	- FELIX	- SC Quad
- Pulsed Magnet	- Pulsed Magnet	
- ATLAS Magnet	- Stability	
- Ore Separation		
- CDF		
- DØ Detector		
A. Herve	R. Niemann	
- 12'	- U-25	
- 12' 4 T design	- UTSI	
- BEBC	- SSC dipoles	
- RCBC	- HTc Powerleads	
- CMS		
P. VanderArend*	P. Marston*	
- 12'	- 12'	
- Tevatron	- Ore separation	
- Ore separation	- Fusion	
	- MHD	
	- GEM	
* Served as consultants to ZGS for the 12' Hydrogen Bubble Chamber Project. from 1966 to 1969:		

In discussion recently, Pete Marston decried the present inability of the US government to follow through on new projects. He noted that none of the large scale programs that he has been connected with in the last 15 years has been completed, and that this lack of support continuity has been a major factor in the loss of the technological leadership that was so clearly established in the exciting days of the ZGS.

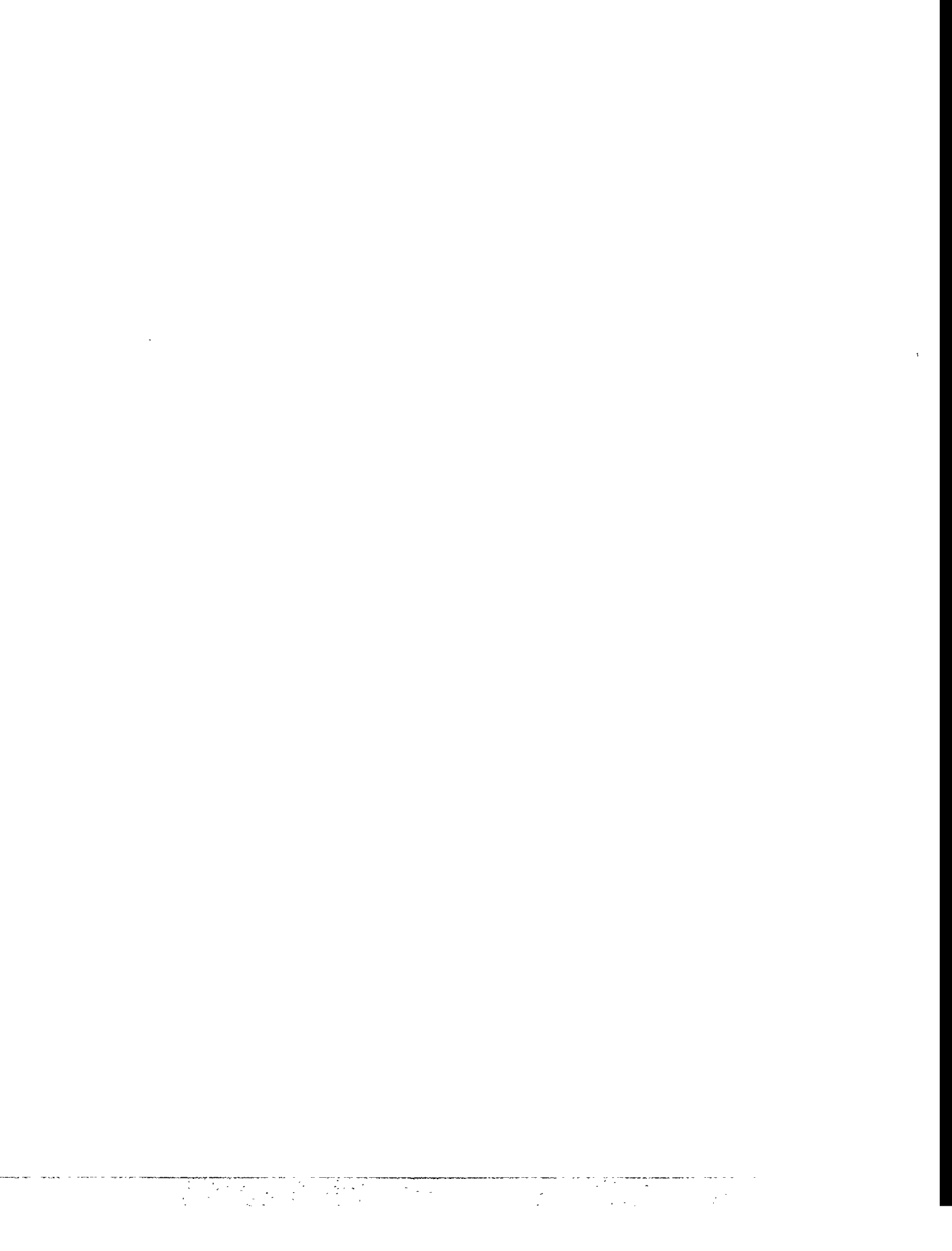
In Conclusion...

In conclusion, let me list significant factors supporting the theme that the ZGS community made basic contributions to the applications of superconducting magnets to high energy physics as well as to other technological areas.

1. ZGS played a key role initially - the AVCO magnet procurement provided a productive, stimulating early focus for superconductivity development at Argonne.

2. The 10" helium bubble chamber magnet was one of the first uses of a superconducting magnet in a high energy physics experiment. This magnet is now in the Smithsonian Institution.
3. The 12' hydrogen bubble chamber magnet was a giant step which demonstrated the technical and economic practicality of large superconducting systems. It took superconductivity from an art to a well engineered technology. At the 75th anniversary of the discovery of superconductivity celebrated at the Applied Superconducting Conference in 1986, John Purcell was invited to tell the 12' magnet story. He was one of nine people so honored at that symposium.
4. The SSR and the POPAE were cutting edge proposals whose approval would have changed the course of U.S. HEP.
5. The ZGS group built and operated numerous devices, e.g., PPT's, the first beam line, the 15' HBC magnet, etc., which demonstrated continued application of superconducting magnets to high energy physics.
6. ZGS people made valuable contributions to fusion, MHD, ore separation, SMES and, indirectly, to MRI. Important factors in these contributions were:
 - Insightful visions of the ZGS leadership group.
 - Prompt reduction to hardware with the emphasis on hardware rather than paper studies.
 - Innovative design
 - Attention to detail
 - Dedicated workers at the ZGS with their outstanding breadth of skills and enthusiastic hard work.





POLARIZED PROTON BEAMS SINCE THE ZGS*

A. D. Krisch
Randall Laboratory of Physics
University of Michigan

I will discuss research involving polarized proton beams since the ZGS's demise. Let me remind you that in 1973 the ZGS accelerated the world's first high energy polarized proton beam; all of us here can be proud of this accomplishment. A few ZGS polarized beam experiments were done in the early 1970's; then from about 1976 until 1 October 1979, the majority of the ZGS running time was polarized running. A great deal of fundamental physics was done with the polarized beam when the ZGS ran as a dedicated polarized proton beam from about Fall 1977 until it shut down on 1 October 1979. The newly created polarization enthusiasts then dispersed; some spread polarized seeds all over the world by polarizing beams elsewhere; some wound up running the High Energy and SSC programs at DoE.

The spin-spin parameter A_{nn} for 90°_{cm} proton-proton elastic scattering is plotted against energy in Figure 1. This graph contains much ZGS data;¹ however, it was not produced until long after the ZGS had stopped.² Notice that at the lowest energy of about 10 MeV, A_{nn} is -1; this means that the protons never scatter when their spins are parallel. Then A_{nn} rises rapidly to +1, which means that the protons never scatter when their spins are anti-parallel. Next note that A_{nn} appears to be oscillating in the so-called dibaryon region near 1 GeV/c. Then as we moved into the ZGS energy region near 3 GeV/c, the A_{nn} parameter decreased sharply. Finally, A_{nn} surprisingly shot up again at the ZGS's highest energies. The last point is actually at 13 GeV/c, which was above the ZGS design energy. We were somewhat concerned that measuring this point might burn up the ZGS; but the ZGS had to soon be decommissioned in any case, so we ran at 13 GeV/c. This sharp rise in A_{nn} at 90°_{cm} convinced most high energy spin physicists that the earlier belief that spin effects would disappear at high energy was just wrong. Many people then started looking for ways to study spin effects at higher energies.

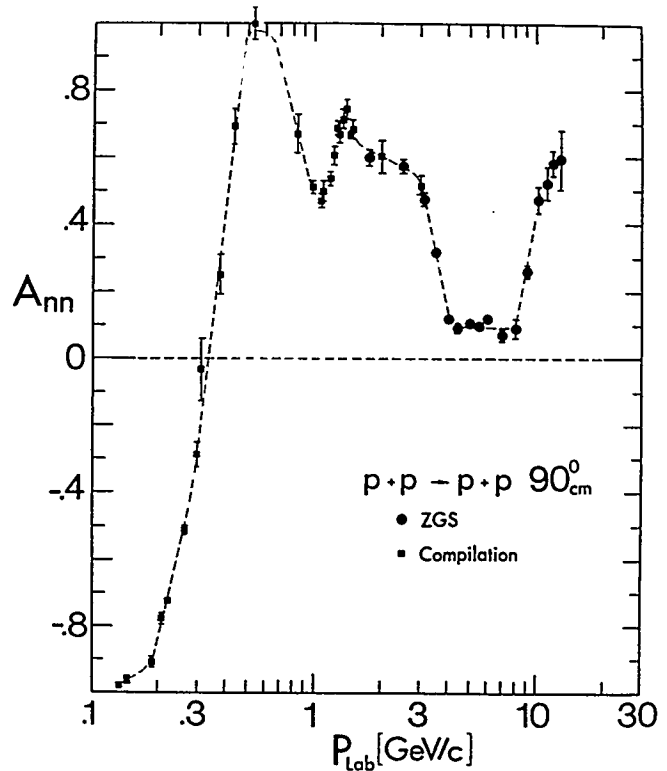


Figure 1. The Spin-Spin Correlation Parameter Plotted Against Momentum.

Around that time, an experiment was done at Fermilab which didn't involve either a polarized beam or a polarized target, but it certainly involved spin in the final state. The experimenters, which included: Gerry Bunce, Tom Devlin, Ken Heller, Oliver Overseth, and Lee Pondrom, found a large polarization in inclusively produced Λ hyperons in 400 GeV proton collisions. Their extensive and precise data³ is shown by the dashed line in Figure 2, where it is compared with 12 GeV data from KEK and 2000 GeV data from the CERN-ISR. Clearly Fermilab, KEK, and the ISR found the same large Λ polarization above $P_{\perp} = 1$ GeV/c. Therefore, the Λ polarization seemed to be a spin effect that is fairly large and independent of energy.

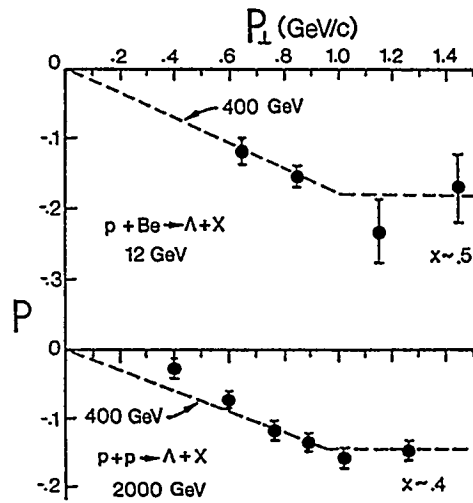


Figure 2. Polarization of Inclusive Hyperons plotted against Transverse Momentum.

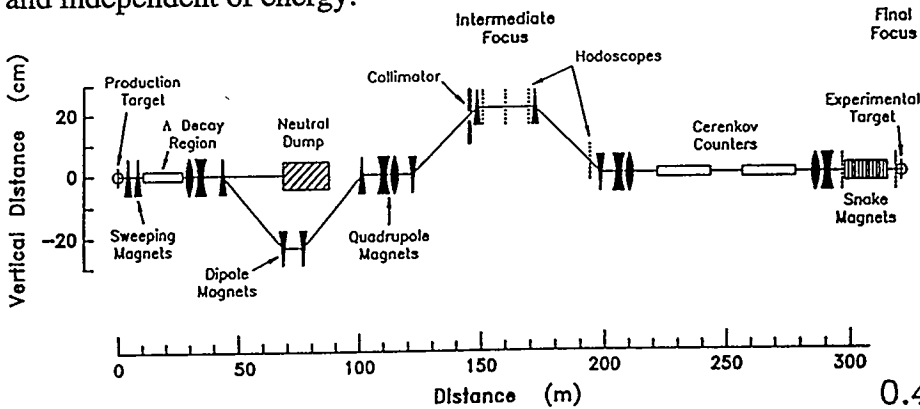


Figure 3. Hyperon Decay Polarized Beam at Fermilab.

One enthusiastic ZGS polarized beam user, Aki Yokosawa, and his colleagues built a hyperon decay polarized beam at Fermilab. They used the fact that the hyperons decay into spin-polarized protons; their beam line is shown in Figure 3. They used this beam for some experiments with both polarized and unpolarized targets. Perhaps their most interesting result⁴ is the recent inclusive π^+ , π^- , and π^0 production, which is shown in Figure 4. Notice that at large Feynman- x , the left-right asymmetry A_n approaches 40%. These data clearly indicate that spin effects are still large and interesting at their beam energy of 200 GeV.

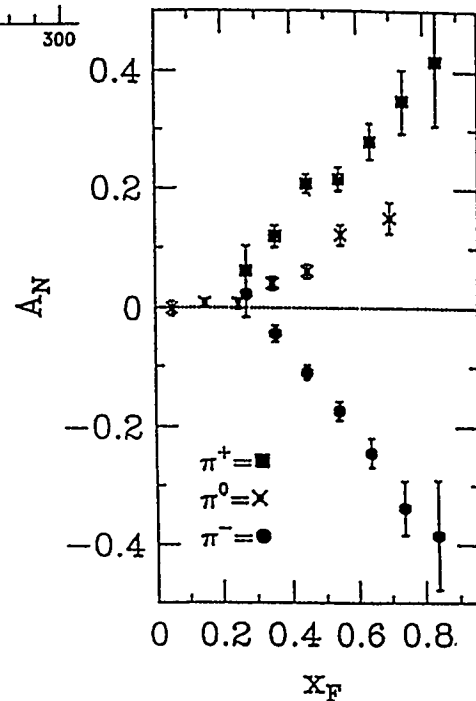


Figure 4. Asymmetry in Inclusive Pion Production.

Some of us attempted to accelerate polarized protons in Brookhaven's strong focusing AGS. There was an earlier ERDA Committee Report, reviewing the future of the ZGS, which stated that it would be "impossible" to accelerate polarized protons in a strong focusing accelerator. When it began to look less impossible at the AGS, Bill Wallenmeyer started worrying about how to rephrase that; I think he finally came up with "impossible or very difficult." Eventually, Jim Kane wrote a final letter to Hank Bohm about shutting down the ZGS, with an official copy to me; the letter said⁵ ". . . the possibility, only recently determined, of establishing a polarized proton capability at BNL and/or Fermilab makes the ZGS shutdown less terminal for high energy polarized proton studies . . .". Ronnie Rau, who was then running the AGS, heard about this letter and eagerly asked for a copy. Being a good administrator, he probably converted the letter into a few million dollars.

Accelerating polarized protons in the AGS was certainly a tough job; we had many strong depolarizing resonances to overcome. As shown in Figure 5, we had to install a great deal of expensive state-of-the-art hardware in the AGS.⁶ We had to build a dozen very challenging pulsed quadrupoles, each with a 1.6 microsecond rise time. We also had to program 96 existing correction dipoles in a very sophisticated way; eight of them were in each of the 12 AGS superperiods. We also built the world's first "on-line" RFQ and installed a new polarized ion source which came from the ZGS along with some dedicated people like Larry Ratner.

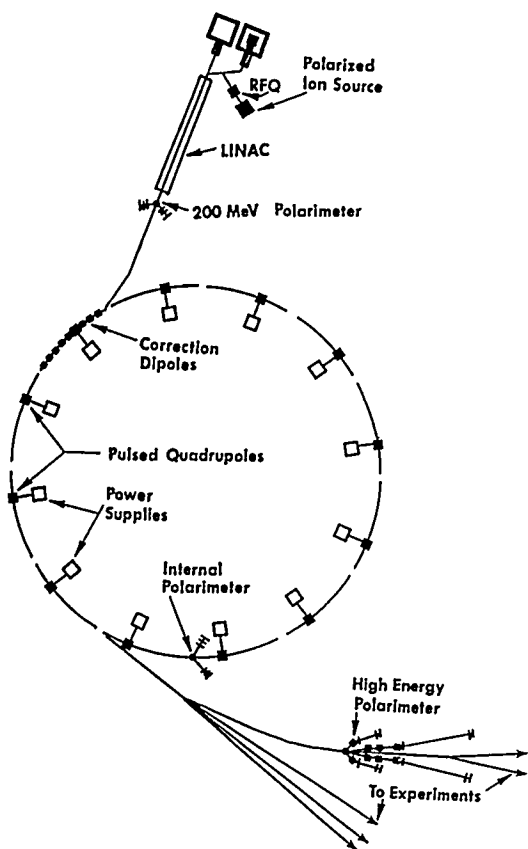


Figure 5. The AGS Polarized Proton Beam.

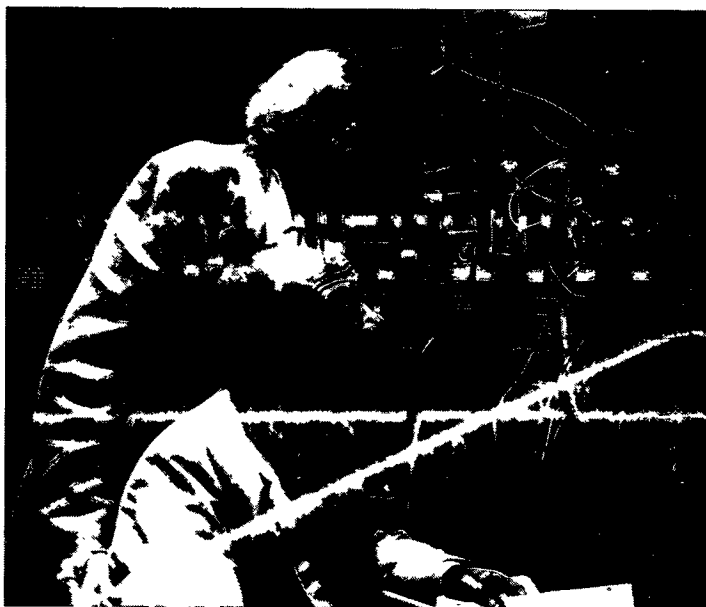


Figure 6. Two Dedicated AGS Polarized Beam Tuners.

Figure 6 shows two hardworking polarized beam tuners around 1984; I think that the one with a lot of hair is Larry Ratner. This nice picture, by the Brookhaven photographer Mort Rosensen, also shows the complex AGS control room scope trace of the polarized beam

accelerating up to 16 GeV. The three sharp dips show the 1.6 microsecond rise-time pulsed quadrupoles overcoming three intrinsic depolarizing resonances. The periodic pulses in the upper trace show the amplitude of the horizontal-field-wave created by the 96 correction dipoles for the sixth harmonic, the seventh harmonic, the eighth harmonic, etc.; these complex harmonic corrections were individually tuned to overcome each of the $G\gamma = n$ imperfection resonances that occur every 523 MeV. We eventually accelerated the AGS polarized beam to 22 GeV by individually overcoming 45 depolarizing resonances; this very intense accelerator research required seven weeks of exclusive use of the AGS. About once a week the Laboratory Director, Nick Samios, would visit me in the control room to politely remind me that "These studies were costing \$1 million a week;" and to ask "how much longer they would continue?"

We eventually did accelerate a polarized proton beam to 22 GeV. However, it was already clear that this technique of individually correcting each depolarizing resonance could not be used at a much higher energy. Starting around 1984, we became interested in trying to polarize the beams at the SSC; we quickly discovered that there would be about 36,000 depolarizing resonances at the SSC. We sadly recalled that it had taken Larry Ratner and me 49 days to overcome 45 depolarizing resonances--roughly one a day. Even if we reduced our time to one resonance per 8-hour shift, it would still take 12,000 days, which is about 35 years. The SSC Director seemed unlikely to approve 35 years of dedicated polarized beam tuning time.

Therefore, we decided to have a Workshop in Ann Arbor⁷ in 1985; it was organized by my late colleague Kent Terwilliger, Ernest Courant, Owen Chamberlain, and myself. The Workshop concluded that Siberian snakes would allow the acceleration of polarized proton beams at the SSC. Siberian snakes were a fairly new idea developed by some Siberians from Novosibirsk--Yaroslav Derbenev and Anatoli Kondratenko.⁸ Derbenev visited Argonne in 1978 to attend the 3rd International Symposium on High Energy Spin Physics;⁹ I still recall his great interest in the ZGS polarized proton beam. A Siberian snake should overcome all depolarization problems by rotating the spin by 180° in each turn around an accelerator ring. To understand a Siberian snake, assume that the spin starts out with its direction vertically up at 0° ; then assume that all the depolarizing magnetic fields in one turn around the ring rotate it by 5° . Next the beam passes through a Siberian snake which rotates it by 180° to 185° . When the proton circles the ring a second time, all of the fields again rotate the spin by 5° ; but the 5° rotation now moves it to 180° . Finally the beam again passes through the snake, which rotates the spin again by 180° to right back where it started at 0° . The Siberian snake is a really clever idea; it basically makes all of the depolarizing fields cancel themselves.

By 1985 the Siberian snake idea had been around for about ten years, but nobody had tested it. Just at that time, the IUCF people were building a Cooler Ring in Indiana. There was already a polarized beam in the IUCF Cyclotron, which was to be the injector for the Cooler Ring. The IUCF people were very experienced with cyclotrons, but synchrotrons were fairly new to most of them. Larry Ratner, Kent Terwilliger, Ernest Courant, and I knew something about synchrotrons, so we proposed a bargain. They approved us to use the Cooler Ring for these Siberian snake studies, and we provided some injection kicker magnets, some other hardware, and some advise about synchrotrons. It turned out to be a very good bargain for everyone.

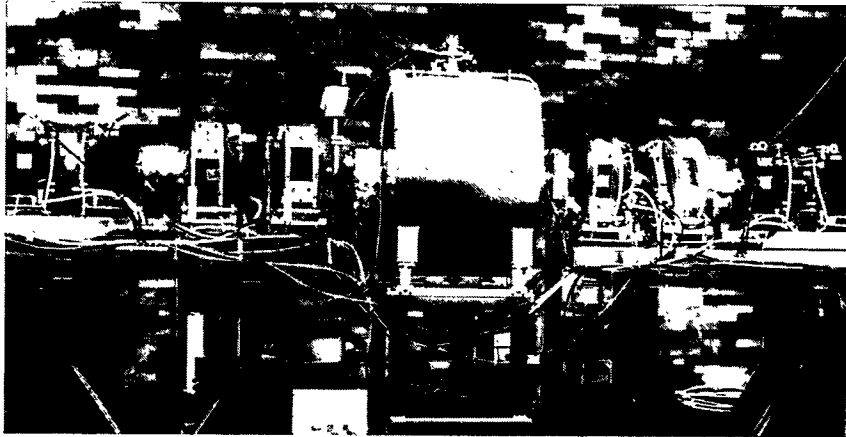


Figure 7. The Siberian Snake at the IUCF Cooler Ring.

Figure 7 shows the Siberian snake installed in the Cooler Ring. This particular snake is a superconducting solenoid magnet with an $\int B \cdot dl$ of about two Tesla-meters which rotates the spin by 180° . The eight small quadrupoles correct the orbit distortions, but they do nothing to the spin. Figure 8 shows the beam polarization at 104 MeV plotted against the imperfection magnetic field integral; this energy is near the $G\gamma = 2$ imperfection resonance which always occurs at 108 MeV. Notice that, when the Siberian snake is off, there is full polarization only if all of the imperfection fields in the ring are exactly corrected. Just a tiny imperfection field causes the polarization to drop rapidly. This curve looks similar to one of the many resonance correction curves that we did at AGS and earlier at the ZGS. Instead, when you turn the Siberian snake on, there is full polarization over the entire measured range of $\int B \cdot dl$; the snake totally overcomes the depolarization.¹⁰ This Siberian snake worked much better than I expected.

The Siberian snake seems a rather marvelous device; once a transverse Siberian snake is set at a fixed DC current, it should work for all depolarizing resonances from 108 MeV up to 20 TeV. In April 1994, Larry Ratner and his colleagues installed a Siberian snake in the AGS and accelerated a polarized beam up to 11 GeV with only a medium loss in polarization.¹¹ It was a partial snake rather than a complete snake; therefore, it only overcame some of the depolarization problems. Nevertheless, it was a great success because it totally overcame all the "imperfection" depolarizing resonances as predicted.

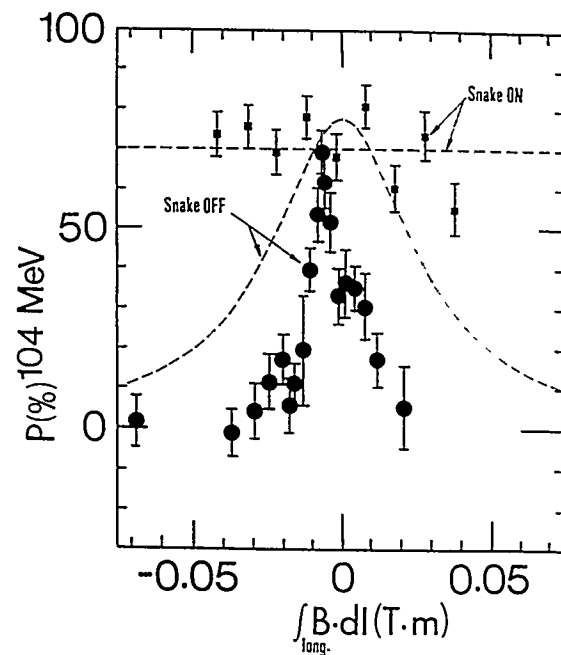


Figure 8. Siberian Snake Overcoming an Imperfection Depolarizing Resonance at the IUCF Cooler Ring.

Now, I will discuss some unpolarized beam - polarized target data obtained while preparing for the first polarized beam experiments at the AGS. This "low-priority test-experiment" studied one-spin effects in proton-proton elastic scattering by scattering the AGS unpolarized proton beam from our polarized proton target. Recall that the ZGS two-spin results were in complete disagreement with the QCD theory of strong interactions; the theorists just didn't know how to deal with this data. However, by the early 1980's they said that, while QCD could not explain the two-spin ZGS data, there was still a firm perturbative QCD prediction that the one-spin asymmetry A must be equal to zero; furthermore, this prediction should improve at higher energies and at higher P_1^2 . We studied A in p-p elastic scattering using the AGS unpolarized proton beam with the Michigan polarized proton target; first we reproduced the CERN/Oxford data at small to medium P_1^2 . Then we started the difficult measurements¹² at larger P_1^2 ; as shown by the squares in Figure 9, the A values started increasing! This caused some problems and embarrassment, but was great fun.

Perhaps hoping to save the PQCD prediction, some people then said that these large P_1^2 points were probably wrong. So in the late 1980's we built a new polarized proton target that operated very well in a beam of 10^{11} protons per second; for some reasons, this target had a 96% proton polarization.¹³ In 1990, we measured A at 24 GeV using this target and beam; the resulting precise data,¹⁴ which are shown as large circles in Figure 9, confirmed that A is quite large at $P_1^2 = 7 (GeV/c)^2$.

Many theorists then said that the AGS energy was not high enough to really test PQCD. Therefore, we decided to search for a place to extend these experiments to higher energy. After several complex and unsuccessful interactions with Leon Lederman, we got involved in a very interesting project in Russia. IHEP-Protvino, which previously was named Serpukhov, was then starting to build the new 400 GeV to 3 TeV UNK accelerator. We formed a Russian-American collaboration to measure A in proton-proton elastic scattering at 400 GeV and then later at 3 TeV. In 1986 we were moving into the era of Glasnost and Perestroika; Bill Wallenmeyer strongly encouraged us to do this experiment partly to help further improve US-USSR relations. Our collaboration of 25 Americans and 25 Russians is shown in Figure 10; we have tried to keep it equally balanced. Our NEPTUN-A experiment plans to repeat the AGS elastic scattering spin experiments at about 400 GeV, and then later at 3 TeV when the superconducting UNK-2 ring starts operation.

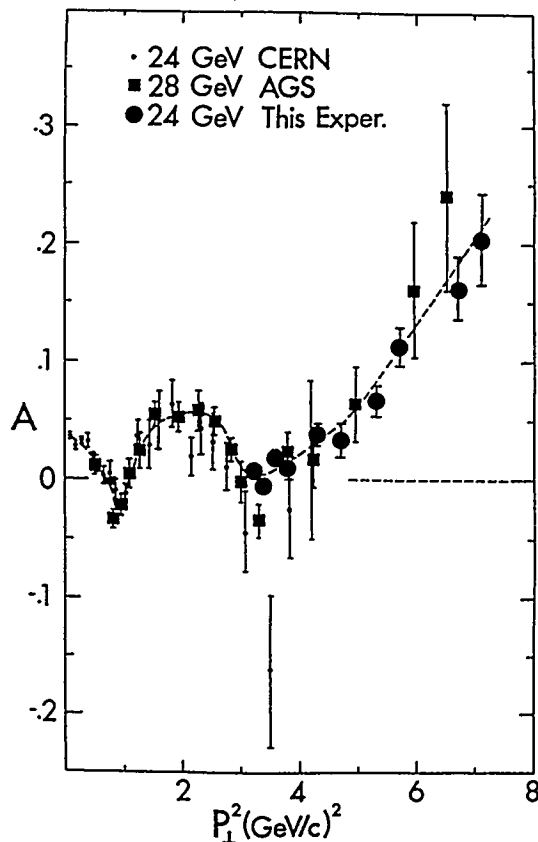


Figure 9. The Analyzing Power or Left-Right Asymmetry is Plotted Against P_1^2 for Proton-Proton Elastic Scattering at 24 and 28 GeV.

G.A. Alexeyev, O.V. Buyanov, V.V. Churakov, O.A. Grachov, V.N. Grishin, G.G. Gurov, V.A. Kachanov, Yu.V. Kharlov, V.Yu. Khodyrev, Yu.M. Melnik, A.P. Meschanin, N.G. Minaev, V.V. Mochalov, S.B. Nurushev, D.I. Patalakha, A.F. Prudkoglyad, V.V. Rykalin, P.A. Semenov, V.L. Solovianov, M.N. Ukhanov, A.N. Vasiliev, A.E. Yakutin; IHEP (Protvino).

V.V. Fimushkin, Yu.K. Pilipenko, V.V. Shutov; JINR (Dubna).

L.V. Alexeeva, J.A. Bywater, D.D. Caussyn, C.M. Chu, D.G. Crabb*, D.A. Crandell, Ya.S. Derbenev[†], S.E. Gladysheva, S-Q. Hu, W.A. Kaufman, A.D. Krisch, A.M.T. Lin, V.G. Luppov, T.S. Nurushev, D.C. Peaslee, R.A. Phelps, J.S. Price, L.G. Ratner, R.S. Raymond, J.A. Stewart[‡], S.M. Varzar, V.K. Wong; MICHIGAN (Ann Arbor).

G.R. Court[‡], D. Kleppner; MIT (Cambridge).

* University of Virginia
 † University of Liverpool
 ‡ Also at CERN

Figure 10. NEPTUN-A Collaboration List.

The UNK Facility is shown in Figure 11. Notice the town of Protvino and the existing 70 GeV accelerator U-70; the much older city of Serpukhov is about 10 km away. The 70 GeV accelerator, which has been operating since 1968, will be the injector into the 400 GeV UNK-1 ring which will later share the main 21-km tunnel with the 3 TeV UNK-2 ring. Our experiment is in the large SS-3 underground cave which is about 11 km from the town.

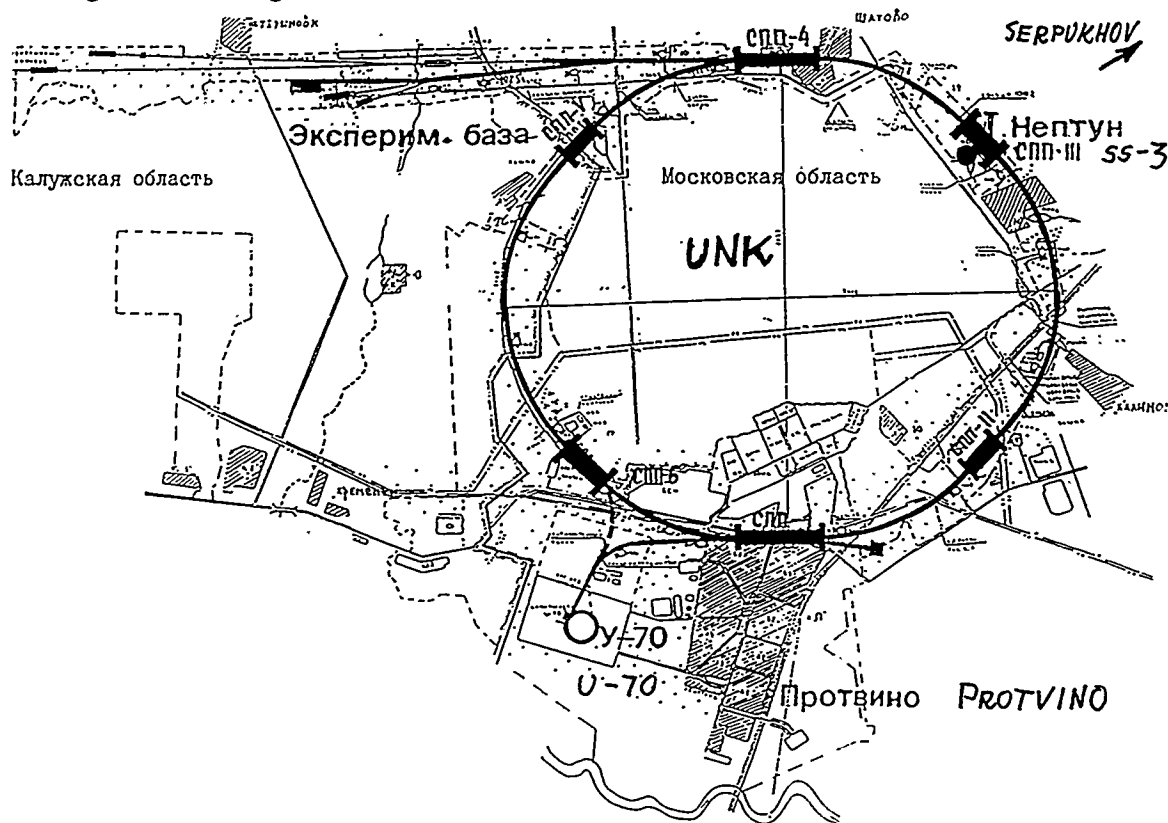


Figure 11. UNK with the Town of Protvino and U-70.

Life in Russia has been complicated recently, but apparently the Russian government has decided to continue its strong support of UNK by getting UNK-1 and several spin experiments in SS-3 operating as soon as possible. Figure 12 shows the 2.7-km-long transfer line from the U-70 accelerator into the UNK tunnel; this transfer line contains standard UNK 6-m-long dipole magnets, quadrupoles, and vacuum pipes. In March 1994, they extracted a beam from the 70 GeV accelerator and efficiently transported it through this 2.7 km line to the UNK tunnel. In the present Russian financial situation, it will still take a few years before UNK-1 is operating. The magnets and construction are paid for using some creative financing.

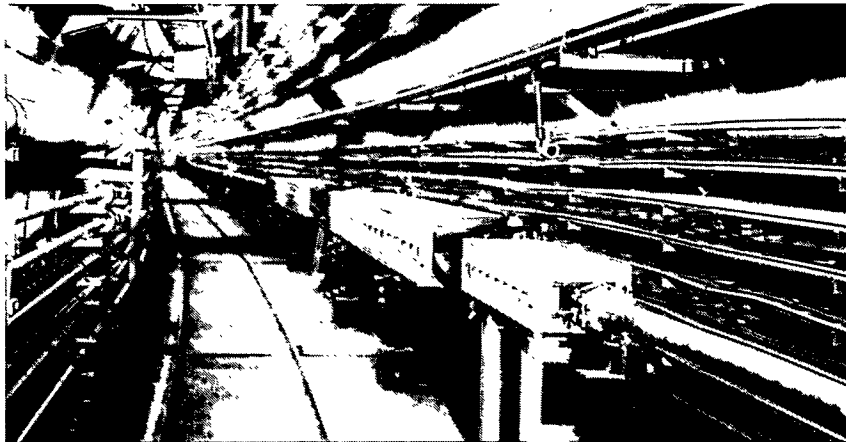


Figure 12. The U-70 to UNK-1 Beam Transfer Line.

Figure 13 shows our large underground hall; the beam enters from the right. The SS-3 main hall is 200 ft. long, 50 ft. wide, and about 40 ft. high; it will contain the Michigan ultra-cold spin-polarized atomic hydrogen jet target and several NEPTUN spectrometers. The long NEPTUN-A tunnel contains our 200-ft.-long spectrometer. The underground electronics hall is also shown. The excavation of this SS-3 cave is finished; IHEP now has about 1500 of the 2200 UNK-1 dipole magnets, and all the quadrupoles.

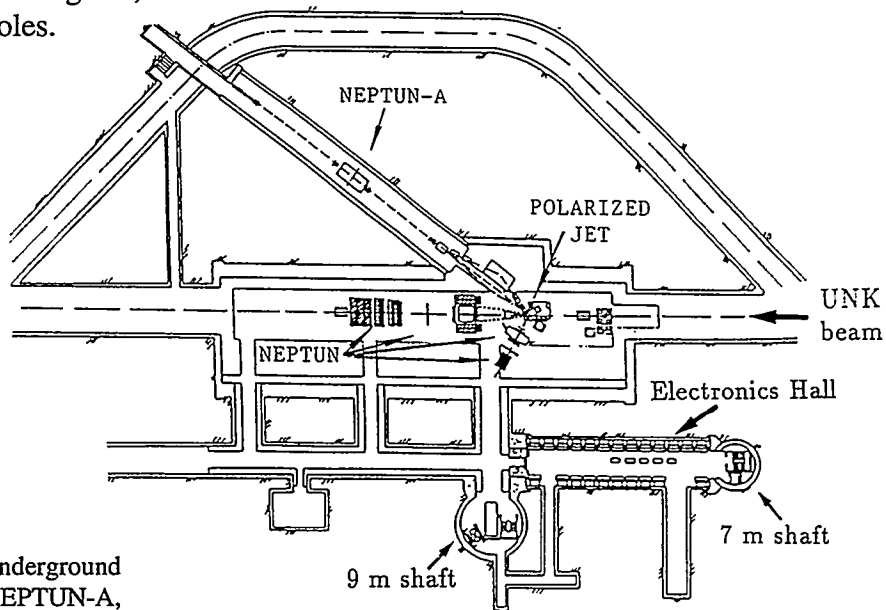


Figure 13. The SS-3 Underground Hall with NEPTUN, NEPTUN-A, and the Polarized Jet.

Recently another group, including many ZGS people and their descendants, started planning a polarized beam program at RHIC. The group includes: Larry Ratner, Aki Yokosawa, Yusef Makdisi, Gerry Bunce, and Thomas Roser. I mentioned earlier that Brookhaven has installed a partial Siberian snake in the AGS and had a successful run;¹¹ they may also accelerate polarized protons in RHIC. The planned layout is shown in Figure 14. Polarized protons in RHIC would allow two-spin experiments on proton-proton collisions at $\sqrt{s} = 400$ GeV. I hope it is funded.

The SPIN@Fermilab collaboration, which is listed in Figure 15, is producing a plan to accelerate polarized protons at Fermilab. This SPIN collaboration was first created to accelerate polarized protons at the SSC, which actually changed its 20 TeV lattice design to leave spaces for possible Siberian snakes. Unfortunately, polarized beam experiments at the SSC now seem unlikely. Fortunately, in 1991 Fermilab commissioned the SPIN collaboration of about 50 accelerator people and 50 experimenters to produce a detailed 144-page report on how to accelerate polarized protons in the Main Injector. This report¹⁵ was submitted in March 1992; the first page is shown in Figure 16.

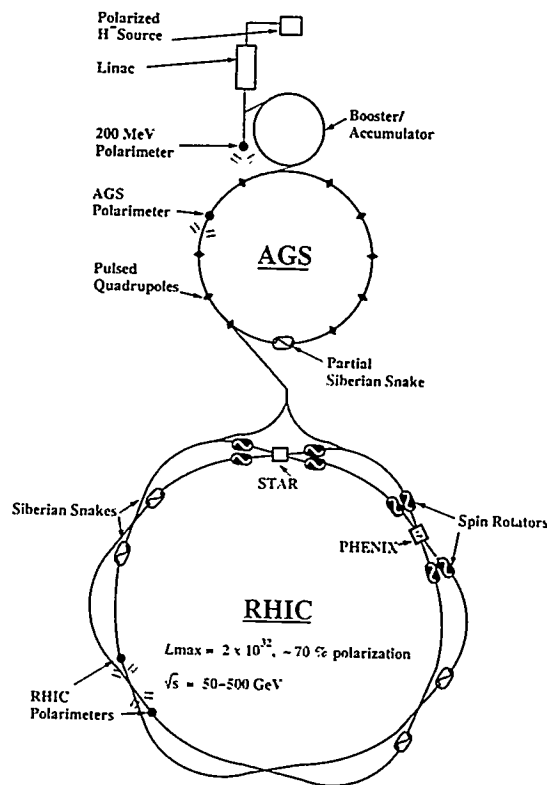


Figure 14. Polarized Protons at Brookhaven.

19 July 1994
 L. V. Alexeyeva*, V. A. Anferov*, B. B. Blinov*, J. A. Bywater, D. D. Caussin, C. M. Chu, E. D. Courant, D. G. Crabb*, D. A. Crandell, Ya. S. Derbenev*, S. V. Gladysheva, W. A. Kaufman, F. Z. Khliari*, A. D. Krish, A. M. T. Lin, V. G. Luppov, T. S. Nurushev, D. C. Peaslee, R. A. Phelps, J. S. Price, L. G. Ratner, R. S. Raymond, J. A. Stewart*, S. M. Varzar*, V. K. Wong
 THE UNIVERSITY OF MICHIGAN, ANN ARBOR, U.S.A.

J. M. Cameron, T. B. Clegg*, V. Derenchuk, T. J. Ellison*, D. L. Friesel, S. Y. Lee, M. G. Minty*, T. Rinckel, P. Schwandt, F. Sperisen, E. J. Stephenson, B. von Przewoski
 INDIANA UNIVERSITY CYCLOTRON FACILITY, BLOOMINGTON, U.S.A.

R. Baiod, C. M. Bhat, G. P. Goderre, P. S. Martin, S. M. Pruss, A. D. Russell
 FERMILAB, BATAVIA, U.S.A.

Yu. M. Ado, V. A. Kachanov, V. Yu. Khodyrev, O. I. Kisly, A. V. Koulsha, V. V. Mochalov, S. B. Nurushev, D. I. Patalakha, A. F. Prudkoglyad, V. V. Rykalin, V. P. Sakharov, D. S. Shoumkin, V. L. Solovianov, V. P. Stepanov, V. A. Teplyakov, S. M. Troshin, A. G. Ufimtsev, M. N. Ukhonov, A. V. Zherchov
 INSTITUTE OF HIGH ENERGY PHYSICS, PROTIVNO, RUSSIA

V. V. Fimushkin, M. V. Kullikov, A. V. Levkovich, V. A. Nikitin, P. V. Nomokonov, A. V. Pavlyuk, Yu. K. Pilipenko, V. B. Shntov
 JOINT INSTITUTE FOR NUCLEAR RESEARCH, DUBNA, RUSSIA

A. I. Demianov, A. A. Ershov, A. M. Gribushin, N. A. Kruglov, A. S. Proskuryakov, A. I. Ostrovodor, L. I. Sarychova, N. B. Sinejr, A. S. Yarov
 MOSCOW STATE UNIVERSITY, MOSCOW, RUSSIA

A. S. Belov, V. E. Kuzik, Yu. V. Plohinskii
 INSTITUTE FOR NUCLEAR RESEARCH OF RUSSIAN ACADEMY OF SCIENCES, MOSCOW, RUSSIA

Y. Mori, C. Ohmori*, H. Sato, T. Toyama, K. Yokoya
 KEK, TSUKUBA, JAPAN

R. Abegg, P.P.J. Delheij, G. Dutto, C. D. P. Levy, C.A. Miller, G. Roy*, P. W. Schmor, W. T. H. van Oers, A. N. Zelenski*
 TRIUMF, VANCOUVER, CANADA

Figure 15. SPIN@Fermilab Collaboration.

31 March 1992
Acceleration of Polarized Protons to 120 and 150 GeV in the Fermilab Main Injector

SPIN Collaboration
 Michigan, Indiana, Fermilab, N. Carolina/TUNL
 Protvino, Dubna, Moscow
 KEK

Abstract

This is a report by the SPIN Collaboration, which has two major goals at Fermilab:
 1. Accelerate polarized protons to 120 and 150 GeV in the Main Injector.
 2. Study spin effects in 120 GeV proton-proton elastic and inclusive collisions using the Michigan Polarized Proton Target in the Proton West Lab.

Table of Contents

Index of Detailed Hardware Plans	Page ii
1. Introduction and Project Chart	Page 1
2. Participants	Page 4
3. Physics Goals at 120 GeV Main Injector	Page 5
4. Physics Goals at 2 TeV Tevatron-Collider	Page 8
5. Main Injector Polarized Proton Beam	Page 10
5a. Budget Estimate	Page 13
5b. Schedule Estimate	Page 14
5c. Management of SPIN	Page 15
5d. Using Siberian Snakes at Fermilab	Page 17
5e. Outline Summary of Polarized Beam Project	Page 21
5f. Request for FY 1992 Funds	Page 28
5g. Related Activities of SPIN Collaboration	Page 29
5h. Status of SPIN at Fermilab	Page 30
6. Goals and Detailed Hardware Plans (Index p. ii)	Page 31
7. References	Page 115
Appendix A Paper by S. M. Troshin	Page 118
Appendix B Penn State Workshop on Polarized Colliders	Page 122
Appendix C Review by O. Chamberlain	Page 124
Appendix D Abridged Review by C. Bourrely et al.	Page 131

Figure 16. Polarized Main Injector Report.

Then John Peoples asked us to make a similar design-study for the Tevatron; we are doing this now. Figure 17 shows what Fermilab might look like with the proposed polarized beam hardware installed. Up to the Main Injector, plans are well-defined with solid cost estimates. They include a polarized source, an RFQ, a low energy polarimeter, another polarimeter after the LINAC, and one in the Booster. The 8 GeV Booster also needs two weak pulsed quadrupoles and one partial Siberian snake. The Main Injector needs two polarimeters and two full snakes. The Tevatron needs two polarimeters, six full superconducting Siberian snakes, and four spin rotators at either end of D0 and CDF to allow either longitudinal or transverse polarization in collider experiments. There might also be internal polarized jet target

experiments in the C0 area using a copy of our large NEPTUN-A spin-polarized ultra-cold atomic hydrogen jet target. A 120 GeV fixed-target polarized beam program might use the Michigan solid polarized target.

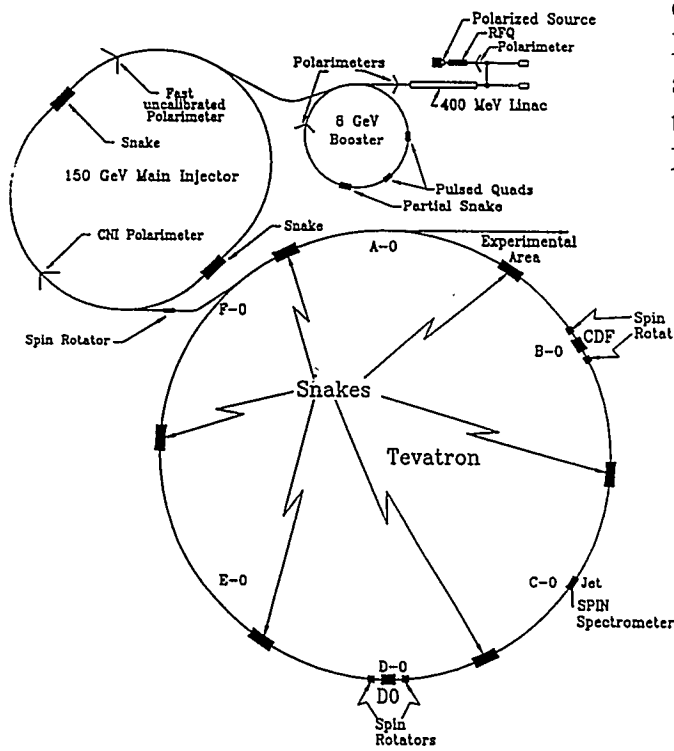


Figure 17. Polarized Proton Beam at Fermilab.

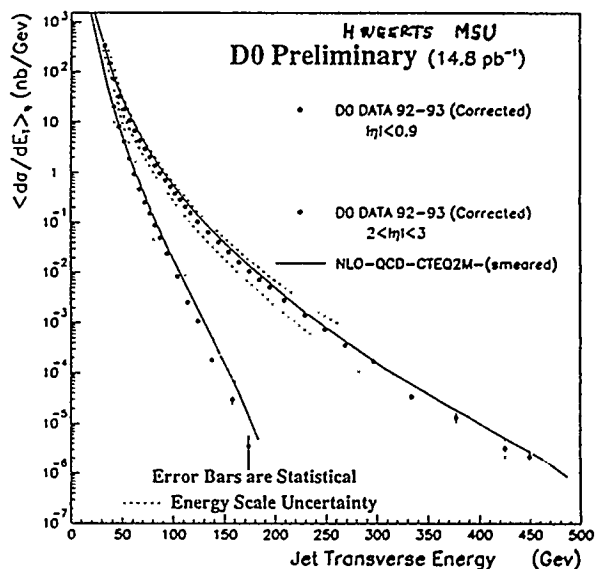


Figure 18. Inclusive Jet Cross-Section at 2 TeV.

Ken Stanfield recently asked us to try to get the collider-detector people interested in the polarized beam plans. We started interacting with some of the D0 and CDF people; we went to some of their meetings and they came to some of ours. At first, it seemed a bit unusual for polarized people to talk to collider-detector people; we are almost divided into two separate communities. However, something good came out of this unusual interaction. Harry Weerts from Michigan State and D0 was in Ann Arbor showing Figure 18 where the jet cross section is plotted against the transverse energy; the CDF people have similar data. I had certainly seen these data at many seminars, but I never before thought of them as being related to polarization. However, when they were shown at our collaboration meeting, I suddenly thought, "My Goodness, our PQCD friends say that the left-right asymmetry A must be zero in any hadronic process, but they essentially ignore all existing spin experiments 'because their energy or P_1 is too low to properly test PQCD.' However, the Inclusive Jet cross section can be measured with

great precision out to a transverse energy of 100 to 200 GeV.” At $P_{\perp} = 100$ GeV/c, one could make a precise measurement of whether there is any left-right asymmetry in jet production in a few hours. It would be somewhat difficult to say that $\sqrt{s} = 2$ TeV and $P_{\perp} = 100$ GeV/c are not high enough to test perturbative QCD. This measurement of A in inclusive jet production could definitively prove PQCD or definitively show that it is not a useful theory. Thus, perhaps something good came out of Ken Stanfield’s twisting my arm to talk to the collider people.

I will end by showing Figure 19, which comes from a 1987 *Scientific American* article.¹⁶ It is a 3-dimensional plot of the ratio of the spin-parallel cross-section to the spin-anti-parallel cross-section for proton-proton elastic scattering; the horizontal axes are incident momentum and P_{\perp}^2 . The 90°_{cm} data that I showed in Figure 1 is shown again. Figure 19 also shows our 12 GeV fixed-energy ZGS experiment¹⁷ which had similar structure at large P_{\perp}^2 . Our 6 GeV data¹⁸ is also shown along with Aki Yokosawa’s 3 GeV data.¹⁹ A few points are also shown from our early AGS polarized beam experiments;⁶ we eventually got some better data,²⁰ but we were never able to do detailed studies as at the ZGS. We were very disappointed with the death of ISABEL; this reduced Brookhaven’s involvement in high energy physics and we were never able to fully utilize the painfully developed AGS polarized beam. I hope that someone at the AGS or elsewhere can someday measure A_{nn} at 90°_{cm} above 13 GeV.

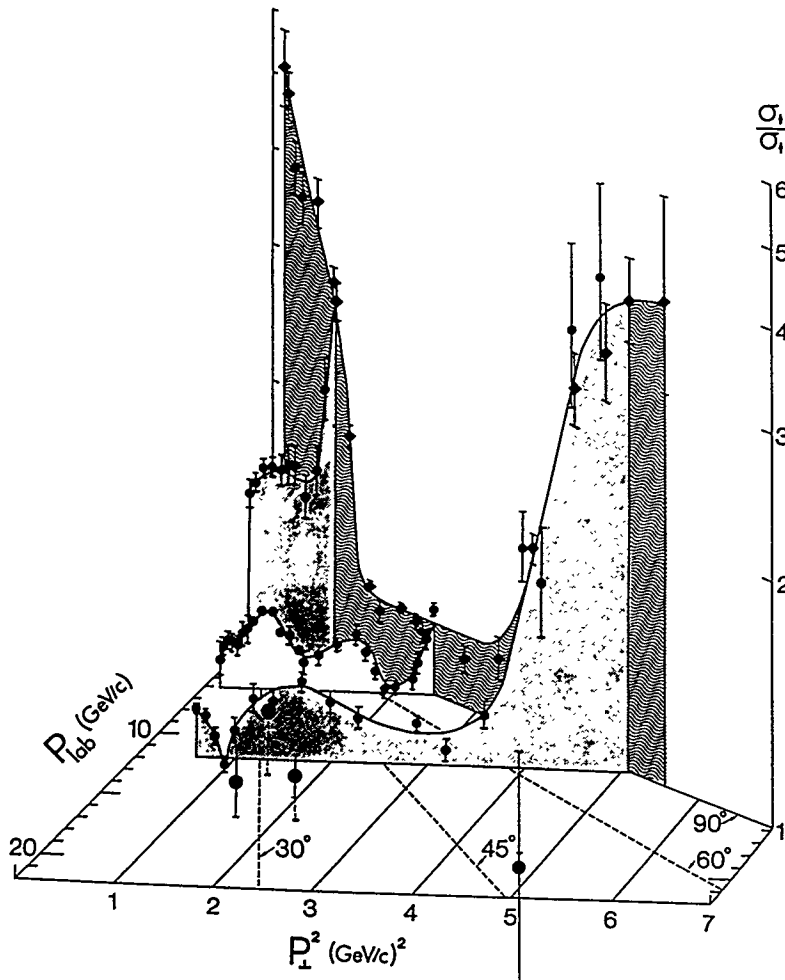


Figure 19. Spin-Spin Ratio in p-p Elastic Scattering.

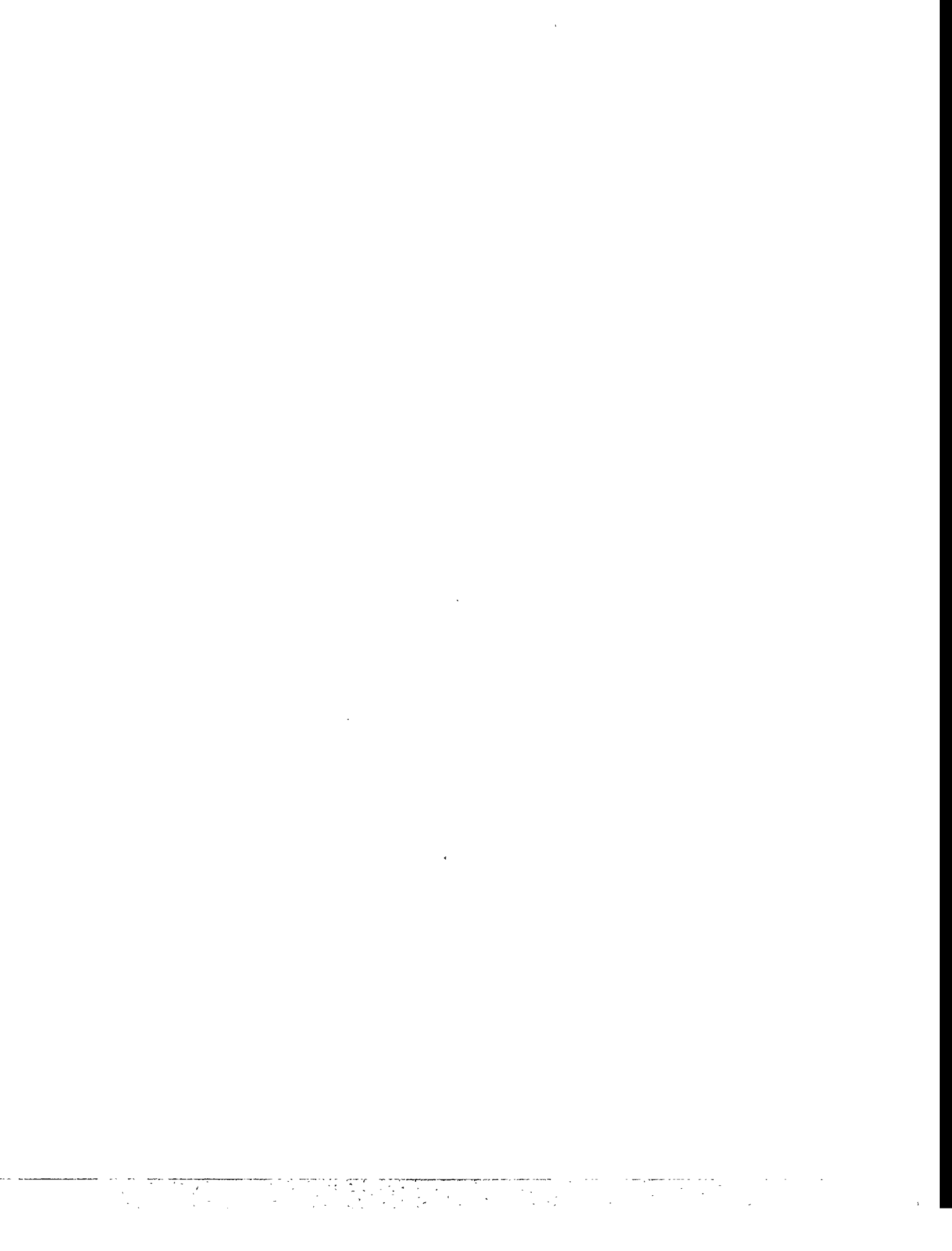
This 3-dimensional graph of two-spin effects shows no evidence whatsoever that spin effects are decreasing at either higher P_{\perp}^2 along the fixed-energy line or at higher energy along the 90°_{cm} line. It seems that there is a lot of structure and that spin effects may even increase at higher energy and at higher P_{\perp} . The still unexplained structure in this graph suggests that spin may be the key to unlocking the mystery of the strong interaction. All of the people associated with the ZGS polarized beam should be proud that they helped to launch this new field of physics.

REFERENCES

*Partially supported by a Research Grant from the U.S. Department of Energy.

1. E.A. Crosbie et al., Phys. Rev. **D23**, 600 (1981).
2. A.D. Krisch, Z. Phys. **C46**, S133 (1990).
3. K.J. Heller et al., Proc. of 7th Int. Symp. on High Energy Spin Physics, eds. L.D. Soloviev et al., **1**, 81 (Protvino 1987).
4. A. Yokosawa, Proc. of 10th Int. Symp. on High Energy Spin Physics, eds. T. Hasegawa et al., p. 93 (Univ. Acc. Press, Inc. Tokyo 1993).
5. J.S. Kane 1979 Letter to H.V. Bohm.
6. F.Z. Khiari et al., Phys. Rev. **D39**, 45 (1989).
7. Proc. Workshop on Higher Energy Polarized Proton Beams (Ann Arbor, 1977), eds. A.D. Krisch and A.J. Salthouse, AIP Conf. Proc. **42** (AIP, New York 1978).
8. Ya.S. Derbenev and A.M. Kondratenko, Part. Accel **8**, 115 (1978).
9. Ya.S. Derbenev, Proc. 3rd Int. Symp. on High Energy Phys. with Polarized Beams and Pol. Targets, ed. G.H. Thomas, AIP Conf. Proc. **51**, 292 (AIP, New York 1979).
10. A.D. Krisch et al., Phys. Rev. Lett. **63**, 1137 (1989); J.E. Goodwin et al., Phys. Rev. Lett. **64**, 2779 (1990); M.G. Minty et al., Phys. Rev. **D44**, R1361 (1991); V.A. Anferov et al., Phys. Rev. **A46**, R7383 (1992); R. Baiod et al., Phys. Rev. Lett. **70**, 2557 (1993); R.A. Phelps et al., Phys. Rev. Lett. **72**, 1479 (1993); B.B. Blinov et al., Phys. Rev. Lett. **73**, 1621 (1994); D.D. Caussyn et al., Phys. Rev. Lett. **73**, 2857 (1994).
11. H. Huang et al., Phys. Rev. Lett. **73**, 2982 (1994).
12. P.R. Cameron et al., Phys. Rev. **D32**, R3070 (1985).
13. D.G. Crabb et al., Phys. Rev. Lett. **64**, 2627 (1990).
14. D.G. Crabb et al., Phys. Rev. Lett. **65**, 3241 (1990).
15. Polarized Main Injector Report, unpublished University of Michigan Report (March 1992).
16. Alan D. Krisch, Scientific American, August 1987, pp. 42-50.
17. J.R. O'Fallon et al., Phys. Rev. Lett. **39**, 733 (1977); D.G. Crabb et al., Phys. Rev. Lett. **41**, 1257 (1978).
18. M. Borghini et al., Phys. Rev. **D17**, 24 (1978).
19. A. Yokosawa, Phys. Rep. **64**, 47 (1980).
20. D.G. Crabb et al., Phys. Rev. Lett. **60**, 2351 (1988).





PULSED SPALLATION NEUTRON SOURCES

John M. Carpenter
Intense Pulsed Neutron Source Division
Argonne National Laboratory

This paper reviews the early history of pulsed spallation neutron source development at Argonne and provides an overview of existing sources world wide. A number of proposals for machines more powerful than currently exist are under development, which are briefly described. I review the status of the Intense Pulsed Neutron Source, its instrumentation, and its user program, and provide a few examples of applications in fundamental condensed matter physics, materials science and technology.

HISTORY OF PULSED SOURCE DEVELOPMENTS AT ARGONNE

This is a day for remembering, reflecting and projecting into the future. Think back to the year 1968, 26 years ago. Please don't fix upon the gathering war half a world away, the burnings in our cities, or the riots in our own Grant Park; these were dark rumblings of political change that even now have not played out. Think instead of the scientific scene. ZGS had already been operating for five years and improvements were afoot. New, bigger machines were being designed and built around the world for high energy physics research. Several high flux research reactors were under design, construction or commissioning: HFBR (Brookhaven), HFIR (Oak Ridge), HFR (ILL Grenoble), A²R² (Argonne), British HFR. Argonne had an already long-established tradition in neutron scattering based on its smaller research reactors, beginning with Enrico Fermi and Walter Zinn at CP-3, and continuing at the 5-MW CP-5.

In January of 1968, as a young and dewy professor of Nuclear Engineering at the University of Michigan, where I had built some instruments for neutron scattering research at the 2-MW Ford Reactor, I was invited to serve in an instrument design group, led by Don Connor of the SSS division, that was supposed eventually to provide instruments for A²R². That group met

just once, early in 1968. Sam Werner, my colleague and classmate at Michigan, then at Ford Scientific Laboratory, was also on that committee. Almost immediately, the A²R² project was canceled.

When it was canceled, A²R² had progressed to the stage of a hole in the ground, a concrete foundation and a reactor mockup facility with a big supply of Beryllium blocks. In May that year, the Laboratory and the AUA established a Committee on Intense Neutron Sources, which was eventually led by Lowell Bollinger and was assigned to look into possible alternatives to the A²R². Bollinger, in Argonne's Physics Division, had a strong program of nuclear cross section measurements at CP-5 and ultimately went on to establish the ATLAS superconducting heavy-ion linac. I have reviewed the meeting minutes, and found the committee membership to have been a somewhat revolving thing. Lee Teng and Tat Khoe took part, but most of the members were reactor types. I learned about spallation sources and the Canadian ING studies. After about one year, examining a wide range of sometimes wild alternatives, we reported the recommendation to pursue a pulsed slow neutron source driven by a proton accelerator. We noted that the main shortcomings of the idea were that we did not know on the one hand the intensity of slow neutrons that such a source would produce, and on the other hand we did not know how effective such a pulsed source would be for neutron diffraction and inelastic scattering studies.

At about this time, Ron Martin returned from a trip to Russia having learned about Dimov's development of a high-current H⁻ ion source. Ron conceived that this source, feeding a 30 Hz rapid-cycling synchrotron through the existing 50 MeV linac, could provide a chain of 500 MeV pulses to the ZGS, increasing its current by a large factor according to $\beta^2\gamma^3$. He arranged to bring the decommissioned 2. GeV electron synchrotron from Cornell, to rig it for a test of the H⁻ injection principle with 300 MeV protons--so-called Booster I, and initiated the design of the 500 MeV Booster II. Jim Simpson took the job of bringing the system to reality. I learned of this in 1969 and dreamed up a proposal to use it to drive a pulsed neutron source during the intervals between ZGS injection pulses. I called it ZIING- the ZGS Injector Intense Neutron Generator. My preliminary estimates of the neutron fluxes indicated that they would be interesting but a little low.

So it stood until 1971, when I came to Argonne on my first sabbatical leave. With Oliver Simpson, SSS Division Director, I spent half my time re-evaluating neutron source options, and half my time making use of the new TNTOS hybrid chopper spectrometer that David Price, Bob Kleb and Mike Rowe had built at CP-5. I had guessed from experience in moderator measurements with Kingsley Graham at Michigan, that a Beryllium reflector could substantially increase the flux in pulsed source moderators; with the moderators decoupled at low energy, the arrangement would preserve the needed short pulses. With Bob Kleb, I worked up the idea for a

pulsed source with a Uranium target, using the Booster-II accelerator. We called it ZING. Don Connor encouraged me to build up a test for this using A^2R^2 Beryllium blocks, the ZING Mockup. I did this, and found that for the simple geometry that I used, the reflector provided a gain of a factor of 10! The factor would be somewhat less for a multi-moderator system. I wrote up the results with Gary Marmer, whom I brought in to keep me honest in matters of the accelerator. I received a patent on the decoupled reflector idea.

I continued to consult at Argonne after my return to Michigan. We drew up a proposal to build ZING and convened a workshop to evaluate its scientific applications, which took place in 1973. About 50 people came; among them was Motoharu Kimura from Tohoku University in Japan. Kimura already had experience using the 300 MeV Tohoku electron linac as a very effective source for neutron diffraction. Others had used powerful electron machines for inelastic scattering, but they were very limited in this application. The ZING spallation source was much more powerful. Kimura made a crucial suggestion--"You must build a prototype!" He stayed on for several months after the workshop and called in his colleague Noboru Watanabe to assist; I took a six-month leave from Michigan in the Fall of 1973 to work on the project.

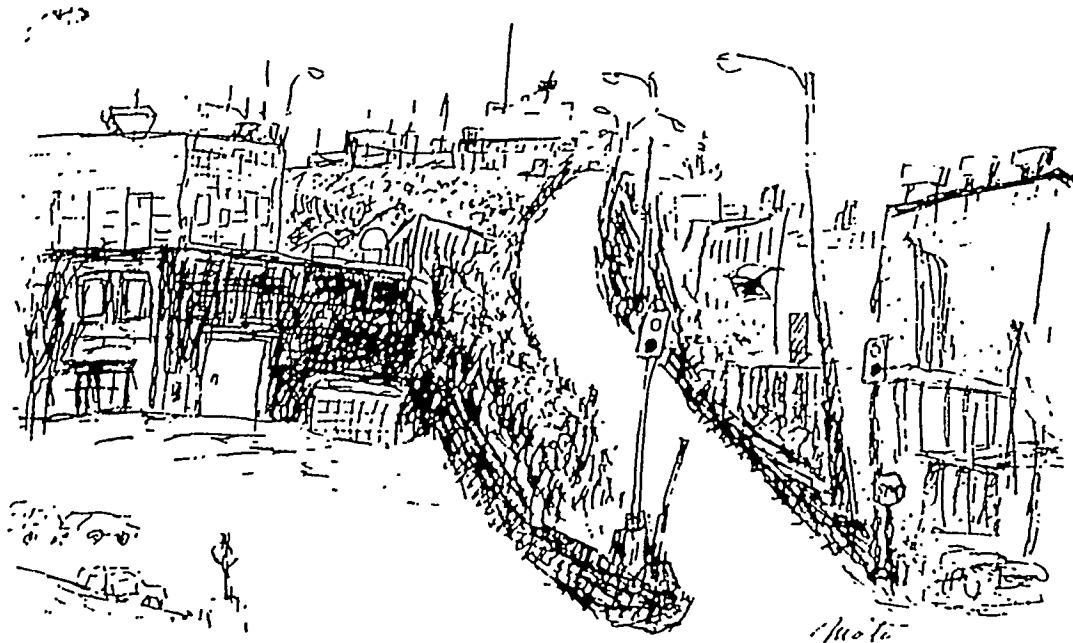


Figure 1. Skunk Hollow, the location of ZING-P, and the entrance ramp to ZGS. Sketch by Motoharu Kimura.

With Bob Kleb's help, we designed a test setup. We called it ZING-P, a little shielded house on top of the beam line between the Booster and ZGS--"Skunk Hollow." Figure 1 shows Kimura's sketch of Skunk Hollow and the ZGS access ramp. The Laboratory eventually

provided \$30,000 for the job, and put Tom Banfield, CP-5 director, in charge. We used a stack of armor plate from the dismantled battleship Indiana (Mike Nevitt's ship when he was in the Navy) in the shielding. Kimura had to return to Japan before the project was authorized. He left in disappointment, feeling that his contribution was being ignored. That was not true, it was only administrative delay. We completed the installation in about three months and ran it first in January, 1974. The target was half of a lead brick, with a copper tube cooling pipe. There were two polyethylene moderators, a decoupled Beryllium reflector and two vertical neutron beams. Watanabe helped to design a neutron diffractometer that was built in the SSS shops. The test proved out the basic principles and the intensity estimates. ZING-P ran at intervals until the end of 1975, when it was time to install Booster-II. Figure 2 is Kimura's drawing of the ZING-P experiment area.

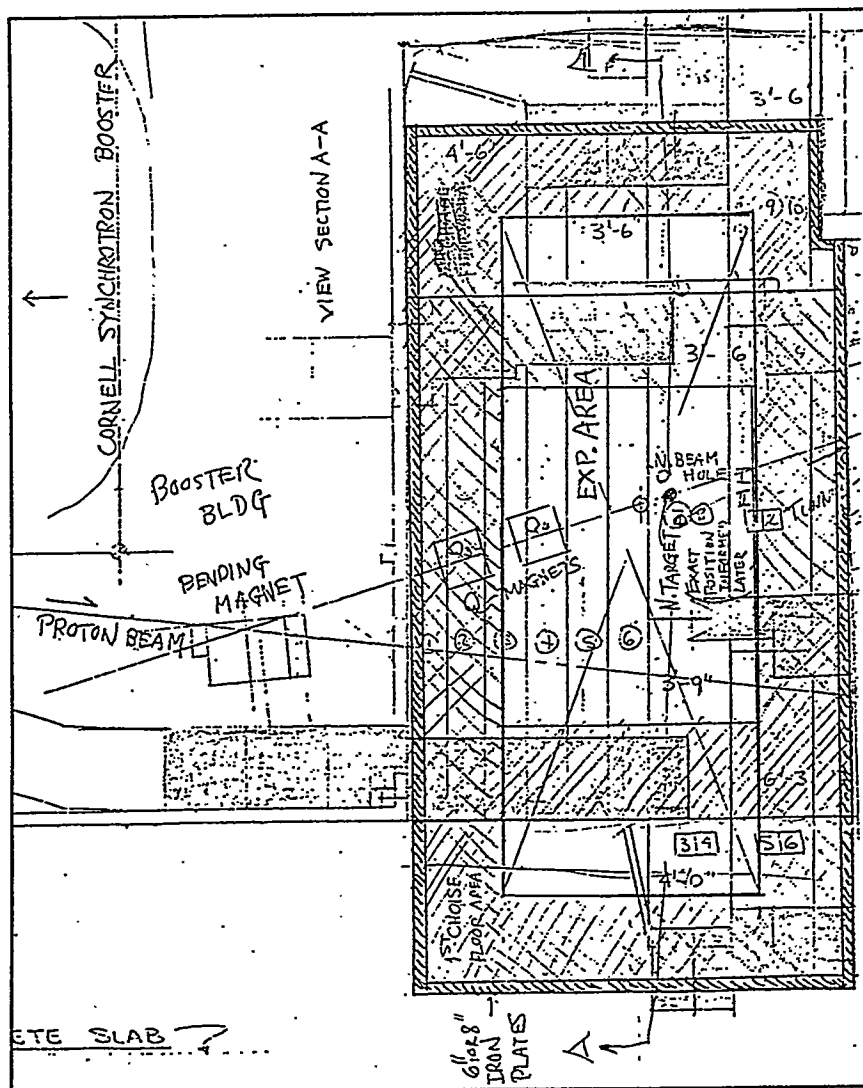


Figure 2. Kimura's drawing of the ZING-P experiment area. The date is May 18, 1973.

Figure 3 shows the lead-brick target and the moderator and reflector arrangement of ZING-P.

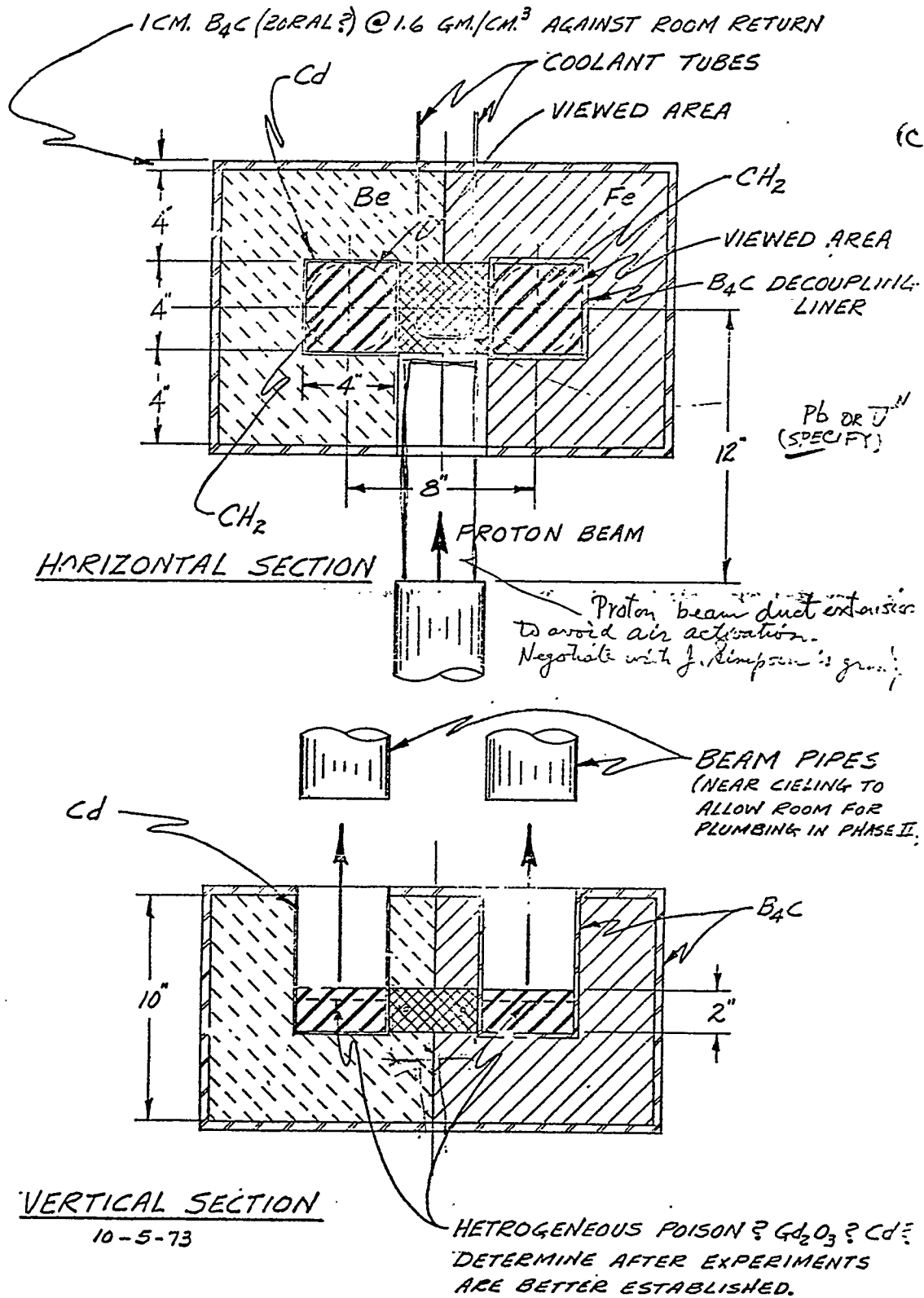


Figure 3. Drawing of the ZING-P target-moderator-reflector arrangement by Bob Kleb.

Figure 4 shows the moderators arranged for time-focusing measurement of the emission-time distribution as a function of neutron wavelength.

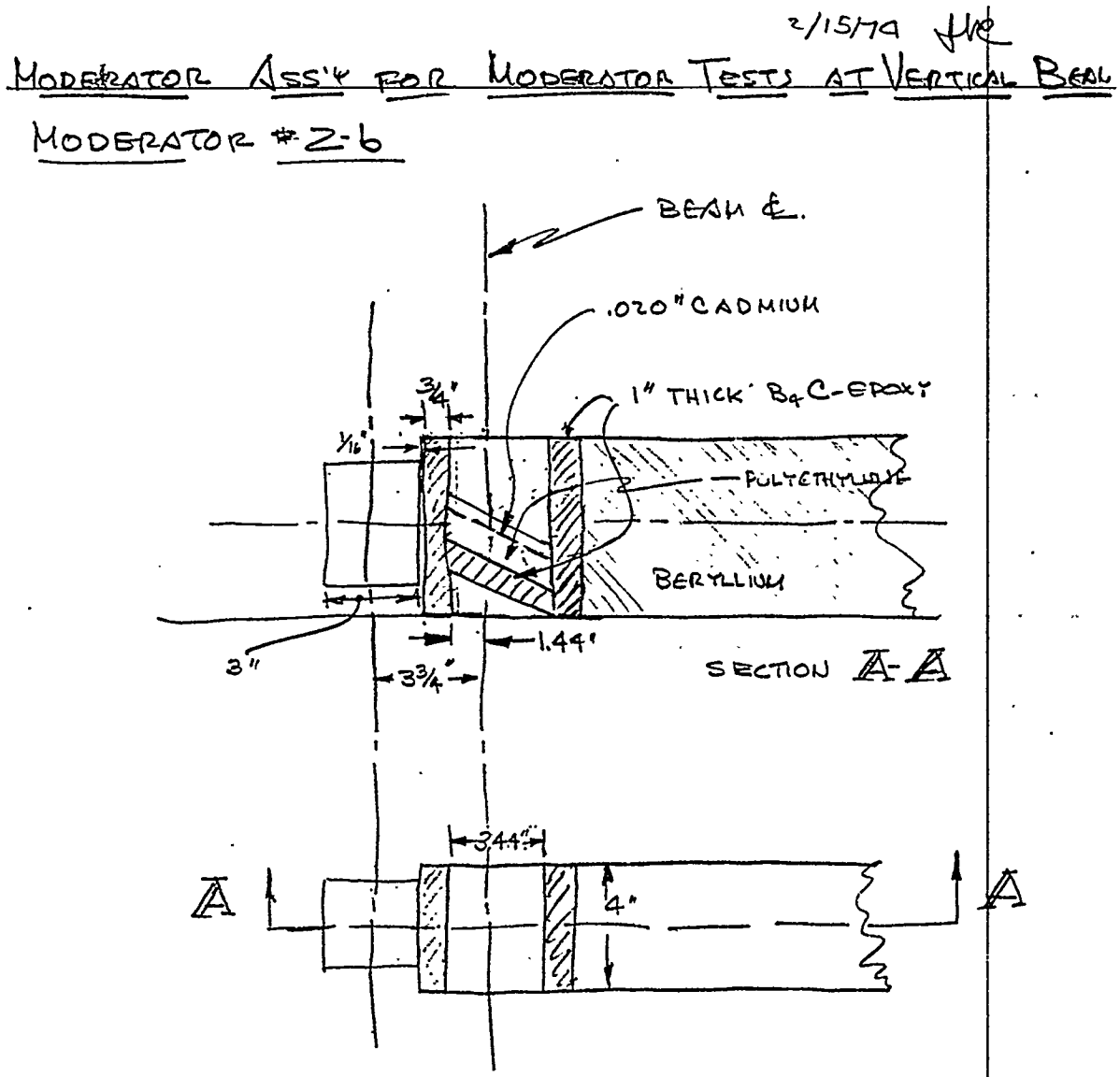


Figure 4. Tilted moderators for time-focused measurements of the shapes of emitted neutron pulses as functions of neutron wavelength.

By then, I had become so involved in the neutron source project that I resigned my full professor position at Michigan and joined Argonne in January, 1975. We designed some modifications to the prototype, including three more horizontal beams and more scattering instruments, to be operated when Booster-II came on-line. That was ZING-P'. Its first target was of W, soon replaced by a target of U, and eventually ZING-P' had a liquid Hydrogen moderator. Prominent in the work were Torben Brun, Bob Beyerlein, David Price, Kurt Sköld, Jim Jorgensen, Bob Kleb, Tom Erickson, Mel Mueller, Selmer Peterson, Art Ries, and Chuck

Pelizzari. Bob Sachs, then Laboratory Director and Mike Nevitt, Deputy Director, encouraged us mightily throughout all this time. ZGS and CP-5 were soon to be shut down and the pulsed source became a matter of higher priority. Kimura returned frequently and assisted with a large number of source performance measurements that were necessary to underpin the IPNS design. In ZING-P and ZING-P' all the essential pieces of the modern pulsed spallation neutron source came together for the first time.

Our ZING proposal ran into trouble in Washington, on the basis that it was too modest-- "Go away and come back with a more powerful version," we heard. Jim Simpson, Martin Foss and others worked up the design of a 800 MeV, 0.5 mA High Intensity Synchrotron, HIS, and we laid plans for a new neutron hall. In 1975 we convened another Workshop to evaluate the new proposal, which Sam Werner chaired with me. Paul McDaniel, AUA head, advised me not to name the newly proposed installation frivolously; "Choose an unpronounceable acronym," he counseled, "Make them say it out." We gave up "ZING" and called it the Intense Pulsed Neutron Source, IPNS. We began firing Schedule-44s to Washington.

Booster-II came up with a low current. It ran until 1980, when the current had risen to about 3 μ A. Everybody worked on the machine, Frank Brumwell, Yang Cho, Ed Crosbie, Marty Knott, Bob Kustom, Jim Norem, Charlie Potts, Walter Praeg, Tony Rauchas, Jim Simpson, Vern Stipp, Bob Wehrli, all had important hands in the synchrotron development over the years. On the neutron side, ZING-P' was extremely successful. It turned out significant research and we established a user program based on the pattern of ZGS, which was very important.

Our proposals ran into more trouble; now the project was said to be too big, too expensive. We included in later versions of our proposals a quickly-accomplishable intermediate step, IPNS-I, based on Booster-II, (now we called the accelerator the Rapid Cycling Synchrotron, RCS) which was to provide experimental capacity and further experience needed before HIS and IPNS-II could be completed. It finally turned out that only the first phase, IPNS-I, received the funding nod. ZGS shut down on October 1, 1979. We began the IPNS construction project in 1978, based on the use of soon-to-be vacated ZGS areas and soon-to-be-liberated components. IPNS was completed in early 1981, on schedule, and (roughly speaking) within budget. First beam was delivered to the target on May 5, 1981, so today, May 6, 1994, is IPNS's 13th anniversary, plus one day! The reasoning by which IPNS was funded was that it was to be an experiment to test the effectiveness of the new way of doing neutron scattering. By now, we can claim resounding success, but there has never been a more ambitious pulsed source project funded in the US.

Figure 5 shows a plan view of IPNS; in the dim reaches beyond the synchrotron is the ZING-P target.

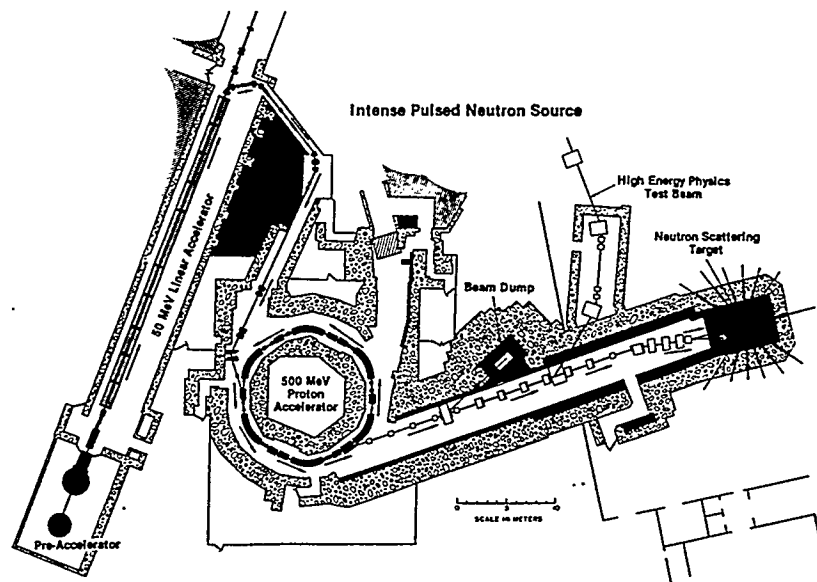


Figure 5. Plan View of IPNS.

Figure 6 shows the experiment hall of IPNS, the former EPB-2 of ZGS. Twelve neutron beams support thirteen neutron scattering instruments. IPNS has three moderators, two of solid methane and one of liquid methane--all cryogenic systems producing cold neutrons as well as copious epithermal neutron beams.

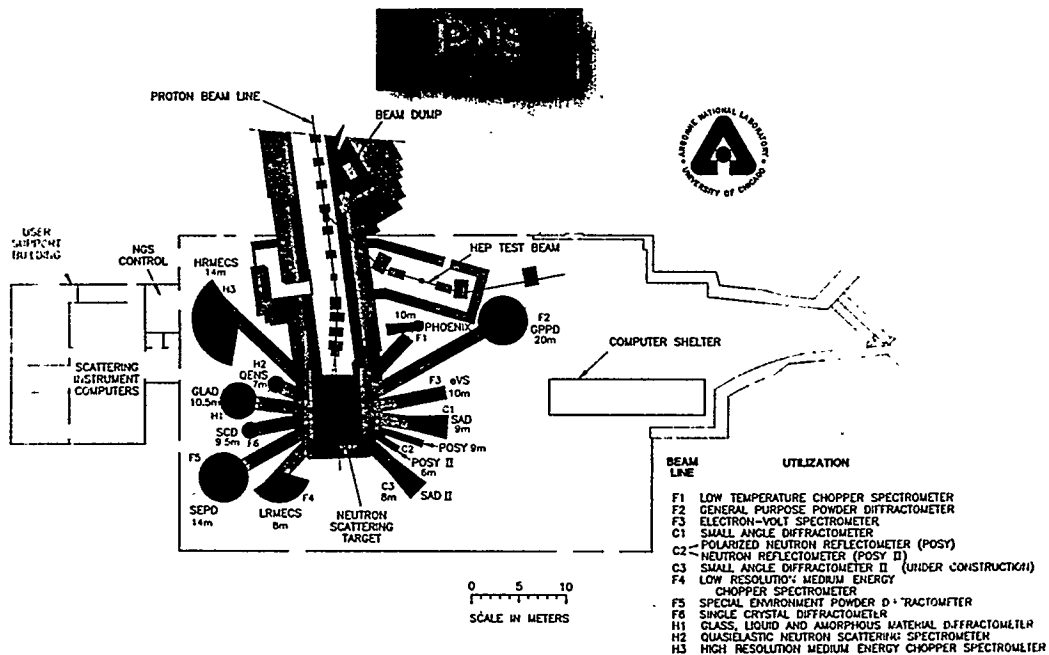


Figure 6. Plan View of the IPNS Experiment Hall.

Figure 7 is a photograph of the IPNS experiment hall.

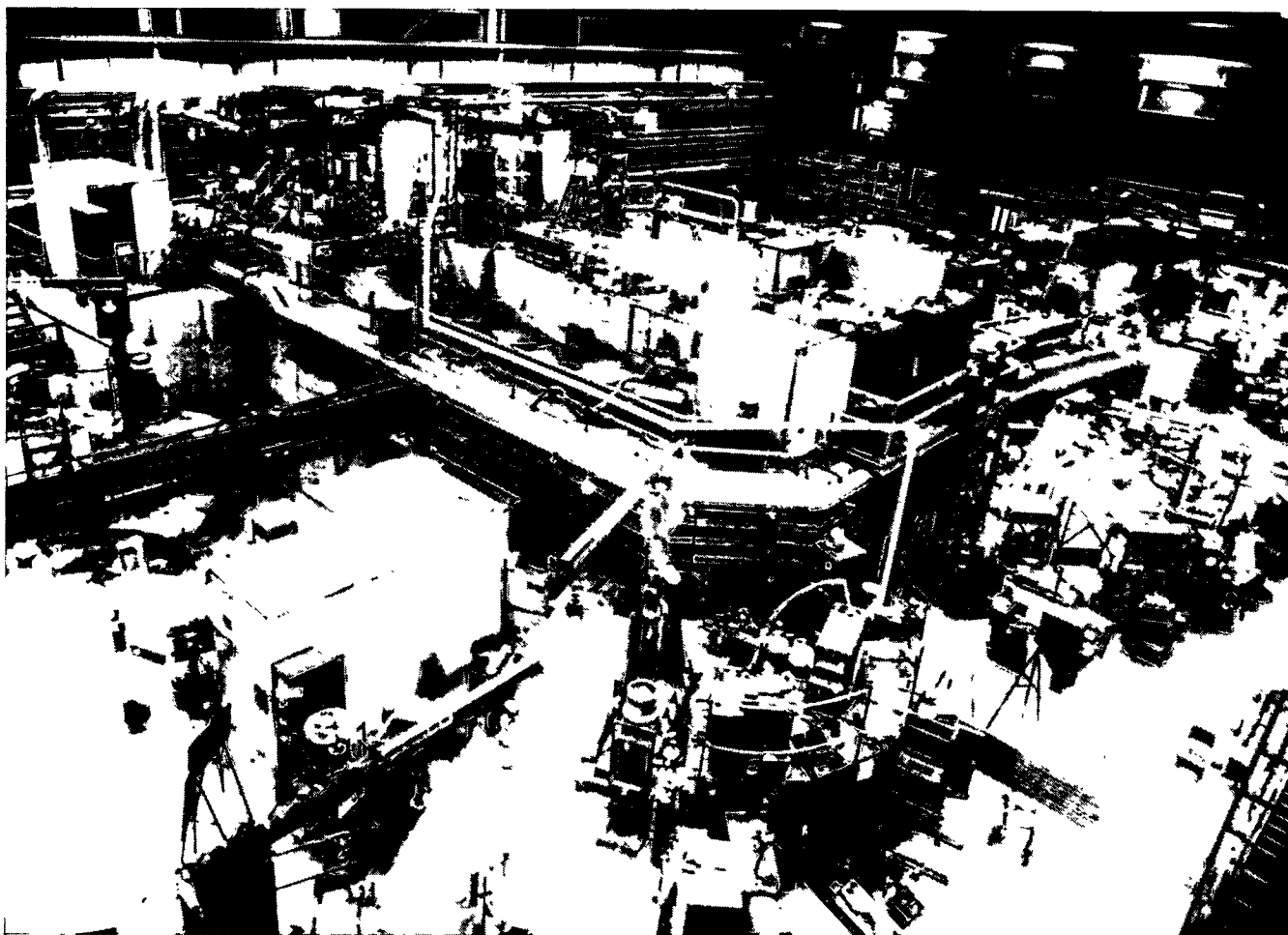


Figure 7. Photo of the IPNS Experiment Hall.

WORLD PULSED SOURCE DEVELOPMENTS

Events transpired elsewhere. In Japan, a pulsed spallation neutron source, KENS, which began operation in 1980 and is an extremely successful, although small research installation, was put up based on the 500 MeV injector to the 12 GeV PS at KEK. The NIMROD accelerator at Rutherford Laboratory in UK was to be shut down. The British adapted the IPNS-II ideas and built what is now ISIS, which started up in 1985 and is now the world leader, an extremely effective research facility. Los Alamos put up a target on LAMPF, originally called WNR, which started up in 1977. It was adapted using a new PSR which started in 1985, now called LANSCE. A giant study was undertaken in Germany, the SNQ, which, unfortunately, never received funding. Construction of a steady spallation source, SINQ, began in Switzerland, which

will be completed in 1995. At the Moscow Meson Factory in Troitsk, work is temporarily stalled but well along toward installing a two-target pulsed/steady spallation source. Table 1 lists the operating pulsed spallation neutron sources and those under construction.

Table 1. Spallation Neutron Sources Operating or Under Construction

Source	Pulsing Frequency	Proton energy, time-average current	Time-Average Beam Power	Startup
KENS (Japan)	20 Hz	500 MeV x 7 μ A	3.5 kW	1980
IPNS (US)	30 Hz	450 MeV x 15 μ A	6.75 kW	1981
ISIS (UK)	50 Hz	800 MeV x 200 μ A	160 kW	1985
LANSCE (Los Alamos)	20 Hz	800 MeV x 60 μ A	48 kW	1985
SINQ (Switzerland)	Steady source	570 MeV x 1500 μ A	860 kW	1995
MMF, INR (Troitsk, Russia)	Pulsed and steady sources	600 MeV x 200 μ A	120 kW	?

We really never quit thinking about newer, larger installations. Bob Kustom conceived an FFAG design called ASPUN, and a smaller, prototypical Mini-ASPUN, put forward in 1984. A few years ago, Jim Norem and I put together a series of modifications to IPNS called PNRF. Now we are working with Yang Cho on the design of a new installation, the IPNS Upgrade, to have a 1-MW time-average proton beam. Los Alamos is pursuing the design of its own version of a 1-MW pulsed source, while Brookhaven National Laboratory is studying a "green field" design that starts at 1 MW and is upgradable to 5 MW. Elsewhere, the Japanese have conceived KENS-II as a part of a new facility, the Japan Hadron Project. Austria and an Eastern European consortium have launched the study of a new facility called AUSTRON. The European Union is sponsoring the study of a 5-MW pulsed spallation source, ESS. Table 2 lists the pulsed spallation source studies now under way.

Table 2. Pulsed Spallation Source Studies Underway

Study	Location	Beam Power
IPNS Upgrade	Argonne	1.0 MW
NGSNS	Los Alamos	1.0 MW
AUSTRON	Austria	0.3 MW
KENS-2	Japan	0.2 MW
ESS	Europe	5.0 MW
PSNS	Brookhaven	1.0 → 5.0 MW

STATUS OF IPNS

The developments that started here at Argonne in 1968 and have proceeded successfully since have spawned this entire new generation of neutron scattering installations, which complement the high flux research reactors and provide capacity for an ever-broadening range of applications of neutrons to the study of materials. Table 3 shows the current status of IPNS. Since startup, the accelerator current has risen while the reliability has stayed at an exemplary 95 %. The original depleted Uranium target was for a time (1988 to 1991) replaced with an enriched Uranium Booster target, which increased the neutron beam intensities by a factor 2.5.

Table 3. What's Happened at IPNS in 10 Years.

Item	Change
Accelerator current	protons $i \times 4$
Booster (U^{235} , $k_{eff} = 0.8$) Target	neutrons $\phi \times 2.5$
Cryogenic moderators	cold neutrons $\phi \times 150$
Number of instruments	4 → 13
Number of experiments	94 → 250
Number of visitors each year	89 → 170
Number of proposals	up 100 %
DOE supported operating time	down 30 %
DOE operating budget (after inflation)	down 9 %
non-DOE operating funds	\$1.5 M

The Booster target suffered a cladding failure after three years and is being replaced. The original moderators have been replaced with three cryogenic moderators, two solid methane moderators producing 150 times greater cold neutron flux and other advantages over ambient temperature systems. The number of experiments completed per year has risen to over 300 and the number of users has increased to about 250 different faces each year. The number of instruments has increased from four to thirteen and the number of requested experiment days has doubled. We have completed about 3000 experiments. However, the budget is down in terms that reflect inflation, and consequently operating time is down 30 %. Occasionally, we do work for others, for which we received \$1.5 M in FY 1993.

Table 4 shows the details of IPNS utilization for the years 1982 through 1993.

Table 4. Summary of IPNS Utilization.

Fiscal Year	82	83	84	85	86	87	88	89	90	91	92	93	Total
Number of experiments performed	94	110	210	180	212	223	257	323	330	273	210	248	2670
Visitors for at least one experiment													
Argonne	37	41	49	44	52	55	57	60	61	60	53	48	
Other government labs	8	9	8	7	11	15	18	16	19	15	14	18	
Universities	27	33	45	51	79	78	89	94	120	92	62	64	
Industry	5	5	9	7	13	24	20	24	36	18	20	16	
Foreign	12	18	39	35	27	24	17	26	18	27	14	25	
Totals	89	106	150	143	182	196	201	220	254	212	163	171	2087
Number of "user" instruments	4	5	6	6	6	6	6	7	7	7	7	6	
Number of "PRT" instruments	1	1	1	2	3	3	4	4	5	5	5	6	

Industrial research groups make frequent use of IPNS. Table 5 summarizes the names of industrial firms that recently used IPNS.

Table 5 Recent Industrial Use of IPNS

Industry Recent Users of IPNS		
3M Corp	Du Pont	Miles, Inc.
Allied Signal*	Eastman Kodak	Mobay Corp.
Amoco	Exxon	Mobil Oil*
ATT Bell Labs	GE*	SDR
BP America*	Goodyear Tire	Shell Research*
Corning Glass	IBM Almaden	Texaco
Dow	Kraft	

* Purchased beam time for proprietary use

Contributors to IPNS Instruments
BP America
Exxon
IBM
SDR
Texaco

SCIENCE AT IPNS

Following are three examples of experiments completed at IPNS, which illustrate the broad range and high significance of science carried out at IPNS.

DEEP INELASTIC SCATTERING AND THE BOSE CONDENSATE FRACTION IN SUPERFLUID HELIUM

The number of atoms per unit momentum \vec{p} in superfluid materials consists of a degenerate zero-momentum component, the Bose condensate, containing a fraction n_0 atoms and a continuous distribution representing the normal atoms

$$n(\vec{p}) = n_0 \delta(\vec{p}) + (1 - n_0) \times \text{continuous function } (\vec{p})$$

If the momentum transfer in scattering is large enough, it is appropriate to represent the scattering function in the "impulse approximation", which describes so-called "deep inelastic scattering,"

$$S(Q, \omega) = \int n(\vec{p}) d^3 \vec{p} \delta\left(\omega - \frac{\hbar^2 Q^2}{2M} - \frac{\hbar \vec{p} \cdot \vec{Q}}{M}\right)$$

Since the momentum distribution is isotropic, the result can be expressed in terms of a function of a single variable,

$$= \frac{M}{Q} J(y);$$

where

$$y = \frac{M}{Q} \left(\omega - \hbar \frac{Q^2}{2M} \right)$$

and

$$J(y) = 2 \pi \int_{|y|}^{\infty} p n(p) dp.$$

Here,

$$\hbar \vec{Q} = \hbar (\vec{k}_i - \vec{k}_f),$$

is the momentum transfer and the (non-relativistic) energy transfer is

$$\hbar \omega = (E_i - E_f), \text{ where } E = \frac{\hbar^2}{2m_n} k^2.$$

Figure 8 shows calculated momentum distribution functions for normal and superfluid liquid Helium.

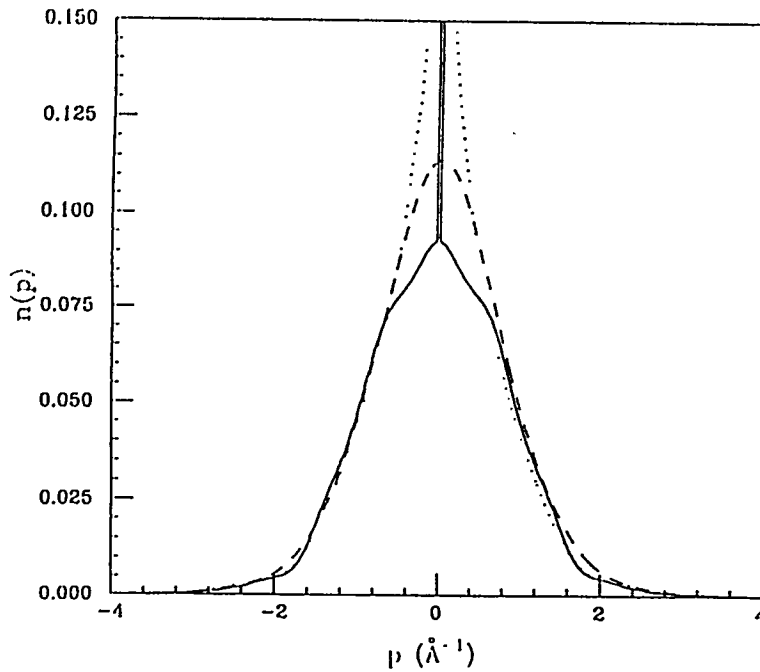


Figure 8. The momentum distribution of normal and superfluid liquid Helium. Solid line, Green's function Monte Carlo; dotted line, variational calculation, dashed line, path integral Monte Carlo calculation for normal liquid.

Measurements are best done at a pulsed source, capitalizing on the high flux of epithermal (higher than thermal) neutrons and the accompanying high pulse resolution, using a chopper spectrometer. Figure 9 shows the results of measurements at IPNS, expressed in terms of $J(\gamma)$, for normal liquid at 3.5 K and for superfluid at 0.35 K.

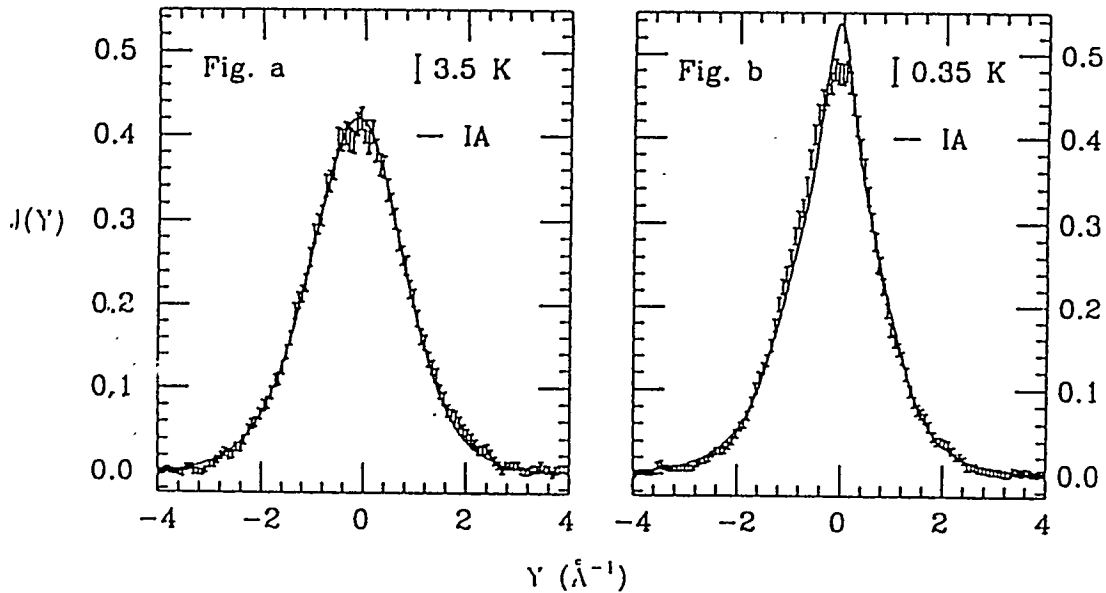


Figure 9. Measured reduced momentum distribution functions $J(\gamma)$, for normal liquid at 3.5 K and for superfluid at 0.35 K.

The impulse approximation (IA) matches the measurements for the normal liquid, but fails in the case of the superfluid. The reason is that the IA fails to account for "final state effects," which broaden both the delta-function and the continuous distribution. Fortunately, theory developed at the same time as the measuring techniques were refined which enabled accounting for these effects, providing the means for extracting the condensate fraction n_0 and producing an essentially perfect fit to the data.

Figure 10 shows the variation of the condensate fraction as a function of temperature for liquid Helium at saturation pressure. The data have been fitted to a function

$$n_0(T) = n_0(0)[1 - (T/T_\lambda)^6] \quad ,$$

with $n_0 = 8\%$ and where T_λ is the superfluid transition temperature, 2.17 K.

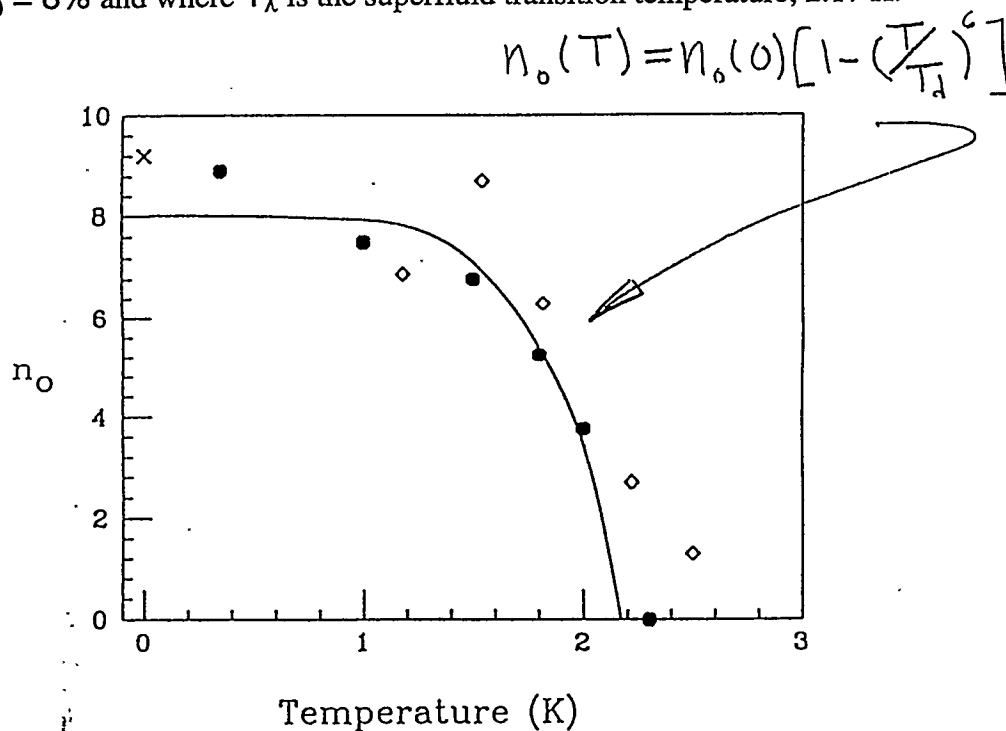


Figure 10. The Bose condensate fraction as a function of temperature. Heavy dots represent the data; the cross is the result of a Green's function Monte Carlo calculation and the diamonds are path integral Monte Carlo results. The solid line is a fit to the data.

The extensive work on this subject has largely been pursued at IPNS, and even began at the prototype ZING-P'. Leading in these accomplishments have been Ralph Simmons (University of Illinois) and Paul Sokol (Penn State University). The work has cleared up many long standing questions of the theory of superfluid Helium, and now has progressed to the study of more complicated systems, He-3/He-4 mixtures, joint pressure and temperature dependence of n_0 , n_0 in restricted geometries (He

in porous and layered materials), and Hydrogenous systems; all of these types of measurements have already been undertaken.

STRUCTURE STUDIES OF HIGH- T_C SUPERCONDUCTORS, $YBa_2Cu_3O_{7-\delta}$, &c.

The discovery in 1986 of the new class of copper oxide superconductors launched world wide studies of their properties. The first determination of the structure of YBCO, as it has come to be called, was done at IPNS in the Special Environment Powder Diffractometer, by Mark Beno and his colleagues. Hi- T_C materials come in indefinite number of varieties: $A_2B_bC_dCu_3O_x$, all polycrystalline ceramics. Neutron diffraction, especially pulsed-source neutron diffraction, it turns out, is THE WAY to explore the structure/function relation relationships in these materials. IPNS and all other pulsed spallation sources are still very busy on these materials. Questions addressed span the range from fundamental to practical, from new superconductors to non superconducting prototypical materials; composition, defects and vacancies, crystallographic phase transitions, multiple phases, *in situ* preparation and treatment variables, texture, composite materials. Jim Jorgensen and his colleagues have led the world in their ongoing program of studying these materials.

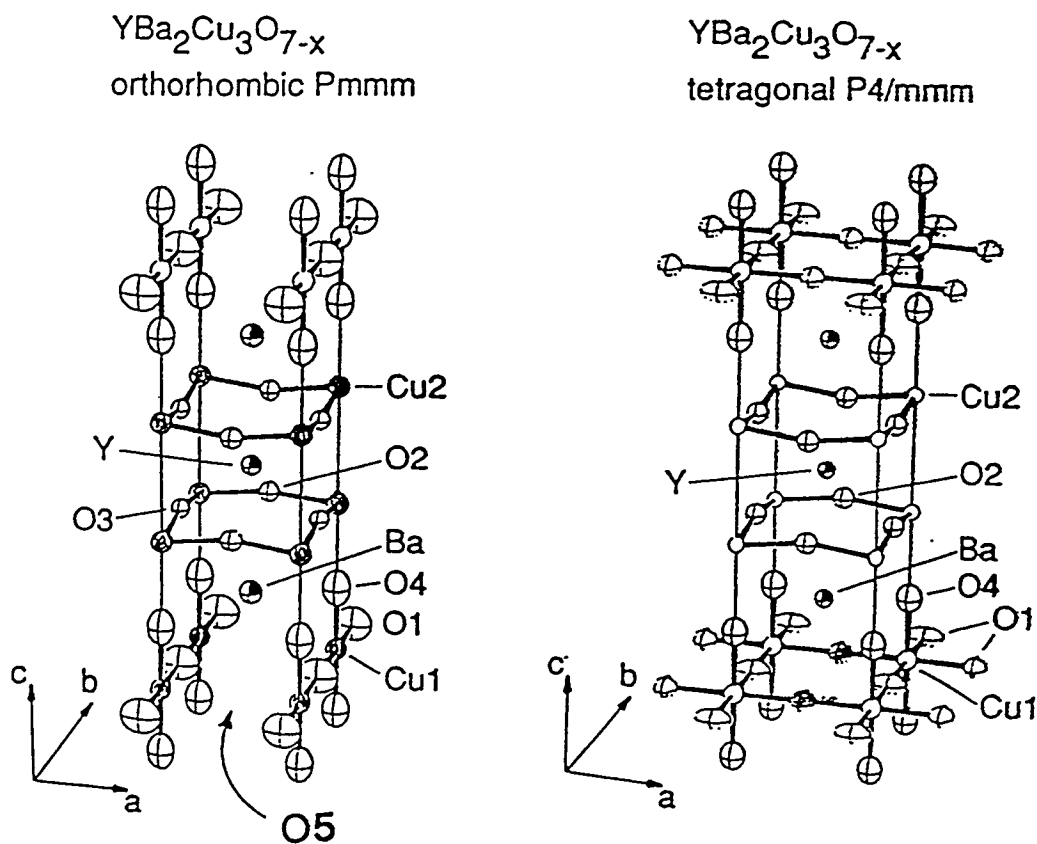


Figure 11. Structures of $YBa_2Cu_3O_{7-\delta}$. Left, superconducting, orthorhombic phase; right, insulating, tetragonal phase.

Figure 11 shows the unit cell structures of two phases of YBCO, the high-temperature tetragonal, normal (insulating) phase and the low temperature orthorhombic, superconducting phase, determined at IPNS. These measurements and an extensive program of further investigations are possible not only because of the power of the pulsed source diffractometers and the well developed analysis techniques, but also because of the presence at Argonne of excellent capabilities for materials preparation and characterization by other methods.

A TEST OF THE REPTATION MODEL OF POLYMER DIFFUSION

The first instrument for neutron reflectometry, POSY, was constructed at IPNS by Gian Felcher and Bob Kleb and won an IR-100 award in 1987. Since its installation, instruments for this purpose have been built in almost all the neutron facilities in the world. The technique is most powerful and flexible in its time-of-flight form, appropriate for pulsed sources. Neutron reflection is similar in its fundamentals to the critical reflection of light, as, for example, from an air-glass interface. There is perfect reflection for angles less than the critical angle, and no information is to be gained. For angles above the critical angle, the reflection probability is less than unity and depends on the neutron wavelength, the incident angle, and the details of the variation of the refractive index below the surface. Since the refractive index for neutrons depends on nuclear scattering lengths which vary irregularly with (A,Z) , the technique is uniquely sensitive to variations of chemical (nuclear, isotopic) concentration beneath the surface. The contrast between H and D, the common and heavy forms of Hydrogen, is especially noteworthy and useful. Because the refractive index varies linearly with wavelength, time-of-flight measurements as a function of wavelength at a fixed angle of reflection reveal the entire variation of the reflectivity. Using polarized beams of neutrons, the reflectivity can be measured as a function of the variation of magnetization density beneath the surface, which is a further unique feature of the method. The measured reflectivities can be analyzed to provide the variation of the index of refraction as a function of depth below the surface.

Bill Dozier (IPNS), Tom Russell (IBM), G. Agrawal (UIC) and others used this method in a series of measurements to investigate the motions of polymer molecules across the interface between two layers. The strength of a polymer interface depends on inter diffusion of molecules across the surface. How this inter diffusion takes place is not only a practical question but also one with deep theoretical implications and is the subject of a theory of DeGennes. The long polymer molecules in the bulk of material diffuse along their length like snakes in a basket of snakes--a motion he dubbed "reptation." The clever IPNS measurements proved out this theory for the first time.

A sample was prepared of two kinds of "block" copolymers. One variant, called HDH, consisted of a block of completely deuterated material in between two blocks of normally hydrogenated polymer. The other variant, DHD, however, was built in the opposite way, a hydrogenated block between two

deuterated blocks. In an ideal case, the materials do not contrast if they can be made to have the same average scattering length densities. A layer of the one was placed on a layer of the other--of course, the two layers are at first distinct. After annealing at elevated temperatures for various lengths of time, the two layers grow together, as shown in Figure 12, illustrated for the case of perfect contrast matching.

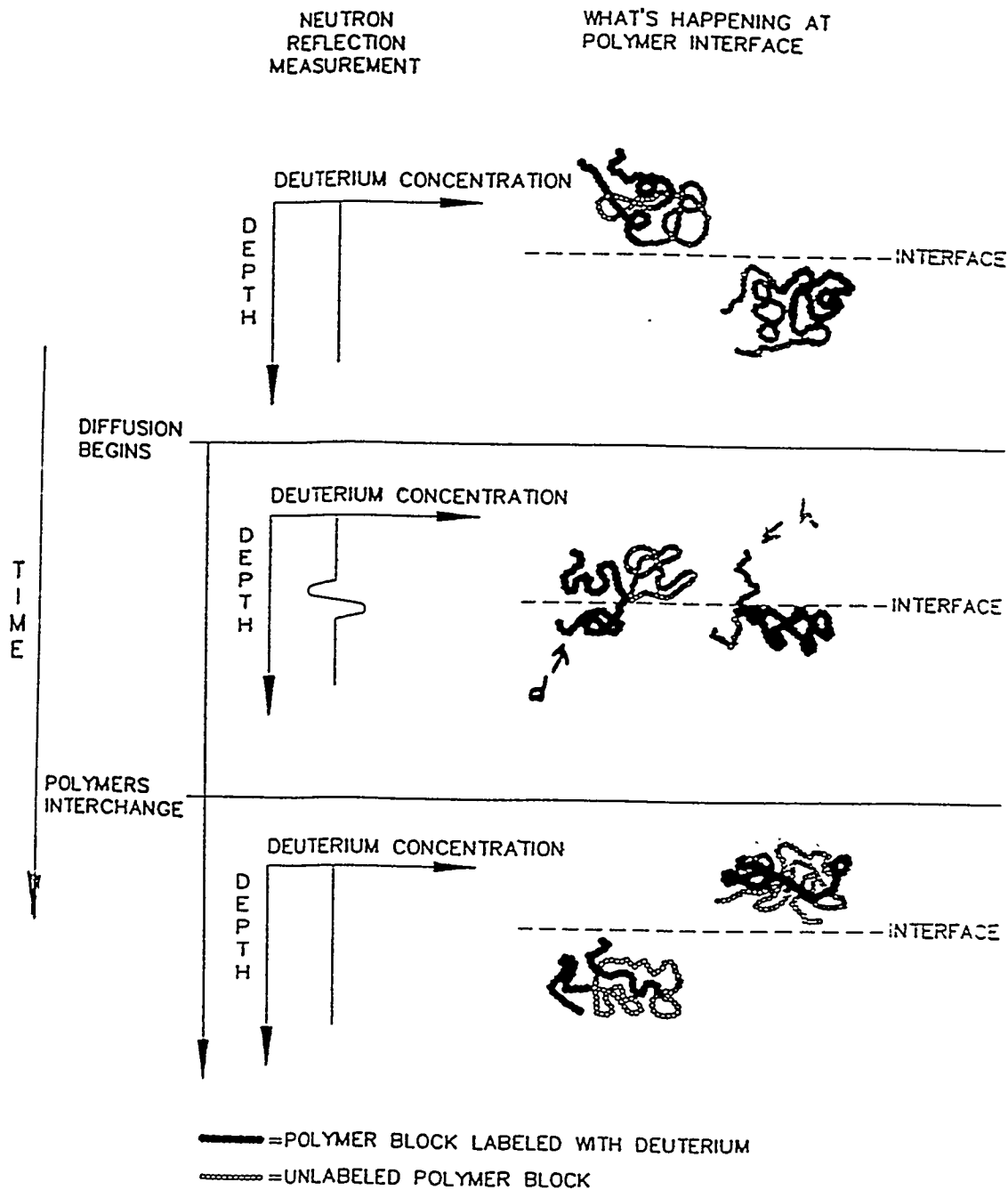


Figure 12. The reptation model of polymer diffusion across an interface. Black spheres represent deuterated polymer blocks, D; white spheres represent normally-hydrogenated blocks, H.

If the reptation model is correct, in early times Ds from the DHD side diffuse into the HDH side and Hs from the HDH side diffuse into the DHD side because these are at the ends of the respective

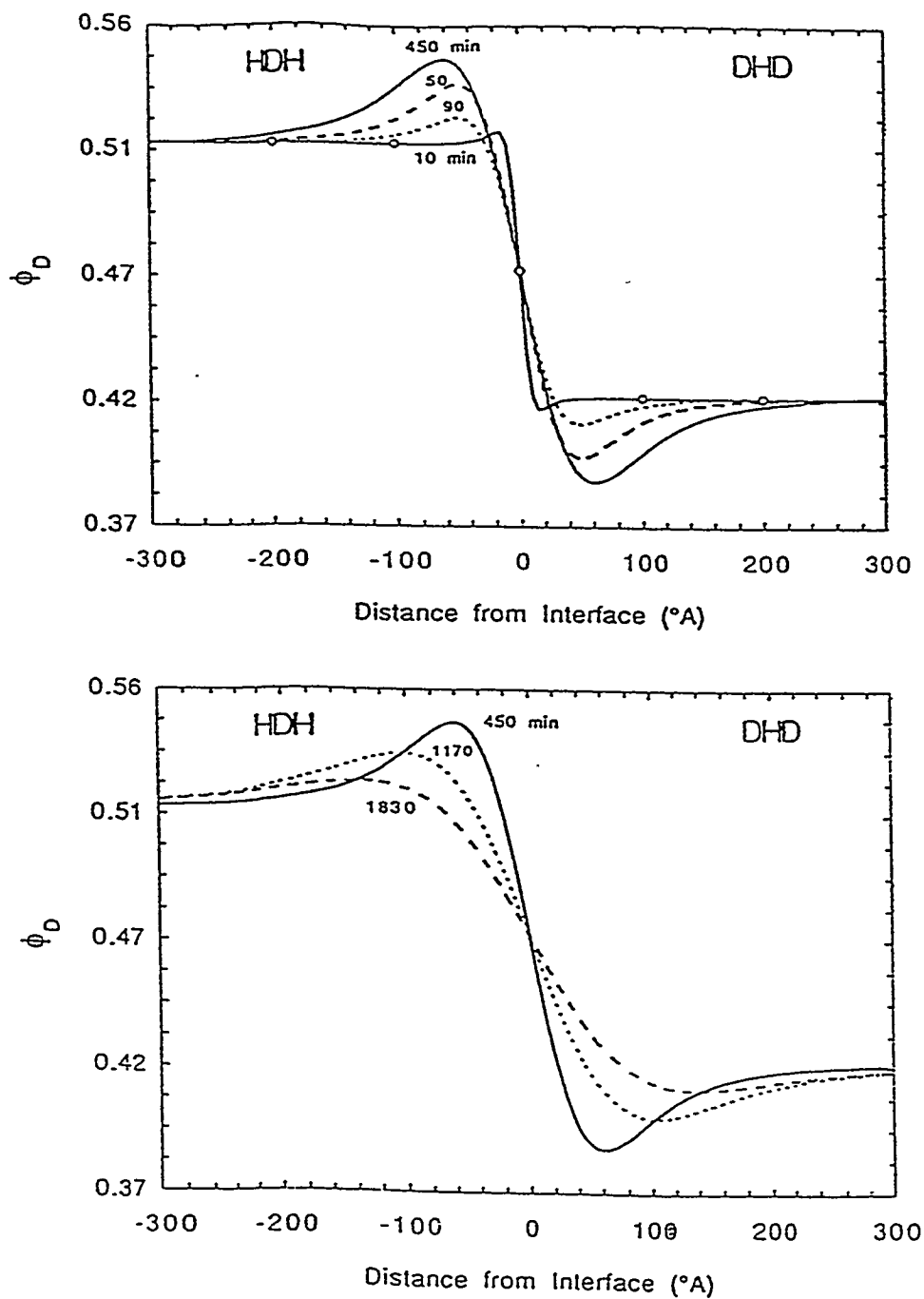


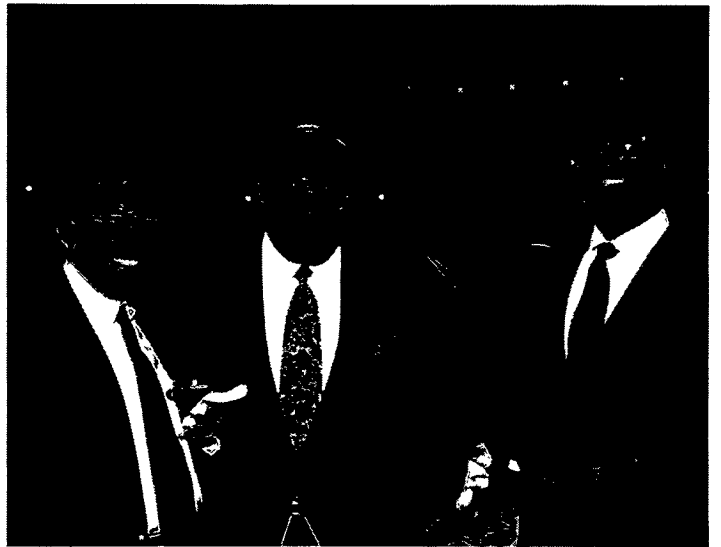
Figure 13. Results of reflectivity measurements of the Deuterium concentration across a labeled polymer interface as a function of distance, for different annealing times.

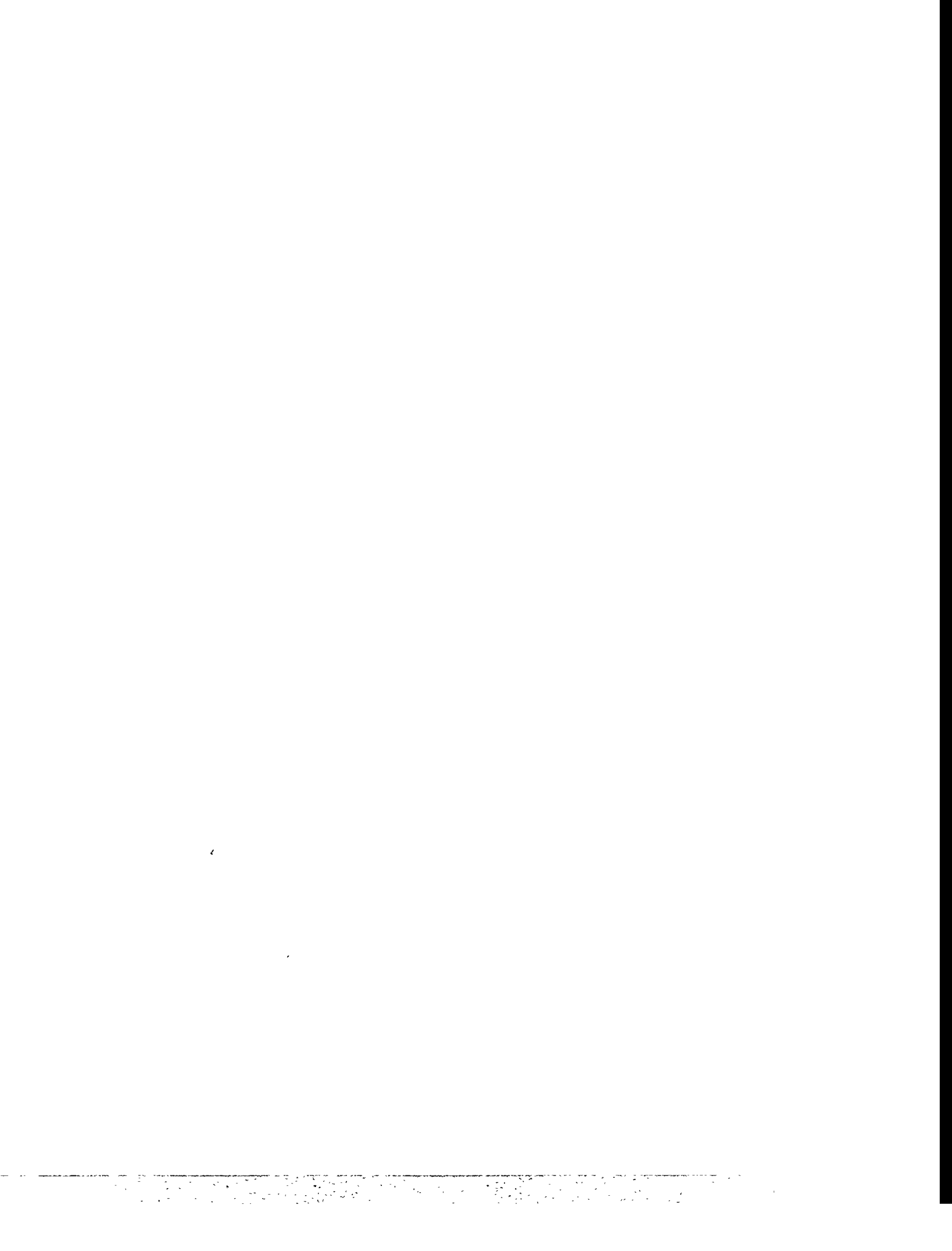
molecules. This produces an enrichment of Ds and corresponding depletion of Hs on one side of the interface and vice versa, so that a region of contrast develops which influences the neutron reflectivity. After long annealing times, when complete molecules have had the chance to pass across, the interface becomes smeared out and the contrast disappears. Figure 13 shows the deuterium density variation as a function of distance, as determined from reflectivity measurements after various annealing times. In the actual measurement, the two materials are not exactly matched in average Deuterium density, so at first there is a sharp step in contrast, then this step spreads out as annealing progresses.

This is the first definitive evidence that polymer diffusion follows DeGennes's reptation model. The demonstration could only have been accomplished with neutrons. It has clear implications for the understanding of polymer bonding and interlayer adhesion.

CONCLUSION

What began as a modest test using Argonne accelerators has grown to represent a highly significant new category of sources for neutron scattering research and other applications, a powerful complement at least and an alternative perhaps, to research reactors for these purposes. Development proceeds on a world wide scale and Argonne's accelerator group, neutron physicists, engineers and materials scientists can justly reflect that they started something good.





SOME NON-HEP APPLICATIONS DEVELOPED AT THE ZGS

Ronald L. Martin
Argonne National Laboratory

Presented at the Symposium on the 30th Anniversary
of the ZGS

May 1994

Introduction

I will talk about 3 programs that have been carried out at the ZGS. These are H^- charge exchange injection, medical applications of protons, and heavy ion inertial fusion. They first appear to be rather different subjects involving accelerator applications for science, medical applications, and energy applications of protons. However there is a common thread that links all three, at least historically. I talked about all three of these subjects at the Symposium on the History of the ZGS in 1979. This talk therefore will briefly remind you of the background of these programs, describe the progress made since 1979, and indicate what I think the future of these programs will be.

H^- Charge Exchange Injection

The negative hydrogen ion is a proton with two electrons bound to it as shown in Fig. 1. The first electron is bound rather strongly while the second is bound much more weakly and can be removed in a strong enough magnetic field or by laser light. Both electrons, however, are removed from the proton whenever the ion passes through even a very thin foil. As a result the ion changes its charge state from - to + and will bend in the opposite direction in a magnetic field as shown in Fig. 1. The proton circulating around the ring may traverse the foil many times but the foil can be so thin that multiple coulomb scattering is not a problem. In traversing the foil the proton does not pick up electrons again so that the process is irreversible and is called non-Liouvillian. This process removes one of the limitations of injection and allows one to continue to inject

for many turns until the circulating current reaches the space charge limit of the ring.

To the best of my knowledge the concept was originated by Moon [1] at Birmingham in 1956 using molecular hydrogen ions. I became aware of it when I visited Dimov at Novosibirsk in 1968. Not only did Dimov [2,3] have the world's most intense negative hydrogen ion source in existence at the time but he was doing charge exchange injection on a small experimental accelerator. We began a development program at Argonne in 1969, and first injected a weak beam into the ZGS [4] in 1969.

The results were most encouraging but the currents were too weak to use this as the operating mode of the ZGS. We proved the principle on the former Cornell electron synchrotron, which was moved to Argonne. The brightness of the circulating beam was increased by a factor of 100 over that of the linac beam, and the reliability of the source and foil proved adequate for use on the ZGS. Charge exchange injection into the ZGS was achieved in 1976 and became the standard operating mode of the accelerator [5]. Thus the ZGS became the first operating accelerator to use this technique. Not only were we able quickly to double the circulating beam of the ZGS but were most pleasantly surprised by an unexpected benefit: the injection conditions were sufficiently relaxed that the pulse to pulse stability of the synchrotron was significantly improved. If the machine were down for any length of time and the start button pushed the very first pulse would be the full intensity. This was unheard of at any working machine at the time.

I had occasion to review the history of non-Liouvillian injection in 1991 at a Symposium on High Brightness Beams at the University of Maryland [6]. I was stimulated to do so by a proposal by Carlo Rubbia [7], Director General of CERN and a Nobel Laureate, to use the non-Liouvillian principle at one stage in the concept of Heavy Ion Fusion. So I produced and published the listing shown in Fig.2. It seems worth reproducing here because it illustrates the connection between what I have been talking about and the initiation of the Heavy ion Fusion Program. I will expand on this connection briefly.

In 1974 I had the idea that, using charge exchange injection, I could store 300 A of 50 MeV protons in a very high field storage ring of about one foot in diameter. Combining the beams from 100 such rings would give a proton beam of one nanosecond duration and 30,000 A peak current. I had never heard of such

currents and thought they might be useful for inertial confinement fusion instead of the laser beams of the Nova program or the (then proposed) electron beams of the Sandia program. Sometime later [8] I had shifted to helium ions rather than protons because it was clear that I could get 4 times the beam energy and still use the charge-changing injection principle. After a few months it became clear that: a) this was not nearly enough energy to ignite the fusion reaction in a reasonably sized pellet, and b) one needed much heavier ions than helium, the heavier the better. Al Maschke [9] of Brookhaven had been talking about using uranium ions at very high energy (up to 100 GeV) to obtain very large beam energies, but did not explain how he would solve the injection problem. It was at about this time that Rick Arnold joined me and we began looking for a non-Liouvillian injection method for heavy ions to make up for the anticipated weak source currents. Rick contacted Joe Berkowitz of Argonne's Physics Division who suggested laser dissociation of the singly charged hydrogen iodide molecule to give neutral hydrogen and singly charged iodine. It would require a Doppler-shifted ruby laser (with 3 volt photons) and intensities that seemed achievable. I believe that it was this non-Liouvillian injection proposal [10] to provide a complete concept for heavy ion fusion that sparked the interest of members of DOE, and the rest is history.

Fig. 2 also lists other accelerator facilities which have adopted the H^- charge exchange injection technique, some because it has proven advantageous, and some (such as ISIS) because it seems the only way to achieve the desired intensity with their existing injection energy and ion source currents. It would appear that H^- charge exchange injection is here to stay and it was planned for the SSC.

Proton Radiography

Many of you will remember the program a large group of us worked on in 1974-76 using 200 MeV protons from the former Cornell synchrotron for diagnostics on human tissue specimens [11].

Proton radiography was pioneered by Andy Koehler [12] of Harvard University and Dr. Steward, a neuropathologist at the University of Chicago, about 1972 using the Harvard 160 MeV proton beam. Dr. Steward approached me about possible use of higher energy proton beams at Argonne. In evaluating how one would do radiography with high energy physics detection techniques (scintillators, phototubes, etc.) I discovered that for a radiation dose to the

patient of 50 mrad only 2×10^8 protons were required for a good image. This intensity is more than four orders of magnitude lower than required for a useful physics machine of the same energy. It meant that a synchrotron designed for this diagnostic application could be simple, relatively inexpensive, reliable, and suitable for use in a hospital. We became very enthusiastic about the practical potential of this program and joined Dr. Steward in the development.

Since normal injection into such a low current machine does not present a problem I proposed to accelerate negative hydrogen ions and use charge exchange as a very simple and inexpensive extraction technique. The alternative, slow resonant extraction, is a very sophisticated procedure. This choice meant using a relatively low magnetic field, 5.6 kG, with a corresponding larger diameter ring, and providing a vacuum of 10^{-10} Torr. Many people object to these requirements. I still believe, however, that the many advantages of H^- acceleration and charge exchange extraction outweigh these disadvantages.

We thought the results we obtained at Argonne, particularly on breast and heart specimens, were spectacular. The radiographs showed differences between the left and right ventricles of the heart (obviously without blood), and showed infected lymph nodes in a breast specimen. Tests on phantoms showed that protons provide significantly higher density resolution than is theoretically possible with x-rays for the same radiation dose to the patient.

We also obtained computed tomography images by rotating the target in a water bath but did not compare the images with x-rays to quantify the results. However, K. Hanson [13] at Los Alamos, at about the same time (1976), did compare proton computed tomography with XCT and came to the same conclusion: protons are definitely superior to x-rays for computed tomography given the same radiation dose. Since a critical issue in any procedure with human patients is the radiation dose that is allowed these should be very important results.

In spite of these positive results we could find no financial support to build the Proton Diagnostic Accelerator and the program died. That would have been the end of this story had not there subsequently occurred a dramatic result in the radiation treatment of cancer using protons.

Proton Therapy

About 1984 major success was announced at Harvard with proton treatment of eye melanomas. These were the results of many years of treatment and focused interest on proton therapy. Eyesight was retained in 93% of the patients treated with protons, whereas the alternative was removal of the eye. Even though only about 1500 people each year have this problem in the US (compared to 500,000 radiation treatments of cancer) it was a turn-around seldom seen in the medical profession. The advantages of protons of allowing better localization of delivered dose for any cancer, first pointed out by Robert Wilson [14] in 1946, became known to many radiation therapists.

These advantages are clear from the graphs [15] of Fig. 3. Energy deposition by x-rays decreases exponentially with penetration depth so that for a deep seated tumor (at 18-23 cm in this example) the dose to healthy tissue in front of the tumor is greater than that delivered to the tumor. Therefore with x-rays treatment must be carried out from many incident directions (a minimum of 4) in order that only the tumor receive a lethal dose with minimal damage to healthy tissue. Energy deposition by protons, on the other hand, is lowest at entrance and increases as the protons slow down, culminating in a sharp maxima called the Bragg peak just before the protons stop. This energy deposition peak is too narrow to cover the longitudinal extent of the tumor so that several different energies (different proton ranges) are required to be used in order to cover the entire tumor with a uniform dose. The resultant dose deposition is shown by the curve called "Spread-out Proton Peak". For a given (required) dose to the tumor less dose is deposited to healthy tissue in front of the tumor and (most importantly) no dose beyond the tumor. The former means that fewer fields (incident beam directions) are required for protons than x-rays to achieve the desired result, and the latter means that one no longer need avoid aiming the incident beam in the direction of a sensitive organ (such as the spinal cord) provided the knowledge of tissue densities is adequately precise. Both of these advantages should simplify the complex task of treatment planning, with implications on the requirements of the beam delivery systems. In addition, the lower dose to healthy tissue with protons can mean either a lower probability of complications or utilizing a higher dose to the tumor for better local control at an acceptable complication rate.

All of the above sounds very positive for the application of protons to cancer therapy. However, along with the advantage of better dose localization goes

the requirement for more precise knowledge of tissue densities (such as 3D computed tomography), and delivery of the 150-250 MeV proton beams are far more complex than for x-ray beams. The added complexity and cost are key issues in the successful development of proton therapy.

Steve Kramer and I, along with John Archambeau, a radiotherapist from Long Island associated with Brookhaven (now at Loma Linda University), met with Jim Slater of Loma Linda to promote the use of protons for therapy. Argonne was a joint sponsor with FNAL of a medical meeting at Fermilab in January, 1985. Out of that meeting grew an organization of physicians, medical physicists, and accelerator physicists called the Proton Therapy Cooperative Group (PTCOG for short). It has become a worldwide organization and is very active. Meetings have been held twice a year since 1985 with the latest one in England. A semiannual newsletter called "Particles", edited by Janet Sisterson at Harvard, shows the status of proton therapy throughout the world. There are presently 16 facilities carrying out proton therapy, and 10 more actively under development. As of January 1, 1994 a total of about 13,000 patients have been treated with protons. About half of these have been treated with the Harvard 160 MeV cyclotron, which has been utilized for this purpose since 1961.

To put this in perspective, the numbers above are very small compared to the number of patients treated with high voltage x-rays. There are about 2000 electron linacs in use in hospitals or clinics for this purpose in the US. There are lots of reasons why x-rays continue to dominate the practice of radiation treatment but one of them is the added complexity of treatment with protons.

Jim Slater has had the first accelerator specifically designed for proton therapy installed at Loma Linda University Medical School. It was designed and constructed by Fermilab and began operation in October 1990. The facility includes 3 isocentric gantries, designed to treat patients from any incident direction. The last of the 3 will be put into operation in the next few months and when the facility is fully utilized it will treat 1000 patients/year with about 30 radiation fractions/patient. In a very few years Loma Linda will overtake Harvard in the total number of patients treated. The gantries are large and expensive. The stated cost for the entire facility, including buildings, is about \$70M.

Massachusetts General Hospital in Boston, the group responsible for the radiation treatments on the Harvard cyclotron since 1961, have contracted with

the Belgium company, IBA, to build and install a 230 MeV cyclotron on the Hospital campus to replace the Harvard cyclotron. The new facility is to include 1 or 2 gantrys and is expected to begin treating patients in 1998.

The little company I formed in late 1984 to promote proton therapy and radiography, ACCTEK Associates (with some of you as partners), has had 5 SBIR grants from the National Cancer Institute. Two (Phases I and II) were on the Proton Medical Accelerator. Prototype magnets and vacuum chambers for my version of the H^- accelerator were built and the projected relatively low cost of a low field synchrotron was confirmed. Two (again Phases I and II) were on the Beam Delivery System. A magnetic raster scanning system for both therapy and radiography was built, along with a rotating beam line I refer to as the low cost alternative to an isocentric gantry. These both worked very well and are presently on display as technology transfer over in the ZGS ring room. The fifth grant (a Phase I) was on a Radiographic Aid to Proton Therapy. The raster scanning system was utilized on a 200 MeV proton beam at the Indiana University Cyclotron Facility to demonstrate data acquisition at a rate that would make proton radiography practical in a hospital setting. More than 50,000 samples were taken, digitized, processed and stored in 1/8 second, adequate for a radiograph if the data had been of radiographic quality. This is to be compared with the 18 minutes per radiograph required in the earlier experiments at Argonne (without the scanning beam). I thought it was the most successful of my Phase I grants. However, applications for the construction and R&D Phase II has been turned down twice. It is all the more disappointing because I think proton radiography, and particularly computed tomography, is very important to the widespread use and success of proton therapy.

No one in this country has acknowledged that the advantages of H^- acceleration and charge exchange extraction for proton therapy outweigh the disadvantages. However, a Russian group has designed a medical facility for a hospital in Moscow using this technique. Given the economic situation in Russia it seems unlikely that such a facility will be built in the near future. More encouraging is the proposal of a group in Milan, Italy to build an H^- medical facility in Verona (near Milan). The facility is to be upgradeable to acceleration of oxygen ions in the future if this option appears advantageous at the time. I have spent about a year (part-time) working with them (with consultants from Fermilab, Brookhaven, and Los Alamos) on the conceptual design of the accelerator. The conceptual design report is to be submitted to the funding authorities in the fall, and the expectation of a positive result are reasonably

high.

To summarize this section on medical uses of protons, I am convinced that a number of new facilities will be built. With the present ideas of the community, however, it might lead only to facilities in a few large regional centers in the United States (perhaps 10-20). If the cost can be substantially reduced, as I have been claiming it can be, the use of protons will be much more widespread. Even if the time scale for such development turns out to be beyond my lifetime someone is sure to pick up the challenge, so I think protons are in your medical future.

Heavy Ion Inertial Confinement Fusion

The connection of the Argonne Heavy Ion Fusion concept to the success of non-Liouillian injection was related earlier. The experimental program, dubbed HEARTHFIRE by Rick Arnold, began in 1976 after the first of four annual workshops. The idea caught on internationally and an International Symposium has been held every two years beginning in 1980 with the latest in Frascati, Italy. The Germans, Russians, and Japanese adopted the RF linac, storage ring approach we proposed, while Lawrence Berkeley Laboratory suggested a single pass at high current through an Induction Linac. About 1981 the United States decided to support only one program on HIF. The LBL approach was chosen and HEARTHFIRE was shut down, in spite of its success up to that time. The Berkeley program has been supported since then at a funding level of 4-5 M\$/year.

Of the foreign programs by far the strongest is at GSI in Darmstadt, Germany. They have carried out a number of pertinent experiments with their two heavy ion rings (mainly used for studies on nuclear physics). In 1982 they produced a design concept of a Heavy Ion Fusion power plant. It was called HIBALL and a line drawing of this concept is shown in Fig. 4. I include this to illustrate a few points that are important in order to understand this program. One is the large size and complexity of such a facility with a 5 km linac, 10 storage rings, 4 large reactors (1000 MWe each), and 20 transport lines into each reactor. The reason for this is that the main question being asked at the time was what was the cost of electricity from fusion. It required a facility of this size to project a cost of 4.5 cents per kilowatt-hour and be competitive with electricity production by nuclear energy or coal. The cost and complexity of such a large plant represent a difficult hurdle to overcome, and perhaps accounts for the relatively slow pace of the development of the concept. Consequently this is not a very encouraging

progress report.

About three years ago the problems of radioactive waste at Hanford and Savannah River, and the problem of spent fuel rods of nuclear reactors was widely discussed in the news. Chuck Bowman [16] of Los Alamos National Laboratory proposed the ATW (Accelerator for Transmutation of Wastes), a very powerful proton linac to produce spallation neutrons for transmuting actinides and long-lived fission products into stable isotopes. At this time I realized that the 14 MeV neutrons of the DT fusion reaction were far more valuable for handling the high level radioactive waste problem of nuclear reactors than they were for producing energy alone. For the same accelerator beam power many more neutrons are produced by fusion (because of the target gain of about 100) than from spallation and the high energy neutrons induce fission in all actinides. Hence the fusion neutrons transmute actinides (with additional energy production) more efficiently than thermal or fast neutrons. The proper question then is not what is the cost of electricity produced by fusion energy, but rather will it work and how does one adapt it to eliminating a major problem of nuclear energy, that of the long-lived high level radioactive waste.

Of course I believe that, given adequate R&D, Heavy Ion Fusion can be made to work and will be economically advantageous as a fission-fusion hybrid system. I have since published two papers [17,18] addressing these issues but have so far not attracted much support. Perhaps it is still premature, but the time for Heavy Ion Fusion will eventually arrive.

References

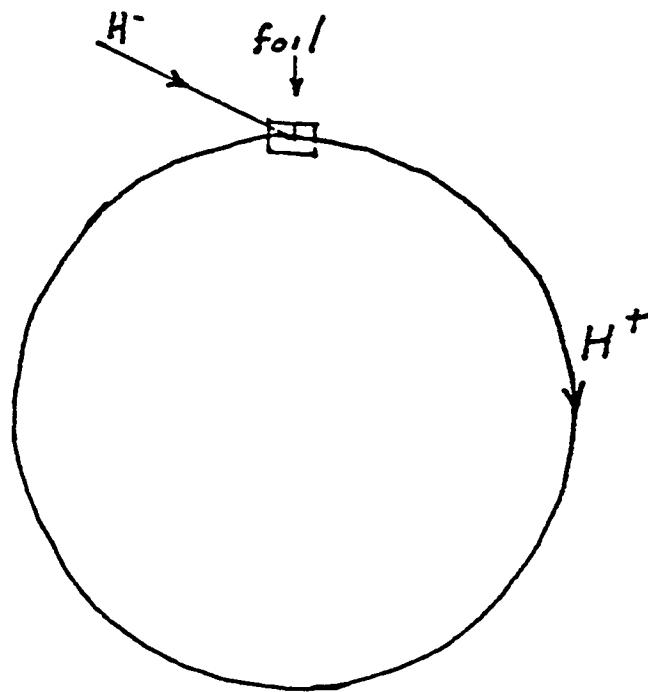
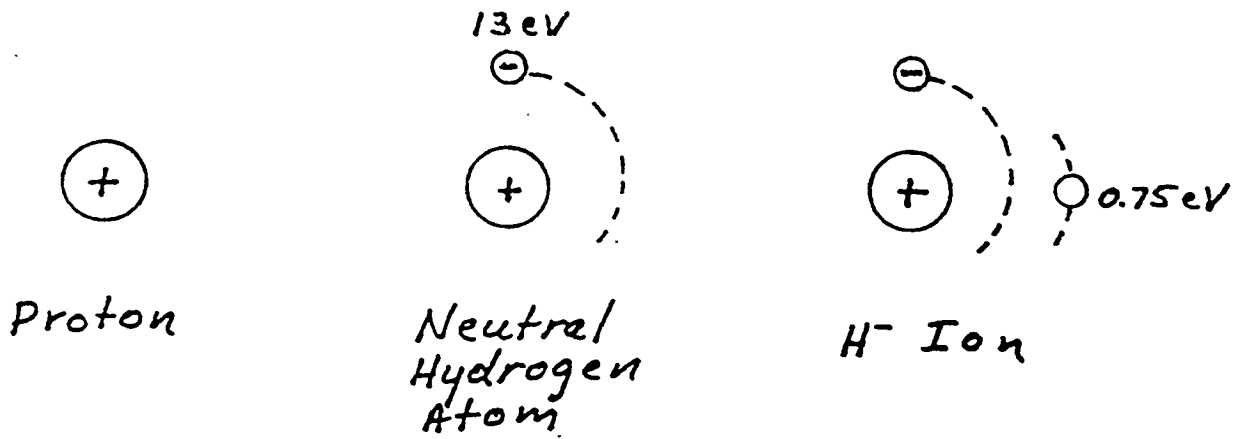
- [1] P.B. Moon. Proposal for Injecting Protons into a Synchrotron by Dissociation of Molecular Hydrogen Ions, CERN Symposium on High Energy Accelerators and Pion Physics, Vol. 1, (June 1956) pp. 231-3.
- [2] G. I. Budker, G. I. Dimov. On the Charge Exchange Injection of Protons into Ring Accelerators, Int. Conference on High Energy Accelerators, Dubna, USSR (Aug 1963). Published by the U.S. Atomic Energy Commission's Div. Tech. Inf., CONF-114, pp. 1372-77.
- [3] G. I. Dimov, et al. USSR National Conference on Particle Accelerators, Moscow, USSR, (Oct 1968).

- [4] R. L. Martin. The Argonne Zero Gradient Booster, IEEE Trans. NS-18, #3, (June 1971) pp. 953-956.
- [5] C. W. Potts. Negative Hydrogen Ion Injection into the Zero Gradient Synchrotron, IEEE Trans. NS-24, #3, (June 1977) pp.1385-89.
- [6] R. L. Martin. Proc. Symposium on High-Brightness Beams for Advanced Accelerator Applications, Univ. Maryland, AIP Conf. Proc. No.253, Particles and Fields Series 47, (1991) pp. 232-5.
- [7] C. Rubbia. Particle Accelerator Developments and their Applicability to Ignition Devices for Inertial Fusion, NIM, A278, (1989) pp. 253-65.
- [8] R. L. Martin. The Ion Beam Compressor for Pellet Fusion, IEEE Trans. NS-22, #3, (1975) p1763.
- [9] A. W. Maschke. Relativistic Heavy Ions for Fusion Applications, IEEE Trans. NS-22, #3, (1975) p1825.
- [10] R. L. Martin, R. C. Arnold. Heavy Ion Accelerators and Storage Rings for Pellet Fusion Reactors, Argonne Internal Report, RLM/RCA-1, (Feb. 9, 1976).
- [11] D. R. Moffett, et.al. Initial Test of a Proton Radiographic System, IEEE Trans. NS-22, #3, (1975) p1749.
- [12] A. M. Koehler. Proton Radiography, Science, Vol. 160, (1968) p 303; V.W. Steward, A. M. Koehler. Proton Beam Radiography in Tumor Detection, Science, Vol. 179, (1973) p 913.
- [13] K. M. Hanson, et.al. The Application of Protons to Computed Tomography, IEEE Trans. NS-25, (1978) p 657; Ibid, NS-26 (1979) p 1635.
- [14] R. R. Wilson. Radiological Use of Fast Protons, Radiology, 47 (1946) p 487.
- [15] Note: Many similar graphs of the comparison of energy deposition by protons and x-rays exist. This one was taken from a Loma Linda brochure on proton therapy.

[16] Los Alamos Internal Report LA-UR-90-4432, A Los Alamos Concept for Accelerator Transmutation of Waste and Energy Production (ATW), Dec. 10-12. 1990.

[17] R. L. Martin. The Fusion-Fission Burner, Proc. Int. Symp. on Heavy Ion Inertial Fusion, Monterey, CA (Dec 1990) pp. 453-7.

[18] R. L. Martin. Prospects for a Fusion-Fission Hybrid, Los Alamos Report UC-940 (Nov 1991), Specialist Meeting on Accelerator-Driven Transmutation Technology for Radwaste and Other Applications, Saltsjobaden, Stockholm, Sweden, June 24-28, 1991, pp.594-600. Compiled by R. A. Jamison.



H^- Charge Exchange Injection

$$H^- \rightarrow H^+ + 2e$$

Irreversible \equiv Non-Liouvillian

Fig. 1. H^- Charge Exchange Injection

NON LIOUVILLIAN INJECTION

$H_2^+ \xrightarrow{\text{gas}} H^+$

Moon (Birmingham 1956)

$H^- \xrightarrow{\text{gas}} H^+$

Dimov (Novosibirsk 1968)

$H^- \xrightarrow{\text{foil}} H^+$

Martin (ANL 1970-76)

ZGS

ZGS BST (IPNS)

100 x Brightness
Stability

KEK BST

FNAL BST

AGS (BNL)

PSR (LANL) (field stripping)

ISIS (Rutherford)

$HI^+ \xrightarrow{\text{Laser}} I^+$

Martin, Arnold (1976) HIF

$Bi^+ \longrightarrow Bi^{2+}$

Rubbia (1988) HIF

$Ba^+ \longrightarrow Ba^{2+}$

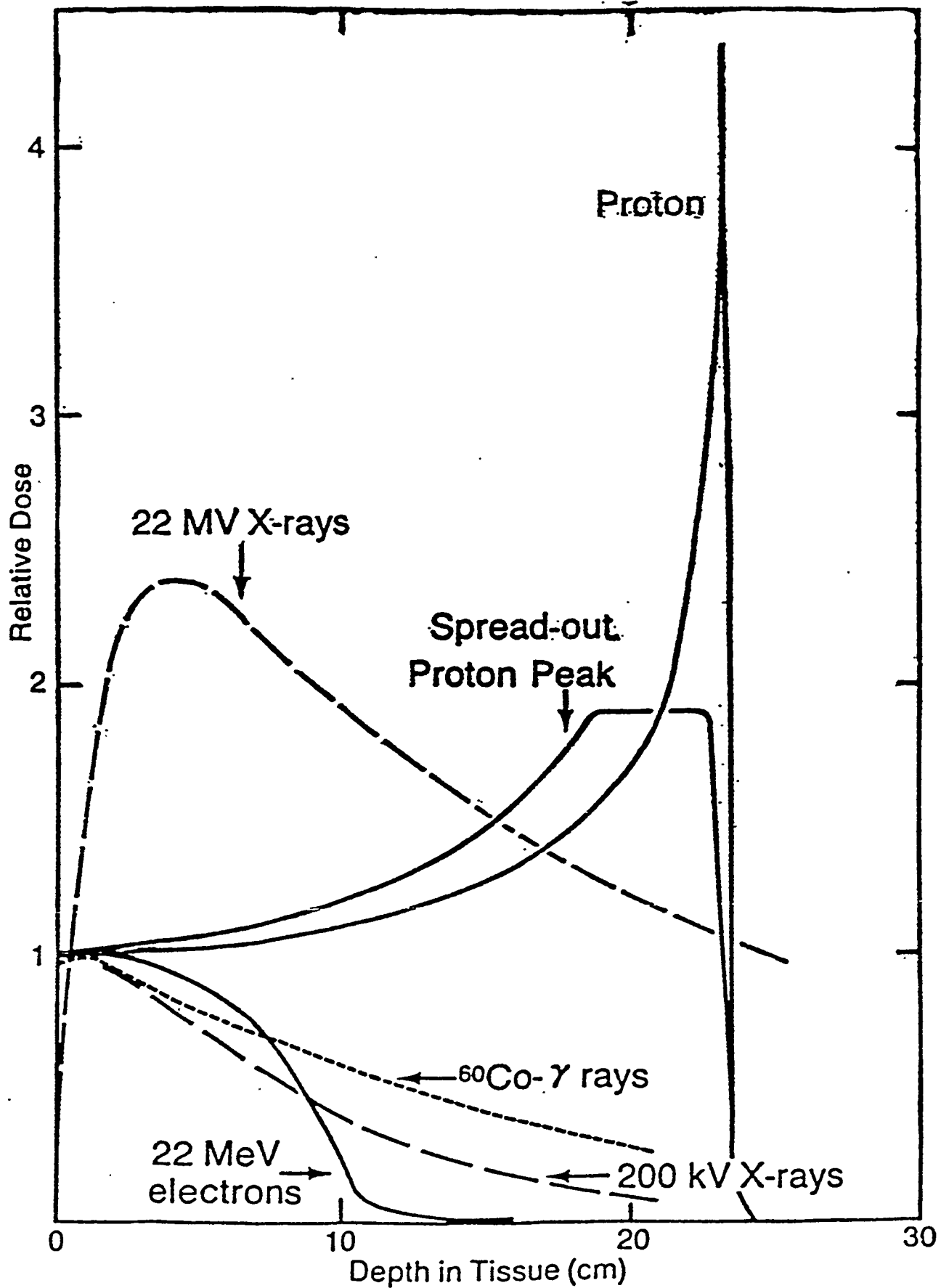
Hofmann (1990) HIF

Extraction $H^- \xrightarrow{\text{foil}} H^+$

TRIUMPF (Vancouver)

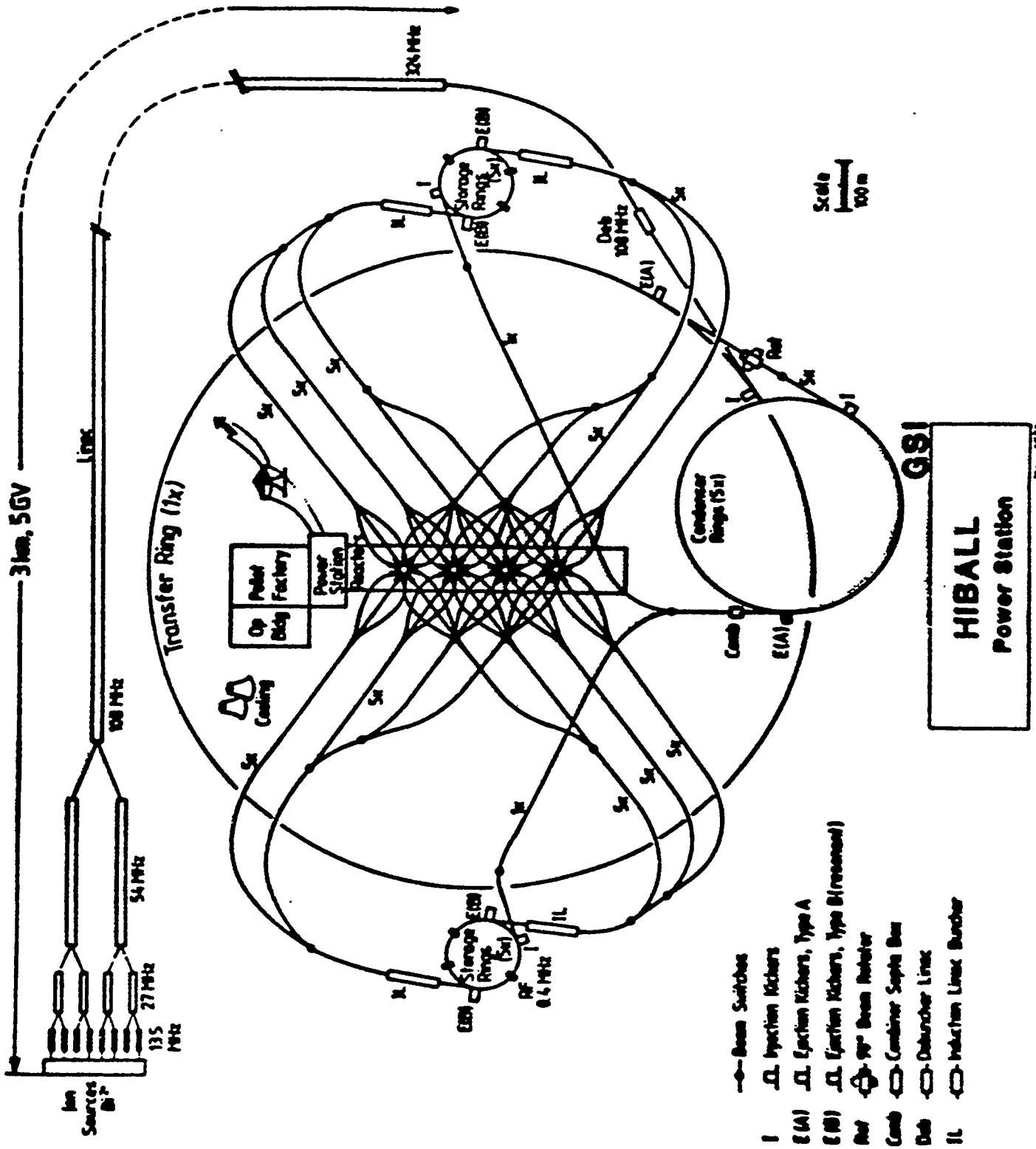
Proposed for ACCTEK Proton Therapy,
Proton Radiography and Computed Tomography

Fig. 2. Non Liouvillian Injection



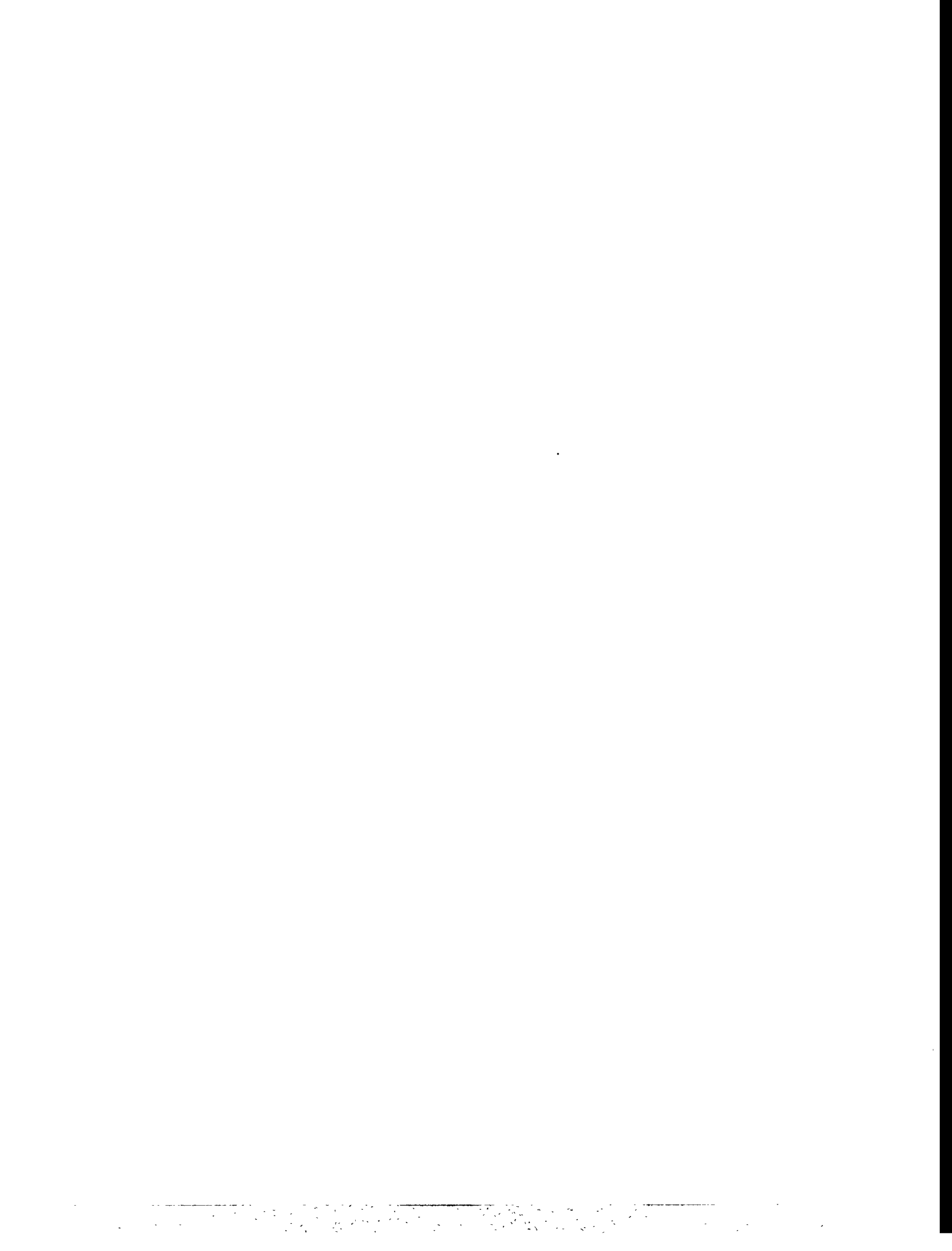
Comparison of depth dose distribution for X-, γ -ray and electron beams with distribution of a proton beam.

Fig. 3. Energy Deposition of Protons and X-Rays

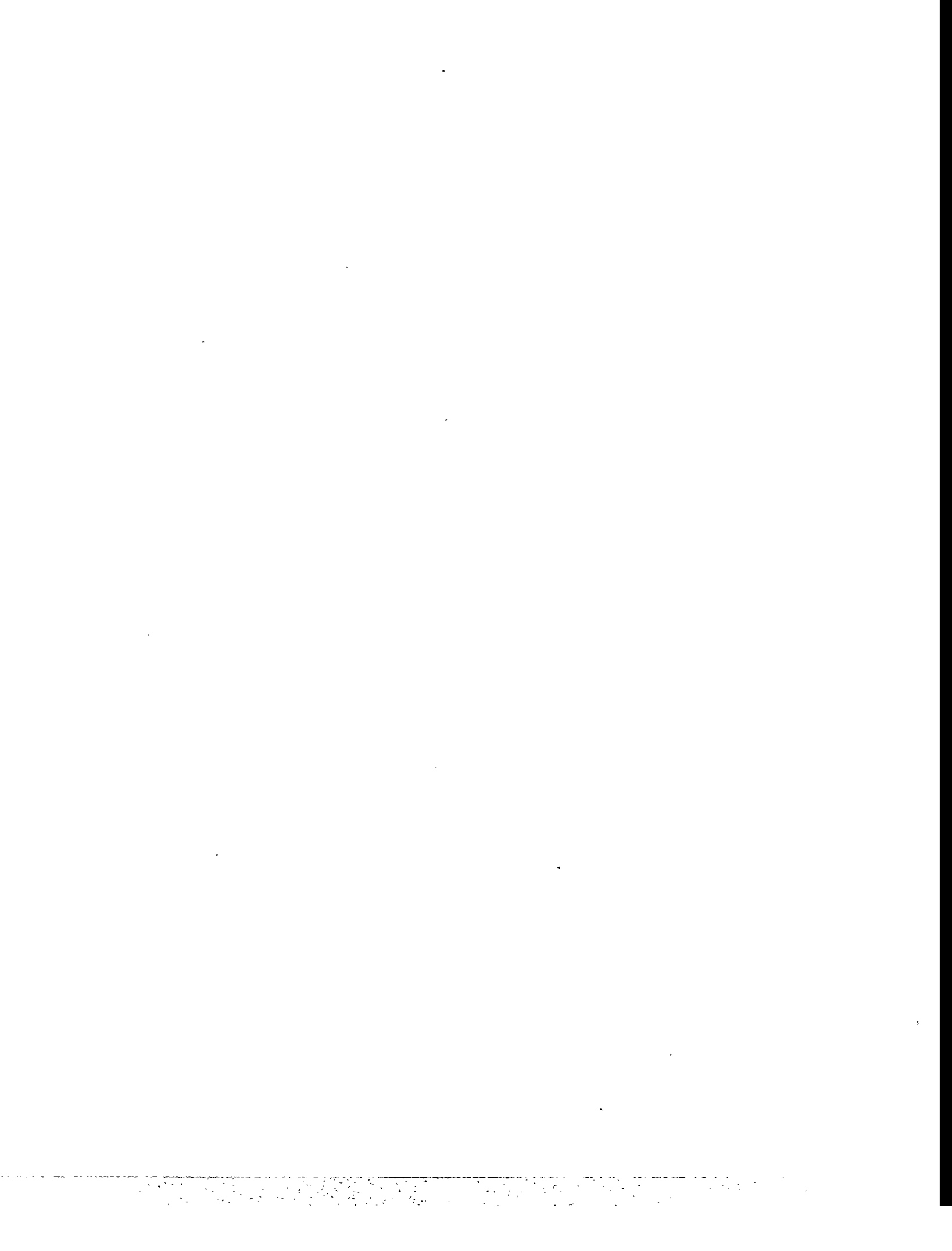


- Beam Switches
- I Ion Injection Kickers
- E (A) E Ejection Kickers, Type A
- E (B) E Ejection Kickers, Type B (recessed)
- RF 90° Beam Rotator
- Comb Combiner Saphire Box
- Deb Debuncher Lines
- IL Induction Lines Buncher

Fig. 4. Hiball Power Station







FROM HYPERONS TO APPLIED OPTICS:
"WINSTON CONES"
DURING AND AFTER THE ZGS ERA

Earl C. Swallow

*Department of Physics, Elmhurst College
Elmhurst, Illinois 60126
and
The Enrico Fermi Institute, The University of Chicago
Chicago, Illinois 60637*

This paper discusses developments in light collection which had their origin in efforts to construct high performance gas Čerenkov detectors for precision studies of hyperon beta decays at the ZGS. The resulting devices, know generally as "compound parabolic concentrators," have found applications ranging from nuclear and particle physics experiments to solar energy concentration, instrument illumination, and understanding the optics of visual receptors. Interest in these devices and the ideas underlying them stimulated the development of a substantial new subfield of physics: nonimaging optics. This progression provides an excellent example of some ways in which unanticipated — and often unanticipatable — applied science and "practical" devices naturally emerge from first-rate basic science. The characteristics of this process suggest that the term "spinoff" commonly used to denote it is misleading and in need of replacement.

INTRODUCTION

Unexpected practical applications arising from research in basic science (or "curiosity driven science" in today's parlance) are commonly viewed as lucky accidents — products of serendipity. When we examine the growth and origins of nonimaging optics and its varied applications, a quite different view emerges.

We find a concrete contemporary example of the **natural progression** which leads from basic science to (*a priori* unanticipated) applications. As is often the case, the intellectual content of the original basic science (elementary particle physics) appears to be quite remote from the areas of final application (solar energy, optics of vision, instrument illumination, *etc.*).

In this paper I chronicle (sometimes quite personally) some significant aspects of this progression for nonimaging optics. I also attempt to elicit from this particular history an understanding of why such a **progression** is, in fact, to be expected even though the **specific outcomes** cannot usually be anticipated. I have drawn substantially on information and ideas originally presented in my earlier *Arthur Holly Compton Lectures*¹. More detailed discussion of nonimaging optics and its applications can be found in a recent advanced text² and in a semi-popular article³ in *Scientific American*.

THE HYPERON CONNECTION

One of the exciting new ideas of particle physics in the early 1960s was the Cabibbo Model⁴ which used ("flavor") SU(3) symmetry⁵ to extend the concept of a Universal V-A Weak Interaction⁶ to strange particles and particularly to hyperon beta decays. An experiment to test this model was a natural feature of the experimental program at the ZGS. The most accessible process was the beta decay of the lambda hyperon: $\Lambda \rightarrow pe^{-}\bar{\nu}$. Such an experiment (E38) was undertaken by a collaboration led by Tom Romanowski (then at Argonne and Ohio State University) and Roland Winston (then a new Assistant Professor at the University of Chicago). I had the privilege of joining this group as a graduate student (working with Peter R. Phillips) from Washington University in St. Louis.

The primary experimental challenges arose from the rarity of $\Lambda \rightarrow pe^{-}\bar{\nu}$ decays: Λ production accounts for only a small fraction of the total cross section,

and the beta decay branching ratio is less than 10^{-3} . The dominant competing charged decay is $\Lambda \rightarrow p\pi^-$, so it is necessary to trigger on electrons and reject pions to study the beta decay. In addition, polarized lambdas were needed to study the structure of the decay interaction directly by measuring parity violating spin correlations of the form $\langle \hat{\sigma} \cdot \hat{p} \rangle$ in the style of the classic Argonne experiment⁷ on polarized neutron decay (performed at the CP5 research reactor).

The reaction $\pi^- p \rightarrow \Lambda^0 K^0$ at 1025 MeV/c (just below ΣK threshold) was known to be a reasonable source of polarized Λ hyperons unencumbered by competing associated production channels. An intense π^- beam at this energy was well within the capabilities of the ZGS. To study the decay products, a large-acceptance magnetic spectrometer capable of analyzing the relatively stiff decay protons as well as the much softer decay pions and electrons was needed. A threshold gas Čerenkov counter with large phase space acceptance was required to distinguish between the desired electrons from $\Lambda \rightarrow pe^- \bar{\nu}$ decays and the more copious decay pions from $\Lambda \rightarrow p\pi^-$ decays. Figure 1 shows our final experimental layout.

To meet the experimental challenges, several significant technical development efforts were necessary. Development of large thin-plate (optical) spark chambers for the magnetic spectrometer and small high-rate chambers for use in the intense π^- beam was undertaken at Argonne. The two of us from Washington University attacked the problem of understanding the highly non-uniform magnetic field of the spectrometer magnet and analyzing particle trajectories in it.

At the University of Chicago's Enrico Fermi Institute (EFI), Roland Winston undertook the design and construction of the required gas Čerenkov counter in collaboration with EFI chief engineer Henry Hinterberger. Because the decay electrons diverge with a wide range of angles from a rather large

apparent source (and the same is therefore true of the faint Čerenkov light), it was necessary to efficiently concentrate the available Čerenkov light onto the photomultiplier tubes (PMTs) in the counter. If the light had been collected with conventional imaging devices, an inordinate number of PMTs would have been required (about 100 PMTs with 11-cm photocathode diameter — a quite manageable system today, but not in 1964-65).

Starting with the recognition that there is no need to "take a picture" of the light source, but only to concentrate the light onto the PMTs, the Chicago intellectual style asserted itself. The problem was examined at the most basic level in an attempt to identify the relevant fundamental limitations on light collection and understand their origins. The Čerenkov light in such a detector can be envisioned as diverging from a surface of effective transverse linear size D with angles ranging between 0° and some maximum value θ_{Max} . If non-absorbing (ideal) reflectors are used to concentrate this light onto a smaller surface of effective transverse linear size d , the angular divergence will increase to θ_f . Phase space conservation then gives the condition for maximum concentration: $D \sin(\theta_{\text{Max}}) = d \sin(\theta_f)$. For plane receivers like our PMT photocathodes, $\theta_f = 90^\circ$ is the largest possible final divergence angle, and thus the maximum possible linear concentration is

$$\frac{D}{d} = \frac{1}{\sin(\theta_{\text{Max}})} . \quad (1)$$

If this linear concentration is achieved symmetrically in both transverse dimensions, then the initial source area (A_i) is proportional to D^2 and the final receiver area (a_f) is proportional to d^2 . The resulting maximum concentration is

$$\frac{A_i}{a_f} = \frac{1}{\sin^2(\theta_{\text{Max}})} . \quad (2)$$

Further, phase space conservation implies that this maximum concentration can be achieved if and only if the light collecting system accepts all rays incident at angles up to θ_{Max} and rejects all rays incident at angles greater than this. That is, the angular acceptance must be a step function. If this is not the case, either some of the incident light is failing to pass through the system, or the system has some unused phase space acceptance which could (in principle) be used to achieve greater concentration.

Figure 2 shows the original construction⁸ for achieving such a maximum concentration in two dimensions (*i.e.*, for meridional rays). A parabolic reflector is constructed starting at point B on the edge of the light receiver (photocathode). The focus of this parabola is at point A on the opposite edge, and its axis is tilted downward at an angle θ_{Max} . Clearly rays entering parallel to the axis and striking the reflector will be focused at point A, and those entering with upward angles smaller than θ_{Max} will be focused somewhere on the receiver between point A and point B. A symmetrical parabolic reflector starting at point A with point B as a focus and axis tilted upward at θ_{Max} then provides a collector which achieves the maximum linear concentration of Eq. 1. A three dimensional (3D) concentrator (frequently called a "cone" or "funnel") matched to the PMT geometry naturally results when this shape is rotated about the z-axis. It is important to recognize that the resulting reflector surface is not a paraboloid of revolution.

The first non-imaging light collector with this shape, later given the descriptive name⁹ "compound parabolic concentrator" or CPC, was built by Roland Winston and his EFI coworkers in 1965. Almost a decade later, in the mid-1970s, we learned that CPCs had also been discussed nearly simultaneously (but in quite different contexts) by V. K. Baranov¹⁰ in the Soviet Union and by M. Ploke¹¹ in Germany.

Interesting theoretical and functional considerations emerged even at the very start⁸. On the theoretical front, the 3D cones do not quite achieve the maximum concentration given by Eq. 2: the angular acceptance only approximates a step function. While the original 2D construction is quite rigorous (yielding the maximum linear concentration of Eq. 1), it applies only to meridional rays in the 3D case. A few skew rays which enter the cone at angles less than (but nearly equal to) θ_{Max} are reflected back out the entrance aperture never reaching the exit aperture.¹² Here was a clear call for additional theoretical investigation of these devices and of light concentration in general.

On the functional front, cones of substantial concentration turn out to be rather long, but they can be truncated at 1/2 to 2/3 the design length with very little loss of aperture. This can make actual cone construction much easier. In addition to the light concentration achieved, placing such cones in front of rigid, encapsulated detectors like PMTs can have significant practical advantages. For example, building a hexagonally close packed array of concentrators with their entrance apertures slightly overlapped makes it possible to collect light from an area much larger than a single PMT can accept while simultaneously eliminating (or at least reducing) the light losses which would otherwise result from dead areas between the photocathodes in a PMT array. When losses are reduced in this way, a proportionate decrease occurs in the net concentration for the array. However, this decrease is quite acceptable when the photons of interest are in short supply.

The E38 gas Čerenkov counter was designed and tested¹³. It employed a total of 28 PMTs grouped in 4 arrays (or clusters) of 7 hexagonally close packed concentrators and PMTs. This reduced dead area losses from 56% (including space for magnetic shielding around the PMTs) to about 5% at a cost of requiring 28 PMTs rather than the absolute minimum of 18. With pion

rejection greater than 1000 and high electron efficiency¹³, the counter performance was outstanding.

Data taking for E38 began at the ZGS in Fall 1967 and continued for about 2 years. This period also gave rise to applications of solid (*i.e.*, dielectric filled) CPCs: (1) to concentrate scintillation light transmitted by total internal reflection through a twisted light pipe¹⁴ and (2) to enhance the concentration of light originating in air or vacuum by the square of the index of refraction (n) of the dielectric¹⁵. Equations 1 and 2 for maximum concentration were thus effectively generalized to

$$\frac{D}{d} = \frac{n}{\sin(\theta_{\text{Max}})} \quad (3)$$

and

$$\frac{A_i}{a_f} = \frac{n^2}{\sin^2(\theta_{\text{Max}})} \quad (4)$$

The theory of these limits and the related devices was also developed more explicitly¹⁶ in the context of Hamiltonian optics¹⁷ including a derivation of the generalized étendue¹⁸ and clarification of relationships to earlier work by Marshall¹⁹, Garwin²⁰, Williamson²¹, Witte²², and Luneburg¹⁷. The "edge ray" and "maximum slope" principles² for designing concentrators, foreshadowed in the original⁸ CPC construction, also began to take shape¹⁶.

Preliminary results from E38 provided the basis for my Ph.D. dissertation, and in July, 1970 I joined Roland Winston at the EFI. Subsequent E38 results²³ were in general agreement with the Cabibbo Model though they indicated a smaller than expected neutrino asymmetry. This indication persists to the present day. They also played an important role in unambiguously establishing²⁴ the relative sign of the vector and axial-vector interactions in strangeness-changing weak processes thereby supporting the need for a charmed quark to suppress

strangeness-changing neutral current processes. The E38 Čerenkov counter was subsequently used in a program of experiments²⁵ at the ZGS Effective Mass Spectrometer.

Ensuing experiments on polarized $\Sigma^- \rightarrow ne^-\bar{\nu}$ at the ZGS²⁶ (E347) and at Fermilab²⁷ (E715) ultimately provided more pointed evidence²⁸ in support of the Cabibbo Model (generalized to Cabibbo-Kobayashi-Maskawa mixing²⁹ for three quark generations). The ZGS experiment (see Figure 3) employed three novel CPC Čerenkov counters³⁰ (see Figure 4) to identify decay electrons. The Fermilab experiment identified beam electrons for calibration with a low-pressure CPC threshold Čerenkov counter. Use of CPCs in both scintillation detectors and Čerenkov counters has become wide-spread in experimental particle physics.

LIGHT FROM THE SKY

Jay Enoch of the Washington University School of Medicine first noted the similarity between CPCs and the tapered portion of cone receptors in the human retina. Further analysis³¹ showed an excellent agreement between the external shape of the tapered portion and a CPC with $\theta_{\text{Max}} = 13^\circ$. Hearing this described at an EFI Seminar, Ricardo Levi-Setti observed that the crystalline cones of the *Limulus polyphemus* (horseshoe crab) eye have a similar shape. The compound eye of *Limulus* has long been a subject of interest³², at least in part because its structures are rather large (the cones are about 0.2 mm in diameter) and therefore amenable to direct investigation. Measurements³³ of refractive index, external shape, and acceptance cut-off angle all match a dielectric CPC with $\theta_{\text{Max}} = 19^\circ$. Of course, the reflection mechanism in these CPCs is total internal reflection. Detailed directional sensitivity and shape measurements³⁴ on turtle photoreceptors also are in excellent agreement with a CPC model. This work substantially clarifies³⁵ the origin of the directional selectivity evidenced by

these visual systems: it arises primarily from the shape and relative refractive index of the individual receptors.

During discussions of the "energy crisis" in the early 1970s, T. M. Knasel and I repeatedly offered the general suggestion that these ideas and devices should be useful for solar energy applications, but to little effect. This changed markedly in mid-1973 when Robert G. Sachs, an EFI Professor then serving as Argonne Director, called attention to a well-defined problem. A study panel examining energy options had concluded that solar energy did not appear to be economically viable. A major reason for this was the high cost of the equipment necessary for large concentrator arrays³⁶ to accurately track the sun's daily motion across the sky.

Before the end of the year, this gave rise to the recognition³⁷ that the original two-dimensional CPC shape (see Figure 2) could be reflected and translated to form a concentrating trough (sometimes called a "2D" or "cylindrical" concentrator) as shown in Figure 5. A trough concentrator with its long axis aligned in the east-west direction can achieve concentrations up to about 10x **without diurnal tracking** of the sun. Concentrations up to about 2x can be achieved with completely stationary systems, while periodic elevation angle adjustment through the seasons of the year is required to achieve values in the 2x to 10x range. With encouragement from EFI Director John Simpson and support from the Greenwalt Fund, a prototype concentrator was completed in September, 1973. In principle, a CPC trough (with reflecting ends) will achieve the maximum concentration given by Eq. 1 (or Eq. 3 if filled with refracting material). The original CPC conception^{8, 14-16} (which assumed a flat receiver at the exit aperture) was soon generalized³⁸ for a variety of receiver geometries.

The evident potential of these concentrators combined with concern about the national energy crisis clearly called for a targeted research effort³⁹. The

University of Chicago and Argonne National Laboratory moved quickly to form a collaboration (with primary financial support from the U. S. Energy Research and Development Administration, predecessor to the U. S. Department of Energy) to develop solar energy applications of nonimaging concentrators. Among the collaborators were William Schertz and Ari Rabl (a senior engineer and a theoretical physicist) at Argonne and Roland Winston, Joseph O'Gallagher, Manuel Collares-Pereira, and Keith Snail (two experimental physicists and two physics graduate students) at Chicago. A test facility located in the overflow parking area across from the front of the Argonne High Energy Physics building (Building 362) is shown in Figure 6.

Over a number of years this group developed additional solar concentrator and receiver designs, analyzed thermal performance, studied collection of diffuse solar radiation, identified promising areas of application, clarified functional advantages and problems, explored materials and methods for concentrator fabrication, examined shape tolerances, pursued industrial technology transfer, tested concentrator assemblies, and initiated large scale demonstration projects. Figure 7 shows one demonstration array. As the energy crisis faded from view⁴⁰, the impetus for commercialization of solar energy in the United States diminished, and pursuit of nonimaging solar concentrator applications shifted to Australia, Europe, Israel, and Japan.

As initial interest in solar energy applications was growing, an exciting scientific application also emerged. Roger Hildebrand of the EFI recognized the potential of nonimaging concentrators for infrared astronomy. There the increase of detector noise with sensitive area is a serious limitation. He and Doyal Harper led a team which developed⁴¹ an infrared CPC coupled to a cavity containing a bolometer and carried out a series of observations⁴². A University of California group⁴³ independently employed nonimaging concentrators to measure the peak

of the cosmic background radiation spectrum. As was the case in Čerenkov counters, these devices offer functional advantages⁴⁴ beyond concentration *per se*. Their use in this field is now nearly universal, including the recent spectacular measurements by the Cosmic Background Explorer (COBE) satellite and systems being designed for the proposed Stratospheric Observatory for Infrared Astronomy (SOFIA).

NONIMAGING OPTICS

The 1970s saw the emergence of nonimaging optics as a new subfield of physics. The late Walter Welford of the University of London joined Roland Winston and several other collaborators in developing a well-defined discipline from the original insights⁸ that some important optical problems do not require image formation and that these problems can be addressed in particularly direct and illuminating ways by the application of ideas from Hamiltonian optics. Two books^{2,45} and a lengthy review article⁴⁶ set forth many of the developments. The edge ray and maximum slope design principles⁴⁷, both implicit in the original⁸ CPC construction, led to many useful insights and concentrator designs. Subsequent formulation of the geometrical vector flux (or flowline) formalism⁴⁸ has led to more detailed understanding as well as new concentrator designs, particularly in 3D cases. The search for additional design approaches is a topic of continuing interest.

To gauge the dramatic growth of this discipline, I performed a rough count of refereed publications⁴⁹ and books dealing with nonimaging optics or involving the use of nonimaging concentrators. This tally shows only 16 publications prior to 1970, compared to 130 from 1970 to 1980, and 320 from 1980 to 1990. Though this is by no means a definitive survey, and the resulting numbers for all three periods are undoubtedly underestimates, it is nonetheless

clear that the dramatic increase over time would not be significantly diminished by a more thorough search.

One intriguing question is why Walter Welford, an outstanding practitioner of the design of imaging optical systems, would become engrossed in the development of nonimaging optics. Certainly his work on the design of wide-angle lens systems like the "fish-eye" lenses for the ZGS 12-foot bubble chamber would lead naturally to an interest in the design of concentrating systems. At a deeper level, his appreciation of direct elegant ideas and his extensive knowledge of classical aberration theory⁵⁰ would have made nonimaging devices like the CPC (which are, after all, essentially *aberration dominated* optical systems) and the straightforward design concepts behind them particularly appealing to him.

MORE RECENT DEVELOPMENTS

It was recognized very early that CPCs could equally well be used "backwards" to produce a light beam with a desired angular divergence issuing from the larger aperture when a small, highly-divergent light source was placed at the small aperture. (Of course this is just a consequence of reciprocity in optics or, more generally, time reversal invariance.) Indeed the earliest photographs of CPC arrays (similar to the cover of the March, 1991 *Scientific American*) were quite naturally taken in this fashion with illuminated colored filters at the small ends. A generalization^{51,52} of the CPC (the " θ_1 - θ_2 transformer") is adapted to half-angles other than 90° at the small aperture.

Such backwards use suggests a wide range of illumination applications⁵³ in conjunction with conventional light sources, lasers, and fiber optics. Indeed one commercial application of nonimaging devices to illumination is ubiquitous, though normally hidden: the expansive tail lights of the Ford Thunderbird are illuminated by a linear array of them with light emitting diodes (LEDs) at the

small ends. Hewlett Packard markets such tailored-beam LED devices. NiOptics, a company dedicated to developing commercial applications of nonimaging optics in a variety of areas, was launched in 1988 by an Argonne-University of Chicago umbrella organization (ARCH).

Devices like the CPC become unreasonably long⁵⁴ when designed for high concentrations. The θ_1 - θ_2 transformer paper⁵¹ also discusses nonimaging "second stage concentrators" which collect and further concentrate light from a primary (imaging) device. In contrast to an entirely imaging system, such an arrangement can allow relaxed fabrication and pointing tolerances for a given concentration ratio, or provide substantially higher concentration for given tolerances. Such concentrators have a variety of applications⁵⁵ involving intermediate to high concentration ratios.

The University of Chicago group, with the support of the Solar Energy Research Institute (SERI), has pursued one of the more exciting applications of second stage concentrators: ultra-high concentration of sunlight to levels near the thermodynamic limit. Viewed from the earth the angular radius of the sun is $\theta_{\text{sun}} = 0.267^\circ$. The corresponding maximum concentration is $1/\sin(\theta_{\text{sun}}) \approx 46,000$ in air and $n^2/\sin(\theta_{\text{sun}}) \approx 46,000 n^2$ in a medium of refractive index n . Thus, even after inevitable losses, a two-stage system with a dielectric secondary could exceed the maximum concentration in air (46,000). Using a silver funnel filled with oil ($n = 1.53$) for the secondary (see Figure 8), initial experiments⁵⁶ achieved a concentration of 56,000. An improved apparatus using total internal reflection in a sapphire ($n = 1.73$) secondary produced⁵⁷ a record solar intensity of 72 W/mm^2 (actually exceeding the 63 W/mm^2 at the sun's surface) at the exit aperture, corresponding to a concentration of 84,000. Such highly concentrated sunlight has potential applications in high-temperature materials processing, development of efficient solar-pumped lasers, and destruction of hazardous

wastes. The National Energy Research Laboratory's experimental High-Flux Solar Furnace now employs (see Figure 9) a refracting nonimaging secondary designed and fabricated by the Chicago group.

Recent changes in the technical and societal climate have renewed interest in solar energy applied to air conditioning. First, technical advances in heat driven air conditioning (conventionally gas fueled) have resulted in systems with significantly higher efficiency. Second, concern over environmental impacts, particularly depletion of the ozone layer, has greatly increased desire for large-scale air conditioning systems which do not use chlorofluorocarbons (CFCs) as their working substances. A new three-stage project is under way to evaluate, develop, demonstrate, and commercialize solar powered air conditioning systems using nonimaging concentrators.

CONCLUSION

Clearly this chronicle is not a finished story. Nonimaging optics is still a young discipline, growing rapidly in both conceptual content and new applications. This means that the full extent of its importance cannot be accurately assessed, but it also means that we have not yet lost sight of its intellectual origins.

The progression outlined here suggests many reasons why innovative ideas for practical applications and devices flow in a natural fashion (which begs for a more meaningful description than the common term "spinoff") from advanced basic research activities. These include the following.

1. Basic researchers have a positive orientation to problem finding and problem definition, allowing them to avoid a narrow focus on seeking solutions to pre-defined problems. This is often needed if one is to translate novel ideas into novel and useful devices.

2. Many basic researchers seek to analyze situations (even "mundane" instrumentation problems) in terms of underlying fundamental principles, thereby pushing back conventionally accepted limitations and barriers.
3. Basic research requires practitioners to *combine* original and critical thinking in a balanced fashion.
4. Successful basic research requires openness to — and even fascination with — new ideas while avoiding uncritical acceptance of them.
5. Substantially (though certainly not totally) open communication with people of great intellectual ability and wide interests is an integral part of the pursuit of first-rate basic science.
6. Advanced basic research often takes place in close proximity to major technical frontiers.
7. The excitement inherent in the enterprise of basic research is an important source of both intellectual energy and the courage to question and innovate.

The intellectual climate of the University of Chicago coupled with the technical and human environment of the ZGS at Argonne provided such conditions in abundance.

ACKNOWLEDGEMENTS

Many years of fruitful collaboration, stimulating conversation, and valued friendship with Roland Winston are gratefully acknowledged. I thank Argonne National Laboratory for support and hospitality during the ZGS era and for the pleasure of working with Tom Romanowski. Likewise, the continuing hospitality of the Enrico Fermi Institute at the University of Chicago is very greatly appreciated. This work was supported in part by the U. S. Department of Energy under grant DE-FG02-90ER40560 (Task B).

REFERENCES

1. E. C. Swallow, *The Arthur Holly Compton Lectures* (fourth series), University of Chicago Enrico Fermi Institute, January 15 - March 19, 1977 (unpublished).
2. W. T. Welford and R. Winston, *High Collection Nonimaging Optics*, (Academic Press, 1989). This book contains a fairly extensive list of publication and patent citations. Reference 46 also provides an excellent review of nonimaging optics applied to flux concentration.
3. R. Winston, *Scientific American* **264**, 76 (March, 1991).
4. N. Cabibbo, *Phys. Rev. Letters* **10**, 531 (1963). See also, M. Gell-Mann and M. Lévy, *Nuovo Cimento* **16**, 705 (1960) and Z. Maki, M. Nakagawa and S. Sakata, *Prog. Theor. Phys.* **28**, 870 (1962).
5. M. Gell-Mann, California Institute of Technology Synchrotron Laboratory Report CTSL-20, 1961 (unpublished) and Y. Ne'eman, *Nuclear Physics* **26**, 222 (1961).
6. R. P. Feynman and M. Gell-Mann, *Phys. Rev.* **109**, 193 (1958); E. C. G. Sudarshan and R. E. Marshak, *Proc. Padua-Venice Conf. on Mesons and Recently Discovered Particles* (1957), and *Phys. Rev.* **109**, 1860 (1958); and J. J. Sakurai, *Nuovo Cimento* **7**, 649 (1958).
7. M. T. Burgy, V. E. Krohn, T. B. Novey, G. R. Ringo and V. L. Telegdi, *Phys. Rev.* **120**, 1827 (1960).
8. H. Hinterberger and R. Winston, *Rev. Sci. Instrum.* **37**, 1094 (1966).
9. From the beginning many of us called these devices "Winston cones," a name which is still common in particle physics, but Roland Winston frequently voiced his discomfort with this. During a discussion of solar energy applications at Argonne in the early 1970s, John Martin suggested the name "compound parabolic concentrator" (CPC). This name correctly acknowledges the importance of the parabolic wall shape while blunting the tendency to confuse this nonimaging device with a conventional (imaging) parabolic mirror. Today the name CPC enjoys fairly wide use. It is sometimes used in a generic sense to denote similar nonimaging concentrating devices even when the curved walls are not strictly parabolic.
10. V. K. Baranov, *Opt. Mekh. Prom.* **6**, 1 (1965), in Russian. See additional citations in reference 2.
11. M. Ploke, *Optik* **25**, 31 (1967), in German. See additional citations in reference 2.
12. See reference 2, pp. 53-76 for a more detailed analysis.
13. H. Hinterberger and R. Winston, *Proc. Int. Conf. Instrum. High Energy Phys.*, 205 (1966) and H. Hinterberger, L. Lavoie, B. Nelson, R. L.

- Sumner, J. M. Watson, R. Winston and D. M. Wolfe, *Rev. Sci. Instrum.* **41**, 413 (1970).
14. H. Hinterberger and R. Winston, *Rev. Sci. Instrum.* **39**, 419 (1968).
 15. H. Hinterberger and R. Winston, *Rev. Sci. Instrum.* **39**, 1217 (1968).
 16. R. Winston, *J. Opt. Soc. Am.* **60**, 245 (1970).
 17. R. K. Luneburg, *Mathematical Theory of Optics* (University of California Press, Berkeley, 1964).
 18. A rather detailed discussion of the relationship between concentration limits, the *throughput* or *étendue* invariant of an optical system, Hamiltonian optics, conservation of volume in phase space, and Liouville's Theorem in statistical mechanics may be found in reference 2, pp. 223-230. Concentration limits may likewise be understood in terms of the Second Law of Thermodynamics (see A. Rabl, *Solar Energy* **18**, 93 (1976); H. Ries, *J. Opt. Soc. Am.* **72**, 380 (1982); and reference 46.) or the unitarity of the time evolution operator in quantum mechanics (see I. M. Bassett and R. Winston, *Opt. Acta* **31**, 499 (1984) and W. T. Welford and R. Winston, *J. Opt. Soc. Am.* **72**, 1244 (1982)).
 19. J. Marshall, *Phys. Rev.* **86**, 685 (1952).
 20. R. L. Garwin, *Rev. Sci. Instrum.* **23**, 755 (1952).
 21. D. E. Williamson, *J. Opt. Soc. Am.* **42**, 712 (1952).
 22. W. Witte, *Infrared Phys.* **5**, 179 (1965).
 23. J. Lindquist, E. C. Swallow, R. L. Sumner, J. M. Watson, R. Winston, D. M. Wolfe, P. R. Phillips, K. Reibel, D. M. Schwartz, A. J. Stevens and T. A. Romanowski, *Phys. Rev. Letters* **27**, 612 (1971) and *Phys. Rev. D* **16**, 2104 (1977).
 24. R. Oehme, E. C. Swallow and R. Winston, *Phys. Rev. D* **8**, 2124 (1973).
 25. For example: S. Kooijman, M. W. Arenton, D. S. Ayres, R. Diebold, E. N. May, L. Nodulman, J. R. Sauer, A. B. Wicklund and E. C. Swallow, *Phys. Rev. Letters* **45**, 316 (1980); M. W. Arenton, D. S. Ayres, R. Diebold, E. N. May, L. Nodulman, J. R. Sauer, C. Sorenson, A. B. Wicklund and E. C. Swallow, *Phys. Rev. D* **25**, 2241 (1982); and M. W. Arenton, D. S. Ayres, R. Diebold, E. N. May, L. Nodulman, J. R. Sauer, A. B. Wicklund and E. C. Swallow, *Phys. Rev. D* **28**, 657 (1983).
 26. P. Keller, A. Lesnik, T. A. Romanowski, W. E. Keig, B. Nelson, D. A. Park, E. C. Swallow, R. Winston, C. E. W. Ward and J. Watson, *Phys. Rev. Letters* **48**, 971 (1982).
 27. S. Y. Hsueh, D. Müller, J. Tang, R. Winston, G. Zapalac, E. C. Swallow, J. P. Berge, A. E. Brenner, P. S. Cooper, P. Grafström, E. Jastrzembski, J. Lach, J. Marriner, R. Raja, V. J. Smith, E. McCliment, C. Newsom, E. W. Anderson, A. S. Denisov, V. T. Grachev, V. A. Schegelsky, D. M. Seliverstov, N. N. Smirnov, N. K. Terentyev, I. I.

- Tkatch, A. A. Vorobyov, P. Razis and L. J. Teig, *Phys. Rev.* **D38**, 2056 (1988).
28. See discussion and references in A. Garcia and E. C. Swallow, *Phys. Rev. Letters* **35**, 467 (1975).
 29. M. Kobayashi and T. Maskawa, *Prog. Theor. Phys.* **49**, 652 (1973).
 30. I. Ambats, E. R. Hayes, C. E. W. Ward, W. E. Keig, D. A. Park, E. C. Swallow, R. Winston and T. A. Romanowski, *Nucl. Instr. and Meth.* **138**, 61 (1976).
 31. R. Winston and J. M. Enoch, *J. Opt. Soc. Am.* **61**, 1120 (1971).
 32. S. Exner, *Die Physiologie der Facettierten Augen von Krebsen und Insekten* (Fr. Deuticke, Leipzig und Wien, 1891).
 33. R. Levi-Setti, D. A. Park and R. Winston, *Nature (London)* **235**, 115 (1975).
 34. D. A. Baylor and R. Fettiplace, *J. Physiol. (London)* **248**, 433 (1975).
 35. See discussion by R. Winston, *Springer Series in Optical Sciences*, vol. **23: Vertebrate Photoreceptor Optics**, (ed., J. M. Enoch and F. L. Tobey, Springer-Verlag, 1981) p. 325.
 36. For direct solar conversion to electricity, concentration is desirable to reduce the number of costly solar cells required — a situation quite analogous to the E38 Čerenkov counter design problem. Alternately, for thermal applications like industrial processes, desalination, cooking, power generation, and heat-driven air conditioning, concentration is necessary to achieve higher temperatures (with attendant increases in thermodynamic efficiencies where relevant).
 37. R. Winston, *Solar Energy* **16**, 89 (1974).
 38. R. Winston and H. Hinterberger, *Solar Energy* **17**, 255 (1975). (One can see the edge ray principle and the maximum slope principle emerging further in this paper.)
 39. For a more detailed discussion of nonimaging concentrator development for solar energy applications, see J. O'Gallagher and R. Winston, *Int. J. Ambient Energy* **4**, 171 (1983).
 40. I do not mean to imply here that our national energy problems actually ceased to exist as oil prices fell and related economic dislocations were relieved, but only that they lost their immediacy and general visibility. With our failure to systematically pursue a multi-faceted national energy resource development program, they are almost certainly lying in wait to attack with a vengeance some time during the first half of the next century.
 41. D. A. Harper, R. H. Hildebrand, R. Stiening and R. Winston, *Appl. Optics* **15**, 53 (1976). This device has been named the "heat trap."

42. R. H. Hildebrand, S. E. Whitcomb, R. Winston, R. Stiening, D. A. Harper and S. H. Moseley, *Astrophys. J.* **216**, 698 (1977) and *Astrophys. J.* **219**, L101 (1978).
43. See D. P. Woody and P. L. Richards, *Phys. Rev. Letters* **42**, 925 (1979) and references therein.
44. See the discussion in reference 2, pp. 215-218.
45. W. T. Welford and R. Winston, *Optics of Nonimaging Concentrators: Light and Solar Energy*, (Academic Press, 1978). (In this book the edge ray and maximum slope principles receive explicit discussion.)
46. I. M. Bassett, W. T. Welford and R. Winston, *Progress in Optics* **27**, 161 (1989).
47. See discussions in references 2, 45 and 46. For a recent examination and topological generalization of the edge ray principle, see H. Ries and A. Rabl, *J. Opt. Soc. Am.* **A11**, 2627 (1994).
48. R. Winston and W. T. Welford, *J. Opt. Soc. Am.* **69**, 532 (1979). Also see R. Winston and W. T. Welford, *J. Opt. Soc. Am.* **69**, 536 (1979); R. Winston and X. Ning, *J. Opt. Soc. Am.* **A3**, 1629 (1986) and discussions in references 2, 45 and 46.
49. For this count I used *The Nonimaging Optics Bibliography* as presented to Roland Winston on the occasion of the *Sede Boqer Symposium on Nonimaging Optics*, Sede Boqer, Israel, March 1, 1992 plus a few additional references. *Selected Papers on Nonimaging Optics* (ed., R. Winston, SPIE, 1995) contains reprints of over 100 original papers.
50. See W. T. Welford, *Aberrations of the Symmetrical Optical System* (Academic Press, New York, 1974) and *Aberrations of the Optical System* (Hilger, London, 1986).
51. A. Rabl and R. Winston, *Appl. Opt.* **15**, 2880 (1976).
52. See reference 2, pp. 82-84 and 247-248.
53. See reference 2, pp. 201-221.
54. For high concentration, and correspondingly small angular acceptance, the length is approximately the entrance aperture radius multiplied by the two-dimensional concentration ratio: $L \approx (D/2)[1/\sin(\theta_{\text{Max}})]$.
55. See M. Collares-Pereira, A. Rabl and R. Winston, *Appl. Opt.* **16**, 2677 (1977); also R. Winston and W. T. Welford, *Appl. Opt.* **19**, 347 (1980) and reference 2, pp. 192-199.
56. P. Gleckman, *Appl. Opt.* **27**, 4385 (1988) and P. Gleckman, J. O'Gallagher and R. Winston, *Nature (London)* **339**, 198 (1989).
57. D. Cooke, P. Gleckman, H. Krebs, J. O'Gallagher, D. Sagie and R. Winston, *Nature (London)* **346**, 802 (1990).

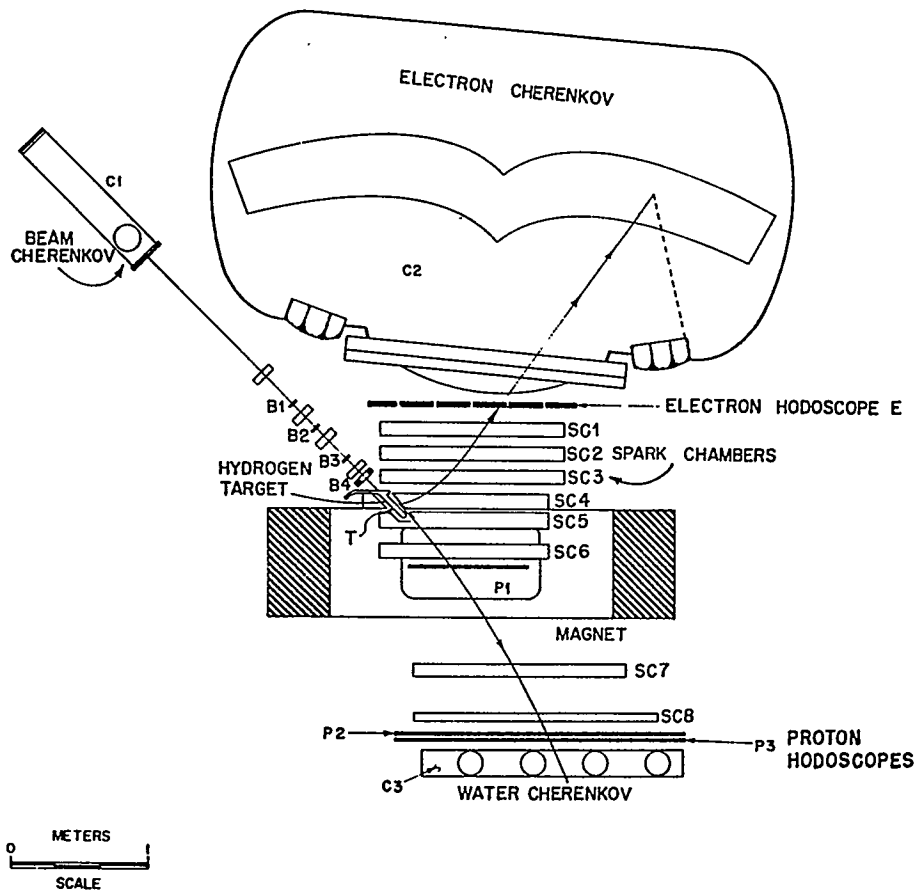


Figure 1. Plan view of apparatus for ZGS $\Lambda \rightarrow pe^- \bar{\nu}$ experiment (E38).

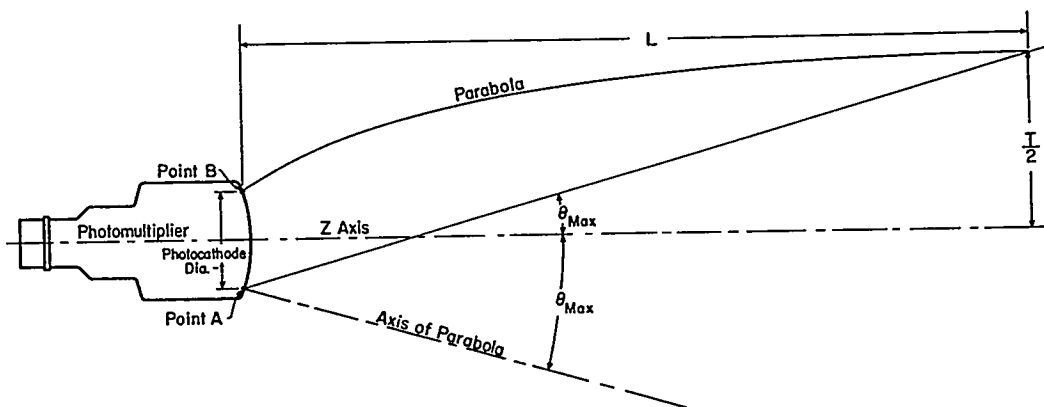


Figure 2. Construction of nonimaging concentrator for E38 Čerenkov counter. Here $\theta_{Max} = 16^\circ$ corresponding to a linear concentration of $T/t = 3.6$.

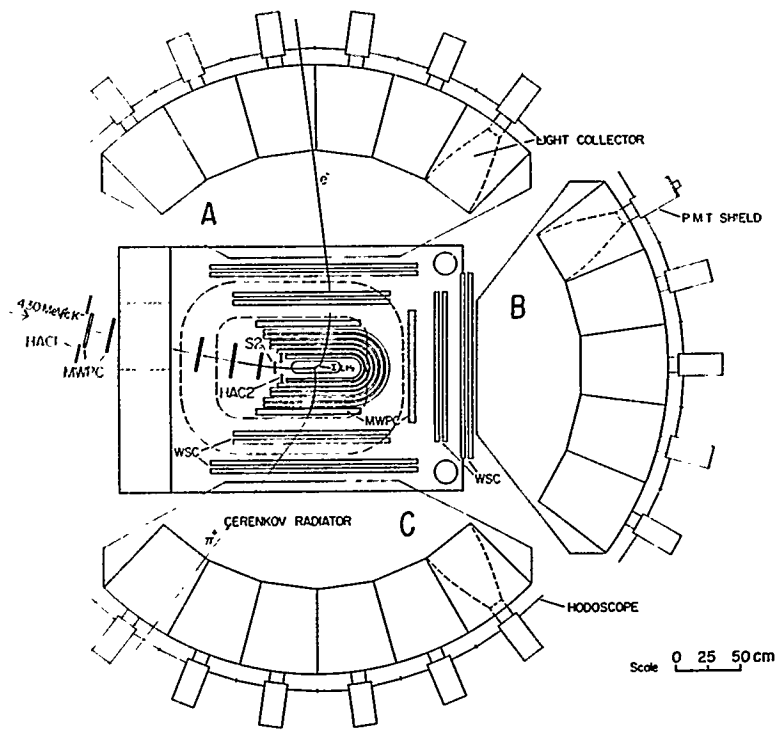


Figure 3. Schematic plan view of ZGS $\Sigma^- \rightarrow ne^- \bar{\nu}$ experiment (E347).

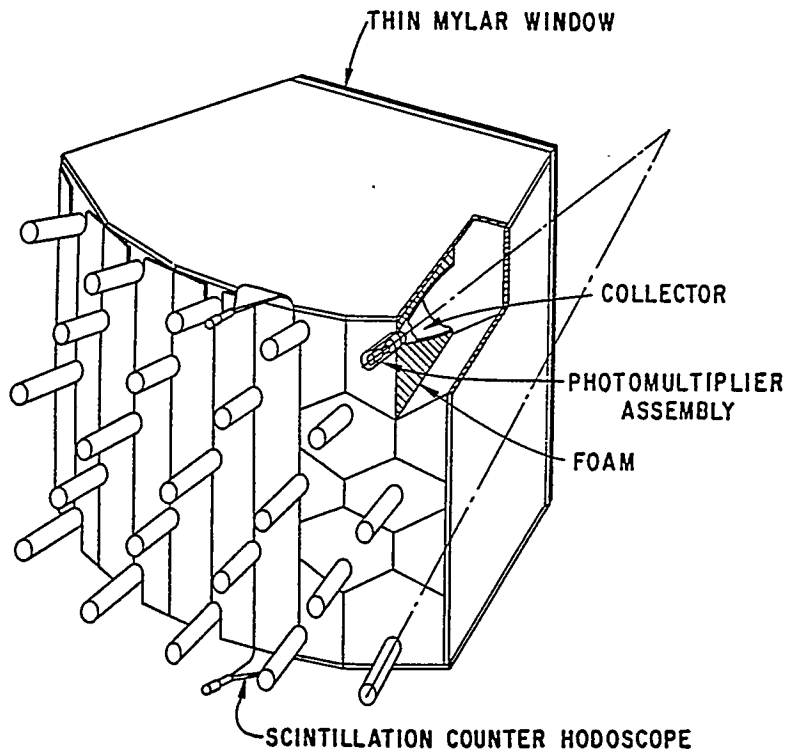


Figure 4. Isometric view of Čerenkov counter assembly as seen from behind.

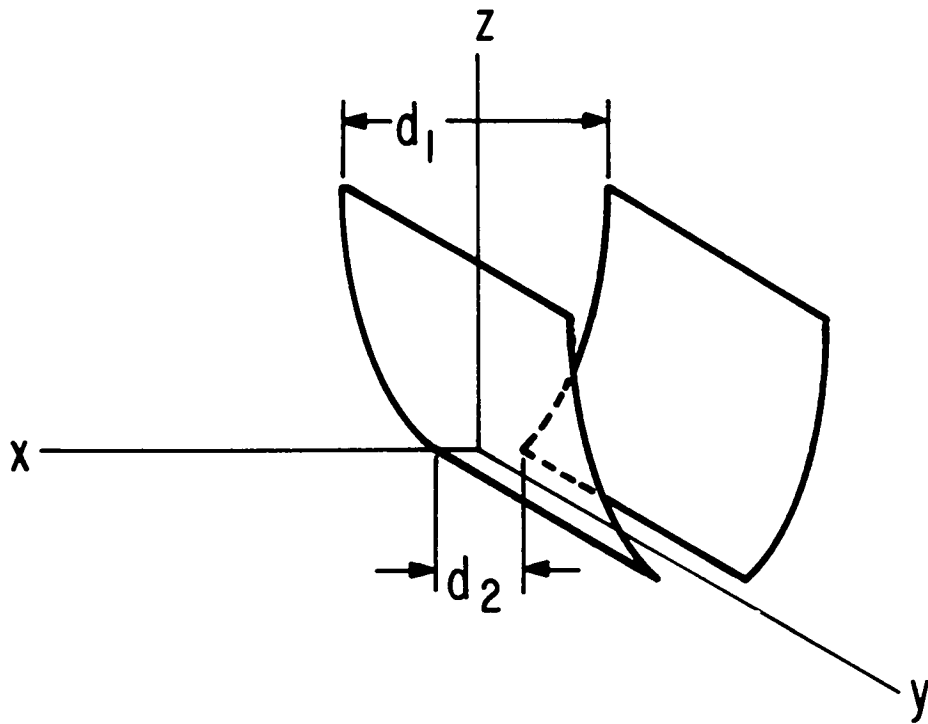


Figure 5. Schematic view of a trough or 2D nonimaging concentrator.



Figure 6. Solar energy concentrator test facility constructed at Argonne National Laboratory in the mid-1970s.



Figure 7. A portion of the 12,000-ft² CPC concentrator array at the Illinois Department of Agriculture building in Springfield, Illinois.

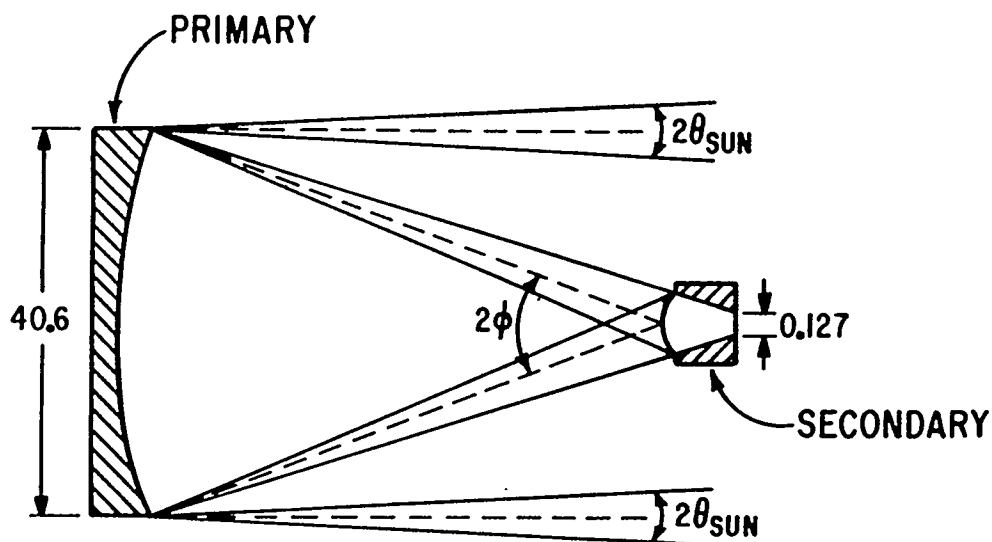


Figure 8. Two-stage concentrator system with an imaging primary and a refracting nonimaging secondary for ultra-high concentration of sunlight.

FOR INFORMATION CONTACT:
Mike Coe (303) 275-4085

NREL RESEARCHERS CONCENTRATE SUNLIGHT 50,000 TIMES

Golden, Colo., April 20, 1994 -- Researchers at the U.S. Department of Energy's National Renewable Energy Laboratory (NREL) have harnessed the power of 50,000 suns, expanding the range of potential applications for concentrated sunlight.

The record concentration was achieved in March at NREL's High-Flux Solar Furnace, located on South Table Mountain in Golden. The furnace was built in 1989 to explore using highly-concentrated sunlight for advanced materials processing and detoxification of contaminated wastes. The furnace uses a series of mirrors to concentrate sunlight into an intense, focused beam.

While the furnace successfully proved sunlight is a clean, effective energy source for numerous manufacturing processes, one goal remained -- achieving a concentration 50,000 times greater than the normal solar intensity found at the earth's surface.

"We wanted to push the limits and thought 50,000 suns was the practical limit given the scale of our furnace," said Allan Lewandowski, NREL project leader for advanced processes.

Researchers used a reflective secondary concentrator to achieve the previous high concentration of 21,000 suns. To achieve 50,000 suns concentration, researchers replaced the reflective secondary with a lens-like refractive secondary concentrator. The University of Chicago designed and fabricated the refractive secondary concentrator under an NREL subcontract. Both secondary concentrators are based on nonimaging optics principles developed by Dr. Roland Winston and his colleagues at the University.

- more -

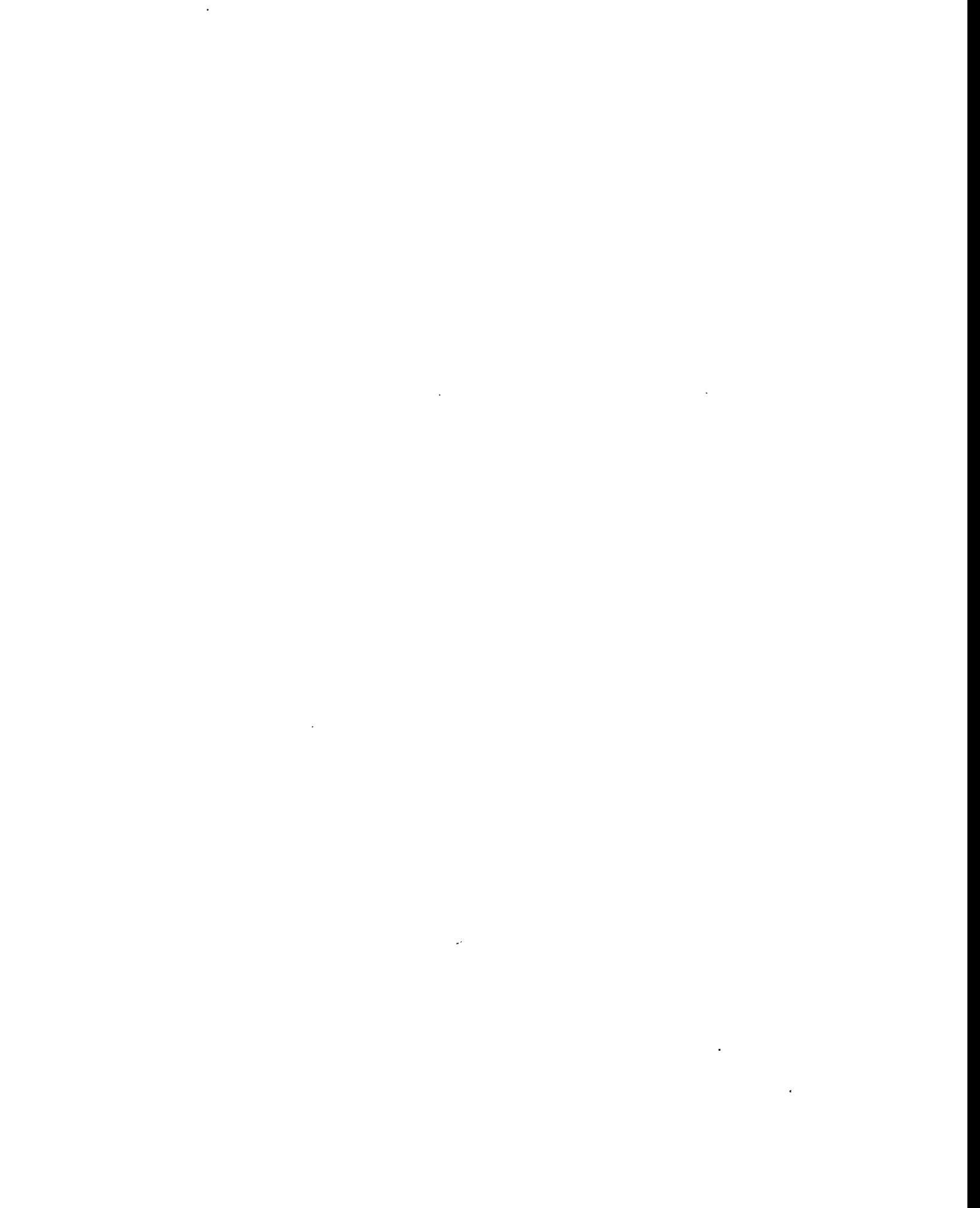
The National Renewable Energy Laboratory (NREL) is operated and managed for the U.S. Department of Energy by the Midwest Research Institute.



Printed with biodegradable ink on paper containing at least 50% waste paper.

Figure 9. Part of a press release issued by the National Renewable Energy Laboratory (NREL) shortly before the ZGS Symposium.





The Quark Revolution and the ZGS - New Quark Physics Since the ZGS

HARRY J. LIPKIN

*Department of Particle Physics
Weizmann Institute of Science, Rehovot 76100, Israel*

and

*School of Physics and Astronomy
Raymond and Beverly Sackler Faculty of Exact Sciences
Tel Aviv University, Tel Aviv, Israel*

ABSTRACT

Overwhelming experimental evidence for quarks as real physical constituents of hadrons along with the QCD analogs of the Balmer Formula, Bohr Atom and Schroedinger Equation already existed in 1966 but was dismissed as heresy. ZGS experiments played an important role in the quark revolution. This role is briefly reviewed and subsequent progress in quark physics is described.

1. Introduction. The Quark Revolution and the ZGS

By 1966 the quark model was taken seriously in Europe and supported by top establishment figures like Bogoliubov, Sakharov, Zeldovich, Gribov, Thirring, Morpurgo and Dalitz. The American approach was stated explicitly by M. L. Goldberger in introducing a colloquium speaker at Princeton in 1967. "A boy was standing on a street corner snapping his fingers and claiming that it kept the elephants away. When told that there had been no elephants around for many years, his response was 'You see! It works!'. And now our speaker will talk about the quark model."

The approach of Galileo that we learn about nature from experiments led people in the East to the conclusion "The quark model works, and we do not understand it. Therefore it is interesting." In the West the particle theorists seemed to have forgotten Galileo. Their conclusion was "The quark model works, but it contradicts the established dogma. Therefore it is heresy and witchcraft."

The simple quark-counting result of Levin and Frankfurt^[1] explained the ratio of 3/2 between nucleon-nucleon and meson-nucleon scattering and again showed that mesons and baryons are made of the same quarks. This was further refined by including the flavor dependence of the scattering amplitudes at the quark level^[2] and led to a remarkable experimental prediction^[3] that was confirmed at the ZGS^[4] and might be considered today as among the first indications of asymptotic freedom.

$$\sigma(K^-p \rightarrow \Lambda\omega) = \sigma(K^-p \rightarrow \Lambda\rho^0) \quad (1.1)$$

This prediction was rejected as nonsense by the referees of Phys. Rev. Letters. The whole quark model was considered to be nonsense, and all the accepted conventional wisdom

noted that the dynamics must be very different for the $\Lambda\omega$ and $\Lambda\rho^0$ states since they have different isospins and are coupled to completely different hadronic channels. PRL accepted our paper only after the ZGS data showed that we were right and the referees were wrong. Although we did not then understand the detailed dynamics, nature was telling us at the ZGS that hadrons were made of asymptotically free quarks, which retained their flavor despite strong interactions, and whose reaction cross sections obeyed simple quark counting rules.

The physics underlying the prediction (1.1) is illuminated by noting the analogy between the four "quark-flavour" vector meson eigenstates $\rho^+(u\bar{d})$, $V_d(d\bar{d})$, $V_u(u\bar{u})$ and $\rho^-(d\bar{u})$ and the four kaon quark-flavour eigenstates: $K^+(u\bar{s})$, $K^0(d\bar{s})$, $\bar{K}^0(s\bar{d})$ and $K^-(s\bar{u})$. In both cases the two neutral states are nearly degenerate and the quark-flavour eigenstates are mixed by their decays into short-lived mesons K_S and V_S (or ρ^0), which decay dominantly into two pions, and long-lived mesons K_L and V_L (or ω), which decay dominantly into three pions.

Neutral kaons are produced as quark-flavour eigenstates K^0 and \bar{K}^0 and decay after leaving the range of all final state interactions as equal mixtures of K_L and K_S . The ZGS experiment showed that neutral vector mesons were produced in the reaction (1.1) as the quark-flavour eigenstate V_u and decayed as equal mixtures of ρ^0 and ω . The surprising result that strong interactions did not change quark flavors could indicate evidence for asymptotic freedom.

Spin physics was also disparaged by the establishment. Nucleons were elementary fermions, behaved like neutrinos at high energy and remained in helicity eigenstates in reactions with no spin dependence or spin flip. The evidence of nontrivial hadron spin physics at the ZGS again showed that nucleons were not elementary fermions and elementary quark spins were interchanged and recoupled in reactions. This led to a very fruitful program for experiments with polarized beams at the ZGS.

Evidence for the quark structure of hadrons kept mounting and was consistently disregarded by the establishment. The basis of QCD was already published in 1966^[5]. A model of colored quarks interacting with colored gauge bosons in the manner described by a non-Abelian gauge theory had so much of the right physics^[6] that it had to lead somewhere. But there are none so blind as those who don't want to see. Andrei Sakharov was a pioneer in hadron physics who took quarks seriously already in 1966. He asked "Why are the Λ and Σ masses different? They are made of the same quarks!"^[7] His answer that the difference arose from a flavor-dependent hyperfine interaction led to relations between meson and baryon masses in surprising agreement with experiment^[6]. Sakharov and Zeldovich *anticipated* QCD by assuming a quark model for hadrons with a flavor dependent linear mass term and a two-body interaction whose flavor dependence was all in a hyperfine interaction with different strengths but the same flavor dependence for qq and $\bar{q}q$ interactions^[6,8].

The mass difference between s and u quarks calculated in two ways from the linear term in meson and baryon masses showed that it costs exactly the same energy to replace a nonstrange quark by a strange quark in mesons and baryons, when the contribution from

the hyperfine interaction is removed.

$$(m_s - m_u)_{Bar} = M_\Lambda - M_N = 177 \text{ MeV} \quad (1.2a)$$

$$(m_s - m_u)_{Mes} = \frac{3(M_{K^*} - M_\rho) + M_K - M_\pi}{4} = 180 \text{ MeV} \quad (1.2b)$$

where the subscripts u , d and s refer to quark flavors. The flavor dependence of the hyperfine splittings calculated in two ways from meson and baryon masses gave the result

$$1.53 = \frac{M_\Delta - M_N}{M_{\Sigma^*} - M_\Sigma} = \left(\frac{v_{ud}^{hyp}}{v_{us}^{hyp}} \right)_{Bar} = \left(\frac{v_{ud}^{hyp}}{v_{us}^{hyp}} \right)_{Mes} = \frac{M_\rho - M_\pi}{M_{K^*} - M_K} = 1.61 \quad (1.3)$$

This striking evidence that mesons and baryons are made of the same quarks and described by a universal linear mass formula with spin corrections in remarkable agreement with experiment was overlooked for amusing reasons^[9-10] and rediscovered only in 1978^[11]. In that same year 1966 Nambu derived just such a universal linear mass formula for mesons and baryons from a model in which colored quarks were bound into color singlet hadrons by an interaction generated by coupling the quarks to a non-abelian SU(3) color gauge field, and spin effects were neglected^[5].

The Nobel Prize for QCD might have been awarded to Sakharov, Zeldovich and Nambu. They had it all in 1966. The Balmer formula, the Bohr atom and the Schroedinger equation of Strong Interactions. All subsequent developments leading to QCD were just mathematics and public relations, with no new physics. But the particle physics establishment refused to recognize the beginnings of new physics and had to wait until new fancy names like chromodynamics, color, confinement, etc. were invented together with a massive public relations campaign. Then they claimed that they had discovered it all.

The color degree of freedom solved the quark-statistics problem for baryons and also provided answers to several puzzles previously unanswered. Colored quarks interacting with a color-exchange potential showed already in 1968 that quarks would be confined in the limit now called large N_c ^[12]. The same colored-quark-color-exchange model explained in 1973 that both quark-quark and quark-antiquark systems are bound but different and gave exactly the observed hadron spectrum with only $q\bar{q}$ and $3q$ states and no exotics^[13]. No simple meson-exchange or other dynamical model gave these properties.

Further evidence for a quark structure of hadrons was found in the so-called ideal mixing pattern of vector and tensor mesons, a mysterious topological quark diagram selection rule now called OZI^[14-16] and peculiar systematics in the energy behavior of certain hadron total cross sections. Total cross sections in channels now called exotic do not have the sharply decreasing behavior found in other channels. This was first described in the additive quark model (AQM) by attributing all the energy decrease to quark-antiquark annihilation amplitudes^[17] and later in a unified picture with AQM couplings of hadrons to exchange-degenerate Regge trajectories^[18-19]. The universality of additive quark couplings to mesons and baryons arose again and again in different contexts in these descriptions.

An s-matrix Regge approach beginning with finite-energy sum rules then led to duality in which the same states appeared both as s-channel resonances and t-channel exchanges and the dual resonance (Veneziano) models^[20] with quark-model constraints on Reggeon couplings and impressive predictive power. The absence of exotics both as resonances and t-channel exchanges led to the OZI rule, while the exchange degeneracy and the dominance of the energy-dependent part of the cross section by quark-antiquark annihilation^[19] led naturally to duality diagrams^[21-22]. The energy independent part of the cross section, later found to be slowly rising, was seen to be related to diffraction, described by Pomeron exchange, with a coupling given by the Levin-Frankfurt quark-counting recipe.

That constituent quarks were real physical objects and that QCD had the right physics to describe strong interaction dynamics was already clear in 1966. That current quarks were different was also clear. But that current quarks could ever be seen as pointlike asymptotically free particles was not even imagined at that time. They provided a mathematical basis for current algebra and were not seen as real physical point-like objects until the SLAC experiments were described by the quark parton model.

There was great resistance to the idea that physical quarks existed but could not be observed as isolated free quarks. But hadrons had a spectrum and therefore a structure, and the energy of the first excited state was already greater than twice the pion mass. The energy required to move these constituents from their lowest orbit into the first excited orbit was already greater than double the rest mass of the lowest bound state. Pumping energy into the proton created pions and other bound states rather than free quarks. The forces and vacuum polarization created by trying to remove a quark from a proton were much too great to allow the quark to be removed like the electron from a hydrogen atom. Already in the late 1960's the hadron spectrum suggested that hitting a quark produced a string of pairs, and that the excitation spectrum looked like the spectrum of a string^[20]. One does not need fancy names like confinement and chromodynamics to understand this simple physics. It should have been obvious that free constituents would not be easily found. But the establishment refused to budge from its reactionary position. The party line that nothing was more elementary than neutrons and protons was sacrosanct and heretics were ridiculed.

2. Victory of the Quark Revolution. New Challenges for QCD

Now the pendulum has swung, everyone recognizes quarks and QCD and the theorists claim that they invented it all. Today many open questions in quark physics remain as challenges for QCD.

1. What is a constituent quark?
2. What is a quark mass?
3. How do quarks and gluons make hadrons?
4. Why does AQM quark counting work?
5. What is the OZI rule?
6. What is the spin and flavor structure of the proton?
7. What is the spin structure of hyperons?

8. What is the explanation of hyperon polarizations?

9. What is the origin of CP violation?

3. Additive Quark Model Counting, Diffraction, the Pomeron and More

Today the simple Levin-Frankfurt additive quark model (AQM) prediction ^[1,2] still fits experimental data up to 310 GeV/c with a discrepancy always less than 7% for the prediction

$$\delta_{AQM} \equiv (2/3) \cdot \sigma_{tot}(pp) - \sigma_{tot}(\pi^- p) \approx 0 \quad (3.1)$$

There seems to be underlying dynamics describing the meson-baryon difference primarily in terms of the number of constituent quarks. Finding a QCD description for the difference between constituent and current quarks along with this simple physics of total cross sections and therefore also diffractive processes presents a challenge to QCD.

The quark model success for total cross section is invariably linked to models for the pomeron, which is believed to dominate high energy diffraction. But fitting present data does not teach us much about the pomeron. A recently proposed phenomenological two Regge model ^[23] (denoted by DL) with a rising "Pomeron" term and a falling "Reggeon" term and a 1974 five-parameter "Two-component Pomeron" model ^[24-25] (denoted by TCP) look very different. Both fit $\sigma_{tot}(pp)$ with two power-law terms, but have very different powers of s or P_{lab} ,

$$\sigma_{TCP}(pp) = 19.5 \cdot (P_{lab}/20)^{0.13} + 19.8 \cdot (P_{lab}/20)^{-0.2} \quad (3.2a)$$

$$\sigma_{DL}(pp) \equiv 21.70 \cdot s^{0.0808} + 56.08 \cdot s^{-0.4525} \quad (3.2b)$$

But present data cannot distinguish between them even though their fits include new values of $\sigma_{tot}(\gamma p)$ ^[26-27] at $P_{lab} = 21322$ GeV/c, interpreted via vector dominance as values of meson-baryon total cross sections at energies where direct cross sections are not yet been measured. Although they look very different the first three terms in their expansions in powers of $x \equiv \log(P_{lab}/100)$ look very similar.

$$\sigma_{TCP}(pp) \approx 38.4 + 0.255x + 0.49x^2 \quad (3.3a)$$

$$\sigma_{DL}(pp) \approx 38.4 + 0.32x + 0.64x^2 \quad (3.3b)$$

$$\sigma_{TCP}(pp) - \sigma_{DL}(pp) \approx -0.065x - 0.15x^2 \quad (3.3c)$$

This difference is seen to be less than one millibarn over the complete range $-2 \leq x \leq 2$ which corresponds to $13.5 \text{ GeV}/c \leq P_{lab} \leq 790 \text{ GeV}/c$. Thus data at present energies do not yet provide sufficient information to distinguish between Pomeron models with very different high energy behaviour.

However, useful information seems to be obtainable by examining the small discrepancies from the asymptotic predictions (3.1). Using modern large- N_c QCD language^[25] we can consider three types of contributions to total cross sections: multi-gluon exchanges, planar quark diagrams and non-planar quark-exchange diagrams. The multigluon contribution is assumed to satisfy both AQM and $SU(3)_{flavor}$ and give a rising cross section which is dominant at asymptotic energies. Its exact energy dependence is not fixed by present data without further assumptions. TCP focuses primarily on flavor and baryon-number dependence, rather than the energy dependence emphasized in other approaches^[23]^[28] and determines the pomeron contribution by fitting data at lower energies expected to exhibit “early asymptopia”; e.g. in channels like ϕp where planar quark and nonplanar quark-exchange diagrams cannot contribute^[24].

There are no data for $\sigma_{tot}(\phi^- p)$. But “early asymptopia” is suggested by the monotonically increasing behavior of the experimental values of the linear combination $\sigma_{tot}(K^+ p) + \sigma_{tot}(K^- p) - \sigma_{tot}(\pi^- p)$ already in the energy range where all cross sections are constant or decreasing. TCP assumes that the asymptotic contribution is given by this linear combination and satisfies the AQM, since it is equal in the AQM to $\sigma_{tot}(\phi^- p)$. Furthermore the same $q-\bar{q}$ annihilation and $q-q$ exchange diagrams contributing respectively to $\sigma_{tot}(K^- p)$ and $\sigma_{tot}(K^+ p)$ appear equally in $\sigma_{tot}(\pi^- p)$ and cancel in this combination. Thus the TCP asymptotic contribution to $\sigma_{tot}(Hp)$ for any hadron H is

$$\begin{aligned}\sigma_{\infty}(Hp) &\equiv (N_q/2)\{\sigma_{tot}(K^+ p) + \sigma_{tot}(K^- p) - \sigma_{tot}(\pi^- p)\} \approx \\ &\approx (N_q/3) \cdot 19.5 \cdot (P_{lab}/20)^{0.13}\end{aligned}\quad (3.4)$$

where N_q is the total number of quarks and antiquarks in H and the parameters 19.5 and 0.13 were determined by fitting the data in the $P_{lab} = 2 - 200$ GeV/c region.

The next TCP contribution is determined by using input from duality^[21,22] or large N_c QCD, where the low energy behavior is dominated by a Regge contribution arising from planar quark diagrams. These are identical to Harari-Rosner duality diagrams^[21,22], which are well known to fit the particle-antiparticle total cross section differences with an energy variation $\approx s^{-1/2}$.

The TCP model first arose from breaking AQM by the most obvious Regge mechanism, a double exchange of a pomeron which couples equally to all quarks and an f which couples only to nonstrange quarks. This led to an equality in remarkable agreement with experiment^[29]

$$\sigma_{tot}(\pi^- p) - \sigma_{tot}(K^- p) = (1/3)\sigma_{tot}(pp) - (1/2)\sigma_{tot}(K^+ p) \quad (3.5a)$$

and also to new predictions for hyperon-nucleon cross sections.

$$\begin{aligned}\sigma_{tot}(\pi^- p) - \sigma_{tot}(K^- p) &= (2/3)\{\sigma_{tot}(pp) - \sigma_{tot}(\Sigma p)\} = \\ &= (2/3)\{\sigma_{tot}(\Sigma p) - \sigma_{tot}(\Xi p)\} = (2/3)\{\sigma_{tot}(\Xi p) - \sigma_{tot}(\Omega^- p)\}\end{aligned}\quad (3.5b)$$

The AQM gives the same hyperon prediction without the violation factor 2/3. The data^[30] confirmed the TCP prediction. The remarkable success of naive TCP without fine-tuning

of its five parameters in fitting and predicting data for all hadron-nucleon cross sections was summarized in the Moriond report of the hyperon experiment^[30], discussed in more detail elsewhere^[31-33] and summarized below.

Rearranging eqs. (3.5) gives baryon-nucleon predictions from only meson-baryon data which are all in surprising agreement at the 1-3% level with experimental values at $P_{lab} = 100\text{GeV}/c$, where data are available,

$$\sigma_{tot}(pp) = 3\sigma_{tot}(\pi^+p) - (3/2)\sigma_{tot}(K^-p) \quad (3.6a)$$

$$38.5 \pm 0.04\text{mb.} = 39.3 \pm 0.2\text{mb.} \quad (3.6b)$$

$$\sigma_{tot}(\Sigma p) = (3/2)\{\sigma_{tot}(K^+p) + \sigma_{tot}(\pi^-p) - \sigma_{tot}(K^-p)\} \quad (3.7a)$$

$$33.3 \pm 0.31\text{mb.} = 33.6 \pm 0.16\text{mb.} \quad (3.7b)$$

$$\sigma_{tot}(\Xi p) = (3/2)\sigma_{tot}(K^+p) \quad (3.8a)$$

$$29.2 \pm 0.29\text{mb.} = 28.4 \pm 0.1\text{mb.} \quad (3.8b)$$

$$\sigma_{tot}(\Omega^-p) = (3/2)\{\sigma_{tot}(K^+p) - \sigma_{tot}(\pi^-p) + \sigma_{tot}(K^-p)\} \quad (3.9)$$

There are as yet no data for $\sigma_{tot}(\Omega^-p)$.

Combining eqs. (3.4) and (3.5a) gives a linear combination of meson and baryon cross sections which also show a monotonically increasing behaviour fit by eq. (3.4)

$$\begin{aligned} (3/2)\sigma_{tot}(K^+p) - (1/3)\sigma_{tot}(pp) &= \sigma_{tot}(K^+p) + \sigma_{tot}(K^-p) - \sigma_{tot}(\pi^-p) \approx \\ &\approx 13.0 \cdot (P_{lab}/20)^{0.13} \end{aligned} \quad (3.10)$$

Such an asymptotically rising component with a power fit to the data violates the Froissart bound^[34] and must break down at higher energies. However replacing the power by logarithmic terms that do not violate the bound gives a prediction indistinguishable from the power law used in the energy region where the data has been fit^[25].

In TCP the asymptotic contribution and the planar quark diagram contributions satisfy both AQM and flavor SU(3) by construction and give vanishing contributions to all linear combinations of cross sections appearing in eqs. (3.5). All AQM and SU(3) violations arise from nonplanar diagrams whose contributions are given by the nonlinear quark-counting recipe obtained from pomeron-f exchange and relate SU(3) breaking to AQM violation. The success of this recipe in fitting and predicting data over a large energy range was

completely unexpected and is still not understood. The energy dependence is not described by any pomeron-f model and is fit by a decreasing power.

$$\sigma_2(Hp) = (N_q N_n) \cdot 2.2 \cdot (P_{lab}/20)^{-0.2} \quad (3.11)$$

where N_q and N_n denote respectively the total number of quarks and antiquarks and the total number of nonstrange quarks and antiquarks in hadron H .

Hyperon data can test the flavor dependence of the AQM violation by separating strange and nonstrange contributions to meson-nucleon and baryon-nucleon scattering^[31]. Assuming the AQM separately for meson-nucleon and baryon-nucleon scattering we obtain

$$\sigma(nN)_B = \frac{1}{3} \cdot \sigma(pN) = 12.9 \pm 0.01 mb. \quad (3.12a)$$

$$\sigma(sN)_B = \frac{1}{3} \{ \sigma(\Sigma N) + \sigma(\Xi N) - \sigma(pN) \} = 7.7 \pm 0.1 mb \approx 6.5(P/20)^{0.13} mb. = 8.0 mb. \quad (3.12b)$$

$$\sigma(nN)_M = \frac{1}{2} \{ \sigma(\pi N) - \sigma(\bar{K}N) + \sigma(KN) \} = 11.2 \pm 0.05 mb. \quad (3.13a)$$

$$\sigma(sN)_M = \frac{1}{2} \{ \sigma(\bar{K}N) - \sigma(\pi N) + \sigma(KN) \} = 7.75 \pm 0.05 mb. \approx 6.5(P/20)^{0.13} mb. = 8.0 mb. \quad (3.13b)$$

where $\sigma(nN)_B$, $\sigma(sN)_B$, $\sigma(nN)_M$ and $\sigma(sN)_M$ denote the contributions respectively of a single nonstrange and a single strange quark baryon-nucleon and meson-nucleon total cross sections. We have assumed that strange quarks and antiquarks contribute equally to meson-nucleon scattering, $\sigma(sN)_M = \sigma(\bar{s}N)_M$ since they have no contribution from the dominant odd-signature exchanges, and substituted the TCP relation (3.4) with no change in parameters to obtain the additional equalities in eqs. (3.12b-3.13b). This surprising result that AQM violation is all in nonstrange contributions while strange quarks contribute equally to meson-nucleon and baryon-nucleon scattering suggests that AQM violation is due to quark exchange diagrams. These cannot involve strange quarks which are absent in the nucleon.

We now note the following surprising equalities.

$$\sigma(nN)_B - \sigma(nN)_M = 1.69 \pm 0.05 mb. \approx 2.2(P/20)^{-0.2} mb. = 1.6 mb. \quad (3.14a)$$

$$\frac{1}{2} \{ \sigma(nN)_M - \sigma(sN)_M \} = 1.73 \pm 0.04 mb. \approx 2.2(P/20)^{-0.2} mb. = 1.6 mb. \quad (3.14b)$$

$$\sigma(nN)_B - \sigma(sN)_B = 5.15 \pm 0.07 mb. \quad (3.15a)$$

$$\frac{3}{2} \{ \sigma(nN)_M - \sigma(sN)_M \} = 5.2 \pm 0.1 mb. \quad (3.15b)$$

These are another form of the relations (3.5) that gave rise to the TCP model and we have here substituted the TCP relation (3.11) with no change in parameters. The difference

between the nonstrange contributions to meson and baryon cross sections is related to the difference between the strange and nonstrange contributions.

The results (ZZ8-3.15) raise several questions which go beyond specific details of the TCP model and suggest the need for new data.

1. Are the strange quark contributions to meson-nucleon and baryon-nucleon cross sections indeed equal over a large energy range, and is all the AQM violation due to nonstrange contributions?

2. Are the flavor-SU(3) and AQM violations related? Are the relations (3.14-3.15) accidental, or do they indicate some underlying physics?

3. Is the difference between strange and nonstrange hadron scattering on nucleons due to: (1) a difference between geometrical properties of strange and nonstrange quarks or hadrons or (2) a difference between the allowed number of quark-exchange diagrams because the target nucleon contains no strange quarks?

Data on meson-baryon cross sections at higher energy would show (a) whether the discrepancy from the additive quark model continues to decrease, (b) whether the $\pi - K$ difference decreases or levels off. More hyperon-nucleon total cross section data would test TCP predictions in a completely different domain. If the prediction (3.5b) is shown to be valid with good precision over a large energy range, it would establish the existence of the "second component" of the Pomeron and provide a challenge for QCD theorists.

Experiments on strange targets would clarify question 3 but are not likely to be performed in the near future. Comparison of meson exchange reactions which enable determination of $\pi\pi$, $K\pi$ and $K\bar{K}$ scattering might be useful. The TCP model assumes that this difference arises from nonstrange quark exchange diagrams that enhance the nonstrange contribution, rather than from flavor-dependent geometrical factors. This view is also supported by the analysis of the existing hyperon-nucleon cross sections in eqs. (ZZ8-3.15). In this case the flavor dependence comes arises from a non-factorizable contribution.

Meson-nucleon and hyperon-nucleon data at higher energies could clarify finer details of flavor and baryon number dependence supporting a hierarchy of contributions inspired by large N_c QCD: (1) multigluon exchange, (2) planar quark diagrams, (3) nonplanar quark diagrams.

4. What is a constituent quark?

Incredible successes of the most naive constituent quark model remain to be explained. QCD input that the hyperfine interaction is produced by one gluon exchange explained the sign of the $\Delta - N$ and $\rho - \pi$ mass splittings^[31-35] and led to a successful prediction for μ_Λ obtained before the experiment^[35] by assuming that the ratio of the quark magnetic moments μ_s^{EM}/μ_d^{EM} is the same as that of the corresponding color magnetic moments which produce the hyperfine splittings,

$$\mu_\Lambda = -0.61 \text{ n.m.} = -\frac{\mu_p \mu_s^{EM}}{3 \mu_d^{EM}} = -\frac{\mu_p \mu_s^{col}}{3 \mu_d^{col}} = -\frac{\mu_p (M_{\Sigma^*} - M_\Sigma)}{3 (M_\Delta - M_N)} = -0.61 \text{ n.m.} \quad (4.1)$$

where μ_f^{col} denotes the color magnetic moment of a quark of flavor f .

Further QCD input suggests that the hyperfine interaction is inversely proportional to the product of the masses of the interacting quarks ^[35] and otherwise flavor independent.

$$v_{ij}^{hyp} = \frac{\vec{\sigma}_i \cdot \vec{\sigma}_j}{m_i m_j} \bar{v}_{ij}. \quad (4.2)$$

where m_i is an effective quark mass and \bar{v}_{ij} is flavor independent. This input was used by Sakharov, working alone in Gorky, to obtain additional mass relations ^[8] discussed below. Cohen and Lipkin ^[36] introduced the additional assumption that the same quark mass parameters appear in the additive mass terms and that these include not only the full single particle energy ϵ_i ; including the kinetic energy but also the flavor-independent part of the two-body interaction; i.e.

$$\sum_i m_i = \sum_i \epsilon_i + \sum_{i>j} v_{ij}^o \quad (4.3a)$$

$$M = \sum_i m_i + \sum_{i>j} \frac{\vec{\sigma}_i \cdot \vec{\sigma}_j}{m_i m_j} v_{ij}. \quad (4.3b)$$

Although the extreme assumption (4.3a) seems highly questionable, the relation (4.3b) has described hadron masses and magnetic moments with remarkable success. In particular relations are obtained between the masses of the five baryons and four mesons in the ground state configuration and which contain no more than one strange quark. Five independent relations are obtained between the nine masses since the formula (4.3b) has four free parameters, the two quark masses and the two interaction strength parameters v_{ij} for mesons and baryons. Two of these are the Sakharov-Zeldovich relations (1.2) and (1.2). Two additional relations for $m_s - m_u$ in baryons and mesons in remarkable agreement with the values (1.2) follow from the extreme assumption (4.3a) that the same effective mass parameter m_i appears both in the first term of (4.3b) and in the hyperfine interaction ^[37].

$$(m_s - m_u)_{Bar} = \frac{M_N + M_\Delta}{6} \cdot \left(\frac{M_\Delta - M_N}{M_{\Sigma^*} - M_\Sigma} - 1 \right) = 190 \text{ MeV}. \quad (4.4a)$$

$$(m_s - m_u)_{Mes} = \frac{3M_\rho + M_\pi}{8} \cdot \left(\frac{M_\rho - M_\pi}{M_{K^*} - M_K} - 1 \right) = 178 \text{ MeV}. \quad (4.4b)$$

The fifth relation follows from assuming the same effective mass parameter m_i in the first spin-independent term in eq. (4.3b) for both mesons and baryons,

$$(m_u)_{Bar} = \frac{M_N + M_\Delta}{6} = 362 \text{ MeV} \quad (4.5a)$$

$$(m_u)_{Mes} = \frac{3}{8} \cdot M_\rho + \frac{1}{8} \cdot M_\pi = 306 \text{ MeV}. \quad (4.5b)$$

We also note three predictions of hadron magnetic moments with no free parameters;

namely (4.1) and

$$-1.46 = \frac{\mu_p}{\mu_n} = -\frac{3}{2} \quad (4.6a)$$

$$\mu_p + \mu_n = 0.88 \text{ n.m.} = \frac{2M_p}{M_N + M_\Delta} = 0.865 \text{ n.m.} \quad (4.6b)$$

The well-known prediction for the ratio of the nucleon magnetic moments (4.6a) follows from the assumption that hadron magnetic moments are obtainable from the constituent quark wave functions with quark magnetic moments proportional to their electric charges. The relation (4.6b) was obtained by using Dirac moments for the quarks with effective quark masses determined from hadron masses and the first term of eq. (4.3b) ^[38-39] The agreement with experiment of this prediction expressing a magnetic moment with a scale determined entirely by masses with no free parameters is impressive.

The success of this model remains to be understood at a more fundamental level. The essential physics underlying these successful relations are:

1. Meson-baryon universality: they are made of the same constituent quarks and must be treated on the same footing. Note that this universality is completely lost in some models like the Skyrminion which treat mesons and baryons very differently.

2. An effective quark mass parameter which has the same value in both mesons and baryons for the hyperfine interaction, the quark magnetic moment and the additive term in the mass operator, where the additive term includes the kinetic energy and the potential energies of the confining potential and all interactions except the hyperfine.

Obtaining these features from a more fundamental description is a challenge for QCD, along with the basic question of what is a constituent quark. Sakharov ^[9,10] noted that the quark masses in these formulas were effective masses including parts of the confining potential. Some indications of the underlying physics has been given in one simple model ^[36] which shows that the effective mass includes to a good approximation some relativistic corrections, kinetic energies and potential energies due to flavor and spin-independent effective quark-quark and quark-antiquark interactions related by the standard color factor of two ^[13,40]. These conclusions have been further supported by a variational treatment which shows that relations between baryon and meson masses are obtained as inequalities by using the exact three-body baryon wave function as a trial wave function for the meson case, and rescaling the wave function to satisfy the virial theorem ^[41].

There is also the problem of relating the constituent quark model with the hadron model consisting of valence current quarks, a sea of quark-antiquark pairs and gluons, which has been used successfully in interpreting results of experiment in deep inelastic scattering. The recent results from polarized deep inelastic scattering have raised a number of unsolved interesting questions on spin and flavor structure of hadrons.

5. The Ongoing Problems of Nucleon and Hyperon Spin and Flavor Structure

New quark physics since ZGS includes the questions of how much of the proton spin comes from quark spins and the role of strange quarks in the proton. Recent analyses of data on nucleon spin structure ^[42-43] confirm the originally surprising conclusion ^[44] of very low quark spin contribution to the proton spin. This result, together with the experimental value $(G_A/G_V)_{n \rightarrow p} = 1.2573 \pm 0.0028$ for the neutron decay suggests that the valence quark contribution to the nucleon spin must be canceled by a sea quark contribution in the EMC and SMC experiments. Their additional conclusion of a high strange quark contribution to the proton spin neglects flavor-symmetry breaking in the sea. The strange quark content of the sea has recently been shown by experiment ^[45] to be reduced roughly by a factor of two from that of a flavor-symmetric sea. Calculations of SU(3) symmetry-breaking in spin physics show that the same factor of two should be used to correct the results of ref. ^[43] for the strange quark contribution to the proton spin.

Meanwhile the experimental data for hyperon magnetic moments and semileptonic decays provide additional contradictions for models of hyperon structure. The essential difficulty posed by the hyperon data is expressed in the experimental value of the quantity

$$\frac{(G_A/G_V)_{\Lambda \rightarrow p}}{(G_A/G_V)_{\Sigma^- \rightarrow n}} \cdot \frac{\mu_{\Sigma^+} + 2\mu_{\Sigma^-}}{\mu_{\Lambda}} = 0.12 \pm 0.04 \quad (5.1)$$

The theoretical prediction for this quantity from the standard SU(6) quark model is unity, and it is very difficult to see how this enormous discrepancy by a factor of 8 ± 2 can be fixed in any simple way.

The expression (5.1) is chosen to compare two ways of determining the ratio of the contributions of strange quarks to the spins of the Σ and Λ . In the commonly used notation where $\Delta u(p)$, $\Delta d(p)$ and $\Delta s(p)$ denotes the contributions to the proton spin of the u , d and s - flavored current quarks and antiquarks respectively to the spin of the proton the SU(6) model gives

$$\Delta s(\Lambda)_{SU(6)} = 1 \quad (5.2a)$$

$$\Delta s(\Sigma)_{SU(6)} = -1/3 \quad (5.2b)$$

and

$$\frac{\Delta s(\Sigma)_{SU(6)}}{\Delta s(\Lambda)_{SU(6)}} = \frac{(G_A/G_V)_{\Sigma^- \rightarrow n}}{(G_A/G_V)_{\Lambda \rightarrow p}} = \frac{\mu_{\Sigma^+} + 2\mu_{\Sigma^-}}{3\mu_{\Lambda}} = -1/3 \quad (5.3a)$$

whereas experimentally

$$\frac{(G_A/G_V)_{\Sigma^- \rightarrow n}}{(G_A/G_V)_{\Lambda \rightarrow p}} = -0.473 \pm 0.026 \quad (5.3b)$$

$$\frac{\mu_{\Sigma^+} + 2\mu_{\Sigma^-}}{3\mu_{\Lambda}} = -0.06 \pm 0.02 \quad (5.3c)$$

The semileptonic decays give a value which is too large for the Σ/Λ ratio; the magnetic moments give a value which is too low. Thus the most obvious corrections to

the naive SU(6) quark model do not help. If they fix one ratio, they make the other worse. Furthermore, the excellent agreement (4.1) obtained ^[35] for μ_Λ by assuming that the strange quark carries the full spin of the Λ suggests that eq. (5.2a) is valid, while the excellent agreement of the experimental value -0.340 ± 0.017 for $(G_A/G_V)_{\Sigma^- \rightarrow n}$ with the prediction $-(1/3)$ suggests that eq. (5.2b) is valid.

The disagreement sharpens the paradox of other disagreements previously discussed because it involves only the properties of the Λ and Σ and does not assume flavor SU(3) symmetry or any relation between states containing different numbers of valence strange quarks. There is also the paradox that the magnetic moment of the Λ fits the value predicted by the naive SU(6) quark model, while the magnetic moments of the Σ are in trouble. In the semileptonic decays the Σ fits naive SU(6) and both the Λ and the nucleon are in trouble. The obvious fix for the semileptonic decays assumes a difference between constituent quarks and current quarks and fits the nucleon and Λ decays, but then the Σ is in trouble.

Interesting open questions remain in the paradoxes of eq. (5.1). Why is the Σ different from all other baryons? The large value in agreement of experiment with SU(6) $(G_A/G_V)_{(\Sigma^- \rightarrow n)} = -(1/3)$ for the simplest weak decay where the prediction is least dependent upon wave function structure implies that the spin projection of the strange valence quark in the Σ is antiparallel to the hyperon spin and has the largest possible value. Yet the contribution of this strange quark spin to the Σ magnetic moment seems to be mysteriously suppressed by a large factor or cancelled by some other unknown contribution. There is no such suppression observed in the contributions to nucleon magnetic moments of the d quark in the proton and the u quark in the neutron, which are directly related by SU(3) to the strange quark contribution in the Σ , and all other weak decays seem to have (G_A/G_V) suppressed by a factor of the order of 3/4.

An apparent inconsistency exists between the excellent agreement of the experimental value ^[46] $(G_A/G_V)_{\Sigma^- \rightarrow n} = -0.340 \pm 0.017$ with the SU(6) prediction of $-1/3$ and the well-known serious disagreement of the experimental value $(G_A/G_V)_{n \rightarrow p} = 1.2573 \pm 0.0028$ with the SU(6) prediction of $5/3$. Finding a model wave function which breaks SU(6) for the neutron decay but not for the Σ^- decay is particularly difficult because the two SU(6) values are extrema for any model in which the axial current is a single-quark operator describing a flavor-changing transition of a valence quark in which all the remaining degrees of freedom are spectators. The possibility of measuring $\Delta u(p) - \Delta d(p) - \Delta s(p)$ directly by elastic neutrino scattering is now under consideration ^[43].

6. The OZI Rule and the November Revolution

The OZI rule was originally proposed to explain the suppression of the $\phi \rightarrow \rho\pi$ decay and has been interpreted as a topological cook-book rule or a dynamical approximation somehow related to asymptotic freedom as revealed by the ZGS result (1.1). However, there is still no real theoretical understanding of this rule and no clue to a quantitative estimate of the forbiddenness factor. An outstanding failure of a quantitative prediction of an OZI-forbidden process was the overestimate^[47] of the width of the J/ψ by a factor of 30 in the big review paper on how to search for charm. Thus no experimenters were told to look for this very striking narrow resonance and the J/ψ was discovered experimentally by pure accident. There was considerable confusion and controversy about the nature of these new particles after the discovery and the issue was not settled until naked charm was actually discovered. The very narrow width was used as evidence against the interpretation of the J/ψ as charmonium. Feynman insisted that this “crazy Zweig rule” could not give such a large suppression, because it was violated by two-step strong interaction processes where each step was allowed and perturbation theory was certainly not valid. There must be some new symmetry principle with a new conserved quantum number.

Today hand-waving arguments supported by model calculations^[48] answer Feynman by suggesting that these second order processes are cancelled by contributions from different intermediate states. This argument also shows that the predicted J/ψ width^[47] was too large because the experimental $\phi \rightarrow \rho\pi$ width was used as input and threshold effects were disregarded. Feynman’s two-step amplitudes via on-shell intermediate states cannot be cancelled by other contributions via off-shell intermediate states. The ϕ mass is above the threshold for the the OZI-allowed $K\bar{K}$ decay, and the $\phi \rightarrow \rho\pi$ decay is dominated by the Feynman two-step OZI-allowed transition $\phi \rightarrow K\bar{K} \rightarrow \rho\pi$ where the intermediate state is on shell and cannot be cancelled by any other amplitude. The J/ψ mass is below the threshold for the analogous OZI-allowed $D\bar{D}$ decay and no OZI-allowed channel is open. Thus all the Feynman two-step transitions involve only off-shell intermediate states and can be strongly suppressed by cancellations.

But there is still no rigorous QCD argument supported by calculations giving quantitative estimates of the strengths of the Feynman two-step contributions.

7. Why are particles different from antiparticles?

7.1 Why have we learned so little in thirty years?

One of the greatest challenges for particle physics in the 1990’s is understanding the broken symmetry of CP violation. C and P violations were observed in 1956, very soon confirmed by many experiments and described by a theory which has stood the test of time and is now part of the standard model. In contrast CP violation has neither been confirmed by other experiments nor described by an accepted theory during the thirty years since its discovery in 1964.

What has happened since the discovery in 1964 of the $K_L \rightarrow 2\pi$ decay? Why no significant new experimental input in almost 30 years? The original $K_L \rightarrow 2\pi$ decay experiment is described by two parameters ϵ and ϵ' . Today $\epsilon \approx$ its 1964 value, ϵ' data are still inconclusive and there is no new evidence for CP violation outside the kaon system. Failure of the standard model to explain CP would indicate the need for new physics

beyond but would not challenge its validity in all other areas.

Why are we still back at Square One with not much new experimental input since 1964? Why is it so hard to find CP violation? How can B Physics Help? Does CP lead beyond the standard model? We investigate these questions with a general pedestrian symmetry approach. The Villains seem to be CPT and $\Delta I = 1/2$ which make life difficult.

Before 1964 the two kaon flavour eigenstates K^0 and \bar{K}^0 carrying strangeness ± 1 were believed to be CP - conjugate $CP|K^0\rangle = -|\bar{K}^0\rangle$, and mixed by a CP-conserving weak interaction into mass eigenstates $|K_S\rangle$ and $|K_L\rangle$ which were also CP eigenstates

$$|K_S\rangle = (1/\sqrt{2})(|K^0\rangle - |\bar{K}^0\rangle); \quad |K_L\rangle = (1/\sqrt{2})(|K^0\rangle + |\bar{K}^0\rangle) \quad (7.1)$$

The transition matrix elements for the CP-conserving $\pi^+\pi^-$ decay satisfy the relations,

$$\langle \pi^+\pi^- | T | K^0 \rangle = - \langle \pi^+\pi^- | T | \bar{K}^0 \rangle \quad (7.2a)$$

$$\langle \pi^+\pi^- | T | K_L \rangle = \langle \pi^+\pi^- | T | K^0 \rangle + \langle \pi^+\pi^- | T | \bar{K}^0 \rangle = 0 \quad (7.2b)$$

Very different lifetimes arise ($\tau_S = 9 \times 10^{-11}$ sec; $\tau_L = 5 \times 10^{-8}$ sec) because the dominant decay mode with largest phase space is allowed by CP for K_S and forbidden for K_L . The discovery of $K_L \rightarrow \pi^+\pi^-$ showed CP violation, which was described by the parameters:

$$\eta_{+-} \equiv \frac{\langle \pi^+\pi^- | T | K_L \rangle}{\langle \pi^+\pi^- | T | K_S \rangle} \equiv \epsilon + \epsilon'; \quad \eta_{00} \equiv \frac{\langle \pi^0\pi^0 | T | K_L \rangle}{\langle \pi^0\pi^0 | T | K_S \rangle} \equiv \epsilon - 2\epsilon' \quad (7.3)$$

So far the only experimental evidence for CP violation is in this case of neutral meson mixing where the two mass eigenstates both decay into same CP eigenstate. One might expect to observe direct CP violation as charge asymmetries between decays of charge conjugate hadrons $H^\pm \rightarrow f^\pm$. So far no such charge asymmetries have been found.

7.2 How CPT complicates detection of CP Violation

At a seminar at Argonne several years ago Barry Wicklund asked the speaker how partial widths for exclusive decay widths could be different for charge conjugate states, when CPT requires the total widths to be the same. Was there any simple way to see this miracle of different partial widths adding up to give the same total width. This question stimulated the following analysis.

Can decays of K^+ and K^- be different? For decays to charge conjugate final states $|f^\pm\rangle$ described by the Fermi Golden Rule, CPT and hermiticity show there is no asymmetry,

$$W_{K^\pm \rightarrow f^\pm} \approx (2\pi/\hbar) |\langle f^\pm | H_{wk} | K^\pm \rangle|^2 \rho(E_f) \quad (7.4)$$

$$\frac{|\langle f^- | H_{wk} | K^- \rangle|}{|\langle f^+ | H_{wk} | K^+ \rangle|} = \frac{CPT |\langle f^- | H_{wk} | K^- \rangle|}{|\langle K^+ | H_{wk}^\dagger | f^+ \rangle^*|} = \frac{|\langle K^+ | H_{wk} | f^+ \rangle|}{|\langle K^+ | H_{wk} | f^+ \rangle^*|} = 1 \quad (7.5a)$$

CPT also requires equal total widths of K^+ and K^- . Since s-wave elastic $\pi^\pm\pi^0$ scatterings go into one another under CPT, $\sigma_{el,s}(\pi^+\pi^0) = \sigma_{el,s}(\pi^-\pi^0)$ is a very narrow Breit-Wigner

resonance at the kaon mass with the same width for both charge states,

$$\Gamma_{tot}(K^+) = \Gamma_{tot}(K^-) \quad (7.5b)$$

Thus the following conditions are necessary for observation of charge-asymmetric decays:

1. Golden rule breaks down. This is exact first order perturbation theory and can only break down where higher order contributions are important. Second-order weak contributions are negligible; thus higher order strong contributions are needed.
2. Conspiracy of several decay modes. Total widths must be equal. Any asymmetry in the partial widths of a pair of conjugate modes must be compensated by opposite asymmetries in other modes.

For kaons all principal decay modes lead to approximate strong S-matrix eigenstates, the golden rule should be a good approximation and all charge asymmetry effects expected to be small. The s-wave $\pi^\pm\pi^0$ state is an exact eigenstate of the strong S-matrix since no inelastic channels are open at the kaon mass. The 3π final states are expected to be dominated by the $I=1$ component and thus nearly proportional to the same eigenstate of the strong S matrix. The $I=3$ amplitude is a $\Delta I = 5/2$ transition and doubly suppressed by the $\Delta I = 1/2$ rule. A similar situation obtains for different partial wave amplitudes where the overall s-wave is expected to be dominant.

7.3 Beating CPT for Charge Asymmetries in B Physics

Can decays of B^+ and B^- be different? Here many more channels are open, different decay modes can conspire to give the same total width and final state rescattering can beat the Fermi golden rule via higher order transitions in strong interactions; e.g.

$$B^- \rightarrow \bar{K}^0\pi^- \rightarrow K^-\pi^0; \quad B^+ \rightarrow K^0\pi^+ \rightarrow K^+\pi^0 \quad (7.6)$$

$$\frac{W_{B^+ \rightarrow K^+\pi^0}}{W_{B^- \rightarrow K^-\pi^0}} = \frac{|S_{el}M(K^+\pi^0) + S_{cex}M(K^0\pi^+)|^2}{|S_{el}M(K^-\pi^0) + S_{cex}M(\bar{K}^0\pi^-)|^2} \quad (7.7)$$

where $M(f^\pm) \equiv \langle f^\pm | H_{wk} | B^\pm \rangle$ and S_{el} and S_{cex} denote strong elastic and charge exchange scattering. This has no simple counterpart in the kaon system. Here both $(K\pi)$ isospin eigenstates $I = 1/2$ and $I = 3/2$ are $\Delta I = 1$ and equally allowed.

We now show how a CP-violating asymmetry arises in a toy model where only $K\pi$ decay modes contribute to B decay. The isospin eigenstates $(K\pi)_I$ are exact eigenstates of the strong S-matrix. Thus for $I=1/2$ and $3/2$,

$$|A\{B^+ \rightarrow (K\pi)_I\}| = |A\{B^- \rightarrow (\bar{K}\pi)_I\}| \quad (7.8)$$

$$\Gamma_{tot}(B^+) = \sum_I \Gamma\{B^+ \rightarrow (K\pi)_I\} = \Gamma_{tot}(B^-) = \sum_I \Gamma\{B^- \rightarrow (\bar{K}\pi)_I\} \quad (7.9)$$

in agreement with the *CPT* requirement of equal total widths. However, asymmetries can

occur for final states which are not strong eigenstates; e.g. $K^\pm\pi^0$,

$$A\{B^\pm \rightarrow f^\pm\} = \sum_I C_I^f |A\{B^\pm \rightarrow (K\pi)_I\}| \cdot e^{\pm iW_I} e^{iS_I} \quad (7.10)$$

where C_I^f denotes isospin Clebsch-Gordan coefficients. Every isospin amplitude is written as the product of its magnitude, and weak and strong phase factors e^{-iW_I} and e^{iS_I} . The weak CP-violating phase reverses sign under charge conjugation; the strong CP-conserving phase remains unchanged. Then $I=3/2 - 1/2$ interference can produce charge asymmetry,

$$|A\{B^+ \rightarrow K^+\pi^0\}|^2 - |A\{B^- \rightarrow K^-\pi^0\}|^2 = -4C_{\frac{1}{2}}^f C_{\frac{3}{2}}^f |A_{\frac{1}{2}} A_{\frac{3}{2}}| \sin(W_{\frac{1}{2}} - W_{\frac{3}{2}}) \sin(S_{\frac{1}{2}} - S_{\frac{3}{2}}) \quad (7.11a)$$

$$|A\{B^+ \rightarrow K^0\pi^+\}|^2 - |A\{B^- \rightarrow \bar{K}^0\pi^-\}|^2 = 4C_{\frac{1}{2}}^f C_{\frac{3}{2}}^f |A_{\frac{1}{2}} A_{\frac{3}{2}}| \sin(W_{\frac{1}{2}} - W_{\frac{3}{2}}) \sin(S_{\frac{1}{2}} - S_{\frac{3}{2}}) \quad (7.11b)$$

The asymmetries are seen to be equal and opposite for the two charge states, cancel in the total rates as expected from CPT and vanish unless *both* $W_{\frac{1}{2}} \neq W_{\frac{3}{2}}$ and $S_{\frac{1}{2}} \neq S_{\frac{3}{2}}$. The vanishing of the asymmetry when $S_{\frac{1}{2}} = S_{\frac{3}{2}}$ is simply interpreted in view of eq. (7.7) since $S_{\frac{1}{2}} = S_{\frac{3}{2}}$ implies no charge exchange, $S_{cex} = 0$. Thus the condition for observing an asymmetry is that at least two amplitudes arising from different strong eigenstates must contribute, and that they must have both different strong phases and different weak phases.

7.4 Charge Asymmetry in Standard Model - Trees and Penguins in $B \rightarrow K\pi$ Decays

In the standard model two diagrams with different weak phases contribute to $B \rightarrow K\pi$ decays via two different strong eigenstates and can produce a CP asymmetry^[49-50] The tree diagram gives only $K^\pm\pi^0$; the penguin only $I=1/2$ $K\pi$.

$$B^+(\bar{b}u) \rightarrow_{(tree)} \bar{u} + W^+ + u \rightarrow \bar{u} + u + \bar{s} + u \rightarrow K^+ + \pi^0 \quad (7.12a)$$

$$B^-(b\bar{u}) \rightarrow_{(tree)} u + W^- + \bar{u} \rightarrow u + \bar{u} + s + \bar{u} \rightarrow K^- + \pi^0 \quad (7.12b)$$

$$B^+(\bar{b}u) \rightarrow_{(penguin)} \bar{t} + W^+ + u \rightarrow \bar{s} + u \rightarrow (K\pi)_{I=1/2} \quad (7.13a)$$

$$B^-(b\bar{u}) \rightarrow_{(penguin)} t + W^- + \bar{u} \rightarrow s + \bar{u} \rightarrow (\bar{K}\pi)_{I=1/2} \quad (7.13b)$$

The radiative penguin transition $b \rightarrow s\gamma$ has recently been observed, and there may be some hope for seeing penguin interference in weak decays. But so far no purely weak penguin contributions have been unambiguously identified and all model calculations should be taken with a grain of salt.

Why is it called Penguin?

7.5 Where has all the antimatter gone?

In 1966 Andrei Sakharov showed how the baryon asymmetry of the universe could be explained by a model in which CP Violation + proton decay can kill all the antimatter produced in the big bang. At that time nobody noticed this work. Today it is a front runner in explaining the asymmetry. We show how it works in a simplified toy model for Sakharov's scenario.

We first note that to kill the antimatter, the difference between the number of nucleons and antinucleons ($n_{\bar{N}} - n_N$) must decrease with time,

$$\frac{d}{dt} \cdot (n_{\bar{N}} - n_N) < 0 \quad (7.14)$$

This must violate baryon number conservation, T and CP, and implies that the proton must decay, but slow enough to explain why it has not yet observed.

But so far CPT seems to be OK and we do not want to require CPT violation. Suppose a very weak gauge interaction with a superheavy boson is responsible for proton decay; e.g. via the decay mode,

$$p \rightarrow e^+ + K^- + \pi^+; \quad \bar{p} \rightarrow e^- + K^+ + \pi^- \quad (7.15)$$

CPT says the lifetimes for p and \bar{p} are equal, $\tau(p) = \tau(\bar{p})$. So proton decay is not enough to produce a baryon asymmetry.

The same very weak interaction that produces the decay (7.15) can be crossed to give the reactions

$$K^+ + p \rightarrow e^+ + \pi^+ \quad (7.16a)$$

$$K^- + \bar{p} \rightarrow e^- + \pi^- \quad (7.16b)$$

. But now CPT says these two transition rates probably equal, so we are not there yet.

Now suppose K^- flux is bigger than K^+ flux. This can kill off \bar{p} faster than p ! But how to get K^- flux bigger than K^+ ? CP Violation in B Decay can produce charge asymmetry to get K^- flux bigger than K^+ . In B decay CPT says $\Gamma_{tot}(B^+ \rightarrow X) = \Gamma_{tot}(B^- \rightarrow X)$ But CPT can be satisfied, CP violated if

$$\Gamma(B^+ \rightarrow K^+ \pi^0) < \Gamma(B^- \rightarrow K^- \pi^0) \quad (7.17a)$$

$$\Gamma(B^+ \rightarrow K^0 \pi^+) > \Gamma(B^- \rightarrow \bar{K}^0 \pi^-) \quad (7.17b)$$

So if B^+ and B^- are produced equally and also p and \bar{p} are produced equally, B^- decays in mode that kills \bar{p} but B^+ decays less in mode that kills p . Thus baryon asymmetry is produced by CP violation.

The Sakharov conditions for baryon asymmetry are thus:

1. Baryon number violation \Rightarrow proton decay
2. No thermal equilibrium.
3. CP violation can produce charge asymmetry

8. Conclusion

Quarks, Gluons and QCD are established, but many challenges remain. There was not time enough to discuss them all in this talk. But the role of pioneering experiments like those at the ZGS should not be forgotten. Nature was revealing asymptotically free confined quarks to blind theorists who did not want to see. And the implications of the ZGS discovery (1.1) are still relevant today. We conclude with an example from today's frontier quark physics.

Weak interaction diagrams tend to produce the ρ^0 and ω via only their V_d or V_u components since the quark lines in these diagrams have definite flavour labels. In the $B^+ \rightarrow K^+\rho^0$ and $B^+ \rightarrow K^+\omega$ decays K^+V_u is produced by both tree and penguin diagrams.

$$B^+(\bar{b}u) \rightarrow_{(tree)} (\bar{u}u\bar{s})u \rightarrow K^+V_u; \quad B^+(\bar{b}u) \rightarrow_{(penguin)} \bar{s}u \rightarrow K^+V_u \quad (8.1)$$

Production of K^+V_d is OZI forbidden. Thus by analogy with (1.1) we obtain

$$BR(B^+ \rightarrow K^+V_d) = 0 \quad BR(B^+ \rightarrow K^+\omega) = BR(B^+ \rightarrow K^+\rho) \quad (8.2)$$

This prediction can be checked directly by experiment. If it is confirmed, the same approach can be used for the more interesting case of $B^0 \rightarrow K^0\rho^0$ and $B^0 \rightarrow K^0\omega$ decays, where the tree diagram again produces V_u but the penguin diagram and all other diagrams which go via an intermediate $\bar{q}q$ pair produce V_d . Tree production of K^0V_d and penguin production of K^0V_u are both OZI and SU(3) forbidden. Thus

$$B^0(\bar{b}d) \rightarrow_{(tree)} (\bar{u}u\bar{s})d \rightarrow K^0V_u; \quad B^0(\bar{b}d) \rightarrow_{(penguin)} \bar{s}d \rightarrow K^0V_d \quad (8.3)$$

$$\frac{BR(B^0 \rightarrow K^0\rho^0)}{BR(B^0 \rightarrow K^0\omega)} = \left| \frac{T+P}{T-P} \right|^2 = \left| 1 + \frac{2P}{T-P} \right|^2 \quad (8.4a)$$

$$\frac{BR(\bar{B}^0 \rightarrow \bar{K}^0\rho^0)}{BR(\bar{B}^0 \rightarrow \bar{K}^0\omega)} = \left| \frac{\bar{T}+\bar{P}}{\bar{T}-\bar{P}} \right|^2 = \left| 1 + \frac{2\bar{P}}{\bar{T}-\bar{P}} \right|^2 \quad (8.4b)$$

where T, P, \bar{T} and \bar{P} denote respectively the contributions to the decay amplitudes (8.4a) and to the charge conjugate decay amplitudes (8.4b) from tree and penguin diagrams.

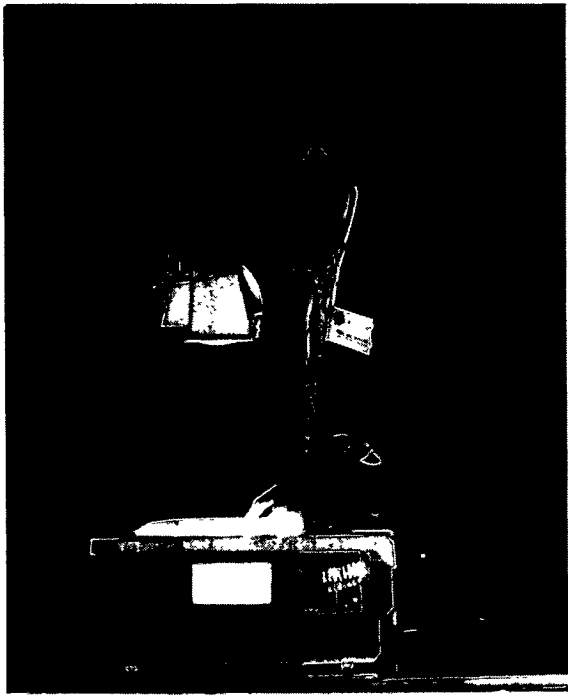
This offers the possibility of detecting the penguin contribution and also measuring the relative phase of penguin and tree contributions, as well as detecting CP violation in a difference between the charge-conjugate ρ/ω ratios (8.4a) and (8.4b). The relations (8.4) provide additional input from $B \rightarrow K\omega$ decays that can be combined with isospin analyses of $B \rightarrow K\rho$ decays to separate penguin and tree contributions [50].

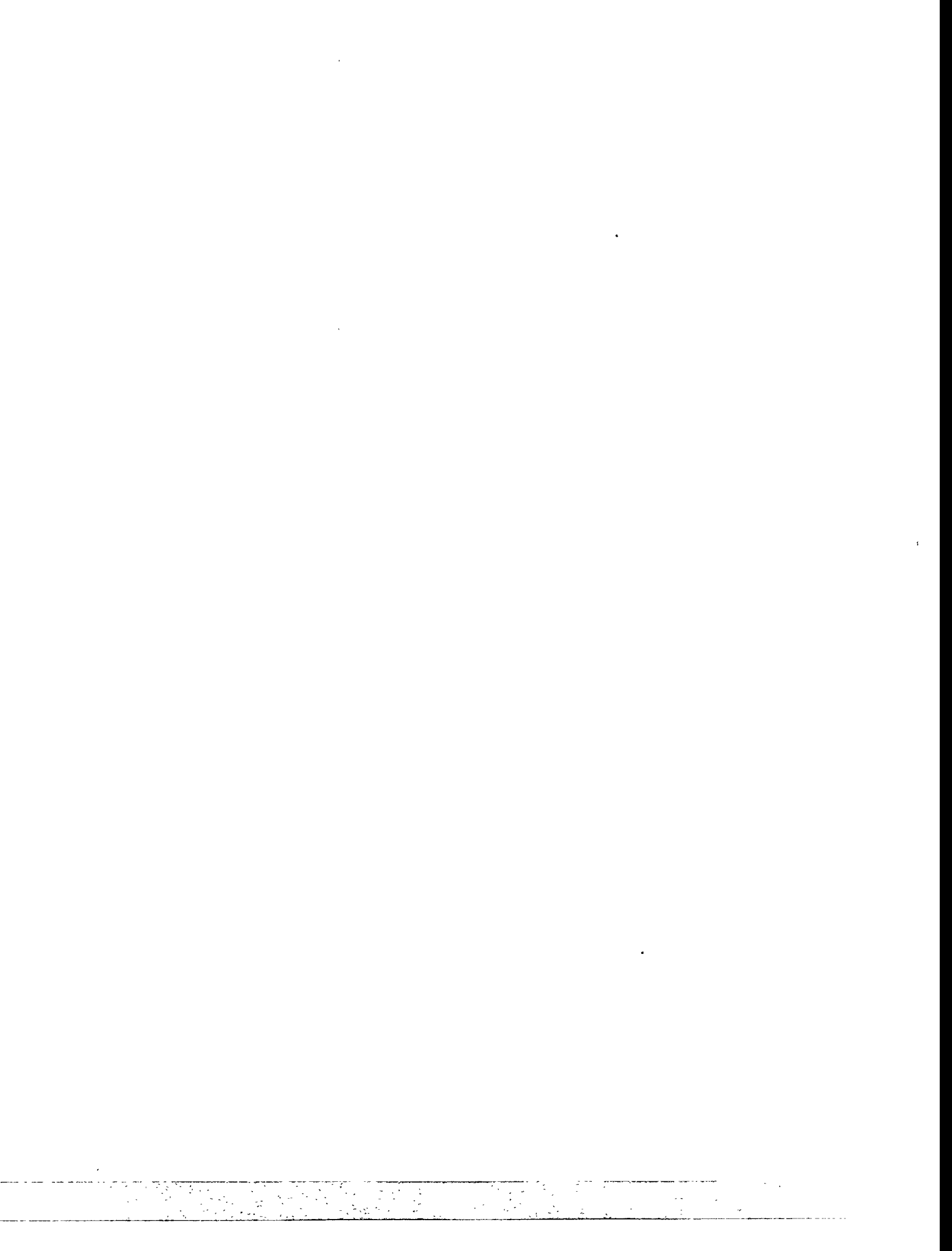
REFERENCES

- 1) E. M. Levin and L. L. Frankfurt, Zh. Eksperim. i. Theor. Fiz.-Pis'ma Redakt 2 (1965) 105; JETP Letters 2 (1965) 65
- 2) H. J. Lipkin and F. Scheck, Phys. Rev. Letters 16 (1967) 355
- 3) G. Alexander, H.J. Lipkin and F. Scheck, Phys. Rev. Lett. 17 (1966) 412
- 4) J. Mott et al, Phys. Rev. Letters 18, (1966) 71
- 5) Y. Nambu, in Preludes in Theoretical Physics, edited by A. de Shalit, H. Feshbach and L. Van Hove, (North-Holland Publishing Company, Amsterdam, 1966), p. 133
- 6) Ya. B. Zeldovich and A.D. Sakharov, Yad. Fiz 4 (1966)395; Sov. J. Nucl. Phys. 4 (1967) 283
- 7) Andrei D. Sakharov, Memoirs, Alfred A. Knopf, New York (1990) p. 261
- 8) A. D. Sakharov, Pisma JETP 21 (1975) 554; JETP 78 (1980) 2113 and 79 (1980) 350
- 9) Harry J. Lipkin, in Gauge Theories, Massive Neutrinos and Proton Decay (Proceedings of Orbis Scientiae 18th Annual Meeting, Coral Gables, Florida, 1981) edited by Behram Kursonoglu and Arnold Perlmutter (Plenum, N.Y., 1981), p. 359
- 10) A. D. Sakharov, private communication; Harry J. Lipkin, Annals of the New York Academy of Sciences 452 (1985) 79, and London Times Higher Education Supplement, January 20 (1984), p.17
- 11) Harry J. Lipkin, Phys. Lett. B74 (1978) 399
- 12) Harry J. Lipkin, in: "Physique Nucleaire, Les Houches 1968," edited by C. de Witt and V. Gillet, Gordon and Breach, New York (1969). p. 585
- 13) H.J. Lipkin, Phys. Lett. 45B (1973) 267
- 14) S. Okubo, Phys. Lett 5 (1963) 1975 and Phys. Rev. D16 (1977) 2336
- 15) G. Zweig, CERN Report No. 8419/TH412 unpublished, 1964; and in Symmetries in Elementary Particle Physics (Academic Press, New York, 1965) p. 192
- 16) J. Iizuka, Prog. Theor. Phys. Suppl. 37-38 (1966) 21
- 17) H. J. Lipkin, Phys. Rev. Letters 16 (1966) 1015
- 18) H. J. Lipkin, Z. Physik 202 (1967) 414

- 19) Harry J. Lipkin, Nucl. Phys. B9 (1969) 349
- 20) G. Veneziano, Phys. Reports 9C (1974) 199
- 21) H. Harari, Phys. Rev. Lett. 22 (1969) 562
- 22) J.L. Rosner, Phys. Rev. Lett. 22 (1969) 689
- 23) A. Donnachie and P. V. Landshof, Phys. Lett. B296 (1992)
- 24) Harry J. Lipkin, Phys. Rev. D11 (1975) 1827
- 25) Harry J. Lipkin, Phys. Lett B242 (1990) 115
- 26) ZEUS Collaboration, Phys. Lett. B293 (1992) 465
- 27) H1 Collaboration, Phys. Lett. B299 (1993) 376
- 28) M. M. Block and R. N. Cahn, Phys. Lett. B188 (1987) 143
- 29) Harry J. Lipkin, Nucl. Phys. B78 (1974) 381
- 30) Pierre Extermann, in *New Flavors and Hadron Spectroscopy*, Proceedings of the Sixteenth Rencontre de Moriond, Les Arcs - Savoie - France, 1981 edited by J. Tran Thanh Van (Rencontre de Moriond, Laboratoire de Physique Theorique et Particules Elementaires, Universite de Paris-Sud, Orsay, France, (1981) Vol. II. p. 393
- 31) Harry J. Lipkin, Nucl. Phys. B214 (1983) 136
- 32) Harry J. Lipkin, Phys. Lett B56 (1975) 76
- 33) Harry J. Lipkin, Phys. Rev. D17 (1978) 366
- 34) M. Froissart, Phys. Rev. 123 (1961) 1053
- 35) A. De Rujula, H. Georgi and S.L. Glashow, Phys. Rev. D12 (1975) 147
- 36) I. Cohen and H. J. Lipkin, Phys. Lett. 93B, (1980) 56
- 37) Harry J. Lipkin, Phys. Lett. B233 (1989) 446; Nuc. Phys. A507 (1990) 205c
- 38) Harry J. Lipkin, In: Proceedings of the 7th International Symposium on High Energy Spin Physics, Protvino (USSR), 22-27 September, (1986) Edited and Published by The Institute of High Energy Physics, Serpukhov (USSR), (1987) Vol. I, p.98
- 39) Harry J. Lipkin, Nucl. Phys. A478, (1988) 307c
- 40) H. J. Lipkin, Phys. Lett. 171B, 293 (1986)
- 41) H. J. Lipkin, Phys. Lett. 172B (1986) 242
- 42) The Spin Muon Collaboration (SMC), CERN preprint CERN-PPE/93-206
- 43) John Ellis and Marek Karliner, Phys. Lett. B313 (1993) 131, and CERN preprint CERN-TH.7022/93, Tel Aviv preprint TAUP 2094-93 hep-ph/9310272, to be published in the Proceedings of PANIC 93, Perugia, Italy

- 44) Stanley J. Brodsky, John Ellis and Marek Karliner, *Phys. Lett.* B206 (1988) 309
- 45) A. O. Bazarko et al (CCFR Collaboration), Nevis Preprint R1502, (June 30, 1994)
Submitted to *Physics Letters B*
- 46) Particle Data Group, *Phys. Rev.* D45 (1992) S1
- 47) M K. Gaillard, B.W. Lee and J.L. Rosner, *Rev. Mod. Phys.* 47 (1975) 277
- 48) Harry J. Lipkin, in *New Fields in Hadronic Physics*, Proceedings of the Eleventh Rencontre de Moriond, Flaine - Haute-Savoie, France, 1976 edited by J. Tran Thanh Van (Rencontre de Moriond, Laboratoire de Physique Theorique et Particules Elementaires, Universite de Paris-Sud, Orsay, France, (1976) Vol. I. p. 169, and *Phys. Lett.* B179 (1986) 278
- 49) Yosef Nir and Helen Quinn *Phys. Rev. Lett.* 67 (1991) 541
- 50) Harry J. Lipkin, Yosef Nir, Helen R. Quinn and Arthur E. Snyder, *Phys. Rev.* D44 (1991) 1715





where M_N is the nucleon mass.

The measured cross section⁽²⁾ for the quasi-elastic reaction (2), shown in Fig. 2a, illustrates this behaviour as do the similar measurements⁽³⁾ of $\Delta(1238)$ production of Fig. 2b. Typical events of the quasi-elastic scattering and single pion production, photographed in the 12-foot bubble chamber, are shown in Figs. 3 and 4, respectively.

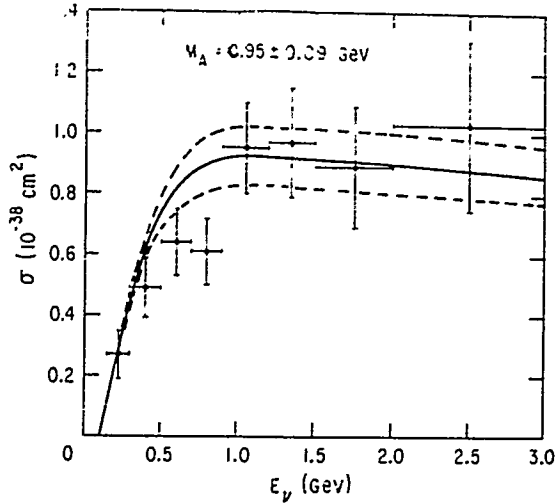


Fig. 2a Total cross section $\nu n \rightarrow \mu^- p$ as a function of neutrino energy. The highest-energy data points extends from 2.0 to 6.0 GeV.

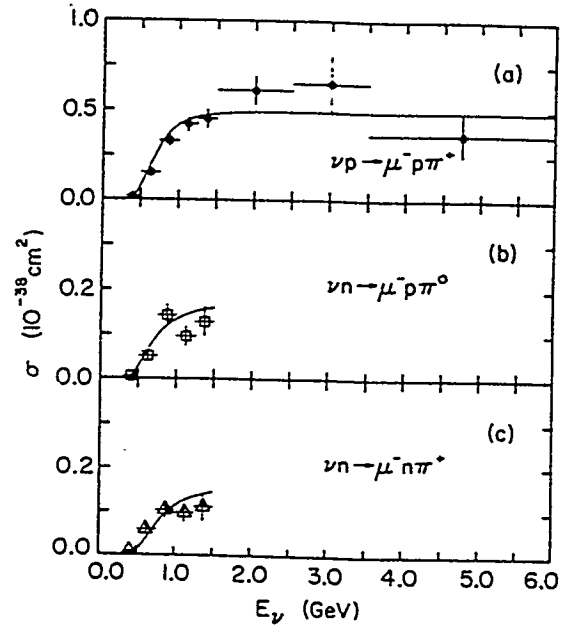


Fig. 2b The excitation functions for the final states (a) $\mu^- p \pi^+$, (b) $\mu^- p \pi^0$, (c) $\mu^- n \pi^+$ with the selection $M(N\pi) < 1.4$ GeV. The curves are the predictions of the Adler model with $M_A = 0.95$ GeV.

We now know that the nucleon is made of three valence quarks, held together by gluons, in addition to a $q\bar{q}$ sea, so the fundamental interaction at the hadron vertex is just the udW coupling in which case the total cross section should rise linearly with neutrino energy as is the case in νe scattering. The inclusive cross section measured in the 12-foot chamber⁽⁴⁾ shows that this simple expectation holds as seen in Fig. 5a. The np cross section ratio also approaches two at the higher energies reflecting the two (one) valence d quarks in the neutron (proton).

The next order of question is how the nucleon momentum is shared between the quarks. This is parametrized by the Bjorken x distribution and the cross section for $\bar{\nu} p$ scattering is written as:



Fig. 3 Low energy quasielastic scattering event photographed in the 12-foot bubble chamber. The neutrino enters from the left. Both the final state proton and μ^- stop in the liquid.

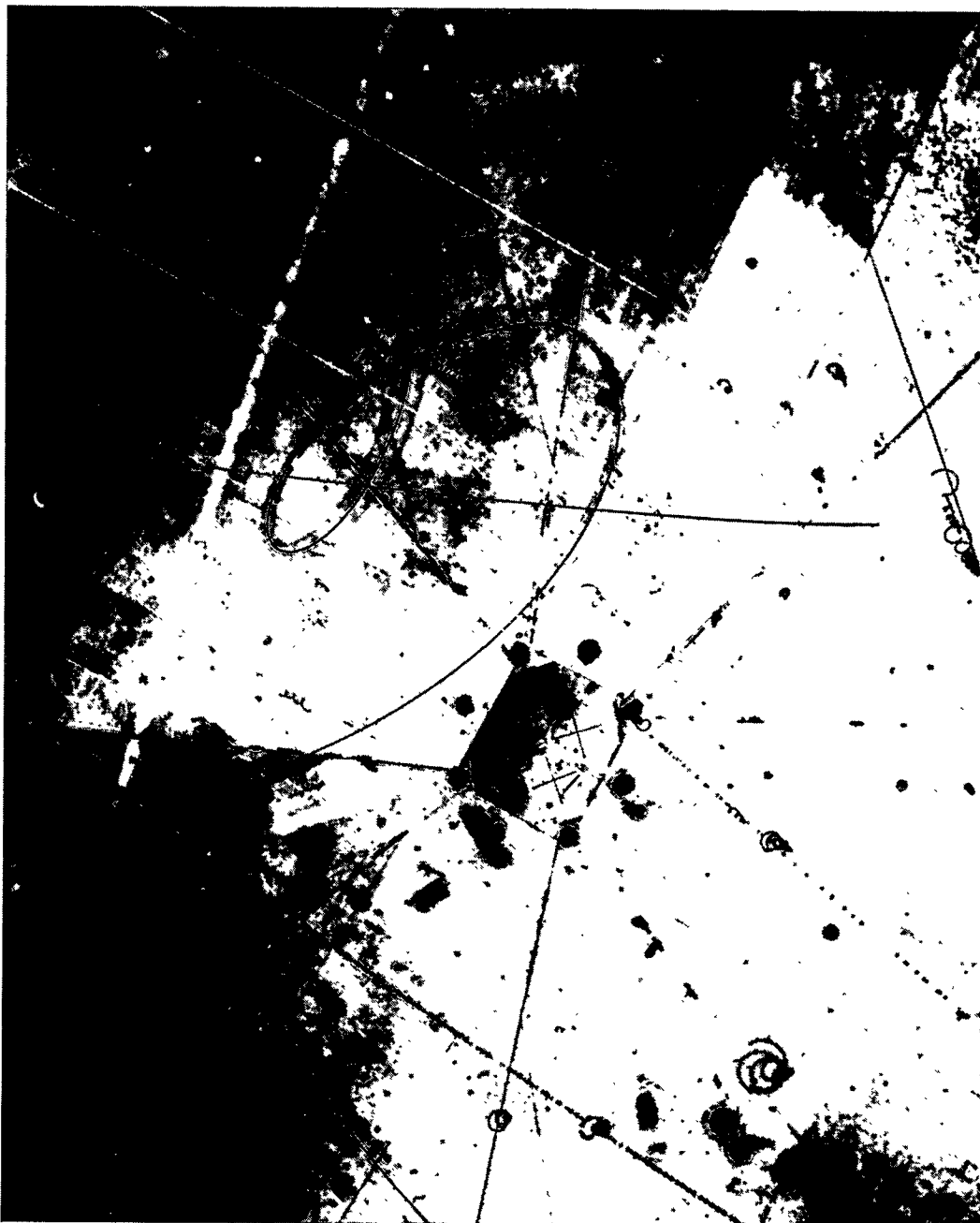


Fig. 4 Single pion production event $\nu p \rightarrow \mu^- p \pi^+$ seen in the 12-foot bubble chamber. The neutrino enters from the top and the π^+ track loops, stops and shows the characteristic $\pi^+ \rightarrow \mu^+ e^+$ decay.

$$\frac{d^2\sigma}{dxdy} = \frac{G^2 M_n E_\nu}{\pi} 2x \left[u(x)(1-y)^2 + (\bar{d}(x) + \bar{s}(x)) \right]$$

where the $u(x)$ is the valence u quark distribution and $\bar{d}(x)$, $\bar{s}(x)$ are the sea antiquarks. The analogy with neutrino and antineutrino electron scattering is evident. To measure the x distributions, we used an antineutrino exposure of the Fermilab 15-foot bubble chamber with a typical neutrino energy of 10 GeV as compared to 1 GeV at the ZGS. By extracting the $(1-y)^2$ and isotropic terms in different x regions, the u valence and the sea quark distributions were measured⁽⁵⁾ as shown in Fig. 6. The sea quark distribution is concentrated at low x .

These studies of neutrino interactions using bubble chambers were done in collaboration with groups from Carnegie-Mellon, Kansas and Purdue.

b) *Charm Spectroscopy?*

Following the discovery of the charm quark, a new spectroscopy opened up and an important question was whether the great success of the hydrogen bubble chambers in studying the spectroscopy of the u , d , s quarks could be repeated.

Since charm production in $\bar{\nu}$ scattering comes from the strange sea via the reaction $\bar{s}W \rightarrow \bar{c}$, only charmed mesons can be produced. With a neutrino beam the reaction is $sW \rightarrow c$, so both mesons and baryons occur in the final state. The decay $c \rightarrow sW$ leads to strange particles in the final state, so the x and y distributions of events with K^0 decays directly reflects the distributions of the strange sea - after correcting for K^0 's made in the fragmentation chain. The results⁽⁶⁾ of our study using the 15-foot chamber are shown in Figs. 7 and 8. The measured momentum fraction carried by the strange sea was $1.9 \pm 0.6\%$.

This small fraction, combined with the complex decay modes of the charmed particles and the difficulty of obtaining very large data samples, particularly at Fermilab, meant that this was not a fruitful program of research although a number of spectacular constrained events were observed with data from both Fermilab and CERN.

To study the spectroscopy of heavy quarks, e^+e^- annihilation was the preferred technique since 40% of the final states contain a pair of charmed particles. So, together with groups from Indiana, Michigan and Purdue, the High Resolution Spectrometer program was mounted at PEP. This spectrometer, shown in Fig. 9, together a good fraction of the collaboration, used the magnet from the 12-foot bubble chamber which became available as the ZGS neutrino program came to an end.

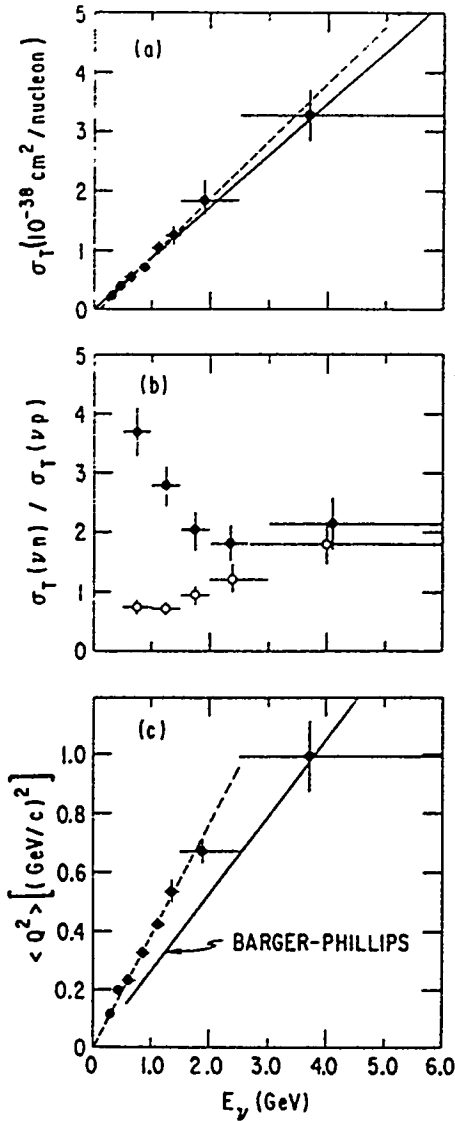


Fig. 5 (a) The total νN cross section, defined as half of $\sigma(\nu d)$, as a function of neutrino energy E_ν . The full line represents a linear fit through the origin, whereas the dashed line is the best linear fit without this constraint. (b) The ratio of the νn to νp cross sections as a function of neutrino energy. The filled circles correspond to all channels, whereas for the open circles, the quasi-elastic events have been removed. (c) Mean four-momentum transfer squared (Q^2) as a function of neutrino energy. The dotted curve represents $\langle Q^2 \rangle = -0.01 + 0.35 E_\nu$; the solid curve is a typical QPM prediction.

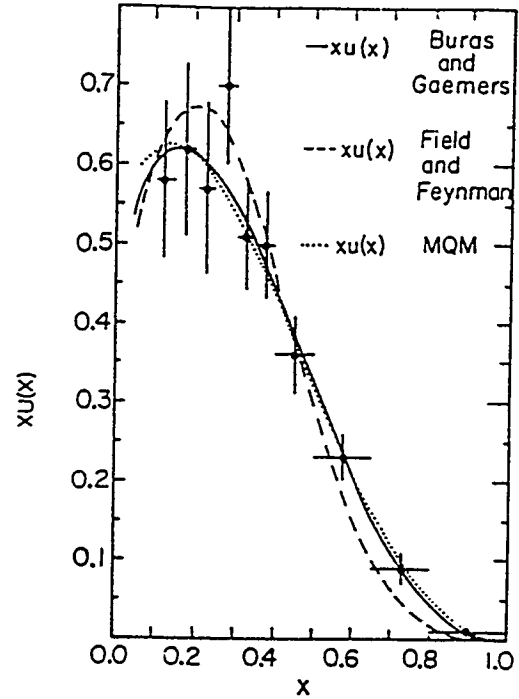


Fig. 6 (a) The up-quark momentum distribution in the proton, $xu(x)$. The data are normalized to the solid curve, which is the prediction of the Buras and Gaemers parametrization at $Q^2 = 4.5 (\text{GeV}/c)^2$. The Field and Feynman and MQM parametrizations are also shown in the dashed and dotted curves, respectively.

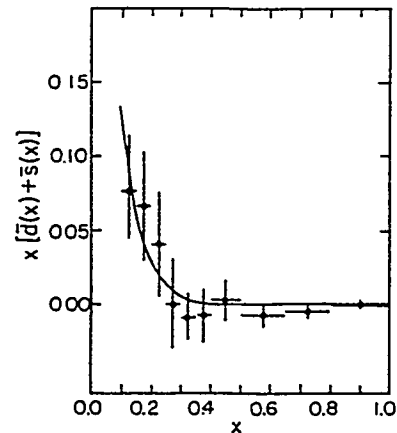


Fig. 6 (b) The antiquark momentum distribution in the proton $x[d(x) + \bar{s}(x)]$. The solid curve is the best fit to the form $A(1-x)^\alpha$ over the range $0.1 \leq x \leq 1.0$.

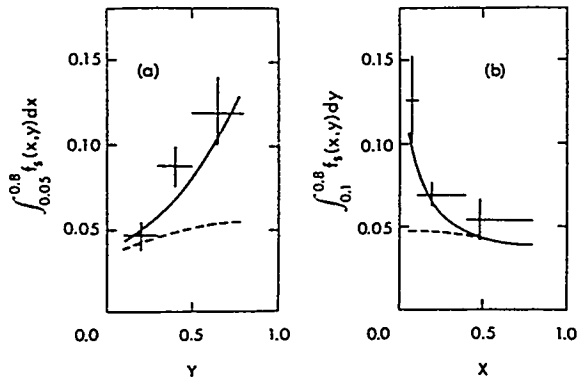


Fig. 7 (a) Strange particle fractions versus y and x . The solid lines are calculated, including the $\bar{s} \rightarrow \bar{u}$ transitions: the dashed lines only the K^0 's produced in the fragmentation chain.

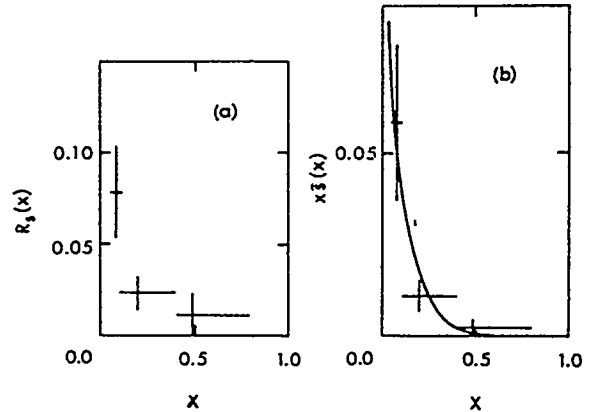


Fig. 8 $R_s(x)$ vs. x . This is the distribution resulting from subtracting the dashed curve from the data in Fig. 7(b). (b) $x\bar{s}(x)$ vs. x . The curve is the FF parametrization.

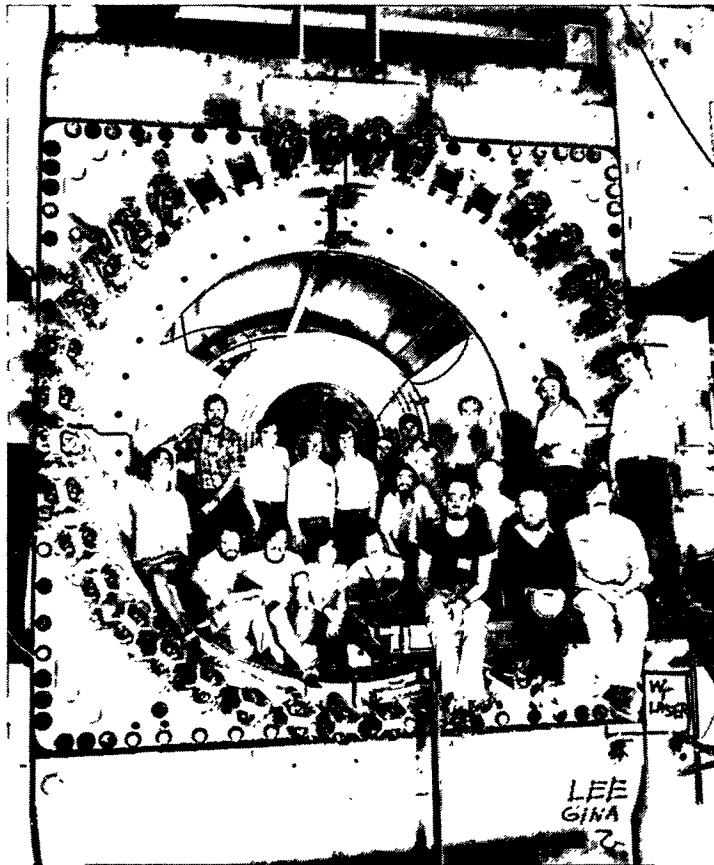


Fig. 9 High Resolution Spectrometer (pole tips removed) and a good fraction of the collaboration.

Typical D and D* signals observed in the HRS^(7,8) in the 1980's are shown in Fig. 10.

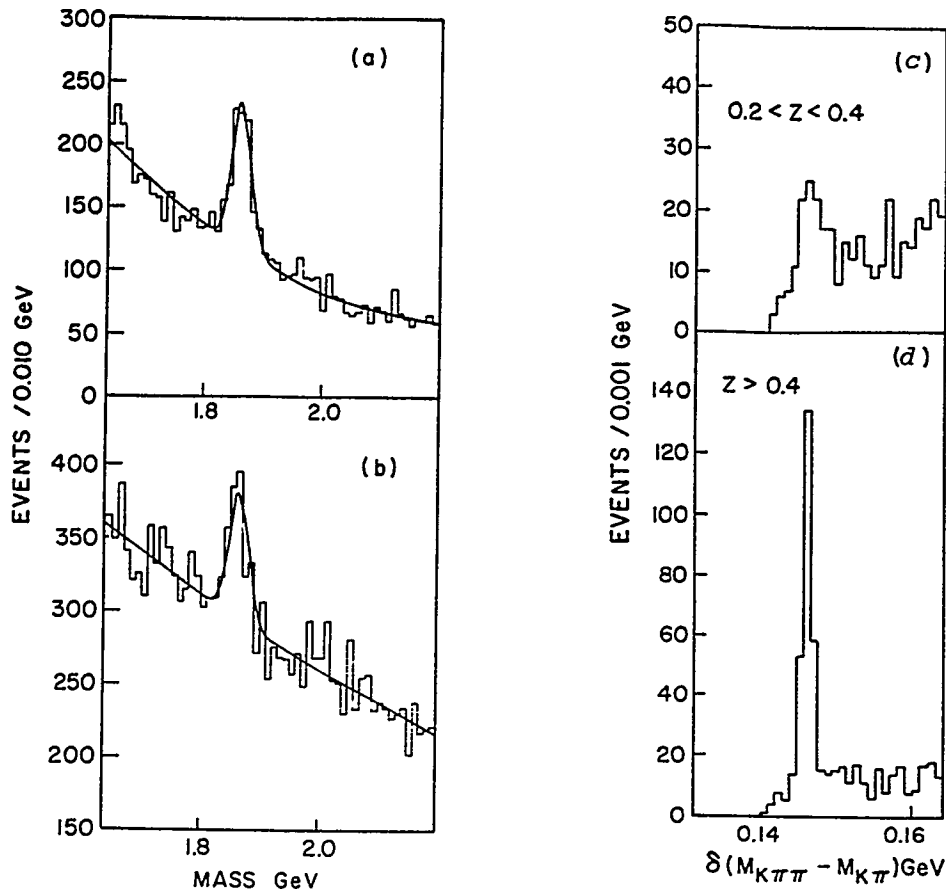


Fig. 10 D and D* signals measured in the HRS. a) mass $K^- \pi^+$, (b) mass $K^- \pi^+ \pi^+$, (c,d) mass difference plots $K \pi \pi - K \pi$ for different z ranges.

c) Neutral Currents

When the question of the existence of neutral weak currents became a major issue in the early 1970's, the first neutrino exposures had been made with the 12-foot bubble chamber and we embarked on a significant search for single pion production⁽⁹⁾ via the reactions:



The first reaction was signed by a π^+ meson originating in the liquid and showing the characteristic $\pi^+ \rightarrow \mu^+ \rightarrow e^+$ decay chain and the second by a pair converted photon pointing at a stopping proton track. The neutron reaction gave two charged particles in the final state that were required to be kinematically consistent with coming from the $\nu p \pi^-$ final state.

The two major difficulties of the experiment were a low event rate and a significant background from the equivalent neutron induced reactions. These were measured from the reaction $np \rightarrow pp\pi^-$ which is charge conjugate to the $np \rightarrow nn\pi^+$ reaction. The final event sample⁽¹⁰⁾ contained 160 neutrino induced events and 80 neutron background events.

In the first data set we did observe⁽¹¹⁾ one event that is a clear smoking gun, establishing, as we noted at the time, the existence of neutral currents. This event, shown in Fig. 11, is associated production by the neutral current: $\nu_\mu n \rightarrow \nu_\mu K^0 \Lambda^0$ followed by the decay of the two neutral particles: $K^0 \rightarrow \pi^+ \pi^-$, $\Lambda \rightarrow p \pi^-$. The background was measured to be 0.021 ± 0.016 events.

These neutral current observations were followed up by a measurement⁽¹²⁾ of the inclusive ratio $R_p^- = \bar{\nu} p \rightarrow \bar{\nu} X^+ / \bar{\nu} p \rightarrow \mu^+ X^0$ using the Fermilab 15-foot chamber. The technique used to identify the NC-events used a variable $u = x(1-y)$ which can be measured from the hadronic system only ($u = P \theta^2 / 2M_n$), where P is the momentum and θ the polar angle. The distributions for the CC $\bar{\nu}_\mu$ and ν_μ events together with the NC data are shown in Fig. 11. The $\bar{\nu}_\mu$ exposure had a significant neutrino background. The resulting value of the Weinberg angle, $\sin^2 \theta_w = 0.190 \pm 0.05$, is shown in Fig. 13(a) using measurements of R_p from other groups. The results from the 12-foot chamber on the single pion production reactions shown in Fig. 13(b) gave the less precise value of 0.26 ± 0.09 . These measurements, which date back to 1982, may be compared to the 1993 value from the CCFR collaboration, based on 10^6 events, of 0.2248 ± 0.0064 , about an order of magnitude improvement in the error in eleven years.

SEARCH FOR THE BOSONS

a) Indirect Observations

Many experiments were done searching for the intermediate bosons W and Z in the period covered by this review. One of the earliest⁽¹³⁾ searched for prompt muons coming from the ZGS proton beam in the simple setup shown in Fig. 14. The reaction was $u\bar{d} \rightarrow W^+ \rightarrow \nu\mu^+$ where the u quark came from the ZGS proton and the \bar{d} from the target. No signal was seen and a mass limit of 3 GeV was placed on the W, assuming a certain cross section.

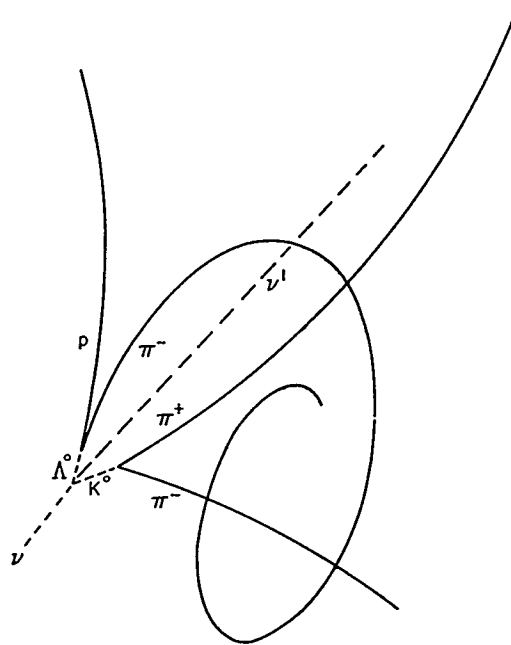


Fig. 11 First example of associated production via the neutral current observed in the 12-foot bubble chamber.

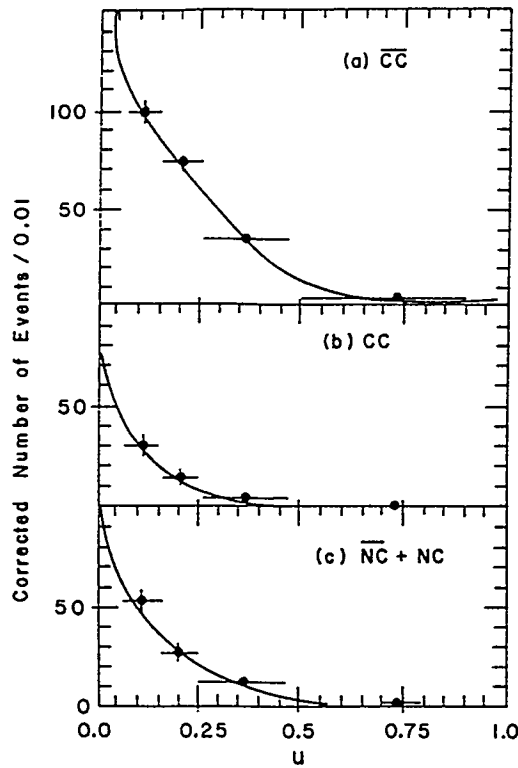


Fig. 12 Experimental differential cross sections dN/du for (a) the \overline{CC} , (b) the CC , and (c) the $\overline{NC} + NC$ events, all for $u > 0.06$. Only the curve for the CC case is area-normalized.

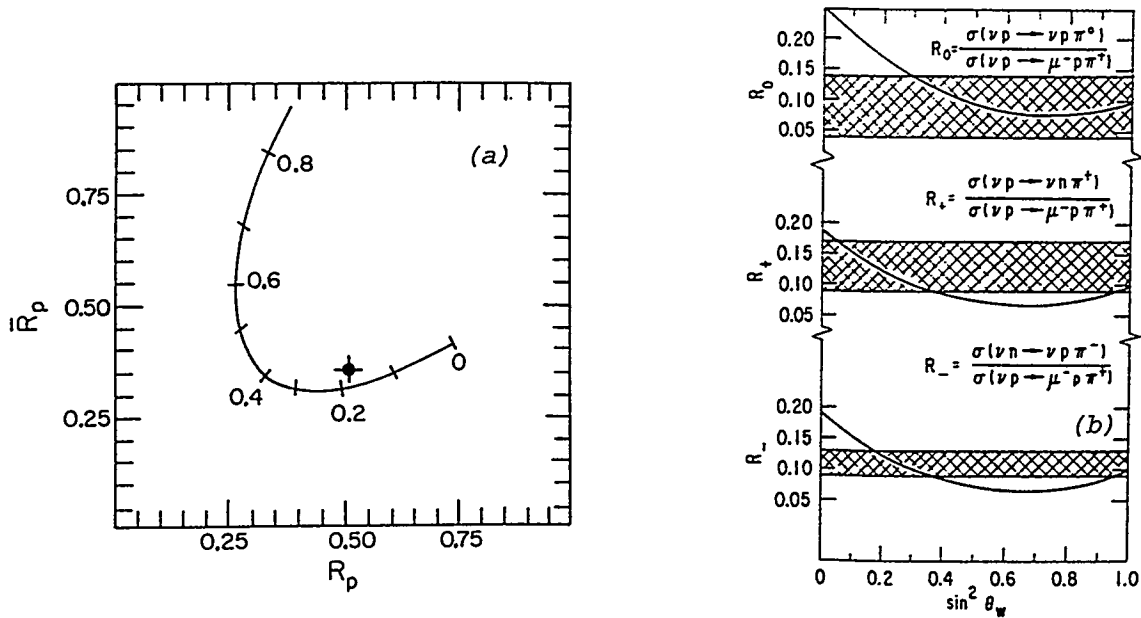


Fig. 13 (a) Measured value of \overline{R}_p vs. the world-average value for R_p . The curve is the Weinberg-Salam prediction with values of $\sin^2 \theta_w$ indicated. (b) Comparisons of our measurements of R_+ , R_0 , and R_- with the predictions of the Weinberg-Salam-Adler model.

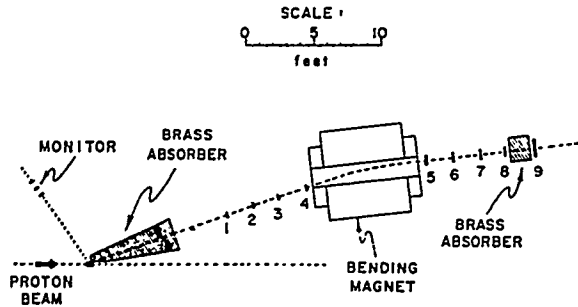


Fig. 14 Layout of experimental apparatus for ZGS W search. Numbers 1 through 9 indicate plastic scintillator counters. Counters and the target are not to scale.

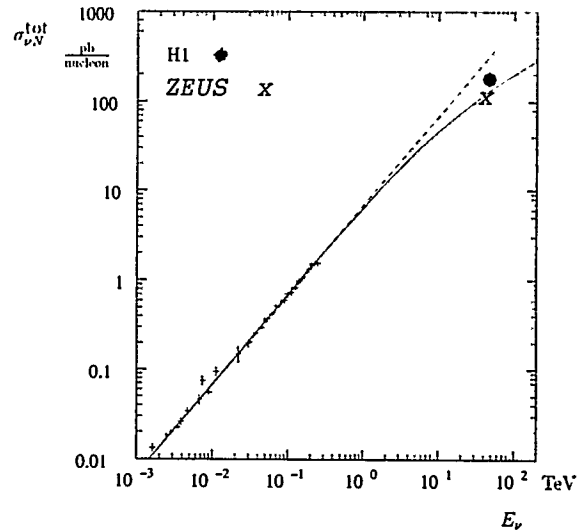


Fig. 15 The energy dependence of the νN cross section. The crosses represent the low energy neutrino data while the full circle refers to result of this analysis which, for the purpose of comparison, had been converted to a νN cross section. The experiment at HERA corresponds to an equivalent fixed target energy of about 50 TeV. The full line represents the predicted cross section, including the W propagator. The dashed line is the linear extrapolation from low energies.

Electromagnetic production in neutrino interactions showed no signal nor did searches for a turn over in the total cross section which will occur at sufficiently high energies in analogy to the cross section for the quasielastic production discussed earlier. The inclusive cross section will include a propagator term and go as:

$$\frac{d^2\sigma}{dx dQ^2} = \frac{G^2}{2\pi} \frac{1}{\left(1 + \frac{Q^2}{M_w^2}\right)} 2 \left[u(x) + (1-y)^2 (\bar{d}(x) + \bar{s}(x)) \right] \quad (6)$$

Such an effect has recently been seen⁽¹⁴⁾ in the H1 and ZEUS experiments at the HERA e-p collider at DESY as shown in Fig. 15. This figure shows the total cross section for neutrino scattering on an isoscalar target as a function of neutrino lab energy. The reaction measured by the HERA detectors is: $ep \rightarrow \nu_e X$. The HERA beam energies of 26.7 GeV for the electrons and 820 GeV for the protons gives a cm energy of 296 GeV or an equivalent neutrino lab energy of 46 TeV, quite an increase over that possible at fixed target facilities. So indeed something did happen when it was possible to reach 300 GeV in the cm system!

An earlier signature of the Z boson came from the forward:backward asymmetry in e^+e^- annihilation to both lepton pairs and quark pairs that arises from the Z- γ interference term. Typical data⁽¹⁵⁾ from the HRS for $e^+e^- \rightarrow \mu^+\mu^-$ and $e^+e^- \rightarrow \tau^+\tau^-$ are shown in Fig. 16. For the charm quark pair production $e^+e^- \rightarrow c\bar{c}$, the asymmetry is given by:

$$A = \frac{3}{2} \frac{1}{q} g^e g^c \frac{G}{2\sqrt{2}\pi\alpha} \frac{s}{1 - s/M_z^2} \quad (7)$$

The expected value of -0.094 may be compared to the HRS measurement⁽¹⁵⁾ of -0.099 ± 0.027 .

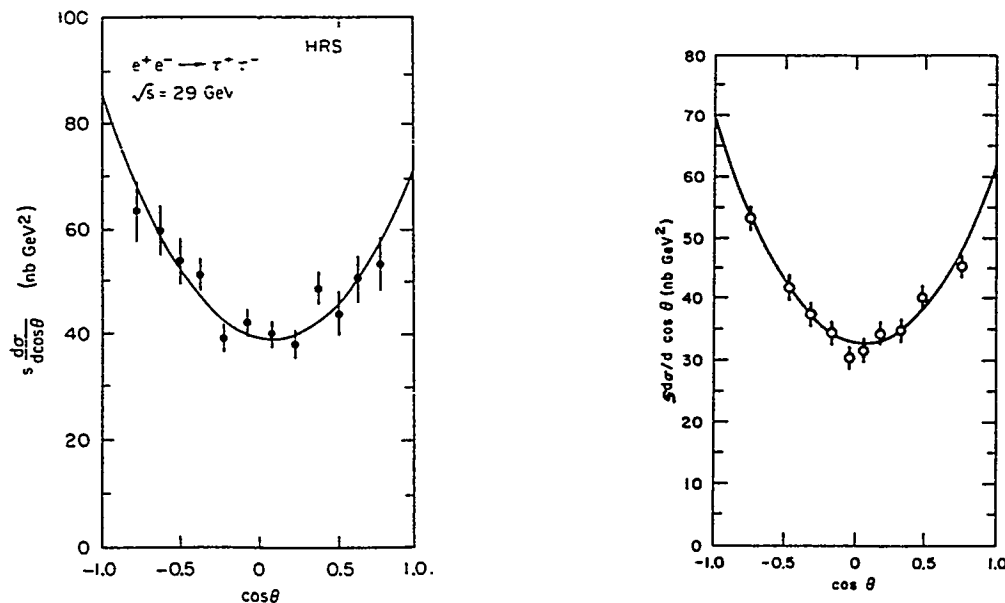


Fig. 16 (a) The angular distribution of muons for 4246 events of the process $e^+e^- \rightarrow \mu^+\mu^-$. (b) The differential cross section for the reaction $e^+e^- \rightarrow \tau^+\tau^-$ at \sqrt{s} at 29 GeV. The curve is the best fit to the data including electroweak interference.

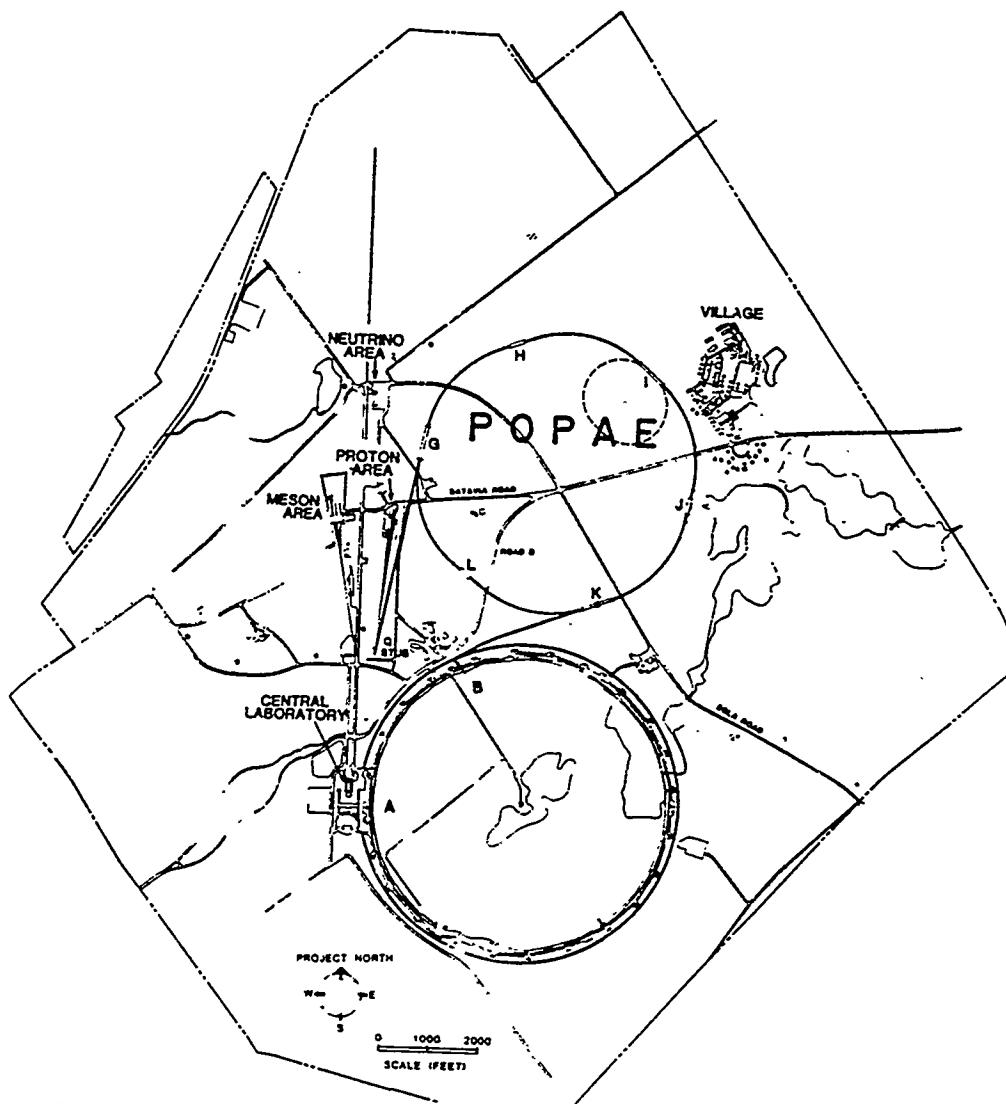


Fig. 17 Location of POPAE on the Fermilab site.

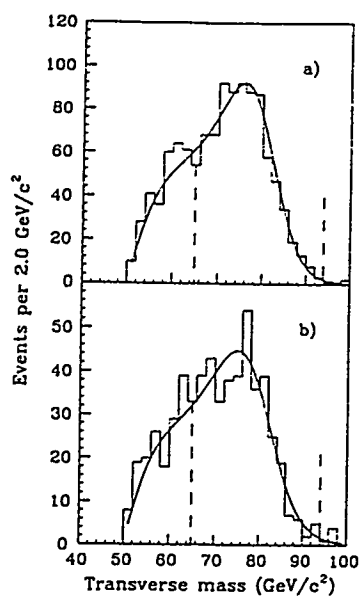


Fig. 18. Transverse-mass distribution for all $W \rightarrow e\nu$ candidates observed in CDF. Overlaid is the best fit to the data. Indicated with dashes is the range of transverse mass used in the fit. (b) Transverse-mass distributions for all $W \rightarrow \mu\nu$ candidates.

b) *Direct Observations*

As is well known the W and Z bosons were directly observed at the CERN $p\bar{p}$ collider in 1984. What is perhaps not as widely appreciated is the joint ANL-Fermilab study carried out, under Bob Diebold in 1976, of a high luminosity 1 TeV on 1 TeV pp collider called POPAE.⁽¹⁶⁾ The foreseen site of this facility is shown in Fig. 17. For various political reasons, the project was never launched and represents one of the major lost opportunities of the U.S. program. One positive outcome of the POPAE study was an early concept of the CDF detector and a significant ANL involvement with that program. Typical transverse mass distributions for $W \rightarrow e\mu$ and $W \rightarrow \mu\nu$ observed in CDF⁽¹⁷⁾ are shown in Fig. 18.

The remarkable agreement between the world average measurements of all of the electroweak parameters and the Standard Model is shown in Fig. 19 where the two variables are chosen as the W mass and the top quark mass. The outer horizontal band is the directly measured W mass and the inner band the LEP measurements expressed in terms of M_W . The measured top quark mass is shown as the vertical band and the family of curved lines are drawn for different values of the Higgs mass.

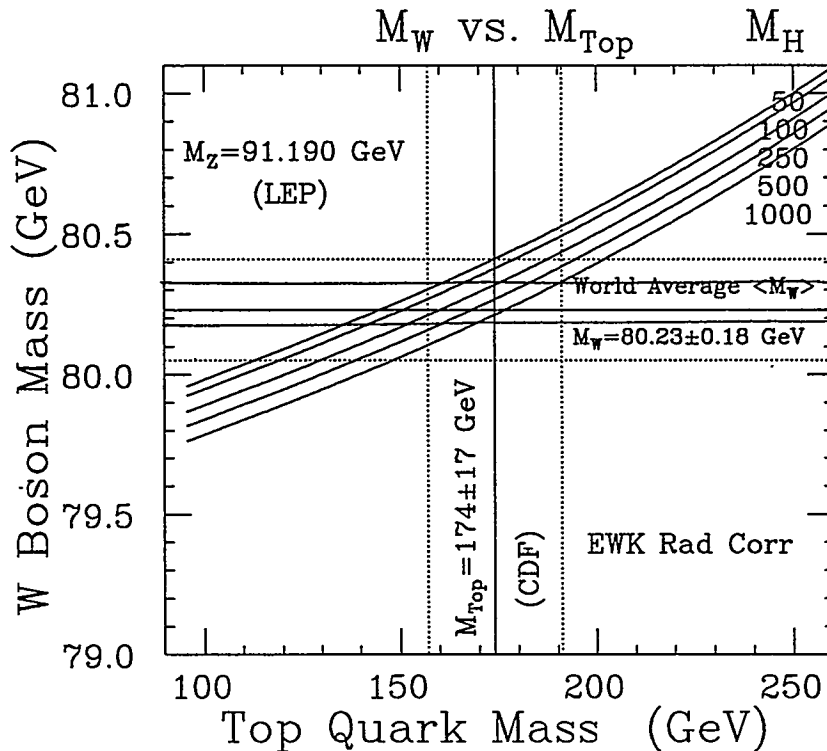


Fig. 19 World average values for the W boson and top quark mass. The diagonal lines are drawn for different assumed values of the Higgs mass.

PROBING THE PROPERTIES OF THE NEUTRINOS

It was once thought that neutrinos have very simple properties: no mass, no magnetic moment and spin one half with negative helicity for the neutrino. However, a simple comparison with the quark sector where the charge one-third quarks are mixed suggests the possibility that this could also hold for the neutrinos. In any case, the issue of neutrino mass is open to experimental investigation.

In the 1966 exposure of the 10-inch helium bubble chamber to a stopping K^- beam at the ZGS, a measurement of the muon range from stopped π^+ decay was used⁽¹⁸⁾ to limit the muon neutrino mass. Two calibration reactions were also measured:

$\pi^- He^4 \rightarrow H^3 n$, $K^- He^4 \rightarrow \Lambda H^4 \pi^0$, to validate the range energy relation.⁽¹⁹⁾ The results gave the limit mass $m_{\nu\mu} < 2.2$ MeV at 90% c.l. The current limit is 0.27 MeV. Stopping protons from the decay $\Sigma^+ \rightarrow p\pi^0$ were also used to measure the Σ^+ mass.

The second neutrino mass limit, published by the HRS Collaboration in 1986, was for the tau neutrino.⁽²⁰⁾ It used the first observation of the $\tau \rightarrow 5\pi$ decay from the HRS to limit the τ neutrino mass to < 76 MeV at 95% c.l. The present limit is about 35 MeV. The HRS results are shown in Fig. 19.

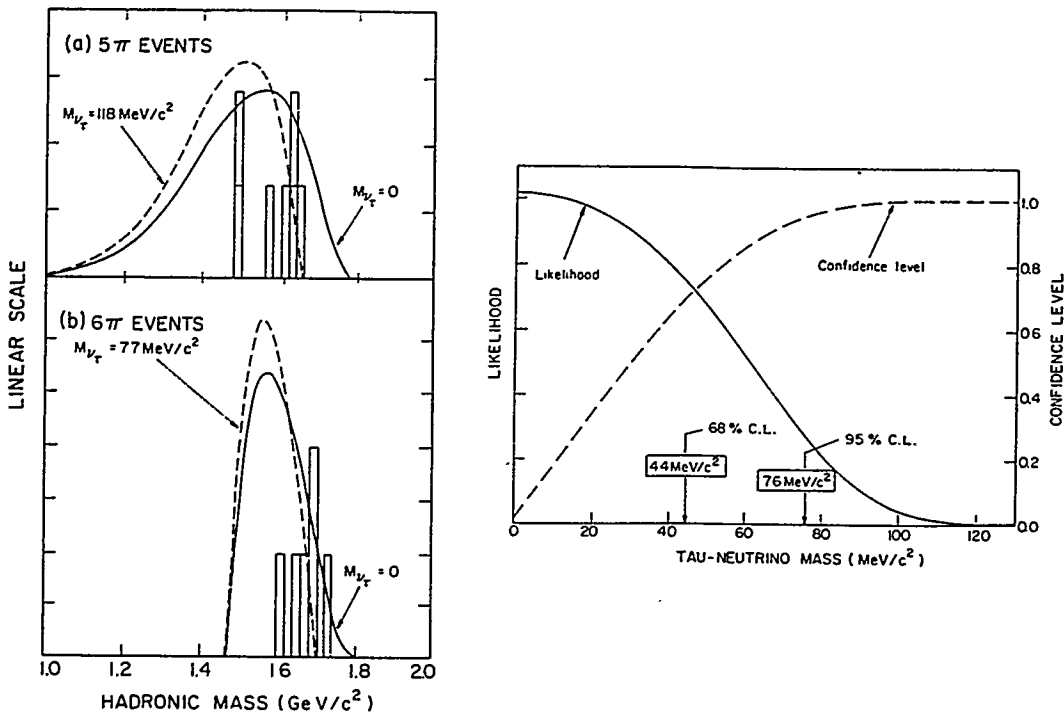


Fig. 19 (a) The hadronic invariant mass of the seven events $\tau \rightarrow 5\pi^\pm \nu_\mu$. The solid line is phase space times the weak matrix element for the best fit $M_{\nu\tau} = 0$. (b) The hadronic invariant mass of the six events $\tau \rightarrow 5\pi^\pm \pi^0 \nu_\tau$. The solid line shown is the best fit, $M_{\nu\tau} = 0$. The dashed lines show the 95%-confidence-level limits of $M_{\nu\tau}$. (c) The likelihood function for the combined $5\pi^\pm \nu_\mu$ and $5\pi^\pm \pi^0 \nu_\tau$ data. The confidence level as a function of τ -neutrino mass is also plotted.

A related search was done in the 12-foot bubble chamber⁽²⁰⁾ looking for the decay $\nu_\mu \rightarrow \nu_e \gamma$. One remembers the importance that the absence of the decay $\mu \rightarrow e \gamma$ played in suggesting that the muon and electron neutrinos were different particles, an hypothesis confirmed by the first AGS neutrino experiment. The experiment in the 12-foot bubble chamber looked for photon conversions to e^+e^- pairs pointing along the beam direction. Since the neutrino mass difference is very small, such photons should have half of the beam energy and be along the beam direction. The mean conversion probability in the deuterium of the bubble chamber was about 4%. The laboratory decay rate, Γ_{lab} , is related to the intrinsic c.m. rate by:

$$\Gamma_{lab} = \frac{m_{\nu_\mu} \Gamma_{\nu_\mu}}{E_{\nu_\mu}} . \quad (8)$$

The result of the experiment was $m_{\nu_\mu} \Gamma_{\nu_\mu} < 4.6 \cdot 10^{-4} \text{ MeV/sec}$ at the 90% c.l.

If indeed neutrinos have a mass, then they could be mixed such that a pure beam of one species would gain an admixture of a second type during the flight time from the production point to the detection point. The mixing probability, P , is written as:

$$P = \sin^2(2\theta) \sin^2 \left[1.27 \Delta m^2 \frac{L}{E_\nu} \right] . \quad (9)$$

where θ is the mixing angle, Δm^2 the square of the mass difference, L the flight path and E_ν the neutrino energy. For best sensitivity one clearly needs a low energy and a long flight path.

Many accelerator experiments have been done, including E645 at LAMPF⁽²²⁾ to which HEPD physicists contributed, but no positive signal has been seen.

There is the well known deficit of neutrinos from the sun which has been interpreted as showing evidence for neutrino oscillations. The situation is quite complex theoretically, depending as it does on solar models and is also experimentally difficult since the extraction efficiency of the daughter atoms must be reliably determined.

In more recent times, evidence has grown that atmospheric neutrino interactions do not show the expected ratio of muon neutrino to electron neutrino interactions. The measurements⁽²³⁾ show a deficit of muon neutrinos as compared to the predicted rate. The neutrinos result from the interactions of high energy cosmic rays with the atmosphere, the muon neutrinos coming from π decay as in a normal accelerator neutrino beam. The

"target" in this case is so dilute that a good fraction of the muons also decay giving rise to the electron neutrinos.

The events are classified as muon like-with a penetrating final state particle, electron-like with a final state shower or "other" which includes neutral current events and inelastic charged current events with a low energy muon or electron in the final state. The results are quoted as a ratio of ratios:

$$R = \frac{(\nu_{\mu}/\nu_e)_{data}}{(\nu_{\mu}/\nu_e)_{Monte\ Carlo}} \quad (10)$$

Data from the 12-foot bubble chamber is used as input to the Monte Carlo simulation since the spectrum of atmospheric neutrinos is quite similar to that from the ZGS.

Two results, listed in Table I, have been reported from the water Cerenkov counters that were originally built to look for nucleon decay. The second values for the water counters comes from the events in which a muon decay was observed. R is expected to be unity so there is a clear deficit as compared to the prediction coming from the Monte Carlo simulation.

Table I
Atmospheric Neutrino Results

<i>Detector</i>	<i>Exposure Kton-Years</i>	<i>R</i>	
Kamioka	6	0.60 ± 0.06	0.64 ± 0.07
IMB	7.7	0.54 ± 0.05	0.69 ± 0.06
Soudan	1.01	$0.69 \pm 0.19 \pm 0.09$	

The Soudan result is not yet precise enough to establish the effect, but by 1998 when 5 kton-years of exposure will have been collected, the error will be ± 0.08 . Since this detector is a tracking calorimeter, it has quite different systematic errors than the water counters and so the Soudan measurement will be very important in establishing the result.

Figure 21 shows the mass difference and mixing angle values that are calculated from the Kamioka data assuming that it results from neutrino oscillations.

If neutrino really are mixed, then a whole new field of research opens up so it is of prime importance to unambiguously establish that this is indeed the case. A good way to do this is to send a neutrino beam from the Fermilab main injector, now under construction, to the Soudan mine, as shown in Fig. 22. The distance of 730 km is about

optimum for neutrinos from the 150 GeV protons of the main injector. Even with the present Soudan detector, a very sensitive experiment can be done in a two-year run as shown by the contour in Fig. 21, which represents the limits that would be obtained if neutrino oscillations do not occur.

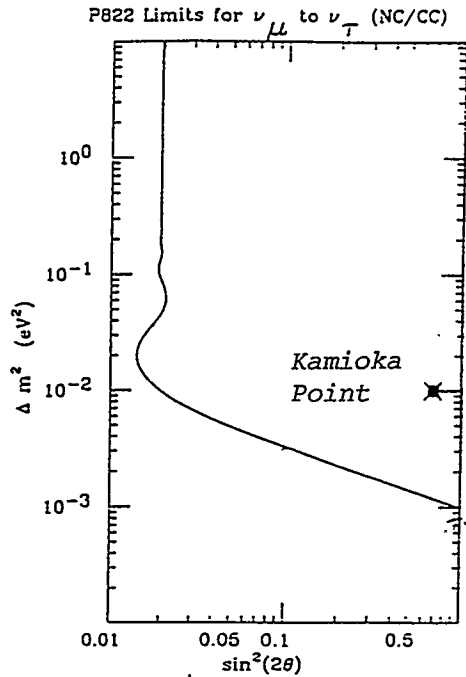


Fig. 21 Contour of sensitivity for the Fermilab to Soudan neutrino oscillation experiment compared to the Kamioka atmospheric neutrino result.

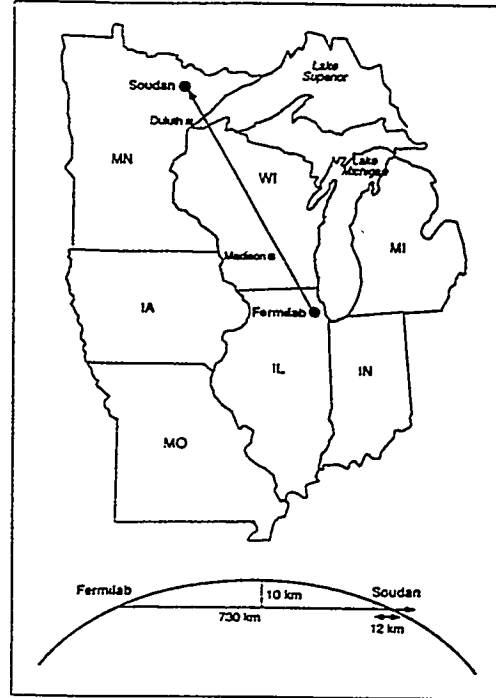


Fig. 22. Proposed neutrino beam from the Fermilab main injector to the Soudan mine detector.

A much larger detector is planned for an extended program of research in the first decade of the 21st century.

CONCLUSIONS

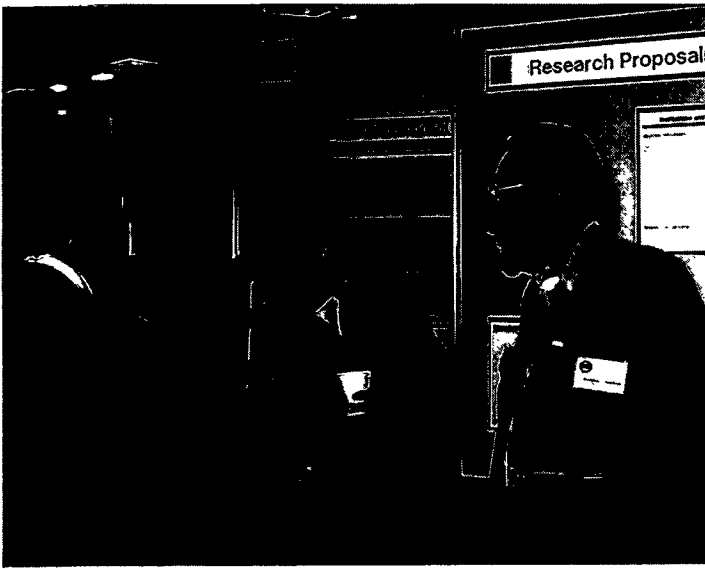
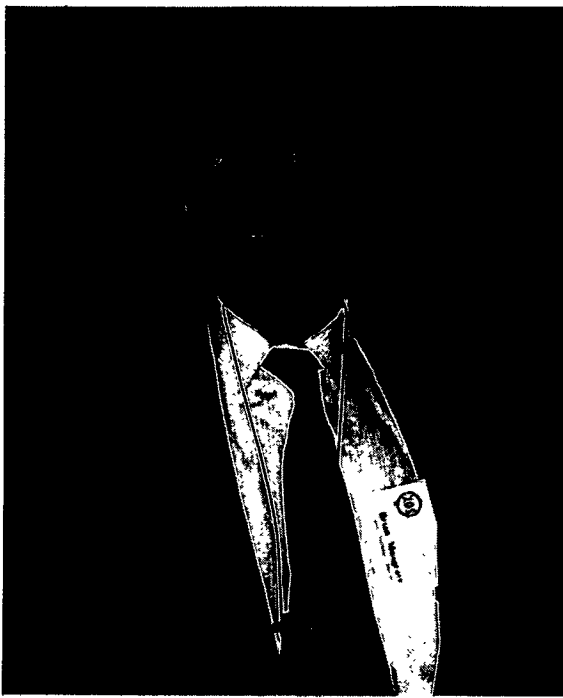
What began 30 years ago as an exploration of weak interactions at energies beyond those available from decays, grew to encompass the whole standard model of electroweak interactions. There are good expectations that the next 30 years will see equally dramatic

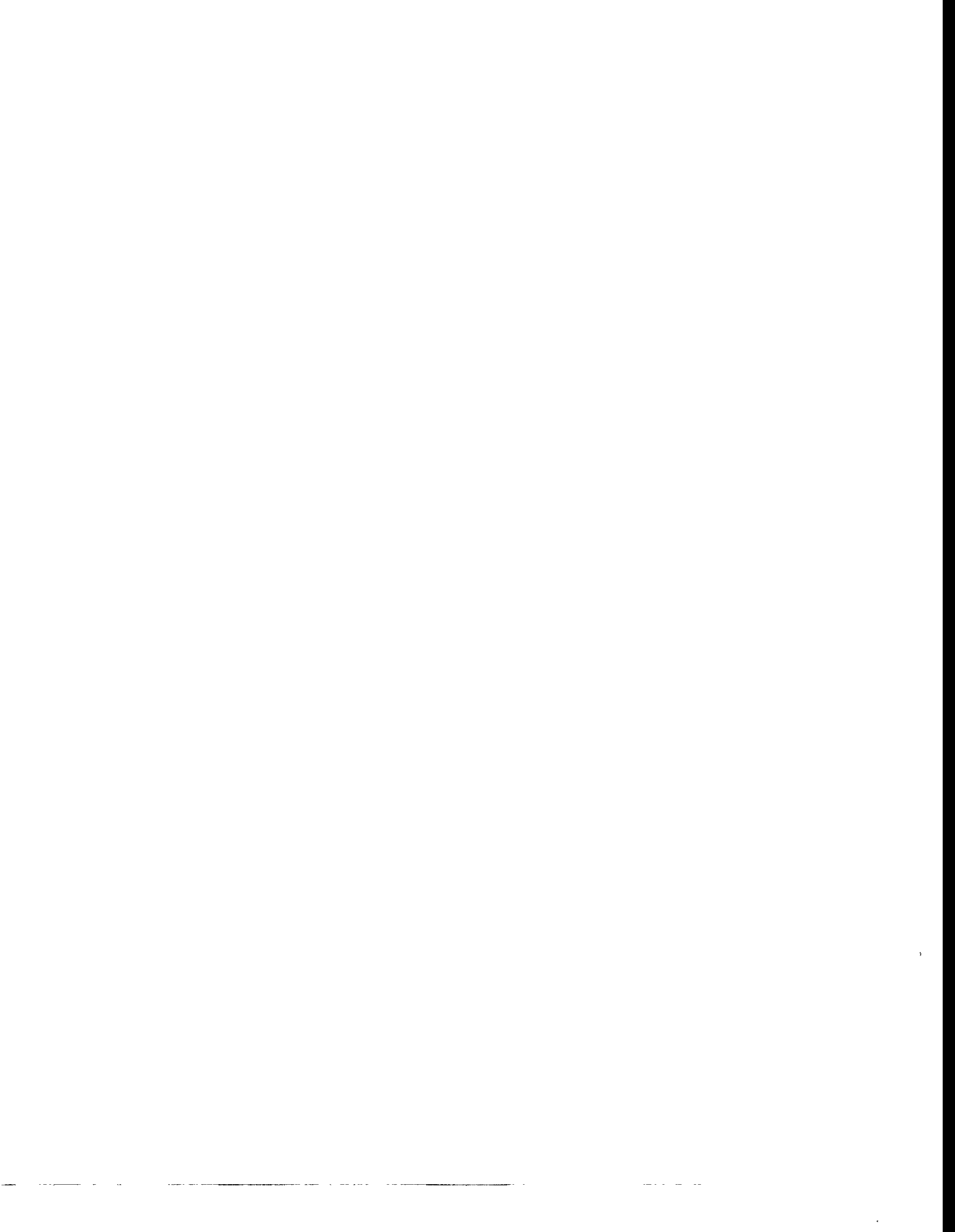
developments, particularly in the neutrino sector and that physicists from Argonne will continue to be deeply involved in the research.

REFERENCES

1. See, for example, M. Derrick in Proceedings of 6th International Symposium on Electron and Photon Interactions at High Energy, Ed. H. Rollnik and W. Pfeil, North Holland (1974).
2. W. A. Mann et al., Phys. Rev. Lett. **31**, 844 (1973); S.J. Barish et al., Phys. Rev. **D16**, 3101 (1977); K. L. Miller et al., Phys. Rev. **D26**, 537 (1982).
3. J. Campbell et al., Phys. Rev. Lett. **30**, 335 (1973);
G. M. Radecky et al., Phys. Rev. **D25**, 1161 (1982).
4. S. J. Barish et al., Phys. Lett. **66B**, 291 (1977); Phys. Rev. **D19**, 2521 (1979).
5. E. Fernandez et al., Phys. Rev. Lett. **43**, 1975 (1979); V. E. Barnes et al., Phys. Rev. **D25**, 1 (1982).
6. S. J. Barish et al., Phys. Rev. Lett. **45**, 783 (1980).
7. S. Ahlen et al., Phys. Rev. Lett. **51**, 1147 (1983).
8. P. Baringer et al., Phys. Lett. **206B**, 551 (1988).
9. S. J. Barish et al., Phys. Rev. Lett. **33**, 448 (1974).
10. M. Derrick et al., Phys. Rev. **D23**, 569 (1981).
11. S. J. Barish et al., Phys. Rev. Lett. **33**, 1446 (1975).
12. M. Derrick et al., Phys. Rev. **D18**, 7 (1978); V. E. Barnes et al., Phys. Rev. **D26**, 2965 (1982).
13. R. C. Lamb et al., Phys. Rev. Lett. **15**, 800 (1965).
14. T. Ahmed et al. (H1 Collaboration), Phys. Lett. **324B**, 241 (1994),
ZEUS results presented at the Glasgow meeting.
15. M. Derrick et al., Phys. Lett. **153B**, 2352 (1985); K. K. Gan et al., Phys. Lett. **153B**, 116 (1985).
16. POPAE, A 1000 GeV on 1000 GeV Proton-Proton Colliding Beam Facility, Fermi National Accelerator Laboratory and Argonne National Laboratory (May 1976).
17. F. Abe et al. (CDF Collaboration), Phys. Rev. **D43**, 2070 (1991).
18. L. G. Hyman et al., Phys. Lett. **25B**, 376 (1967).
19. M. Derrick et al., Phys. Rev. **A2**, 7 (1987).
20. I. Beltrami et al., Phys. Rev. Lett. **54**, 1775 (1985); S. Abachi et al., Phys. Rev. Lett. **56**, 1039 (1986); Phys. Rev. **D35**, 2880 (1987).
21. V. E. Barnes et al., Phys. Rev. Lett. **38**, 1049 (1977).

22. S. J. Freedman et al., Phys. Rev. **D47**, 811 (1993).
23. A. Yu. Smirnov, Proceedings of the XVI International Symposium on Lepton and Photon Interactions, Ed. P. Drell and D. Rubin, AIP Press (1993).





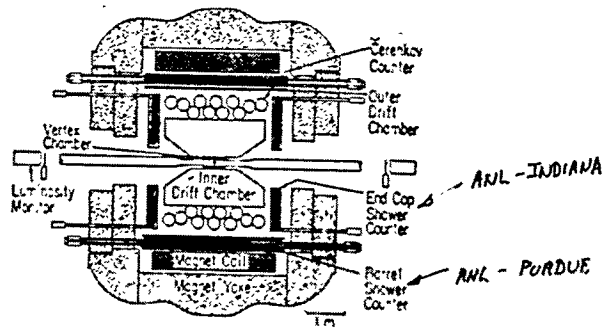


Figure 4 Isometric and Cross-sectional view of the HRS detector

Fig. 4

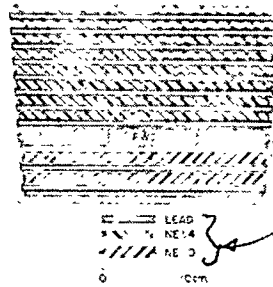


Fig. 5 Cross-sectional view of a module from the HRS barrel calorimeter system

Barrel Shower Counter
40 modules
Technique: Sampling Calorimeter



Fig. 5

This was the first of a series of calorimeter projects in which the HEP Division was to be involved. One of the 40 calorimeter modules is shown in Fig. 5. Compared to the calorimeter modules later constructed for detectors at hadron and electron-proton colliders, this appears small. At PEP, hadron calorimetry was not required and the HRS barrel electromagnetic calorimeter was very successful even though only 11 X_0 in depth, because leakage corrections could be made based on test beam data and Monte Carlo simulation.

The HRS operated successfully for the whole period of PEP operation and collected 300 pb^{-1} of integrated luminosity with about 150,000 hadronic events. Although the precise resolution provided by the HRS did not result in discovery of any narrow resonant studies, it did allow some of the best studies at the time of the properties of the D , D^* , and F mesons, in the notation of the time. The HRS established the existence of decays $\tau \rightarrow 5\pi^\pm \nu_\tau$, $5\pi^\pm \pi^0 \nu_\tau$ and contributed to reducing the errors on the mass of the tau neutrinos. In Fig. 6 one sees an example of the clean di-jet final states encountered at PEP energies. Scanning such computer-generated displays as this is to be compared to scanning bubble chamber pictures in conjunction with the computer printout of the spatial reconstruction of track measurements. Another example of di-jet production, in this case $F\bar{F}$ production, is seen in Fig. 7. This also illustrates the detailed spatial information provided by the vertex detector, an HRS upgrade, which allowed lifetime measurements of such mesons to be made. As one might expect, the extensive experience of bubble chamber physicists played an important role in producing the tracking software and the on-line displays for data analysis.

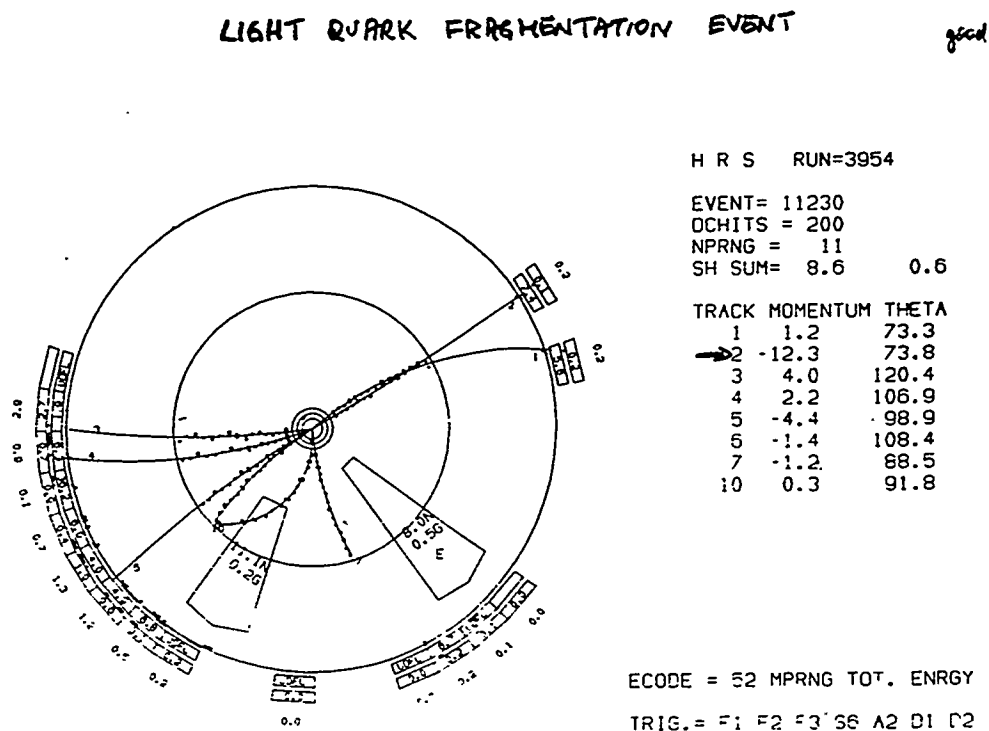


Fig. 6

The involvement of the HEP Division in detectors for hadron colliders goes back to the 1976 POPAE proposal in which a 4π magnetic detector was described. This involvement continued with the Tevatron initiative at FNAL leading to the Colliding Detector Facility, CDF. As seen from Fig. 8, ANL, through Bob Diebold, were charter members of CDF. The ANL interest was in providing the central electromagnetic calorimeter for CDF, the component expected to make possible the clean identification of electrons from the large hadronic background and photons from the background of π^0 decays. This is expressed in Fig. 9, copied from the CDF design report.

The CDF was realized by a large international collaboration and was arguably the first full solid angle hadron collider detector, as is seen schematically in Fig. 10. Following the design report of 1981, construction began in 1982 and first collisions with the partially completed detector were seen in 1985. The central hadronic-electromagnetic calorimetry was complete for the initial run. One of the 48 half wedges of the central calorimeter is shown in Fig. 11. The electromagnetic parts of these wedges were fabricated in the ANL Central Shops and in Fig. 12 one sees one of these, together with the group responsible for the design and construction. The technique, sampling calorimetry, used wavelength shifter readout of the scintillator light. The technique for making the complicated wavelength shifter-lightguides was developed by Bill Evans who exhibits one in Fig. 13. The CDF is shown during its assembly in Fig. 14.

The combination of charged particle tracking and electromagnetic calorimetry, allied with the enhanced spatial resolution of the wire chamber located at shower maximum, allows observation of π^0 and η decays into photons and the reconstruction of mesons such as the rho. Effective mass plots reminiscent of those from bubble chamber studies are shown in Fig. 15. Figure 16 shows one of the top quark candidates in the on-going CDF study to establish the existence of this missing quark. The electromagnetic calorimeter is a crucial component in this search.

The electron-proton collider, HERA, at Hamburg, Germany is unique and makes possible the extension of deep inelastic scattering to probe the structure of the proton down to 10^{-18} cm. Detection of particles from the collision of 27 GeV electrons with 820 GeV protons using calorimetry involves similar design demands as for CDF but with one important difference. The charged current reaction, $ep \rightarrow \nu + X$, where the neutrino carries off energy and momentum which are not detected, means the calorimetry must be hermetic with the best possible hadronic energy

*Production of ϕ and $F \rightarrow \phi\pi$. First seen by CLEO as narrow $\phi\pi$ state at 1970 MeV.
 Lowest order charm-strange First seen at PEP by HRS.*

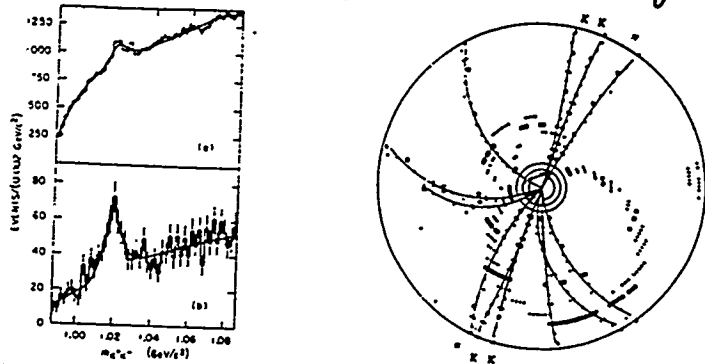


FIG. 1 The K^+K^- invariant-mass spectrum for (a) $z(K^+K^-) > 0.1$ and (b) $z(K^+K^-) > 0.4$.

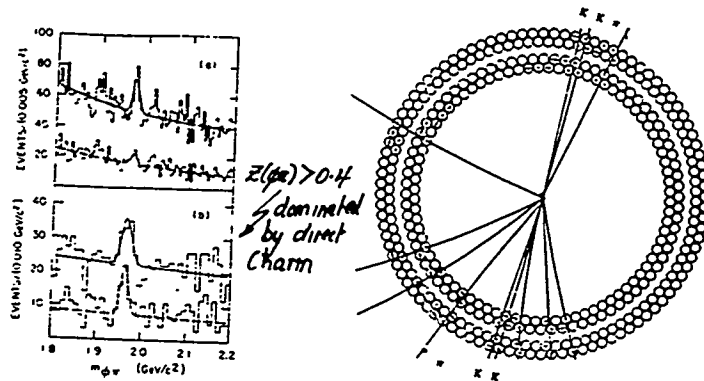


FIG. 3 The $\phi\omega$ invariant-mass spectrum for events with (a) $0.2 < z(\phi) < 0.4$ and (b) $z(\phi) > 0.4$. The lower histograms are selected in particular ranges of the decay angles as discussed in the text.

Figure 22 Back to back F event, Vertex chamber hit

Fig. 7

COLLIDER DETECTOR AT FERMILAB - CDF
EARLY ANL INVOLVEMENT

M. Magnetic detector
Measurements of secondary particle momenta will allow a calculation of the true rapidity. In addition, transverse momentum distributions can be measured and studied as functions of rapidity for each type of particle, and for all multiplicities from $\sqrt{s} = 200$ to 2000 GeV. One can also look at other correlations such as rapidity gaps between particles of different charge and type. The detection and energy determination of ν^{μ} will be an enormous aid in this kind of work.
Measurements of resonance production can be undertaken; $p, \Lambda, \Sigma, K^*, \phi, A_2$ and η yields can be determined. It will be interesting to know how the ratios of ν^{μ}/ν^e and ν^{μ}/ν^p behave as a function of topology and kinematic variables such as the transverse momentum. These measurements will be important in interpreting the high p_T phenomena, in addition to their intrinsic importance in clarifying central-region physics.

1976
POPAE
R. Diebold
et al

Fig. 8

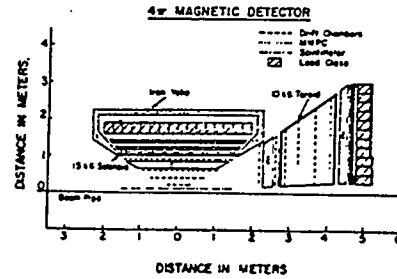


Fig. 11-26. Cross sectional view of the 4w magnetic detector. Only one of the forward detectors is shown.

CDF - 1

CDF Note

Parameters of Colliding Beam Detector

R. Diebold, A. Tollestrup, T. Collins, S. Ecklund, J.K. Walker
23 Jan 78

Constraints

1. Kissing scheme for beams.
 2. Maximum energy of MR/ED beams = 150/1000 GeV for pp and 1000/1000 fc.
 3. Conventional magnets for the MR normal operation.
 4. Low β achieved without loss of part of the 50m long straight.
- (Note: R. Diebold paper #1 of Summer Study assumes 46m is free.)

CDF MILESTONES

- 1978 CDF GROUP FORMS
- 1984 TECHNICAL DESIGN REPORT

LARGE
INTERNATIONAL
COLLABORATION

DESIGN REPORT
FOR THE
FERMILAB COLLIDER DETECTOR FACILITY
(CDF)
AUGUST, 1981

From Design Report

Hadron Rejection

The shower counter is a powerful identifier of electrons. Hadron rejection will be achieved by cuts on various pieces of information:

1. Energy deposited in the shower counter compared to that measured by the magnetic curvature, $E/p \approx 1$.
2. Early development of the shower, i.e. large signals in the wire chambers.
3. Relatively well collimated showers in the wire chambers.
4. Little energy remaining in the shower to penetrate the hadron calorimeter.

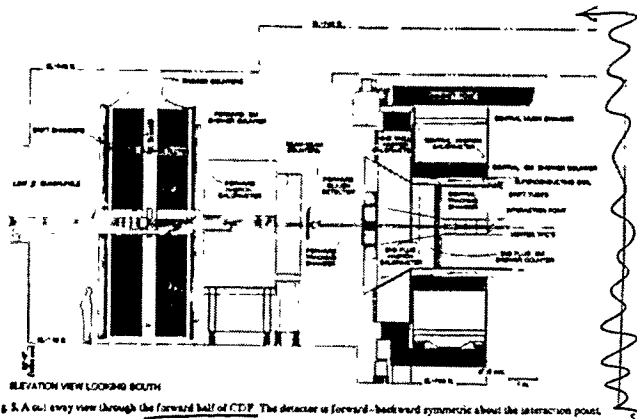
Using E/p and the pulse height in a proportional chamber, Singer (CDF-25) obtained the results shown in Fig. 4.13 for test data with momentum spread $\Delta p/p \approx 1\%$; even without cuts 3 and 4 he obtained rejections of a few thousand for 30 GeV pions.

Fig. 9

- 1982 CONSTRUCTION UNDER WAY
- 1985 OCTOBER. FIRST COLLISIONS WITH PARTIAL DETECTOR
- 1987 JAN - MAY FIRST PHYSICS RUN WITH FULL DETECTOR

CDF - First Full Solid angle hadron collider detector
 Uses Solenoidal Magnet like e^+e^- detectors
 Diameter 3m, Length 5m, 15KG.

Charged particle tracking down to 3.5° from beam
 Using Four Separate tracking Systems

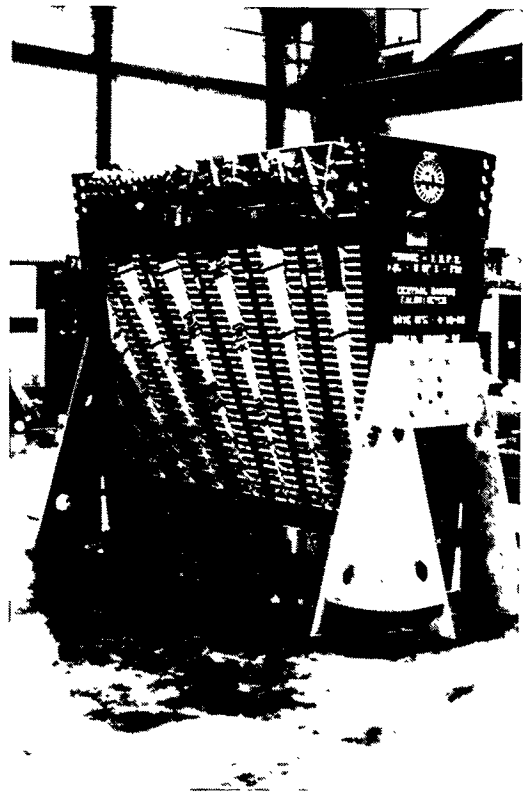


* Calorimetry Sampling Calorimeter; EM Shower Counter followed by hadronic section
 ANL SHOWER COUNTER PWC after $6X_0$ to separate e/h and detect single γ

Muon detection Instrumented Absorber-Toroids

Leading Particle Spectrometer Roman Pots with scintillator and drift chamber

Fig. 10



WEDGE MODULE WITH WAVESHIFTER/LIGHTGUIDE ASSEMBLIES INSTALLED

Fig. 11

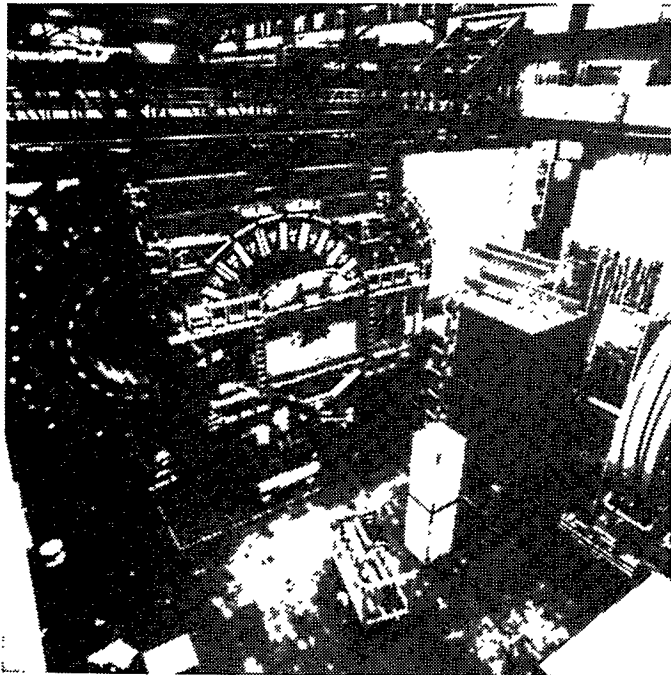


ARGONNE CDF LRM IN SUMMER 1982

Fig. 12



Fig. 13



ASSEMBLY - SUMMER '86

Fig. 14

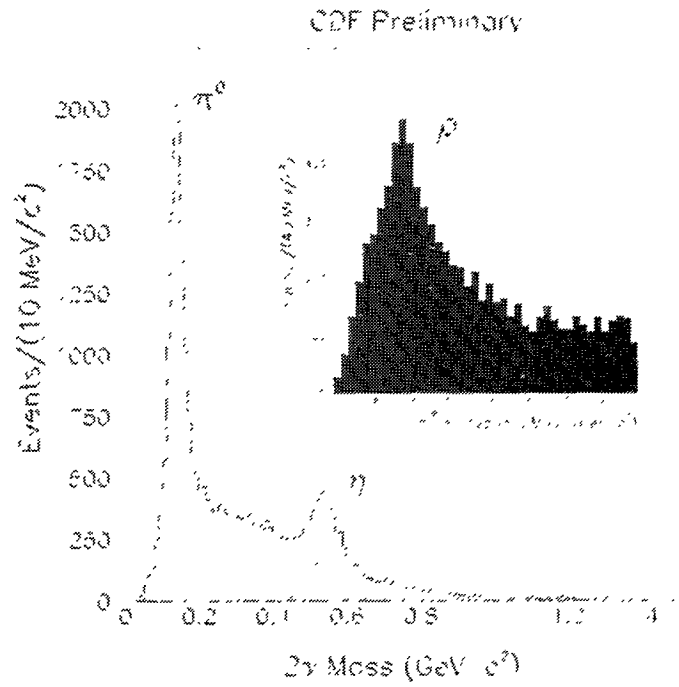


Fig. 15

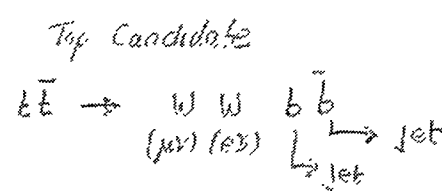


Fig. 16

resolution since all the measureable information is contained in the recoiling hadronic system. The solution adopted was that of compensating calorimetry; a sampling calorimeter consisting of alternate layers of uranium and scintillator will provide identical response to electrons and hadrons of the same energy, which dramatically improves the hadronic energy resolution. The calorimeter uses the same technology everywhere, unlike the solution adopted by CDF.

Together with a group of five U.S. universities, ANL began the design and R&D for the barrel calorimeter of a general-purpose detector, ZEUS, at HERA. The ANL group on the HRS experiment moved to ZEUS when the PEP program terminated and were able to build on the calorimetry experience accumulated with that detector and also through the CDF experience. The calorimetry was defined in the technical report of 1986. Following a period of R&D and prototype construction, actual construction of the 32 barrel calorimeter wedges started at ANL in 1989.

The collaborative effort was very successful with each group providing components they had developed and produced, which were then assembled at ANL. The collaboration was able to take advantage of the laboratory infrastructure to set up the facility needed to handle the 300 tons of depleted uranium plate, each plate was to be clad with stainless steel sheets, and assemble it into calorimeter wedges, each weighing 10 tons. Wedges were tested at ANL using a cosmic ray test station. Just as with the HRS and CDF, ANL provided much of the engineering expertise essential in the design and construction of such large-scale calorimeters as these were.

A schematic of the ZEUS detector, shown in Fig. 17, illustrates the differences and similarities to a hadron collider detector such as CDF. While both contain a central tracking detector coupled with a solenoid magnet, complete calorimeter coverage and muon detection, the ZEUS detector is not symmetric about the interaction point. This is because reaction products are mostly carried in the direction of the 820 GeV proton, so a greater depth of calorimetry is required for energy measurement there.

An isometric view of a barrel calorimeter wedge is shown in Fig. 18. Each wedge was segmented in depth into three compartments, the first electromagnetic followed by two hadronic energy measurement sections. The stacking of a wedge is shown in Fig. 19 and the installation of the wavelength shifter lightguides on a stacked wedge is seen in Fig. 20.

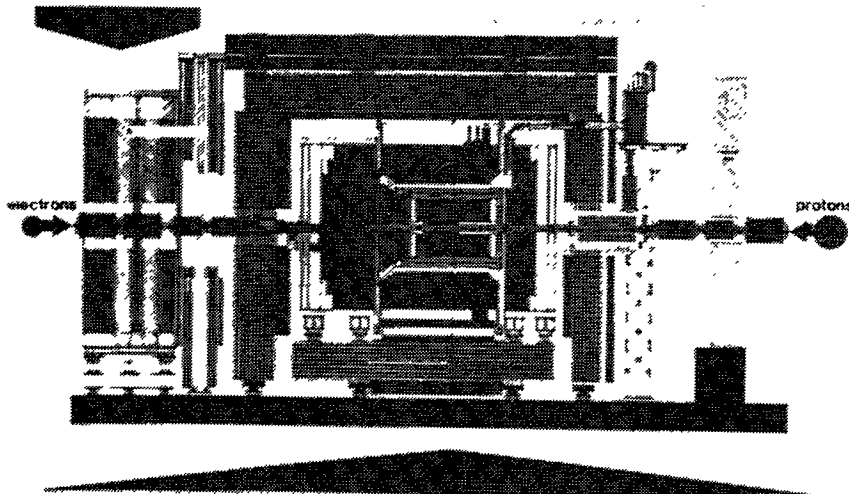


Fig. 17

Fig. 18

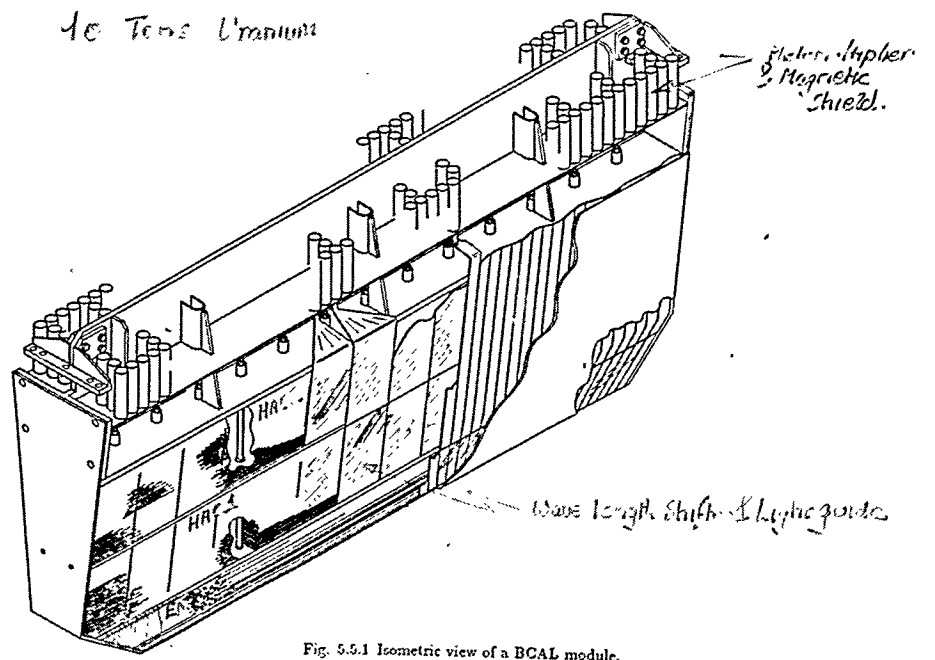


Fig. 5.5.1 Isometric view of a BCAL module.

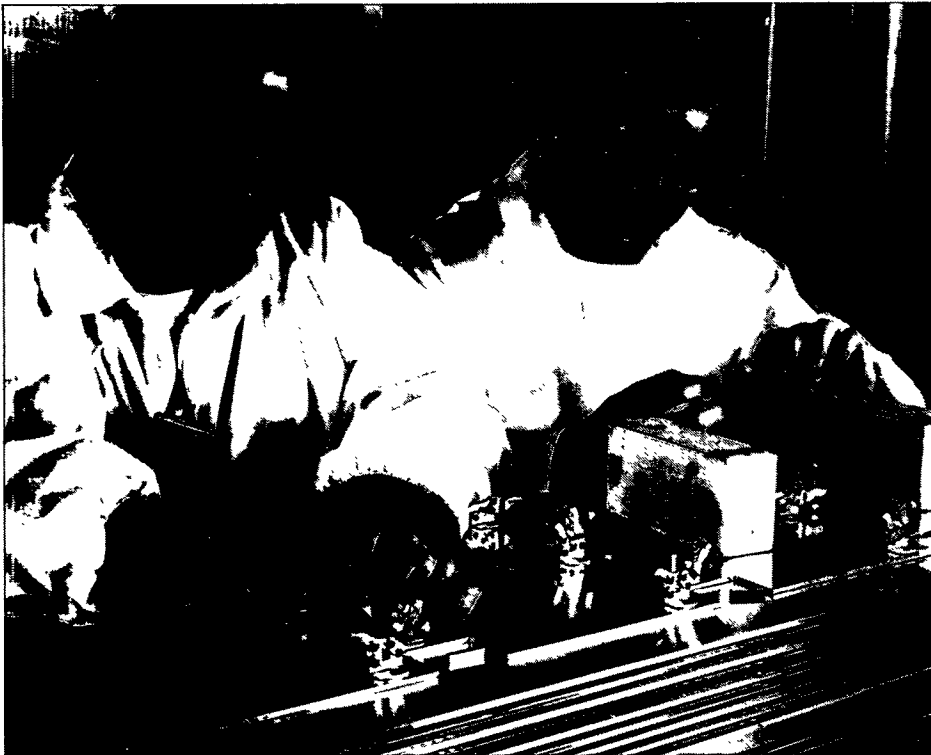
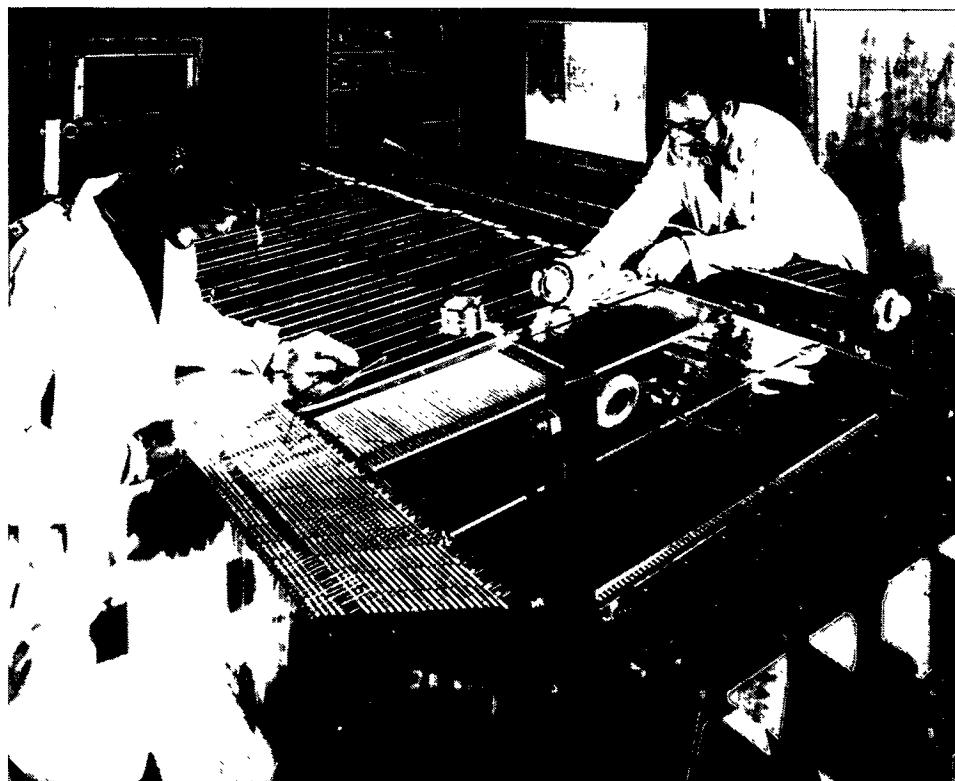


Fig. 19

Fig. 20



ZEUS: Fermilab Test Beam Data

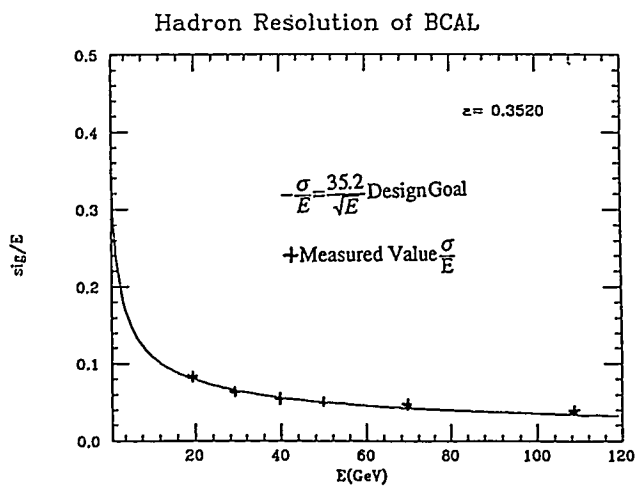
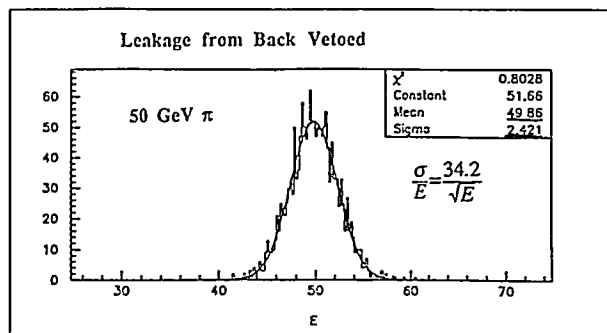


Fig. 21

The calorimeter was shown to achieve the design resolution in test beam studies at FNAL. Results are shown in Fig. 21.

Another example of the way in which Argonne was able to help the collaboration was in handling the transportation of the wedges to Hamburg. Figure 22 shows a wedge ready to be lowered down into the interaction hall and in Fig. 23, one sees a wedge being installed into the detector. This phase of the assembly was handled by ANL and the University of Wisconsin. The obligatory picture of the completed detector and collaboration is shown in Fig. 24. Some familiar faces from ZGS days can be recognized.

Examples of event displays of e-p interactions are shown in Figs. 25-26. In addition to the orthogonal views of the charged particle tracking, displays of the energy deposition in the calorimetry are shown.

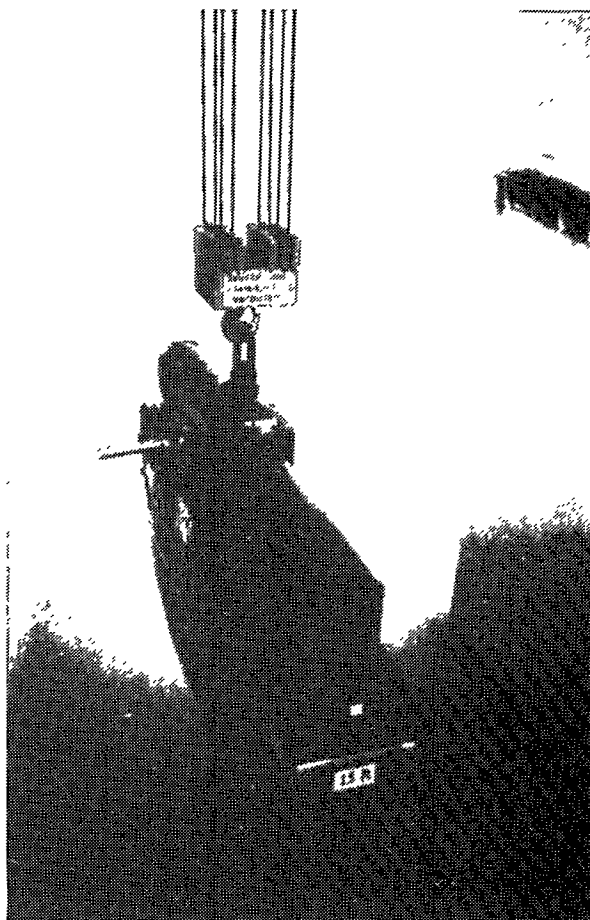


Fig. 22

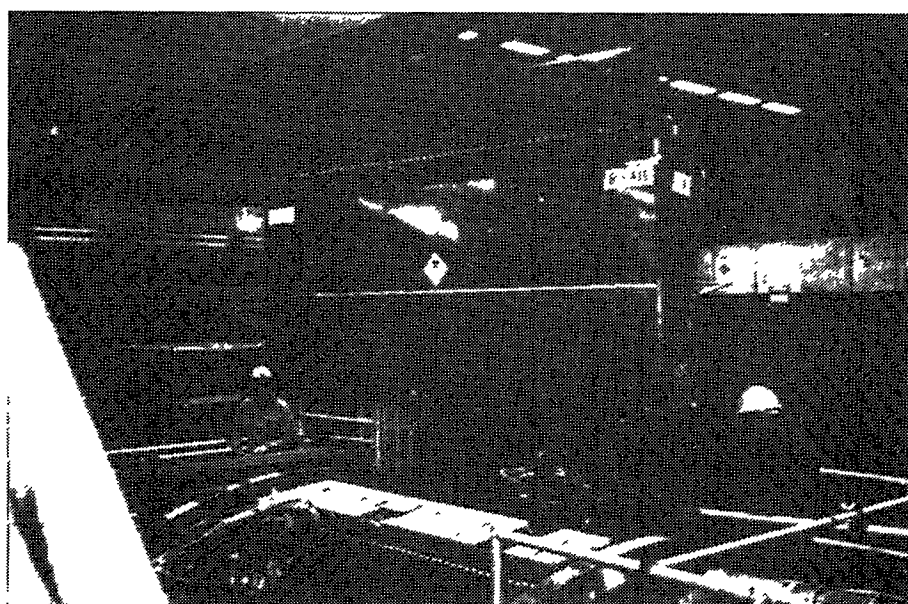


Fig. 23

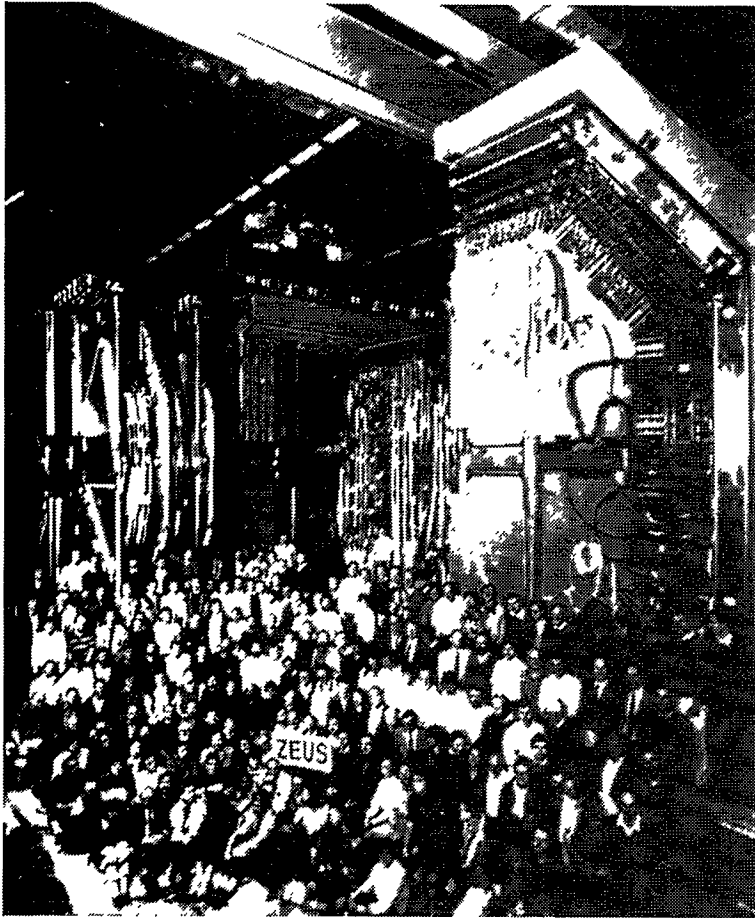
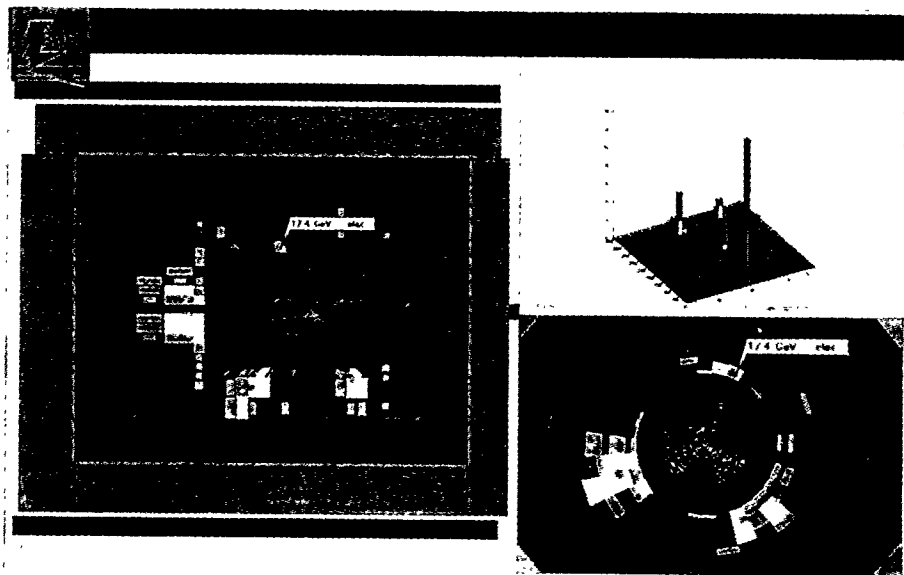


Fig. 24

Fig. 25



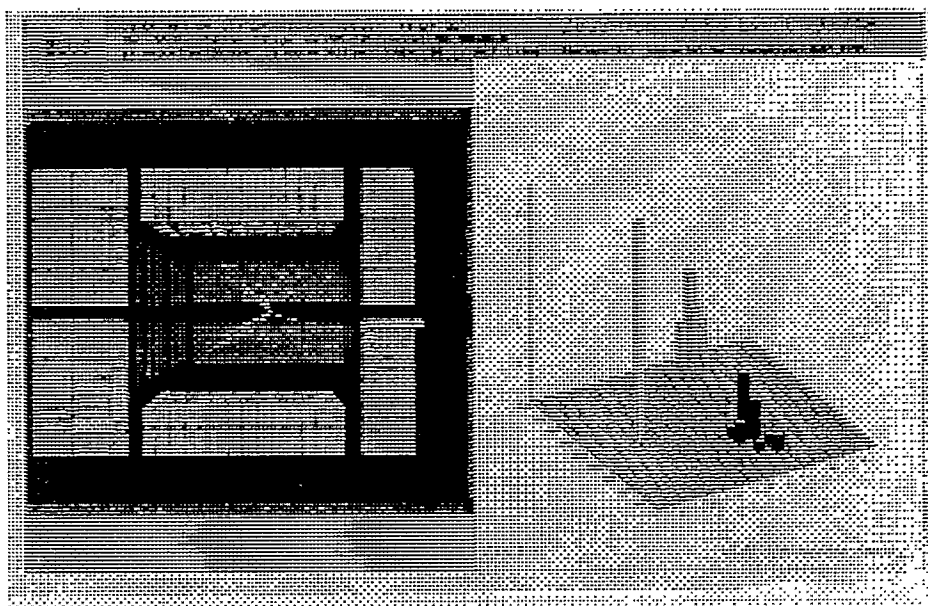


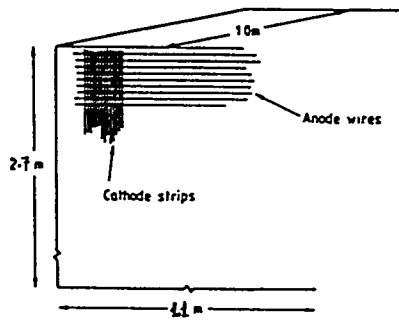
Fig. 26

HERA began operations in 1992 and despite the low luminosity (the integrated luminosity accumulated by ZEUS in 1992 was 30 nb^{-1}), the initial survey of a new kinematic region yielded several interesting results. The measurement of the total cross section for γ - p interaction at an energy, $\sqrt{s} = 200 \text{ GeV}$, ten times higher than previously possible, indicated only a shallow increase with energy. Hard scattering in photoproduction was clearly observed for the first time and diffractive production was found to constitute a surprisingly large fraction, about 10%, of the deep inelastic ep cross section. Analysis of the 1993 data, now in progress, has shown extrapolations into the HERA kinematic region using deep inelastic scattering data from lower energy fixed target experiments do not describe the measured proton structure function. The HERA kinematic region is throwing new light on the structure of the proton.

All of the detectors so far described take advantage of particle production by colliding beam facilities. The Soudan detector, at least initially, was proposed to look for the decay of the nucleon. The Soudan detector is a tracking calorimeter which provides much of the information typically extracted from a bubble chamber picture, charged particle tracking, particle identification by ionization energy loss and particle energy measurement. After a prototype stage, Soudan 2 began as a collaboration between ANL, Minnesota, and Oxford University. The collaboration was soon joined by Tufts University and the Rutherford-Appleton Laboratory. Much of the same relationship existed between Oxford and the Rutherford Laboratory as that between ANL and the U.S. university groups with the National Laboratory providing strong engineering support and assembly - service support for detector construction to complement the experience in underground laboratory techniques at Minnesota and the experience with cosmic ray physics and long drift particle detection techniques at Oxford.

Soudan 2 was proposed in 1981 as a 1000-ton tracking calorimeter for nucleon decay. Each module was an assembly of drift tubes located in a matrix provided by a stack of corrugated steel sheets, as illustrated in Fig. 27. Ionization on the path of a charged track is drifted over as much as 50 cms, with (x, y) coordinates provided by anode wire and cathode pad readout and z information from the arrival time of a digitized group of hits. The long drift technique retains good spatial resolution, of the order of a few mm, for a reasonable number of electronic readout channels, usually a large fraction of a tracking detector cost.

LONG DRIFT TECHNIQUE



Retain good spatial resolution (\sim few mm)
 WITH
 Reasonable number of electronic readout channels
 Channels/module =

Fig. 27

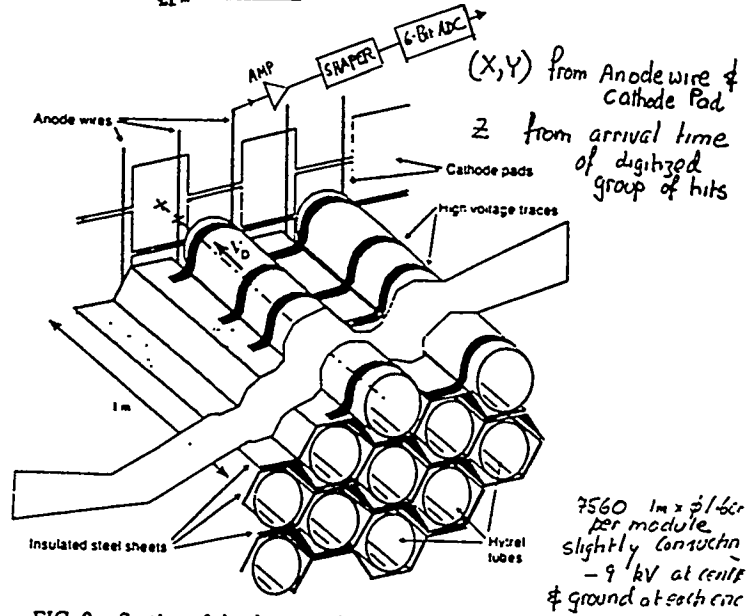


FIG. 2. Section of the detector showing drift tubes in the corrugated steel stack.

Line Data
 Run 35209 Event 670
 09-Apr-1992 11:30:39.98

Fully contained events

Fig. 3. Neutrino interaction candidate $\bar{\nu}_e$ event in Soudan 2.

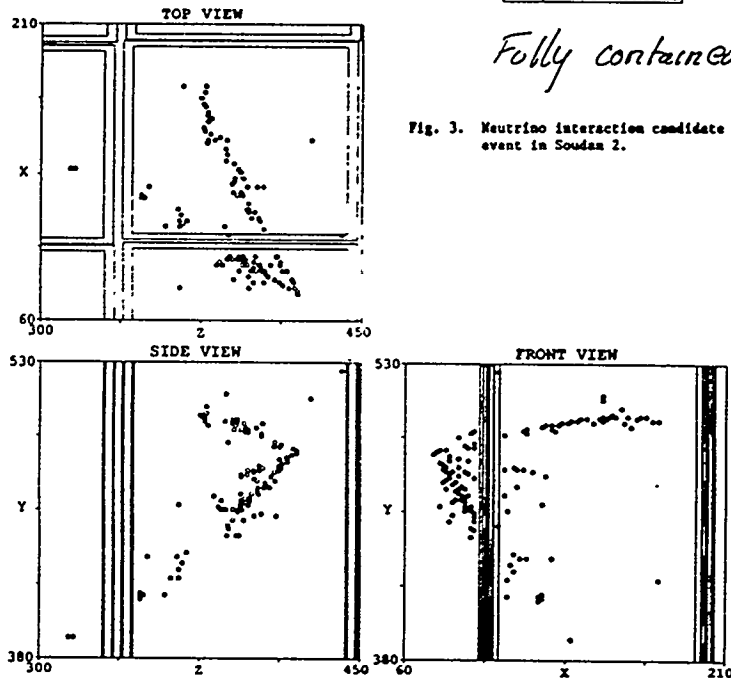


Fig. 28

Modules were assembled at ANL and at the Rutherford Laboratory and transported to the underground laboratory located in an iron mine in Tower, Minnesota. The depth of the laboratory, 655 m, is important in rejecting muon-induced backgrounds but other serious backgrounds to nucleon decay, such as depth-independent neutrino interactions, must still be rejected. The detector technique chosen complemented others such as the water Cerenkov detector. Candidates for neutrino interactions in the detector are shown in Figs. 28-29.

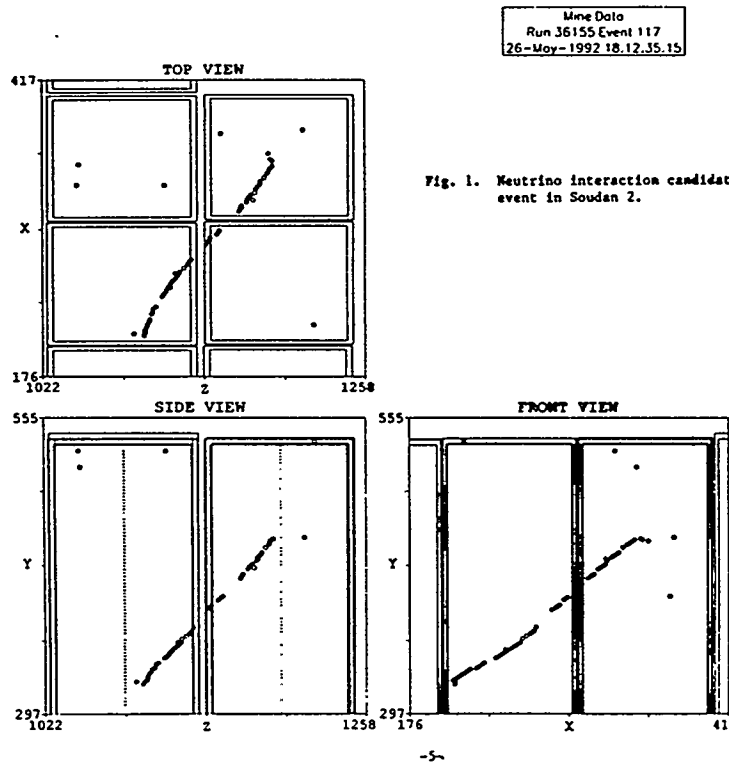
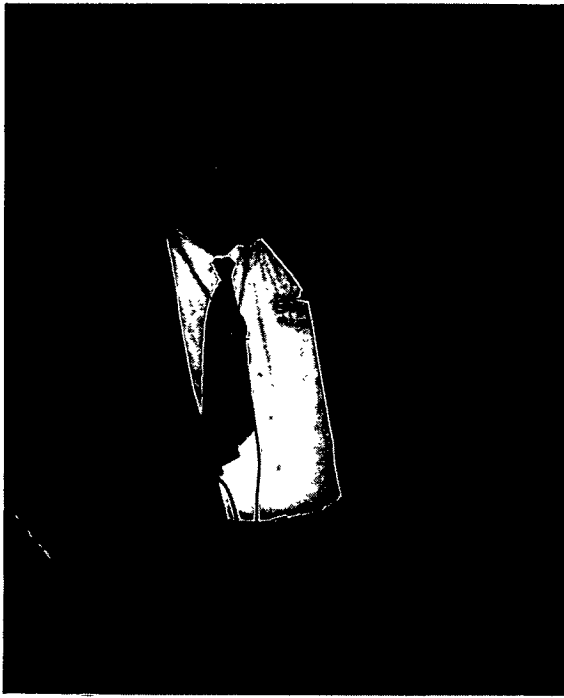


Fig. 1. Neutrino interaction candidate track event in Soudan 2.

Fig. 29

Because the detector was modular in concept, it has been possible to take data as the detector was completed and assembled over a period of some years. The first year of operation with the completed detector has been achieved. Besides accumulating data on particularly favorable nucleon decay modes, the experiment is also pursuing the important issue of the atmospheric ν_μ/ν_e ratio, for which anomalous results have been reported in other experiments. This measurement is well matched to the good tracking and particle identification capabilities of Soudan 2.

Over the years since the ZGS, ANL has worked productively with a number of University groups in a relationship which can be compared favorably with a similar role discharged by the Rutherford-Appleton Laboratory in the United Kingdom and Saclay in France. The expertise accumulated in calorimetry at Argonne promises to be important in the future in several experiments: detector upgrades at ZEUS, CDF; participation in the ATLAS detector for the CERN LHC, and the barrel shower counter for the STAR detector at the RHIC facility.





Moving on to Brookhaven (Fig. 3), we see the last year of construction of the AGS and a sharp rise in the operating budget. One can see major capital equipment expenditures as well as the AGS and computer upgrades. Here you may also recognize the Isabelle support around 1980. Recent years have shown a steady erosion of support at Brookhaven since they are the lowest energy machine operating in the HEP DOE program. When I present this curve at AGS users groups, it is a sort of a good news/bad news curve. The bad news is that the trend over these last many years has been down. Of course physicists like to fit data. If you fit it, the budget runs to zero in the not too distant future. The good news is this is still a substantial amount of money, about \$75M in 1994. They are still doing a lot of physics at the AGS. Of course, this is just high energy physics so the RHIC construction does not show up. If we were to show that, there would be a big bump in the Brookhaven budget. Whether or not there will be high energy physics done on RHIC remains to be seen.

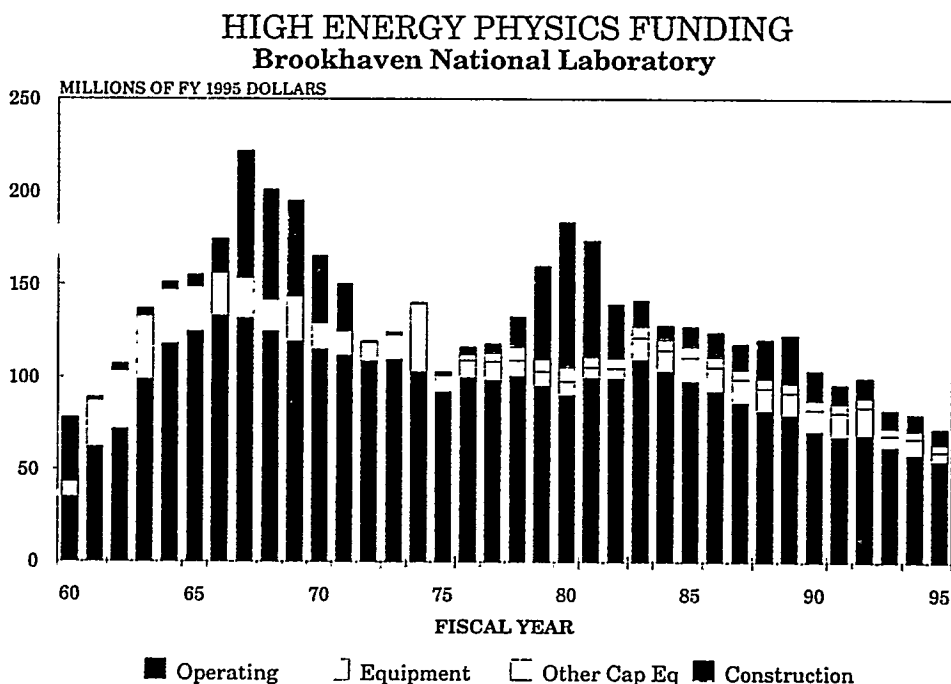


Fig. 3

Now for SLAC (Fig. 4) - We can really see the Laboratory starting: there is an enormous increase in construction. It is interesting that the major construction projects at SLAC stand out rather cleanly including the construction of the original linac and the associated laboratory. Here in 1975-1980 is PEP construction and then ten years later, the SLC. We can also see the B-factory coming in at the end of the chart.

Many of you will know that SPEAR was not a construction project. It was done solely out of capital equipment funds and is spread out over the three years in the late 1960's. The big spike in 1973 was a major computer upgrade, all the money of which occurred in one year.

Be careful that when you look back at these numbers they seem huge, we're inflating backwards 35 years and that can do strange things to numbers. Later we will take a look in a little more detail at both Isabelle and PEP and its relationship to the ZGS.

HIGH ENERGY PHYSICS FUNDING Stanford Linear Accelerator Center

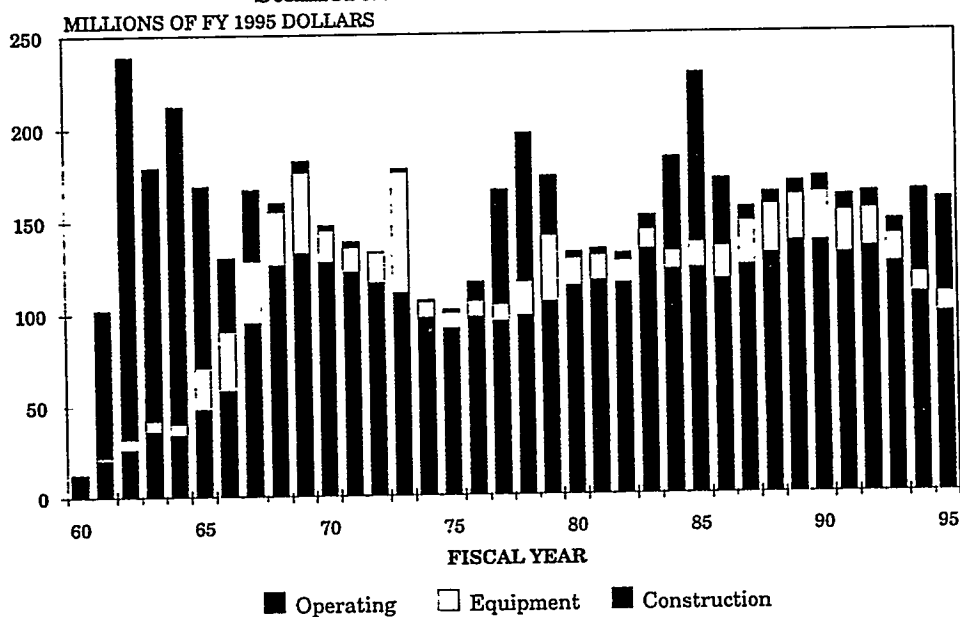


Fig. 4

HIGH ENERGY PHYSICS FUNDING Fermi National Accelerator Laboratory

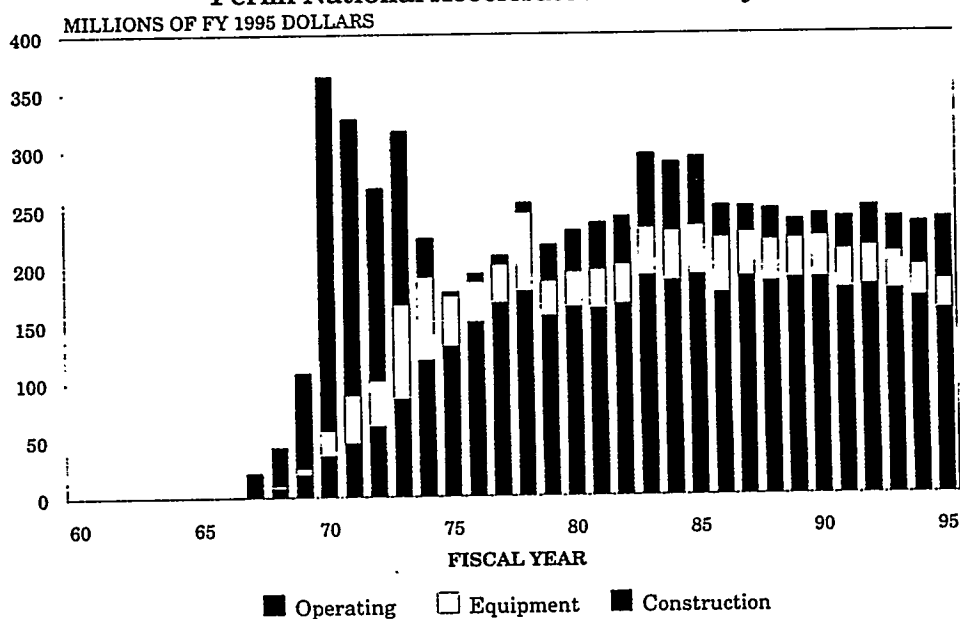


Fig. 5

Fermilab (Fig. 5) - You see a rapid increase in construction starting in 1967 and going up to a very high level. Again you won't recognize the numbers because they are 1995 dollars. There was a corresponding increase both in the operating budget and in the capital equipment. Later, in the 1970's and early 1980's, there is a period of construction of the energy saver, TeV I and TeV II. This is spread over a number of years, but it is in this time frame. It doesn't stand out so boldly as a sharply defined construction project standing by itself and spread over in a few years. Again we see in the last few years the falloff of the operating budget of Fermilab. You see some recent increase in the construction because of the main injector and the linac upgrade. Finally, in 1995, this green bar is all main injector. It is moving ahead quite well.

One more laboratory before we get to ANL: the SSC (Fig. 6) plotted on the same time scale. One of the biggest tragedies of our field is that we spent about \$2B dollars on this project and now it has been terminated. The green area is actual federal money spent on construction; the rest is non-federal money, essentially all from the State of Texas. The last two bars show the 1994 closeout money and what's been requested. The latter request is for \$180M and I'll be surprised if that 1995 money actually shows up for that purpose. I think some of us who are worried about the funding of the base program would rather see that money applied different ways.

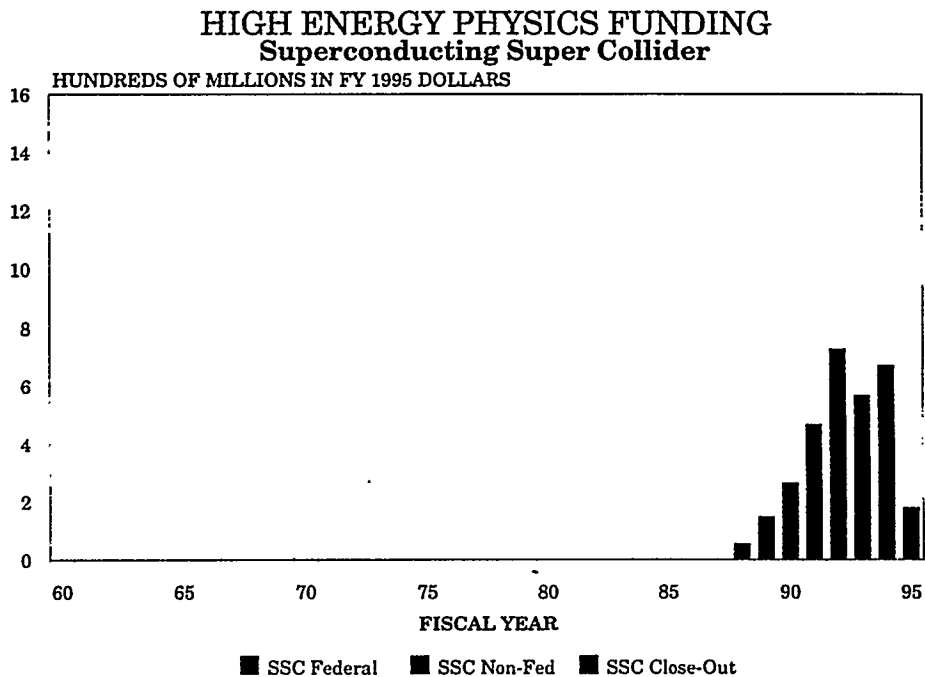


Fig. 6

Perhaps we should all stop and think about what went right and what went wrong with the SSC project: see if there are lessons to be learned, so that we don't repeat history.

Argonne (Fig. 7) - Again, we are picking this up only in the 1960's. The start of the ZGS construction occurred before that. We see, in the last few years of construction, substantial capital equipment and a rapidly increasing operating budget to support the Laboratory. Also in the mid-1960's is the 12' bubble chamber construction and the expansion of the experimental areas, both of which were done primarily with capital equipment. Then the struggle: the budgets started falling off. It seems that Argonne always had a continuing struggle after the good years of the early-to-mid 60's. The peak in 1973 is a computer upgrade. The discussion and arguments

HIGH ENERGY PHYSICS FUNDING Argonne National Laboratory

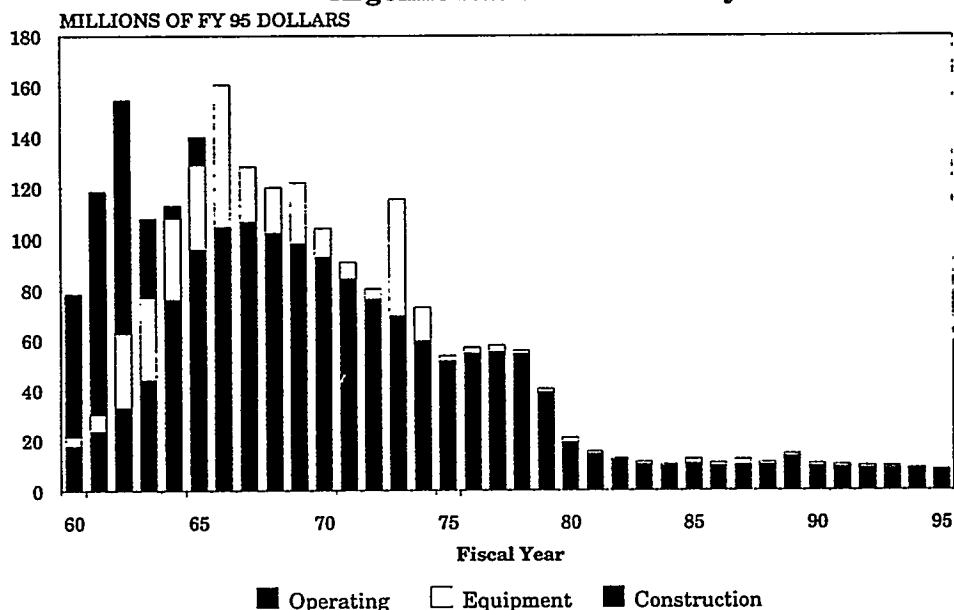


Fig. 7

of the various review panels about the future of the ZGS were occurring in the mid-1970's. The last few years of the program was run primarily for polarized beam so that there was a plateau in the operating costs until 1979, the last year of ZGS operation. Then the budget fell to a level which, on this scale, looks small but it is still significant.

The discussions that you have heard and the experimental talks in the last couple of hours show that a lot of good physics is being done by the HEP group at Argonne. While this money appears to be small, it is supporting a group that is very effective in carrying out work that has enabled the HEP program to participate in ways that it would otherwise would not be able to. I particularly like the example of Argonne playing a significant role in the construction of the barrel calorimeter for ZEUS. They had the expertise to do the calorimeter and had the Laboratory's infrastructure to handle the substantial administrative problems, as well as the technical problems associated with a large amount of uranium in one place.

Now I'd like to jump back a little bit to remind you of the construction bumps at SLAC for PEP (Fig. 8) and BNL for Isabelle (Fig. 9). At SLAC, I just isolated the PEP construction money. This little box in 1983 indeed isn't a misprint. It took them three years to close out the books, so there was a final expenditure of a couple of million dollars or so. It's sort of interesting to lay these two plots on top of each other. The construction for PEP fits rather nicely on top of this plateau of the ZGS. Wisecracks have been made that the ZGS was used twice, once to pay for PEP and once to pay for Isabelle. Well, there's some logic to it although the numbers don't quite fit. The declining ZGS budget, plus the PEP construction, gives a total funding that is not so different from earlier years. In fact, we can play a similar game with the Isabelle numbers. In 1979 the ZGS goes off completely, and the Isabelle construction takes up the difference. The vertical scales about the level of funding are about the same on both of these graphs. So the good old ZGS, even in its last gasp, helped the field in various ways, including helping other projects, PEP and Isabelle, get on their way.

HIGH ENERGY PHYSICS FUNDING PEP Construction

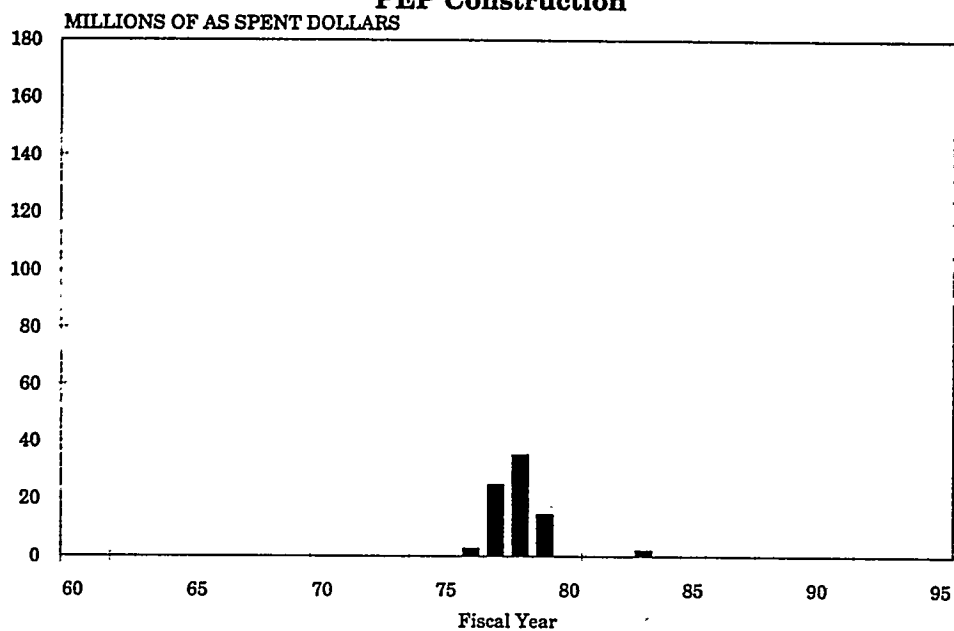


Fig. 8

HIGH ENERGY PHYSICS FUNDING ISABELLE Construction

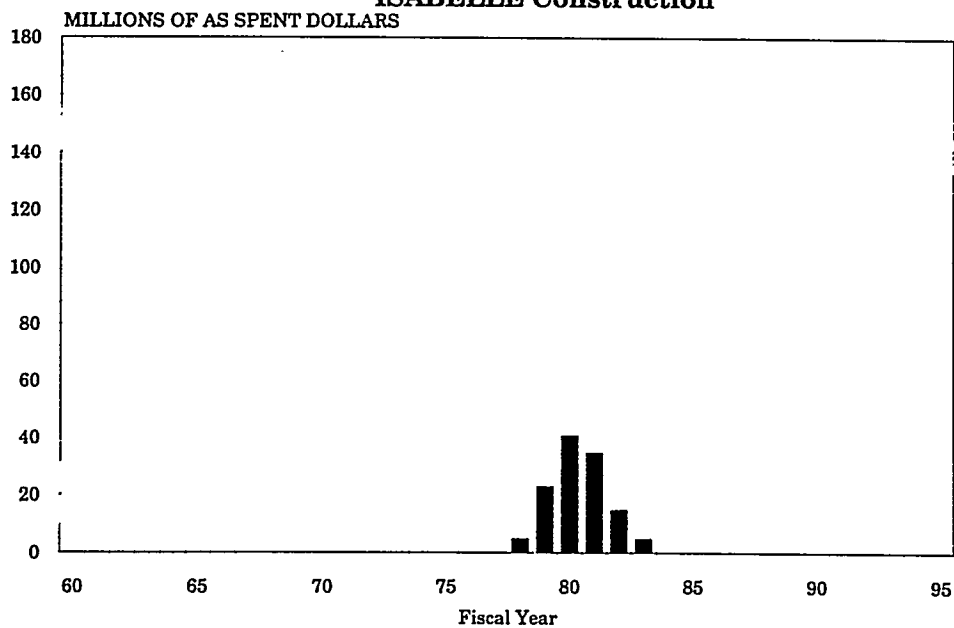


Fig. 9

Now to summarize in a rather sweeping way, Fig. 10 shows all of the accelerator construction projects over the last 35 years. In the early 1960's we had four projects under construction at the same time: PPA, CEA, ZGS, and AGS. The AGS was completed but SLAC started, so again we had four accelerators being built at the same time in four separate laboratories.

HIGH ENERGY PHYSICS FUNDING Construction

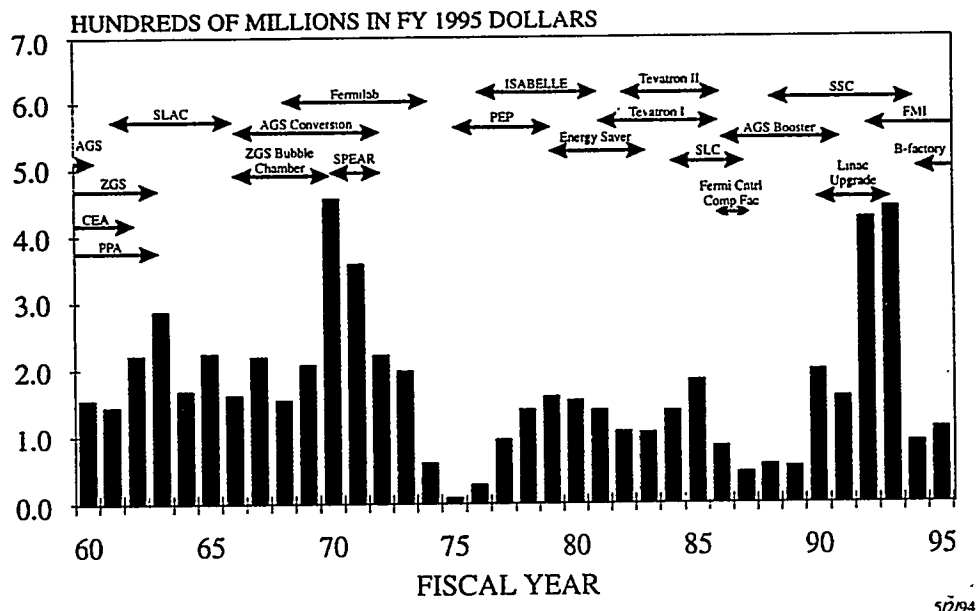


Fig. 10

The ZGS bubble chamber, the AGS conversion and SPEAR came into predominance in the late 1960's. Of course, in addition, there was the start of Fermilab in the late 1960's which continued into 1973-74. We then have the low point in the program in 1975 (remember this is just construction money), PEP started and was appropriately finished. Isabelle, however, was started but then terminated. This was followed by three upgrade construction projects at Fermilab. Then came the second low period, although we had with some overlap, the SLC, the Fermilab central computer, and the AGS booster,

The AGS booster is a rather modest project, about \$30M, but it is spread over about 4-5 years. It is a project that, if appropriately funded, could probably be completed in 2-3 years. Then you see the linac upgrade at Fermilab and the Fermilab main injector. Again, here's a case where a project that is quite straightforward and could be completed in about 3 years, with appropriate funding, will probably take about seven years, if we are lucky; perhaps longer. The B factory has also just been started. This project is benefitting from the fact that it has been designated as a Presidential Initiative. Late in the budget process for FY1994, just as we were about ready to go to Congress, we got a phone call saying that \$36M has been added for the B-factory at SLAC. Life works in strange ways. The money was added and the budget went up. We would have preferred to push ahead rapidly and finish the main injector.

Figure 11 is a general interest chart. It shows most of the accelerators that have been in operation or are planned. The graph shows center-of-mass energy, even though many of these are fixed target machines and not colliders. To put them all on the same graph, we assume that the beam is colliding with a liquid hydrogen target in calculating the effective luminosity for a

HIGH ENERGY PHYSICS

WORLD ACCELERATOR AND COLLIDING BEAM FACILITIES

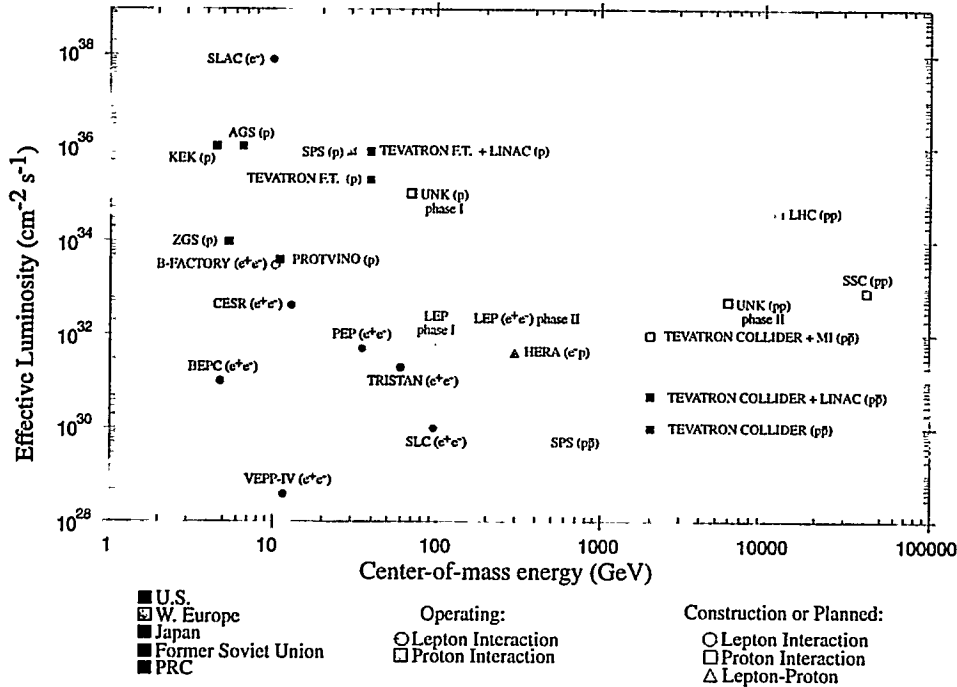


Fig. 11

fixed target facility. Here you can see the ZGS. It is a little clearer to see this if we take off the electron machines (Fig. 12) to see where the ZGS is relative to other proton machines. Its effective luminosity was very respectable for the time.

Generally later machines have higher energy so that you move off to the right in time, although this is not a time plot. The SSC is still there. We haven't updated the graph yet. The LHC shows a higher luminosity but a lower energy.

We are accused, from time to time, of never shutting off a machine. That is not true; a number have been closed as can be seen in Table I. The numbers are in as-spent dollars (dollars actually spent to build that facility), so they are not normalized to any one fiscal year. We can see that about \$124M was spent on Isabelle before it was terminated in 1983. We even show the old Caltech electron synchrotron. In those days one could build an accelerator for a modest amount of money, although CEA and PPA were more expensive. The table shows the total project cost for the SSC, and not the amount that was spent, although a significant fraction was. Those are the machines that have been retired or terminated over the years. Table II gives a quick rundown of some of the information that has been presented in graphical form. The table lists several Total Estimated Costs (TEC). The AGS had a cost estimate in 1956 of \$31M. It was completed in 1960, but the books were not closed until 1965 when the TEC was \$30.6, so that estimate was very well done. The AGS conversion, a few years later, was more expensive than the original machine.

The Fermilab TEC was \$248M in 1968: in 1976, when the books were closed, you see it coming in under budget by \$6.2M which was returned to the U.S. Treasury. The Energy Saver didn't change much although it went up some. The other upgrades didn't fare as well, particularly TeV I, which involved the construction of the antiproton source. The first design didn't seem to be panning out, so they took a different approach which cost substantially more.

HIGH ENERGY PHYSICS WORLD ACCELERATOR AND COLLIDING BEAM FACILITIES

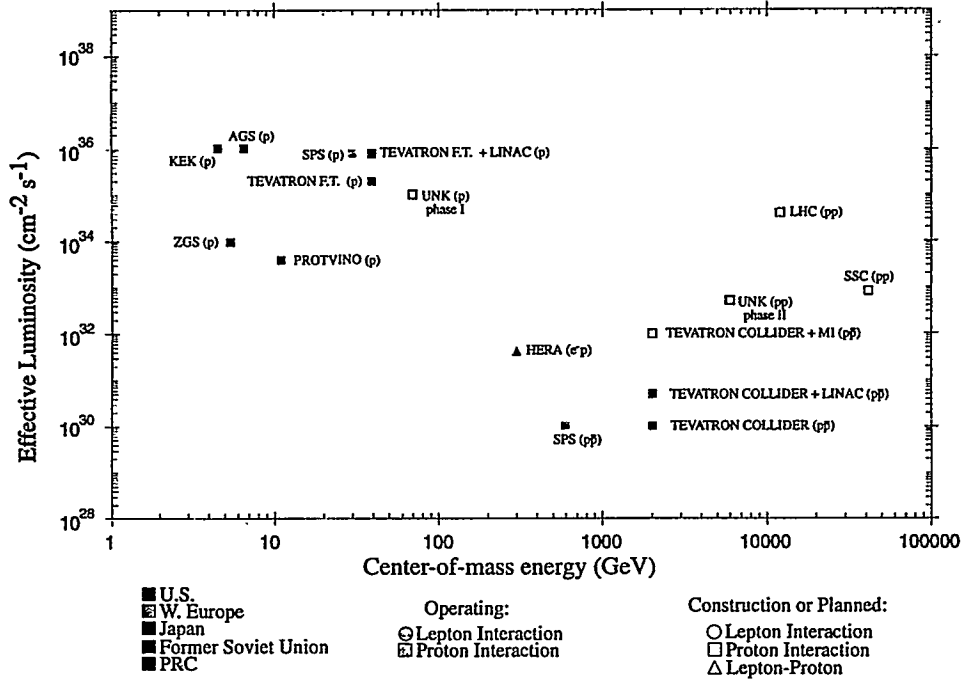


Fig. 12

HIGH ENERGY PHYSICS DOE MACHINES RETIRED OR TRANSFERRED IN LAST 20 YEARS (Dollars in Millions)

Institution	TEC	Date Auth	Completion Date	Date Retired
Argonne National Laboratory				
Zero Gradient Synchrotron (ZGS)	\$ 51.3	FY 1957	1963	1979
ZGS Bubble Chamber & Exp. Areas	\$ 17.8	FY 1966	1970	1979
Brookhaven National Laboratory				
COSMOTRON	\$ 10.5	FY 1949	1952	1967
ISABELLE	\$ 123.8	FY 1978		1983 (Term.)
Lawrence Berkeley Laboratory				
BEVATRON	\$ 9.9	FY 1950	1952	1975*
BEVATRON Improvement	\$ 10.0	FY 1961	1965	1975*
California Institute of Technology				
Caltec Electron Synchrotron	\$ 1.6	FY 1950	1952	1970
Harvard University				
Cambridge Elec. Accel. (CEA)	\$ 10.2	FY 1956	1962	1973
Princeton University				
Princeton Penn. Accel. (PPA)	\$ 11.6	FY 1956	1963	1971
PPA Addition	\$ 10.8	FY 1961	1965	1971
Superconducting Super Collider	\$8,249.0 (TPC)	FY 1988		1993 (Term.)

*After shutdown was incorporated in BEVALAC

Table I

**HIGH ENERGY PHYSICS
LOCATION AND COST OF
U.S. HIGH ENERGY PHYSICS MACHINES**
(Dollars in Millions)

<u>Institution</u>	<u>TEC</u>	<u>Date Auth</u>	<u>Completion Date</u>
Brookhaven National Laboratory			
Alternating Gradient Synchrotron (AGS)	\$ 30.6	FY 1956	1960
TEC \$31.0 in FY 56			
TEC \$30.6 in FY 65			
AGS Conversion	\$ 48.5	FY 1966	1972
TEC \$47.3 in FY 66			
TEC \$48.5 in FY 75			
AGS Booster	\$ 31.7	FY 1986	1991
Fermi National Accelerator Laboratory			
Fermilab & 200 BeV Accel.	\$241.8	FY 1968	1974
TEC \$248.0 in FY 68			
TEC \$241.8 in FY 76			
Energy Saver	\$ 50.8	FY 1979	1983
TEC \$38.9 in FY 79			
TEC \$46.6 in FY 80			
TEC \$46.9 in FY 81			
TEC \$50.8 in FY 82			
Tevatron I	\$ 84.0	FY 1981	1986
TEC \$39.5 in FY 80			
TEC \$41.5 in FY 81			
TEC \$82.5 in FY 82			
TEC \$84.0 in FY 85			
Tevatron II	\$ 49.0	FY 1982	1986
Linac Upgrade	\$ 22.8	FY 1990	1993
Main Injector	\$229.6	FY 1992	1999 (est.)
TEC \$177.8 in FY 92			
TEC \$229.6 in FY 94			
Stanford Linear Accelerator Center			
Stanford Linear Accelerator Center	\$114.0	FY 1961	1966
SPEAR	\$ 5.3	FY 1970	1972
Positron-Electron Project (PEP)	\$ 80.2	FY 1975	1979
TEC \$78.0 in FY 75			
TEC \$80.2 in FY 83			
Stanford Linear Collider (SLC)	\$115.4	FY 1984	1987
TEC \$112.0 in FY 83			
TEC \$115.4 in FY 84			
PEP-II Upgrade (B-factory)	\$177.0	FY 1994	1998 (est.)

Table II

We are out of time. I would like to close with a few words about the current status. Figure 13 is a slightly different graph. It shows the whole program with the SSC sitting on top. The point I would like to make is that as the SSC went up, the base program went down. Now the SSC is gone. We think that it is time to recover. The budget request for 1995, if you set aside the construction projects, is about 4% lower than 1994. These are not inflation corrected, so inflation adds to this. The 1994 numbers are about 4% lower than 1995, 1993 is 4.5% below 1992. In 1992 we had the same budget as 1991, although when you add in inflation, there is hardly any increase.

HIGH ENERGY PHYSICS FUNDING

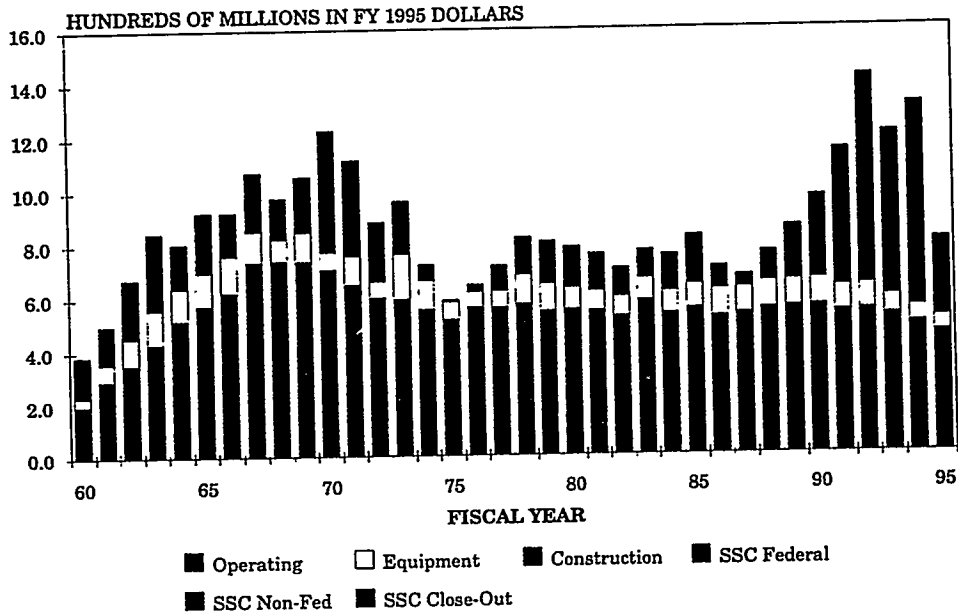


Fig. 13

HIGH ENERGY PHYSICS Percent of HEP Budget (Operating + Capital Equipment)

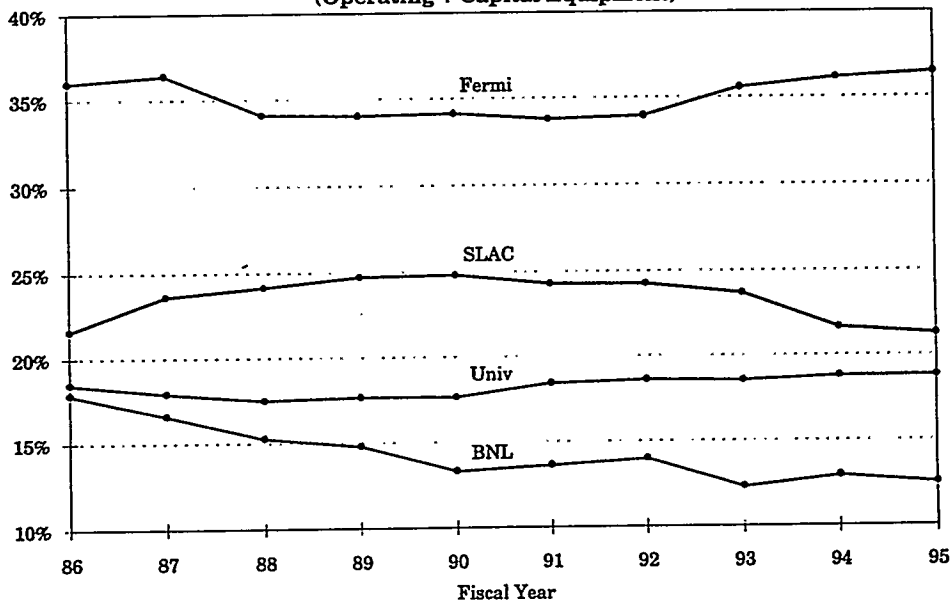


Fig. 14

So in fact, one can look at it in the following way: Over the last few years, we've taken on the two construction projects, the SLAC B factory and the Fermilab main injector in an essentially constant budget. As a result, the operating budget has really been going down in the last few years. If you are funded by DOE, your budget has been pinched. There it is folks. In 1995 we would have to add \$170M to get back to the buying power of 1990 which demonstrates why you are feeling such tight budgets.

Let me just close with two charts to show how we are dividing up the major pieces of the HEP budget. Figure 14 shows the percentages of operating plus capital equipment. Fermilab has the major share and in recent years, its share has stabilized and even gone up a little. The university program is similar; it also has stabilized and gone up a little. The university funding has not gone down. Those two pieces of the program account for over half the budget so, in the total program, somebody has to come down. The two somebodies are SLAC and BNL. In future years, BNL will become primarily a heavy ion facility rather than just high energy physics.

HIGH ENERGY PHYSICS FUNDING

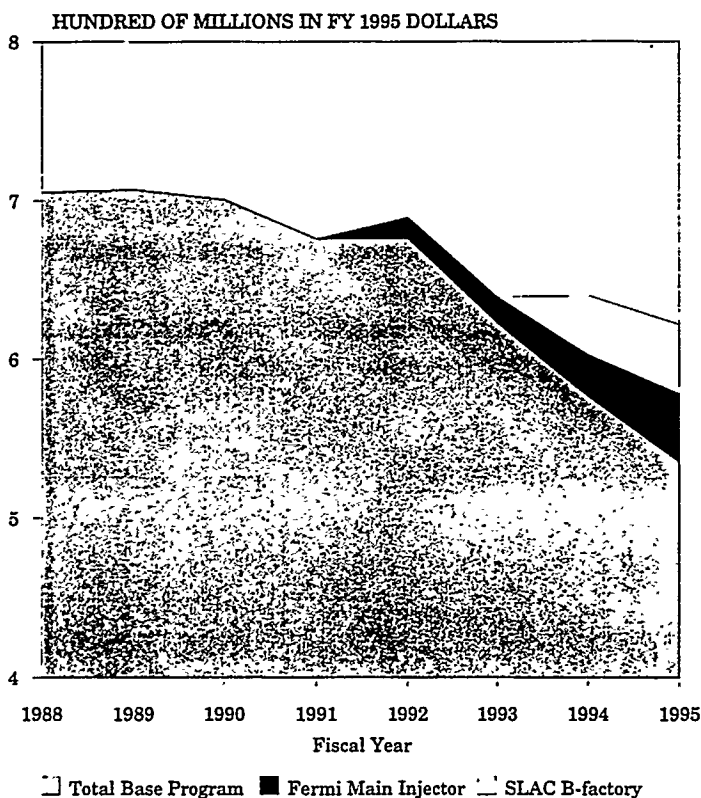


Fig. 15

The SSC is terminated, but we do have two major construction projects on the way: the Main Injector and the SLAC B factory, shown in Fig. 15.

With the termination of the SSC, U.S. involvement in the LHC at CERN is a question that's on the table. There is strong opinion in the community on both sides. Should we participate in the LHC and, if so, at what level? One level is to participate in both of the detectors, ATLAS and CMS and assist in the construction of the machine - something that CERN is almost certain to insist upon if we have major involvement in the detectors. So that's an issue. However, our base program has many current and near-term physics opportunities. We do have the world's highest energy machine, both fixed target and collider, and the highest

luminosity. The SLAC SLC, the e^+e^- linear collider is finally working well, with 70% plus polarized electron beams. They are producing a lot of good physics. BNL has very intense kaon beams and is doing a number of important rare decay experiments. ANL and LBL are playing important roles throughout our national program as major users at other facilities, and the university groups carry out about 75% of the actual physics research.

HIGH ENERGY PHYSICS PROGRAM STATUS AND FUTURE

Construction Projects--Where are we now?

- o SSC Terminated
- o Fermilab Main Injector underway
- o SLAC B-factory underway
- o U.S. involvement in LHC at CERN under consideration

Current and Near-Term U.S. HEP program opportunities

- o Fermilab--world's highest energy and luminosity hadron collider
- o SLAC--50 GeV electron beam, 70% polarized; e^+e^- linear collider
- o BNL--intense kaon beams
- o ANL and LBL user groups
- o University groups

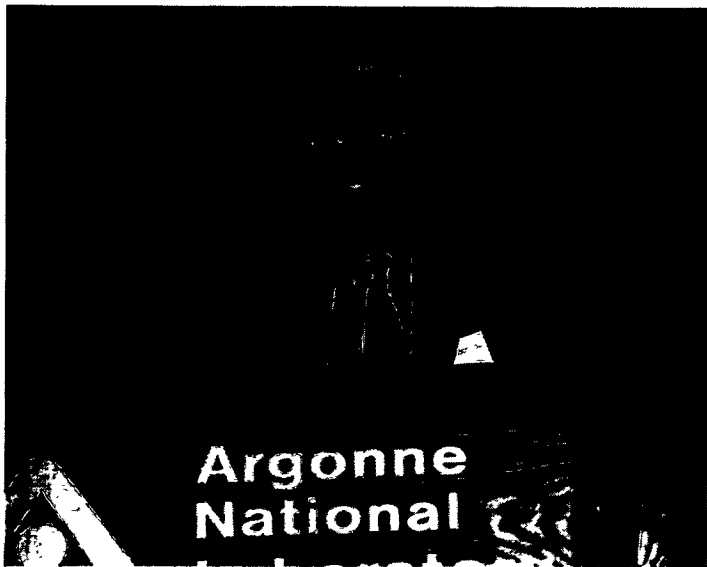
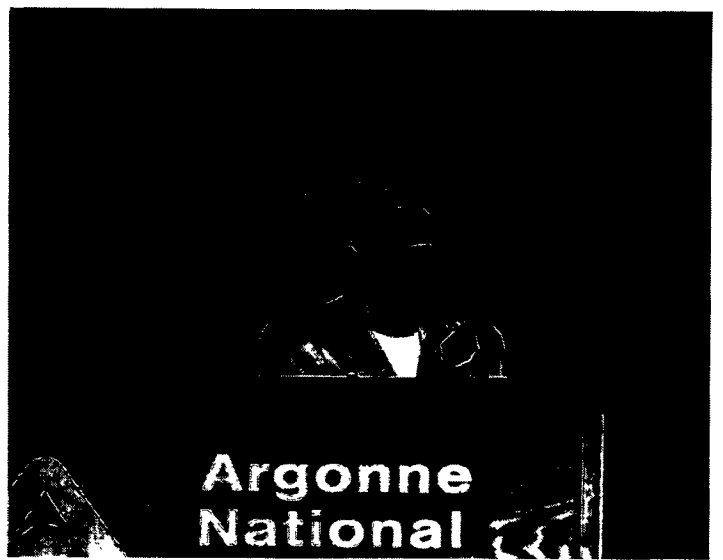
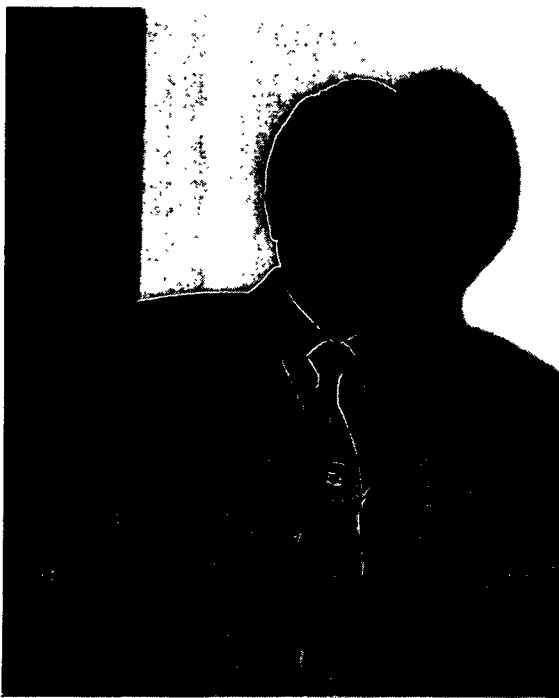
The Future

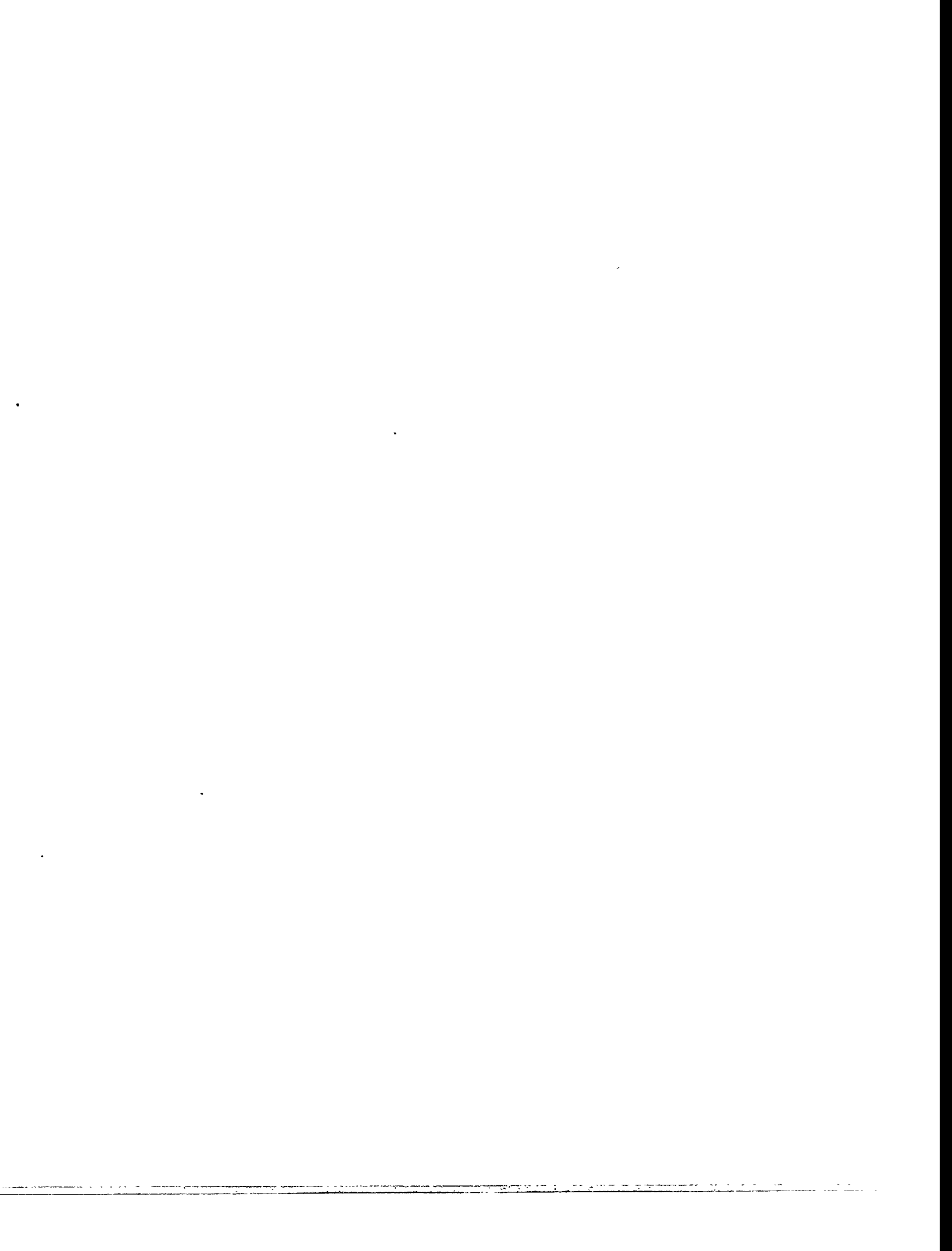
- o HEPAP Subpanel (Sid Drell, Chairman) to provide a vision
- o Possible U.S./CERN collaboration
- o High Energy Linear Collider (HELIC)
 - R&D underway
 - International memorandum of understanding signed by all major players
Cost, schedule, and location uncertain
- o FHC (Future/Final/Fermilab? Hadron Collider)
 - Follow-on to LHC
 - Energy?; greater than 30 x 30 GeV
 - Location?? Schedule??

Table III

What does the future hold. The HEPAP subpanel, chaired by Sid Drell, is to provide us with a vision. Their report is due to HEPAP on May 23, so we'll soon hear. Certainly one of the issues is a possible US/CERN collaboration on the LHC. Of other things that are floating around in the more distant future, there is the possibility of a high energy linear collider. There is substantial R&D underway. A Memorandum of Understanding has been signed by all the major players world-wide: SLAC, Fermilab, DESY, CERN, KEK, Novosibirsk. However, there are still a lot of uncertainties about whether or not a machine can be built, as well as what the energy should be, the costs, the schedules, and the location.. What about beyond the LHC - the FHC. What does that stand for? Who knows? Future, Final, Fermilab? I had a discussion with an old friend last night. He said maybe the F stands for Fantasy. Who knows, but I think there will be something beyond the LHC in hadron colliders. And that somewhere in our future, the energies will be substantially more than what we're looking for in the LHC, but no one knows what its cost, location and schedule might be.

We clearly have some financial difficulties, but we do have a lot of opportunities with our current program. I find it very encouraging to visit Argonne; we had our DOE program review of HEP here at ANL just earlier this week. They are, for their size, carrying out important work, contributing significantly to our program. It is very gratifying. We have a lot that we can do nationally. We still have a world leadership facility. We certainly do have some problems, perhaps the most important one is to turn around the slide down in our budget.





What remained from the ZGS accelerator components was the injection system, shown in Fig. 3, consisting of the preaccelerator, the 50 MeV linac and the 500 MeV rapid-cycling synchrotron (RCS). The second preaccelerator, for polarized protons, was taken to BNL and used for the polarized proton physics program on the AGS. The accelerator system remaining at ANL has been used for about 15 years to make spallation neutrons from the target shown at the right in Fig. 3. The way this developed is discussed in detail in the talk by Jack Carpenter. The next two pictures show part of the RCS ring (Fig. 4) and the transport line to the spallation target (Fig. 5). The magnets in the latter are old ZGS



Fig. 4. Picture of the RCS ring.

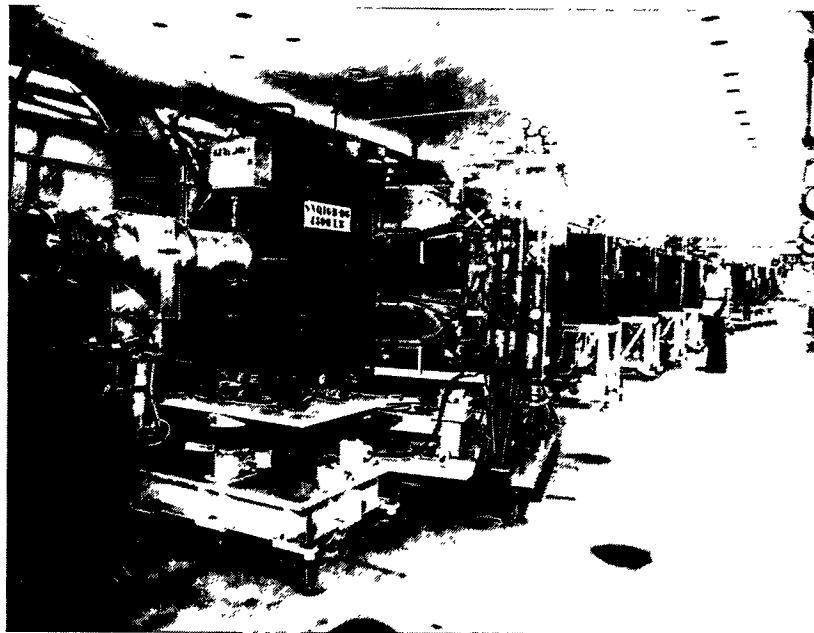


Fig. 5. 500 MeV transport line to the IPNS spallation target.

beam transport magnets-plus some that were originally built for the Cambridge Electron Accelerator!

The next picture (Fig. 6) will be familiar to many of you. It shows part of the ZGS main ring plus one of the eight long straight sections with the manipulators for the Piccioni extraction targets mounted on the top cover. The extracted proton beams came out at 90° from this position. The meson beams from internal targets exited to Building 370 at center left. A number of us spent quite a bit of time inside this straight section box. The vacuum pumping was done by 48" diffusion pumps mounted below-something that can be done today with a 16" cryopump.

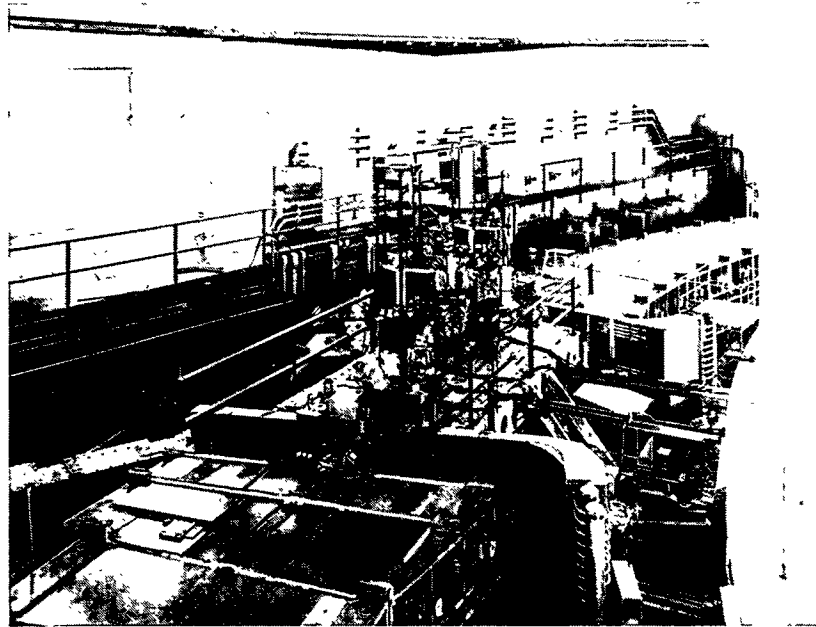


Fig. 6. Part of the ZGS main ring and a long straight section.

The meson area (370), on the far side of the wall, was used in the post-ZGS era to house a number of projects, including two large ones. The first was a test set up for heat exchangers that operate with a small temperature difference, important for Ocean Thermal Energy Conversion (OTEC). Figure 7 shows the large ammonia storage tanks and some of the plumbing. The second was a test of ship propulsion using a magnetohydrodynamic generator (MHD). The water loop linking the large superconducting dipole magnet, built at Argonne, can be seen in Fig. 8. Figure 9 shows the coils of this U-25 magnet being wound in the Building 362 High Bay. The magnet was originally built for use at the MHD Laboratory in Tennessee, but the program was cancelled before it could be delivered. Another magnet that was built and operated in Building 370 is shown in Fig. 10. This was a pulsed, conventional magnet used to study eddy current effects in 3-D. There was no 3-D computer code available at that time. Funding came from the fusion program.

In addition to the continuing IPNS program, the 50 MeV linac beam was used in a series of experiments with both negative and neutral hydrogen beams. The main interest was in measuring various cross sections and developing diagnostic devices of importance to the Strategic Defense Initiative (SDI). Foil and gas neutralizers were tested, neutral beams with very small divergence were developed, and the survivability of electronics in a radiation field was tested. More than 40 experiments were done by sixteen different organizations using the beam layouts shown in Fig. 11. As is evident, the beams were built in the ZGS ring building, taking up about half of the circumference. The large cross section of this space allowed plenty of room as well as a good working environment. Photographs of the set ups can be seen in Figs. 12 and 13.

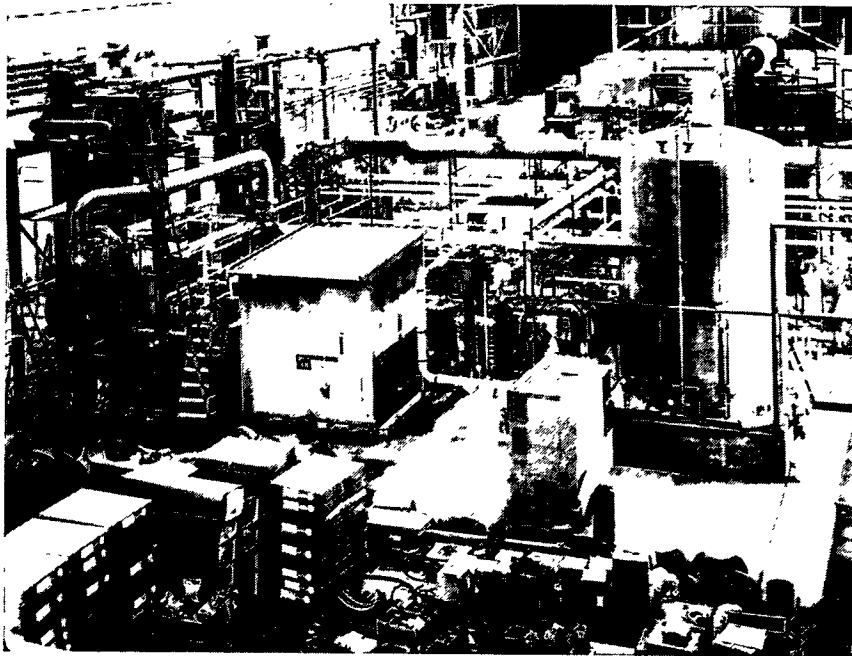


Fig. 7. OTEC test setup.

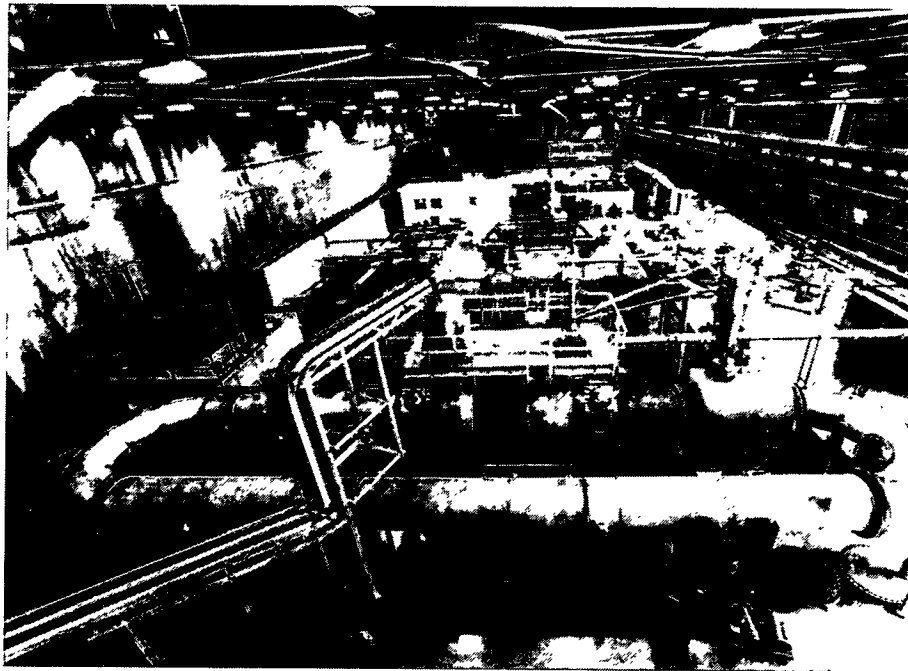


Fig. 8. Ship propulsion test using the large superconducting dipole.

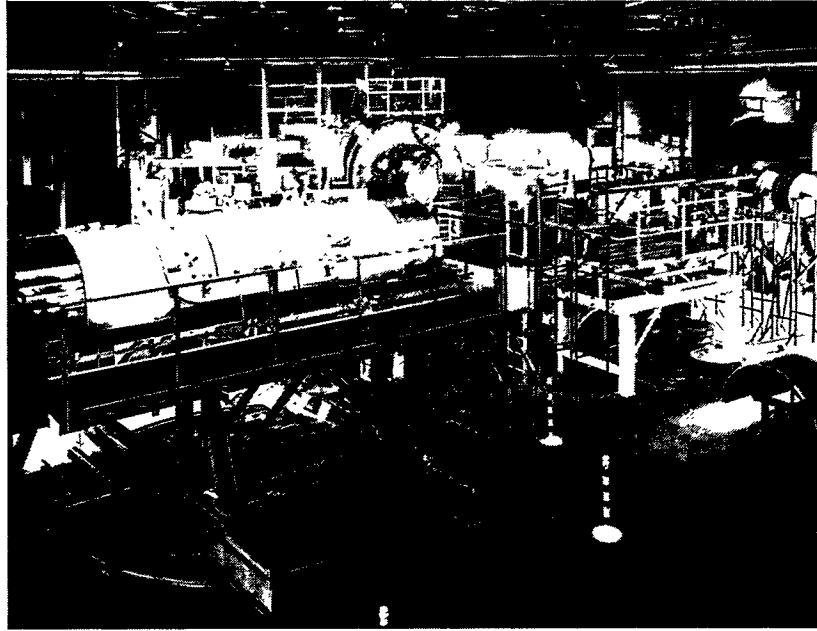


Fig. 9. The superconducting dipole for the U25 MHD channel under construction in the 362 High Bay.

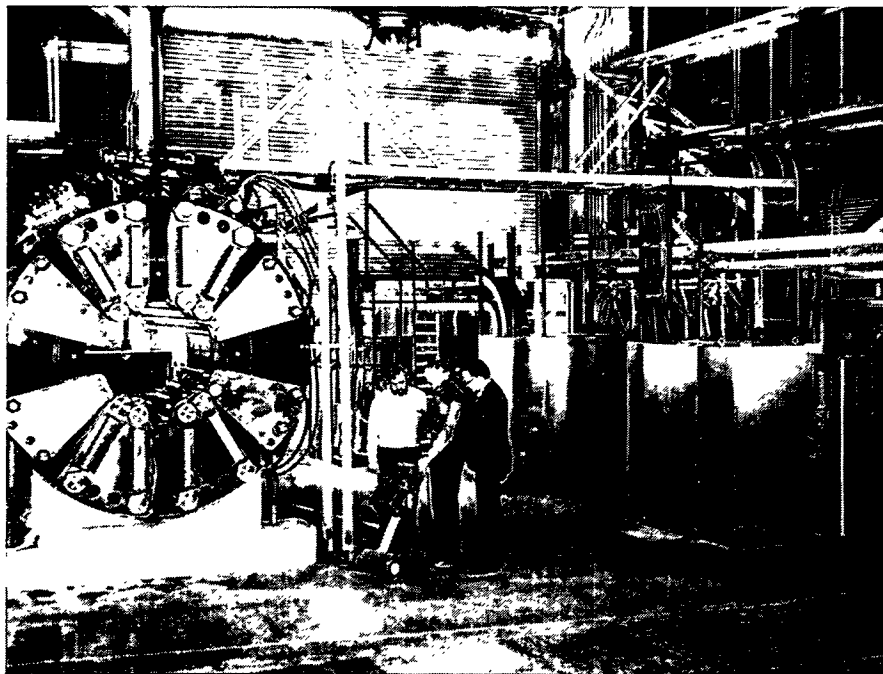


Fig. 10. Pulsed magnet used for eddy current studies.

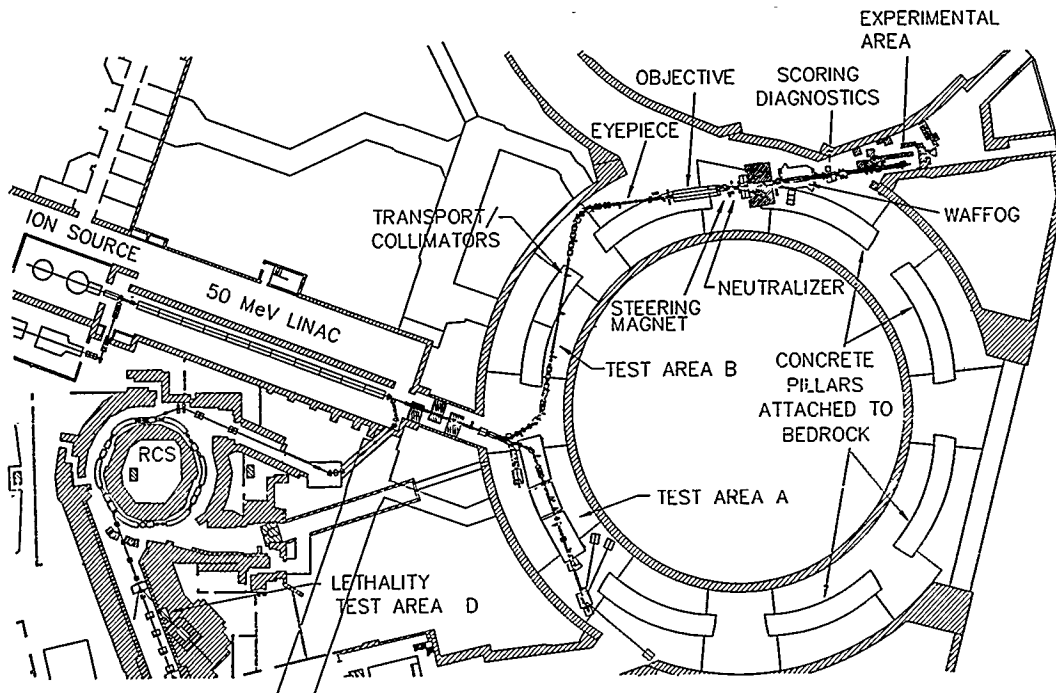


Fig. 11. Layout of 50 MeV beams in the ZGS ring building.

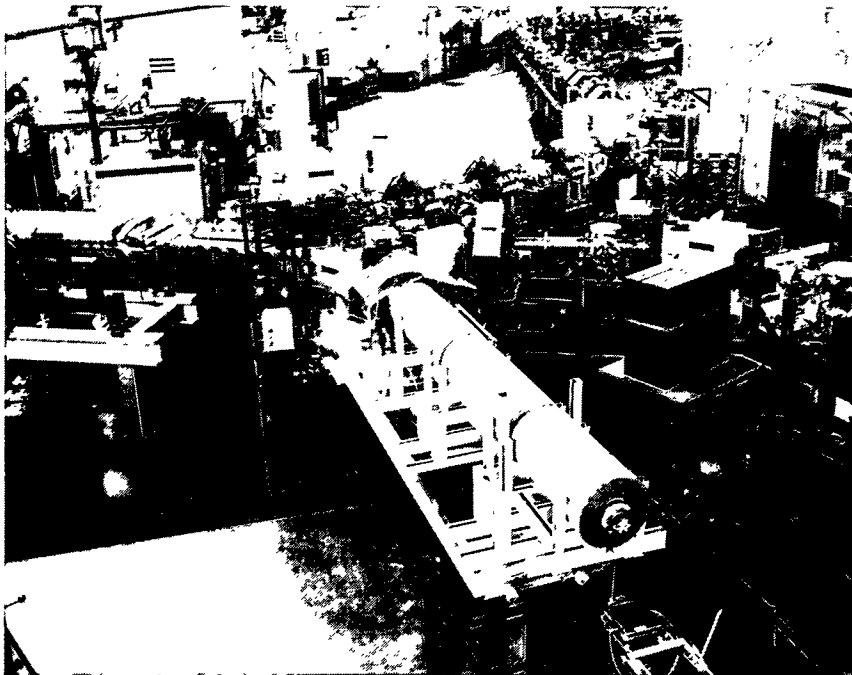


Fig. 12. Beam line setups for the SDI measurements.

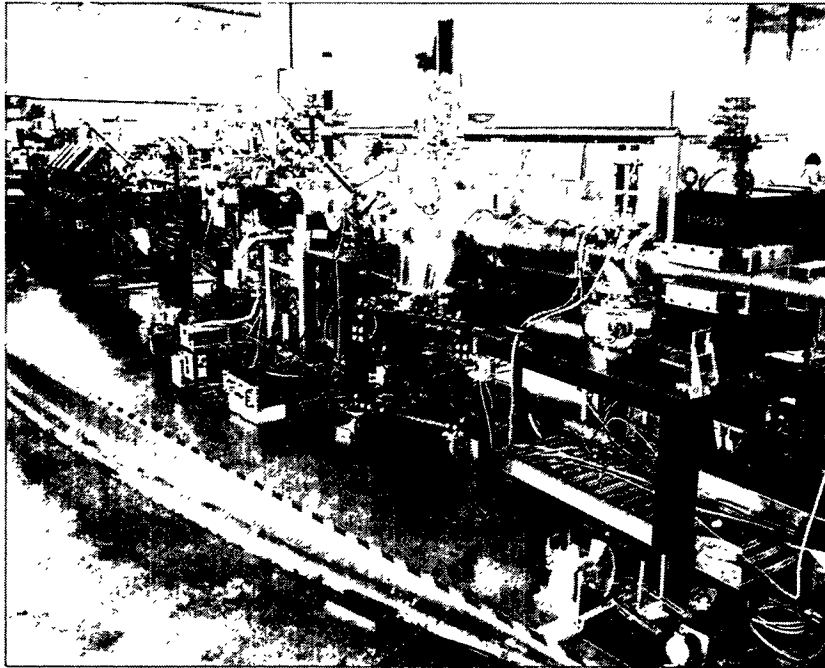


Fig. 13. Magnetic telescope objective under test for the SDI program.

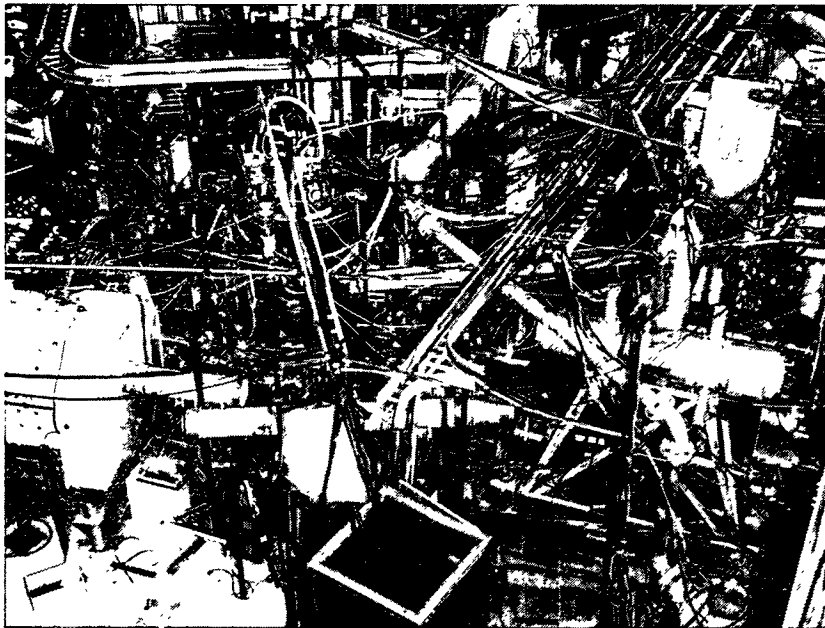


Fig. 14. View of a typical HEP experiment in the ZGS time.

Now let's remind ourselves what a typical HEP experiment looked like in the ZGS time (Fig. 14). Laughter! You can see that it was possible to do things even before the days of Tiger Teams and OSHA jurisdiction over Argonne.

CWDD FACILITY

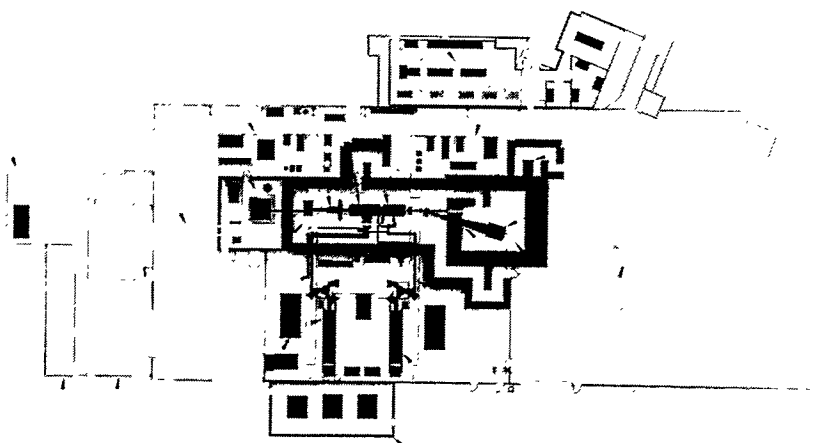


Fig. 15. Layout of the CWDD accelerator system.

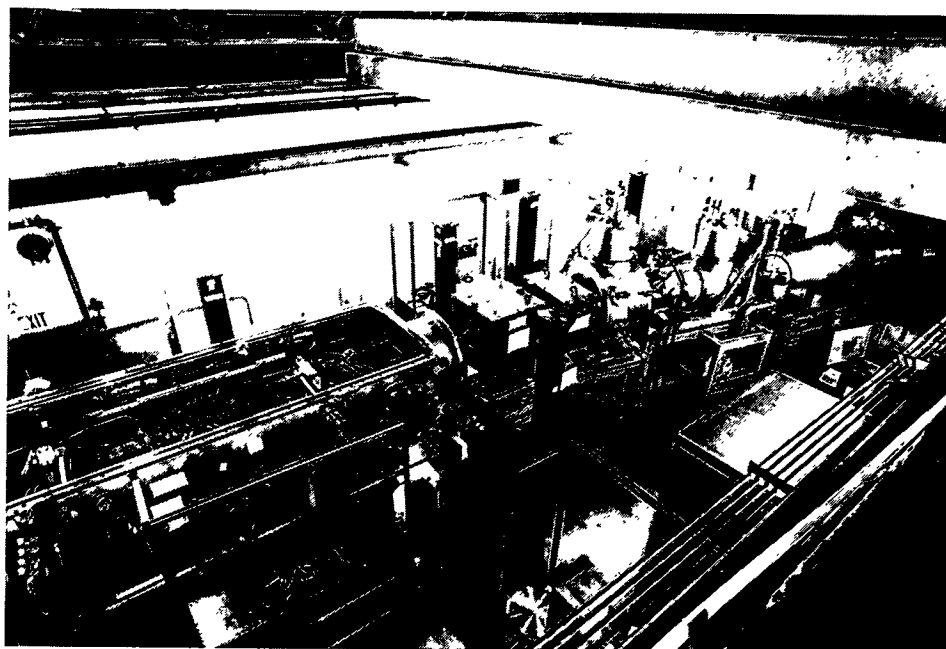


Fig. 16. Picture of the CWDD accelerator in Building 369.

The EPB-I Building (369) was used to house the Continuous Wave Deuterium Demonstration facility (CWDD), a high-current deuteron linac: another SDI project. It consisted of a 90 mA 200 KeV d-source, built by the Culham Laboratory in England, a 2 MeV RFQ and, finally, a 7.5 MeV drift tube linac, as shown in the layout of Fig. 15 and the photograph of Fig. 16. The ion source, pictured in Fig. 17, was operating 5 minutes with 20 mA before the program was terminated. The accelerator, shown in Fig. 16, is somewhat neater than the HEP experiment of Fig. 14 but, of course, it never operated in contrast to

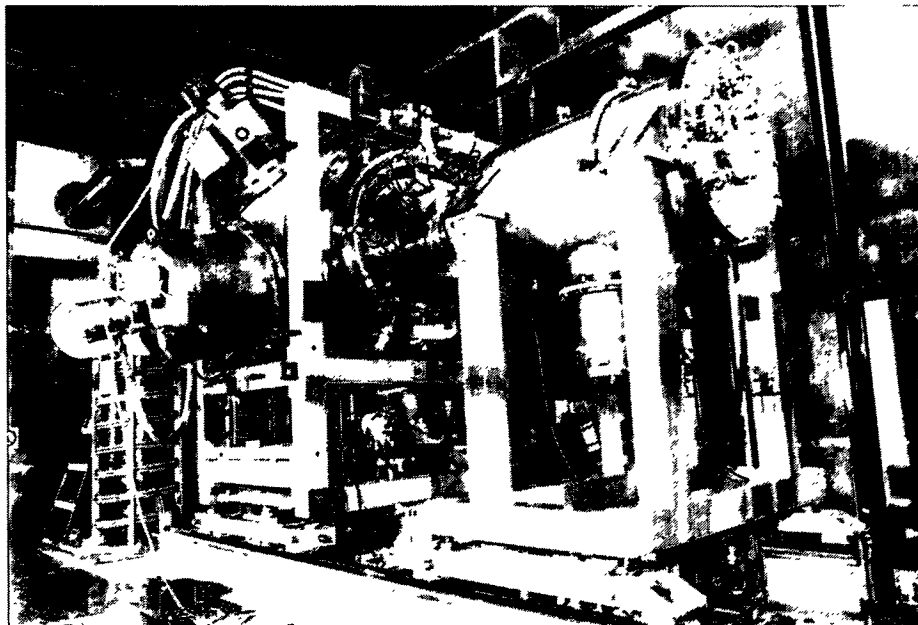


Fig. 17. Ion source of the CWDD accelerator.

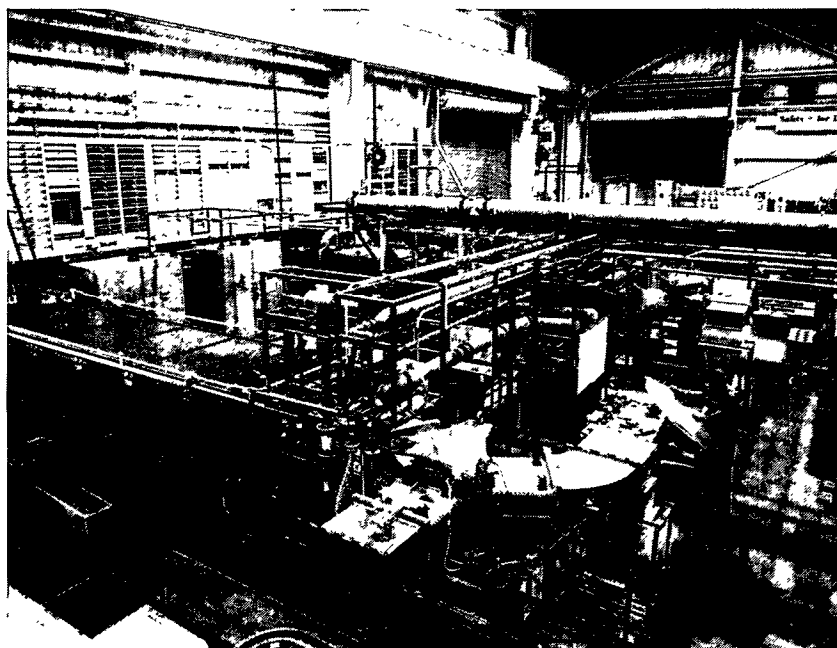


Fig. 18. Klystron housing and waveguides of the CWDD accelerator.

the HEP experiments. The RFQ used 352 MHz klystrons, the same frequency as the APS. The lead shielded klystron housing and the RF wave guides can be seen in Fig. 18.



Fig. 19. The ring magnet power supply for the ZGS.

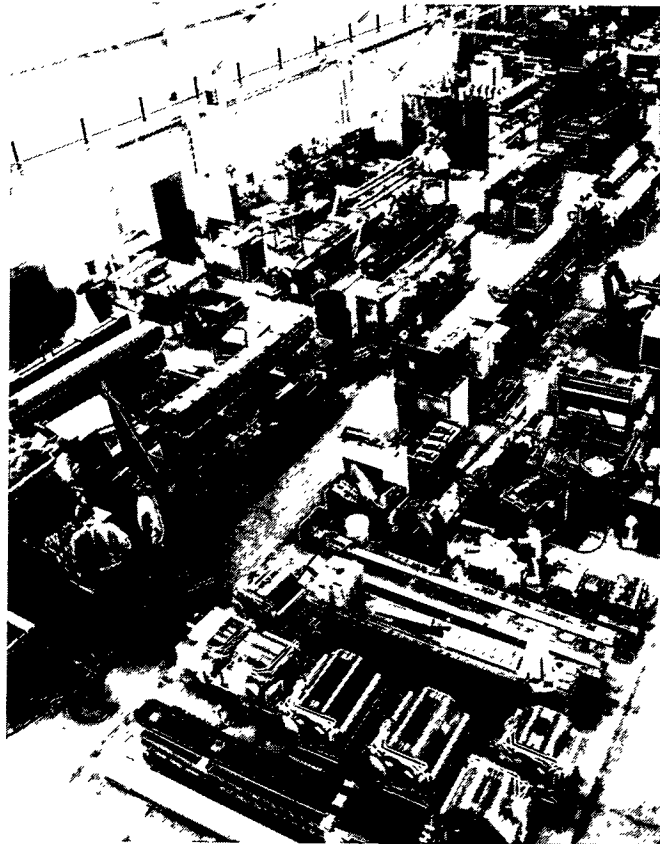


Fig. 20. APS magnet factory in Building 376.

The Ring Magnet Power Supply for the ZGS was the big motor/generator set seen in Fig. 19. This was removed and the building (376) put to good use as a magnet factory for the APS, as seen in Fig. 20. Building 382 was used for fabrication and testing of APS vacuum chamber components, Fig. 21, and tests of components of the X-ray beam lines were tested, Fig. 22, in the 362 High Bay.

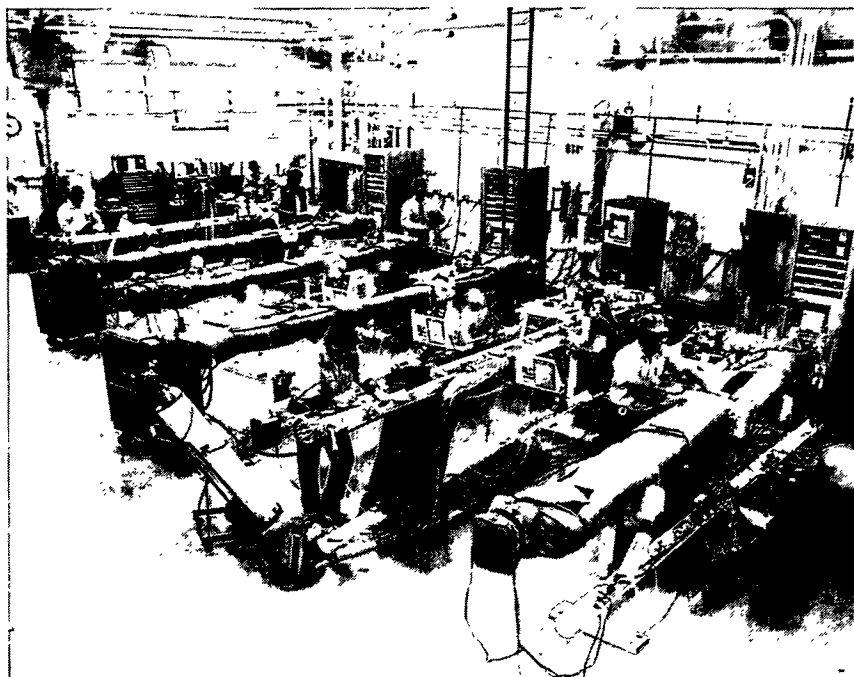


Fig. 21. Vacuum sections of the APS under bakeout and test in Building 382.

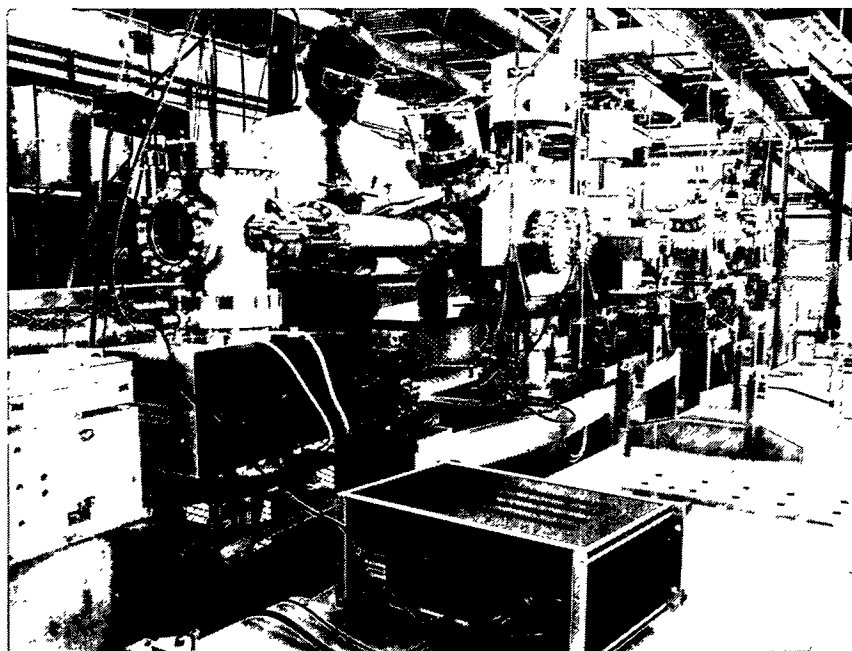


Fig. 22. Test setup of X-ray beam in Building 362 High Bay.

Unlike many of the projects I have discussed, the APS has actually been completed and will have a productive scientific life that is measured in decades. It is clear that the collection of facilities surrounding the ZGS have been crucial in the development and timely construction of this new facility, which will ensure the continuing viability of Argonne as a first-class research Laboratory.

The continuing HEP research program also used the ZGS buildings, particularly the EPB-I extension (366). The first project to modify the magnet of the 12-foot bubble chamber was done in the bubble chamber building. The rotated coil is seen in Fig. 23. The barrel calorimeter modules for CDF at the Tevatron Collider (Fig. 24) and the ZEUS detector for the e-p collider at DESY (Fig. 25) were built in Building 366. Finally, there is a continuing program studying wakefield acceleration using specially designed equipment shown in Fig. 26. The first phases of this program used the 20 MeV electron linac in the ANL Chemistry Division.

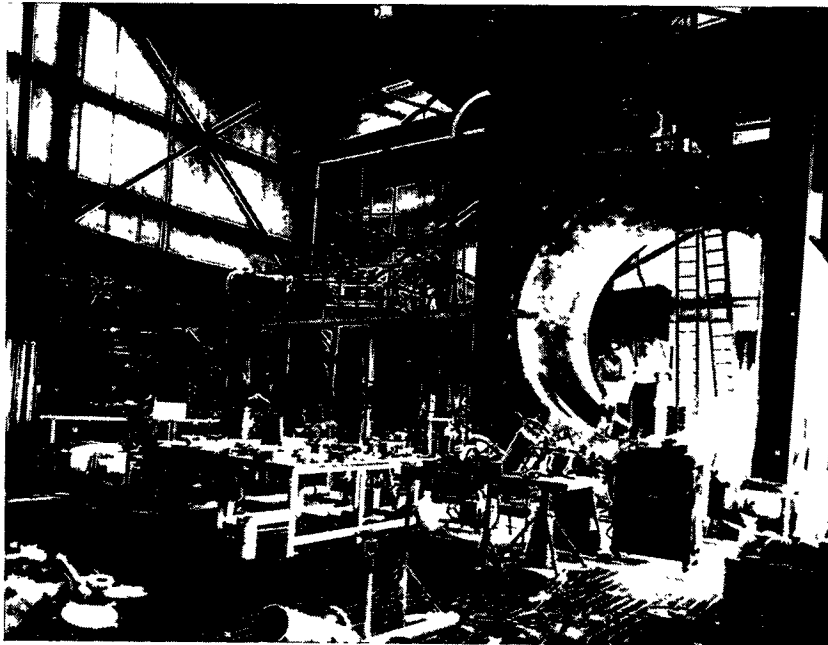


Fig. 23. Super magnet coil built for the 12-foot bubble chamber after modification for the High Resolution Spectrometer (HRS).

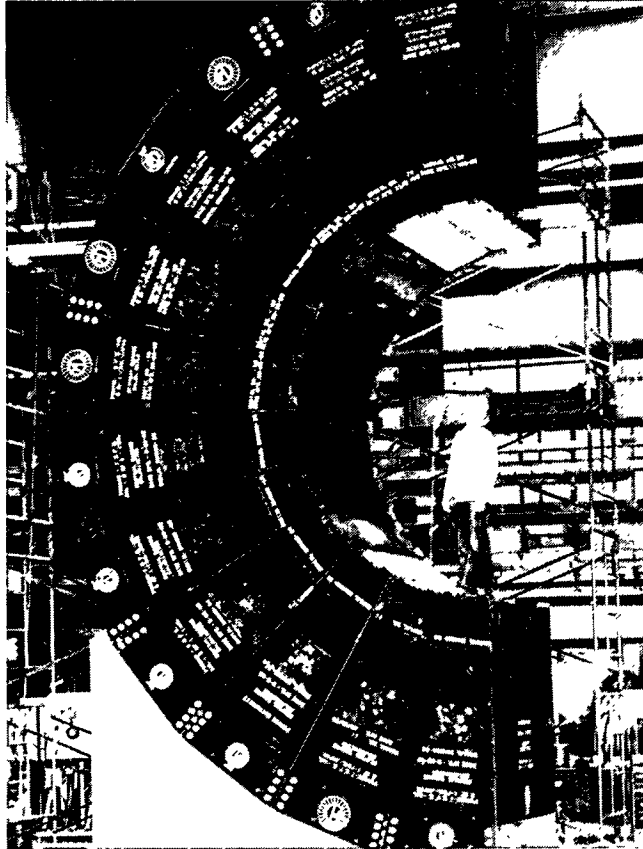


Fig. 24. Barrel calorimeter half for the Collider Detector Facility (CDF) at Fermilab.

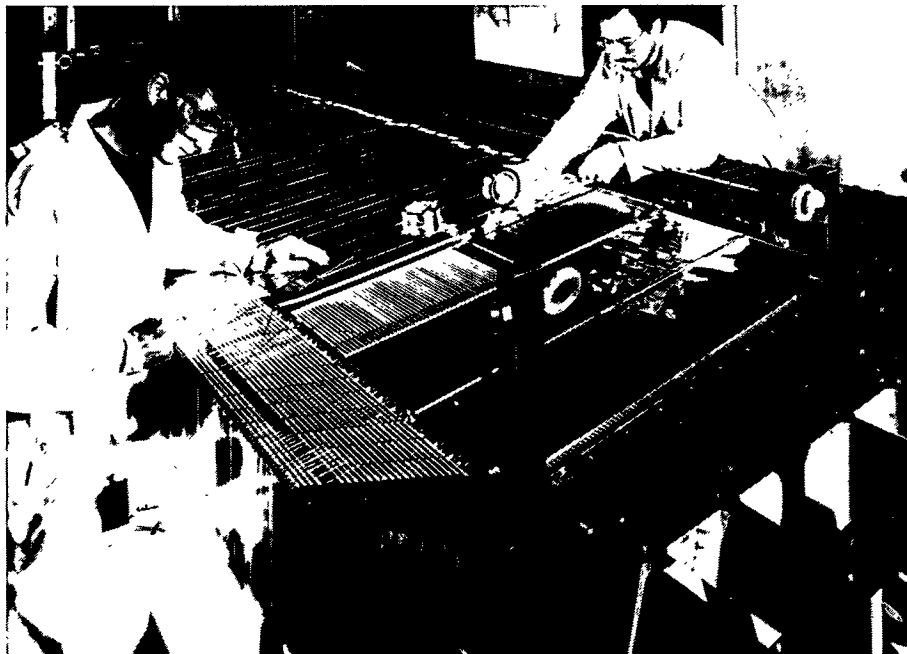


Fig. 25. A barrel calorimeter module for ZEUS under construction in Building 366.

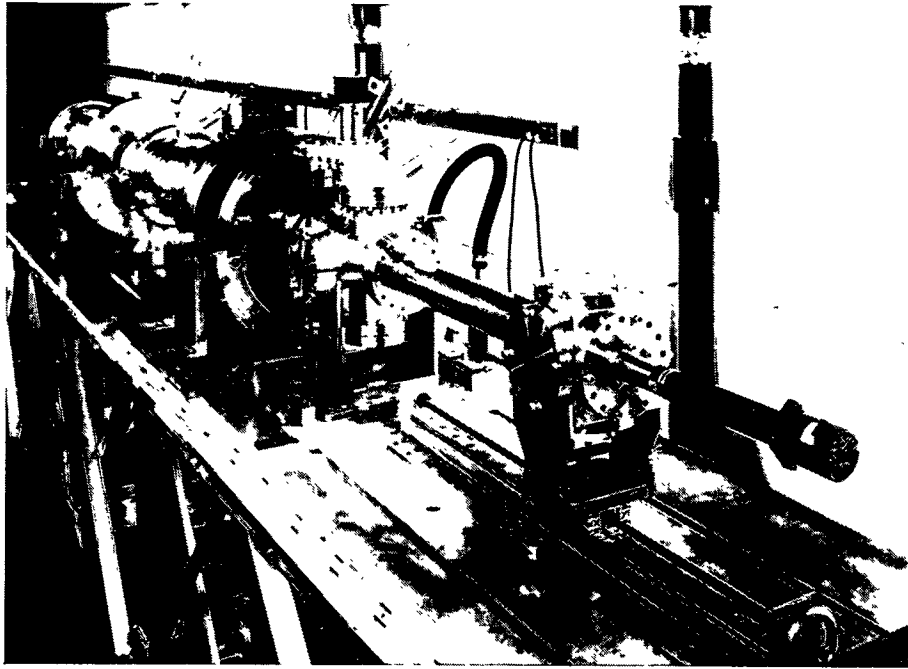
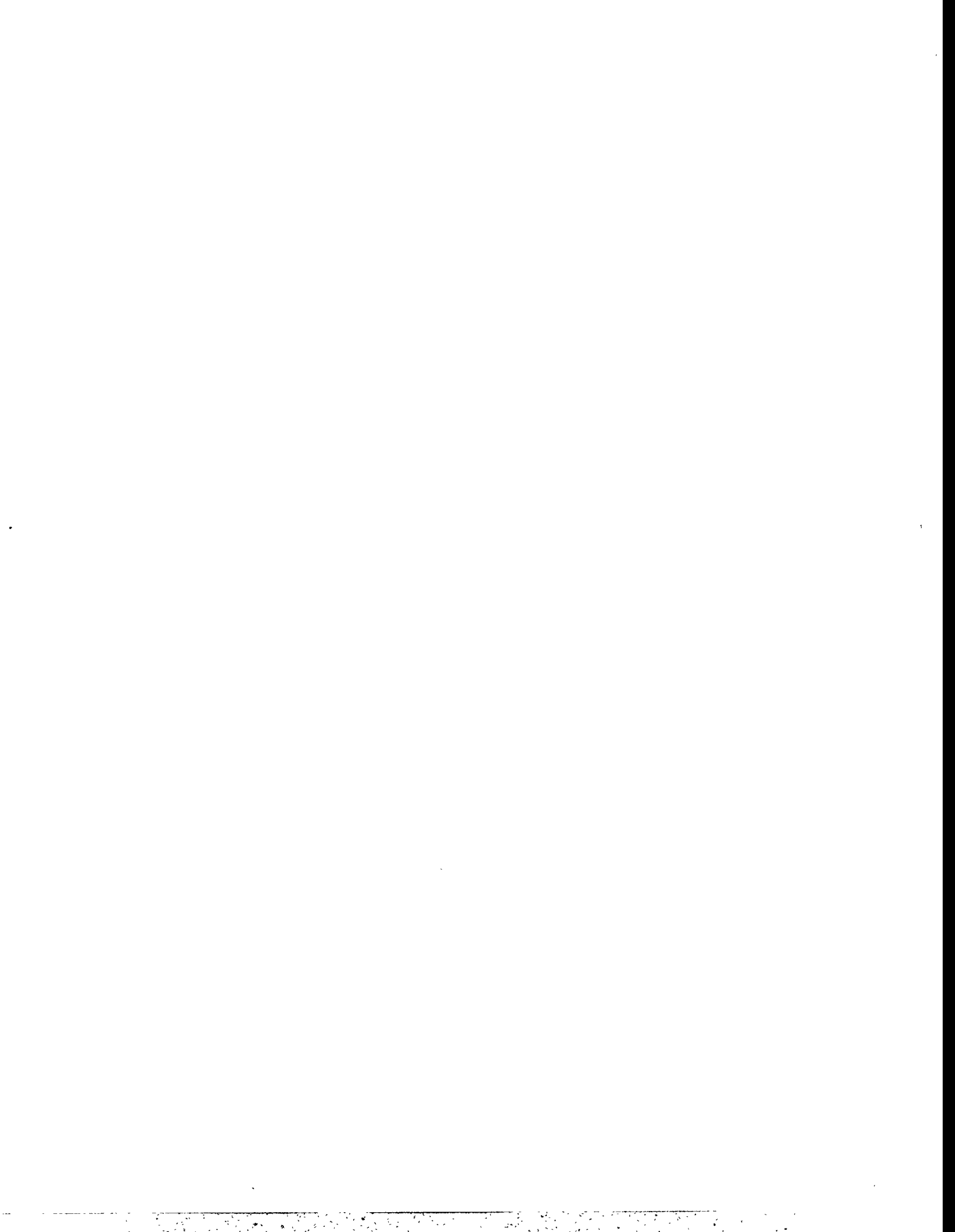


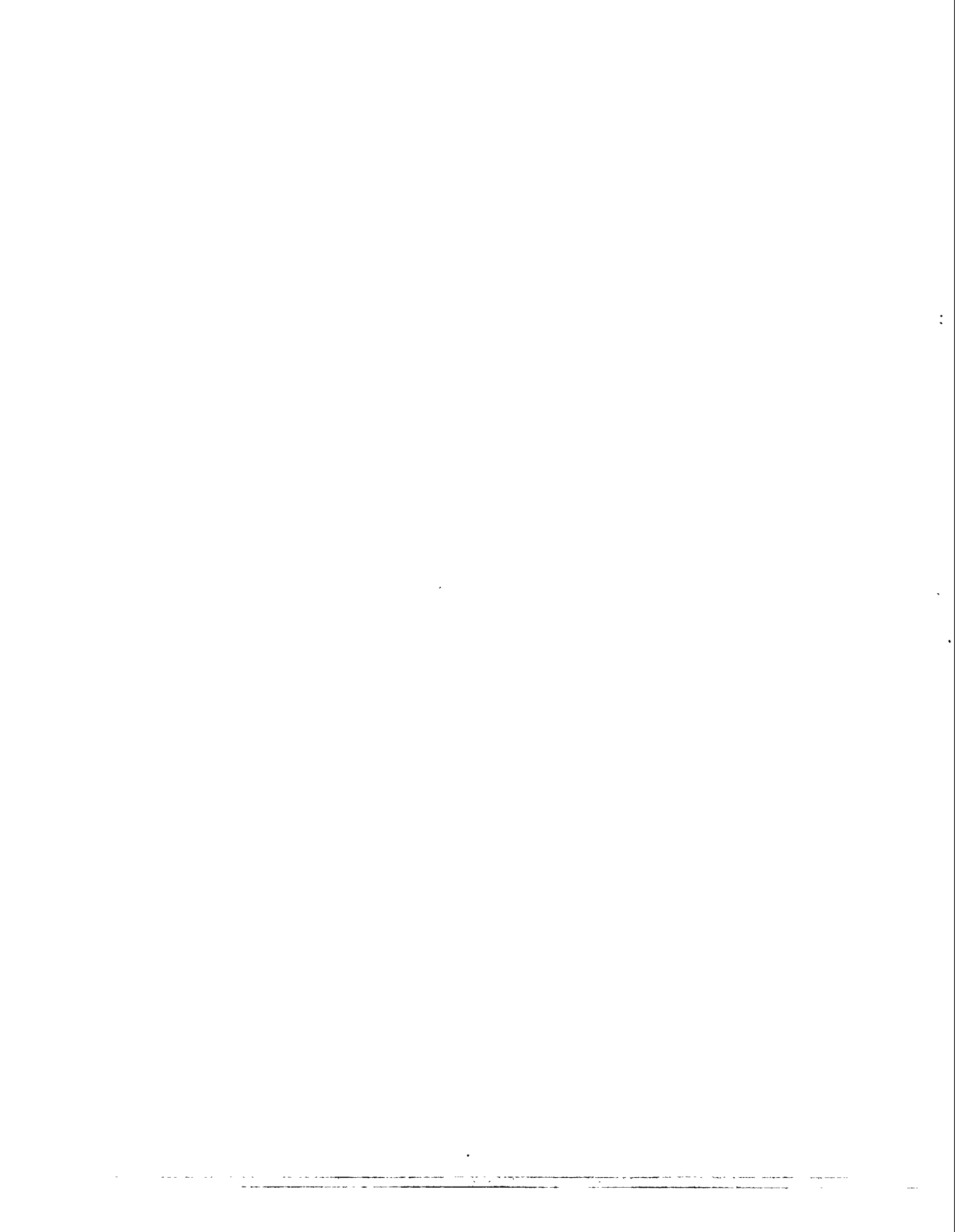
Fig. 26. Part of the Argonne Wakefield Accelerator in Building 366.

We have now completed our whirlwind tour. What conclusions can we draw? I can think of three. The first is that the termination of a program like the ZGS has an up as well as a down side; it provides resources and opportunities for work in new research areas. The second is the contribution that the assets of the terminated program make to the continuation of the Laboratory. The ZGS facilities were able to serve a variety of new Argonne programs. Finally, everything depends on having a staff of people who can see and exploit unique opportunities to further the U.S. R&D activities.











They were later joined by other ZGS people, like Al Moretti, Tony Passi, John Gonczy and Ed Heyn, who went to build the hardware, and Argonne physicists, who carried out research programs there, such as Tom Fields' and Rich Singer's jet experiment, and the neutrino experiments manned by veteran "bubblers" from the ZGS 12-foot and other chambers.

At Argonne, other programs had been firing up. Like Hearthfire, a heavy ion fusion concept developed by Ron Martin, aided and abetted by Jerry Watson, Ken Menefee, Dave Leach and others. Figure 3 shows the Hearthfire crowd, minus Ron, who was probably off in Russia at the time.

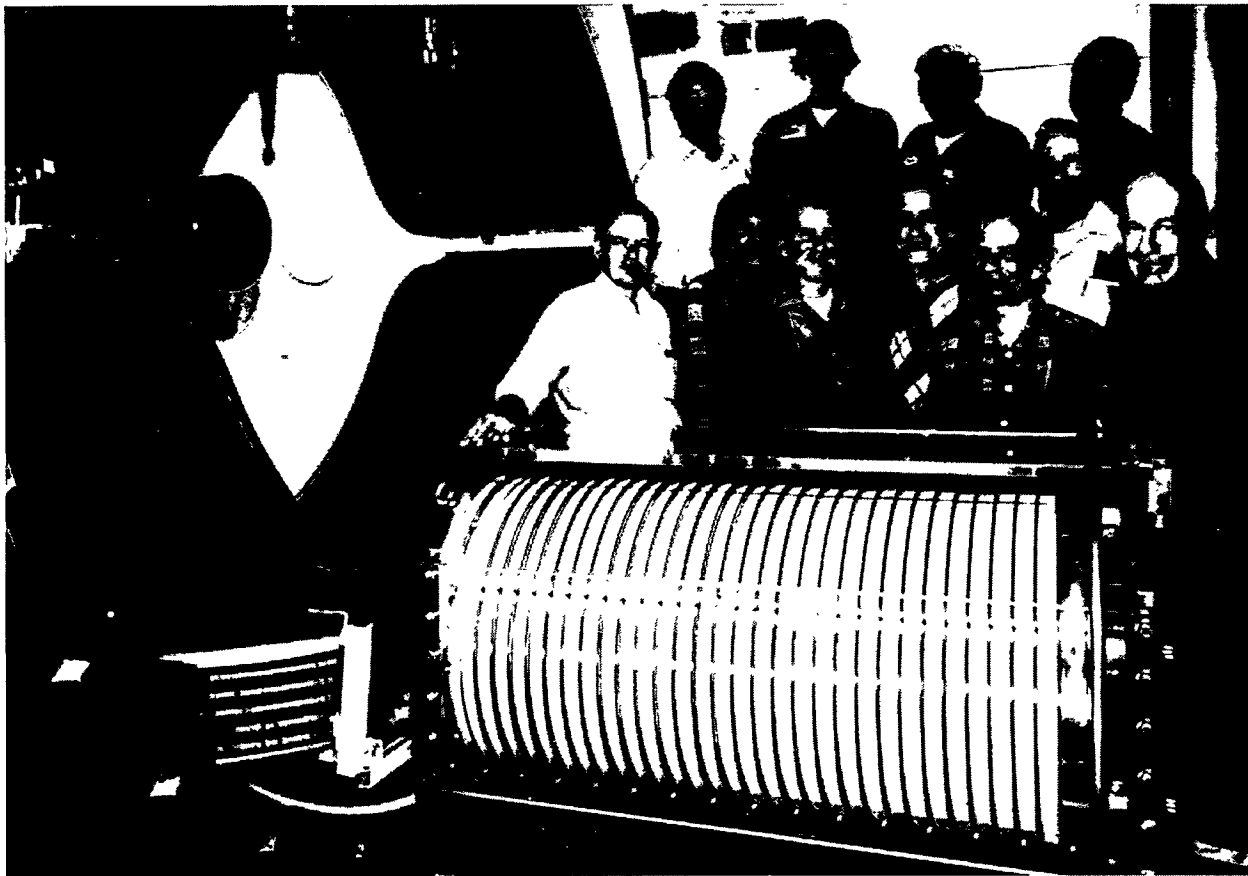


Fig 3. Hearthfire development group with Dynamitron high-voltage column.

The Superconducting Magnet Group was very busy building large magnets, such as the U-25, which was shipped off to Russia, along with a bunch of our experts. The group shown in the picture (Fig. 4) was indeed expert at many things. One of them was ferreting out the Marine Corps Bar in Moscow, another was adding people to photographs. On the far right of the picture below is a dubbed-in Rich Smith, who was unfortunately not available for that historic photo-opportunity.



Fig. 4. U-25 Magnet team prior to departure for Moscow on USAF C5A transport aircraft.

A look at organization charts of the Accelerator Research Facilities Division (ARF), starting in 1975 and going through to 1979, shows the changing direction of the division. By 1975 a fairly large solar energy activity was under way, and in 1976 the superconducting group appears. In 1978, ion beam fusion had been added, along with the start of a closing group. As shown in Fig. 5, on that fateful October day in 1979, a large closing group existed, ion beam fusion had become heavy ion fusion, solar energy had toddled off into the sunset (or more precisely to another part of Argonne), a FNAL pbar group was on the map, and an operations group for the Intense Pulsed Neutron Source (IPNS) was identified.

Although you could never tell it from any of the High Energy Physics Division's (HEP) organization charts (they all tended to look somewhat generic, like the example shown in Fig. 6), in fact, the HEP people had been very busy shifting their research.

A program led by Malcolm Derrick, Brian Musgrave and others recycled the 12-foot Bubble Chamber magnet into the centerpiece of the High Resolution Spectrometer detector used on PEP at SLAC. Just getting the 100-ton magnet

ACCELERATOR RESEARCH FACILITIES DIVISION
ARF DIVISION OFFICE

10/1/79

<u>CLOSING GROUP</u>	R. L. Kustom E. F. Parker R. Bouie J. Cotts R. Kickert R. Thompson A. Bakke	Director Deputy Assistant Executive Assistant Budget Safety Secretary* Secretary*	<u>HEAVY ION FUSION GROUP</u> R. L. Martin - Manager A. Noretta N. Sesol R. Stockley J. Watson S. Fenster G. Magelssen R. Wehrle M. Mazarakis A. Wright K. Menofee
<u>TECHNICAL SUPPORT GROUP</u>	R. Hoffett - (Acting) Group Leader R. Mandernack D. McGhee J. Moenich A. Passi W. Pelczarski M. Pracy K. Thompson R. Ziemann G. Fouts R. Puccetti C. Putman T. Saddler R. Seglem G. Sprau D. Voss E. Stringer*	R. Kustom - (Acting) Manager V. Stipp D. Suddeth G. Volk L. Donley W. Sullivan L. Johns R. Kliss D. Piatak S. Reinke P. Roth C. Saunders R. Smith R. Sobanski W. Horn B. Marzec*	R. Blackman (Eff. 1/1/80) D. Leach (Eff. 1/1/80) M. Rebuehr R. Ward R. Zoldecki J. Heami (Eff. 1/1/80) K. Volk* J. Worn*
<u>EXPERIMENTAL PHYSICS GROUP</u>	R. Moffett - Group Leader L. Balka E. Colton S. Kramer T. LaChance R. Barner S. Phillips G. Featherstone*	E. Parker - (Acting) Manager Y. Cho R. Lari L. Ratner H. Takeda T. Khoo	<u>SUPERCONDUCTING MAGNET GROUP</u> R. P. Smith - (Acting) Group Leader L. Genens H. Ludwig K. Hataya R. Niemann J. Hoffman S. H. Kim L. Turner M. Lieberg S.-T. Wang H. Chen Y. Huang R. Lanham J. Urban A. Paugys R. McHenry*
<u>ACCELERATOR PHYSICS GROUP</u>	R. Hoffett - Group Leader L. Balka E. Colton S. Kramer T. LaChance R. Barner S. Phillips G. Featherstone*	E. Parker - (Acting) Manager Y. Cho R. Lari L. Ratner H. Takeda T. Khoo	<u>FNAL P GROUP</u> J. Simpson - Manager T. Hardek

*Secretarial

Fig. 5. ARF 1979 Organization Chart

November, 1981

HIGH ENERGY PHYSICS DIVISION

Administrators

Robert E. Diebold
Brian Musgrave
Joanne S. Day

Physicists (Experimental)

Michael Arenton
David Ayres
Daniel E. Bender
Malcolm Derrick
William R. Ditzler
Thomas H. Fields
Enrique Fernandez
Stephen Gray
Ray T. Hagstrom
Lloyd G. Hyman
Kenichi Imai
Paul Kooijman
James S. Loos
Howard Ludwig
Edward May
Lawrence Nodulman
Lawrence Price
Hajime Shimizu
Harold Spinka
Robert Stanek
Koichi Toshioka
Thomas Trinko
David Underwood
Robert Wagner
Jeffrey Weiss
A. Barry Wicklund
Akihiko Yokosawa

Physicists (Theoretical)

Edmond L. Berger
David Callaway
Louis Clavelli
Porter Johnson
Daniel Jones
David J. Maloof
Dennis Sivers
Cristian Sorensen
Gerald H. Thomas
Nigel Wright

Engineers and Applied Scientists

Kenneth Coover
John Dawson
Daniel A. Hill
Norman Hill
H. Bruce Phillips

Computer Scientists

James Schlereth
Barbara Pancake

Technical Staff

Ivars Ambats
Leonard Balka
B. Harvey Blair
Wilton J. Evans
William N. Haberichter
Donald J. Jankowski
Thomas Kasprzyk
Carl Klindworth
Robert Laird
Robert C. Miller
Ronald Rezmer
Joseph F. Sheppard
Eugene Walschon

Technical Hourly Personnel

Donald Emery
Robert S. Johnson
Lawrence Kocenko
Arthur M. Rask
Robert Taylor
Steve Zelipsky

Fig. 6. High Energy Physics Division organization chart.



Fig. 7. High Resolution Spectrometer, et.al.

modified and shipped off to California was a major job for many people, Klaus Jaeger and Russ Klem among them. Figure 7 shows members of the HRS collaboration standing inside the detector.

Neutrino oscillations claimed the attention of Lloyd Hyman, Tom Romanowski and Bob Stanek, and they formed a collaboration with the Argonne Physics Division to do an experiment at LAMPF. They had been preceded there by Aki Yokosawa's group, which was dividing its time between Los Alamos, Fermilab, and anywhere else they might be able to get a proton to polarize. Figure 8 shows a portion of the polarized beamline at Fermilab, along with two mainstays of the group, Dan Hill and Joe Sheppard.

The Collider Detector Facility (CDF) collaboration, led at first by Bob Diebold and later by Larry Nodulman, became a major activity of the Division. Argonne was charged with construction of the calorimeter, and that activity kept a large portion of HEP and Argonne's Central Shops very busy indeed.

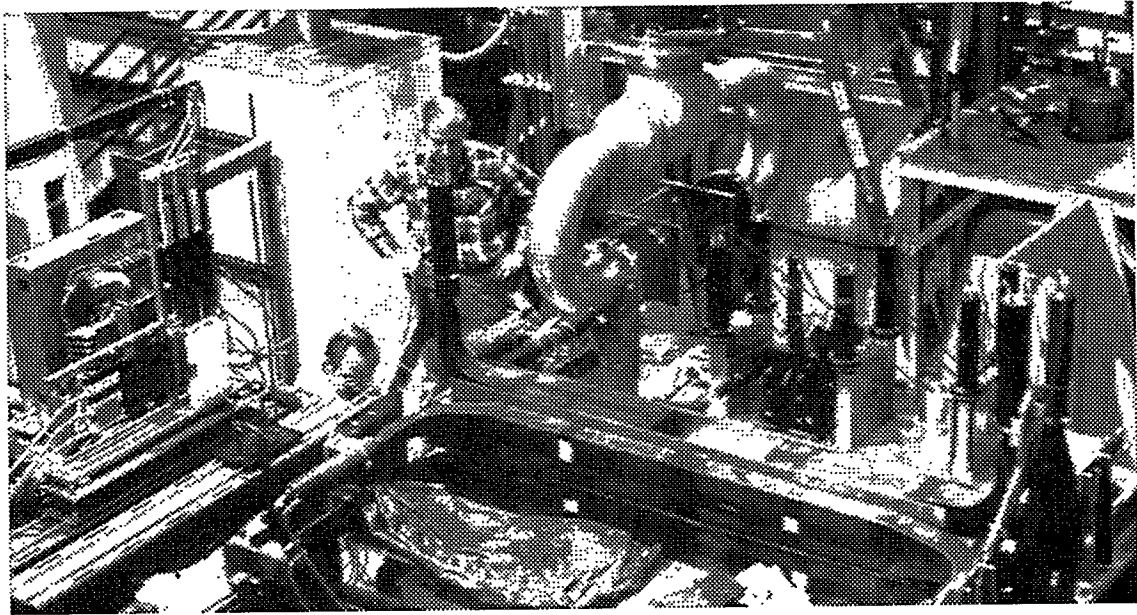


Fig. 8. E-704 polarized beamline apparatus.

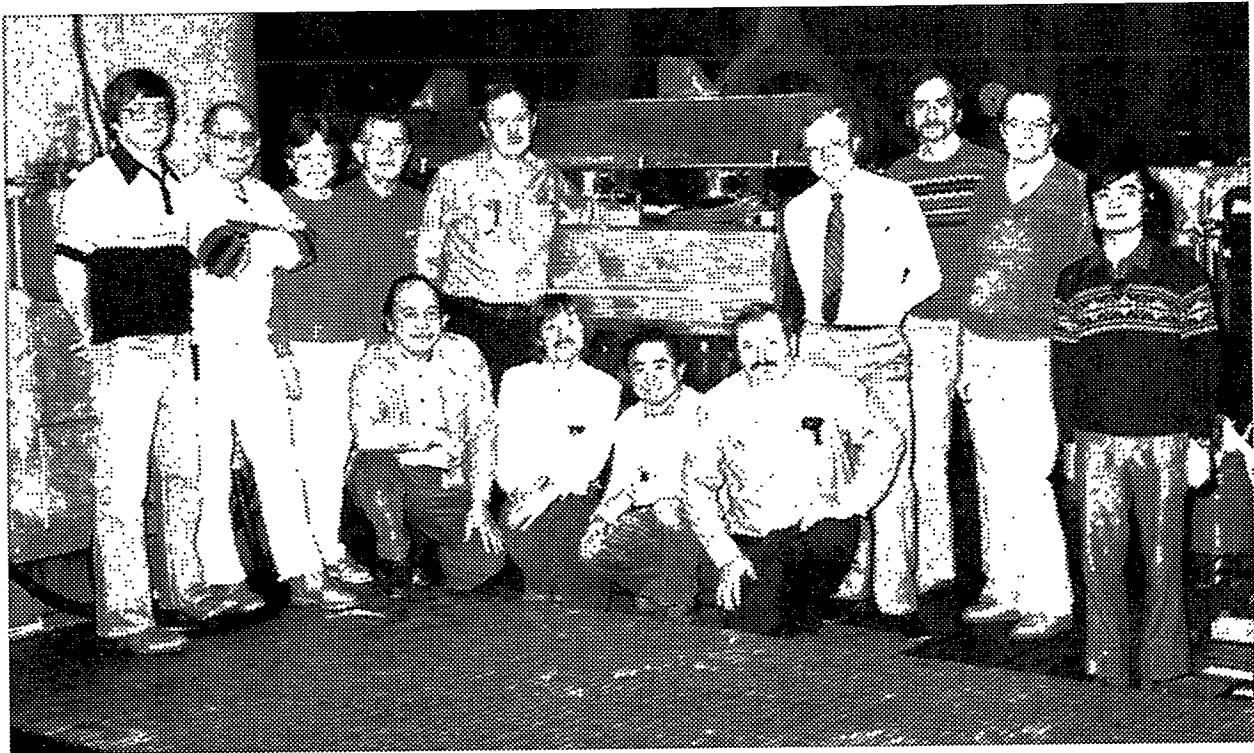


Fig. 9. The CDF group photographed with a calorimeter module.



Fig. 10. Members of the proton decay collaboration.

Dave Ayres, Ed May and Don Perkins, along with Marvin Marshak and Keith Ruddick opted to find out if the proton decays, and formed a collaboration that proceeded to build an underground laboratory in an iron mine in northern Minnesota on the shores of beautiful Lake Vermillion. A majority of the group is shown in Fig. 10. Please note that the locomotive has nothing to do with the experiment.

After the HRS at PEP, the Lepton group entered into a collaboration to build the ZEUS detector, destined for the HERA accelerator facility at DESY laboratory in Hamburg, Germany. Building on the High Energy Physics Division's experience with the CDF calorimeters, this time Argonne took on the calorimeter design and fabrication. Figure 11 shows team members posing on the stacking fixture.

Back on the accelerator side of the house, Bob Kustom, Ed Crosby, Tat Khoe and others were busy designing an accelerator for medium energy physics named GEM. Jim Norem and Len Balka built something called APEX in the Building 363 high bay; in the Building 370 area, FELIX and ALEX were keeping about 30 people gainfully employed, including Walter Praeg, Larry Turner, Don McGhee, Ed Wallace, and Andy Kelly.

Medical accelerators have been around for a long time - just ask Art Creer, who's been running them at the University of Chicago. But a whole new generation of medical accelerators have benefitted from the expertise of ex-ZGS people. Phil Livdahl and Al Moretti contributed to the development of the Loma Linda University Hospital accelerators. Ron Martin has been pursuing proton therapy, founding a new company, Acctek, with the help of grants from the National Cancer Institute, and drawing on the expertise of many ZGS people, Bob Wherle, Ken Menefee, and Bob Ward among them.



Fig. 11. Argonne contingent of the ZEUS collaboration.

Advanced accelerator research is currently being carried out in the High Energy Physics Division, where Jim Simpson has a group building the Argonne Wakefield Accelerator Facility.

The operations group called out in the 1979 ARF organization chart eventually turned into the IPNS Division. Its current complement of 68 people includes 22 former ZGS employees.

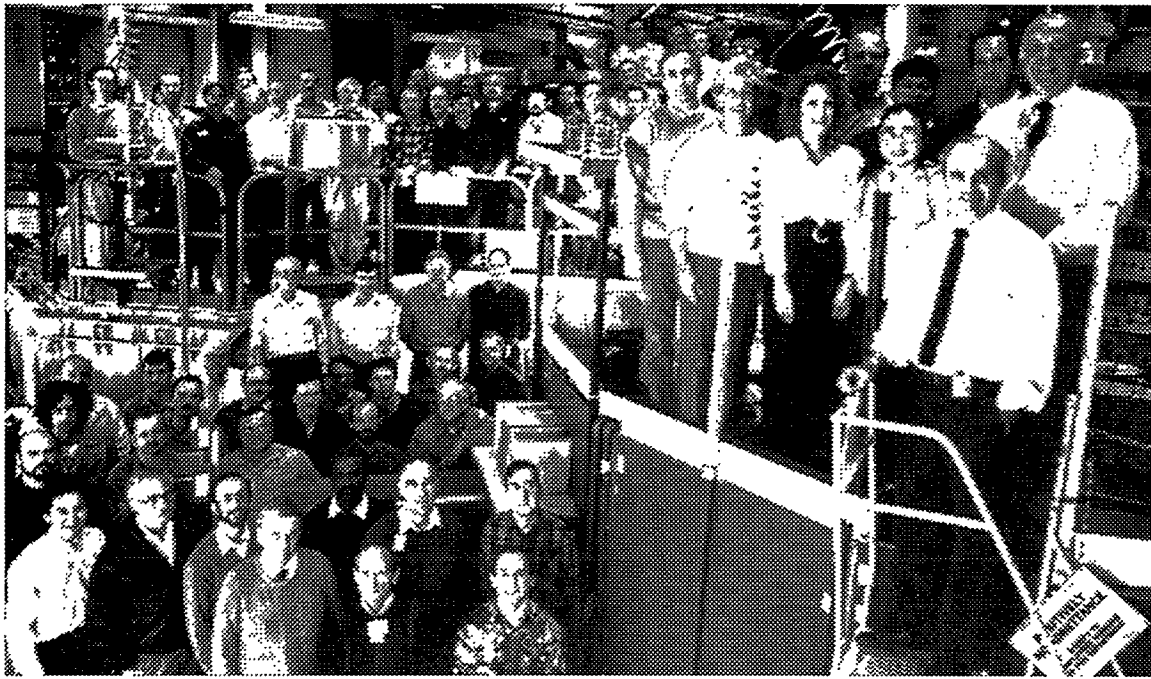


Fig. 12. Staff of the Intense Pulsed Neutron Source Division on the tenth anniversary of the 1981 start of operation.

And, as you have all heard, the Advanced Photon Source project claimed the attention of many of us. The accelerator design started with a nucleus of ZGS people, as you can see from Fig. 13. There are now 500 FTE's working on the project, 53 of whom had ZGS experience.

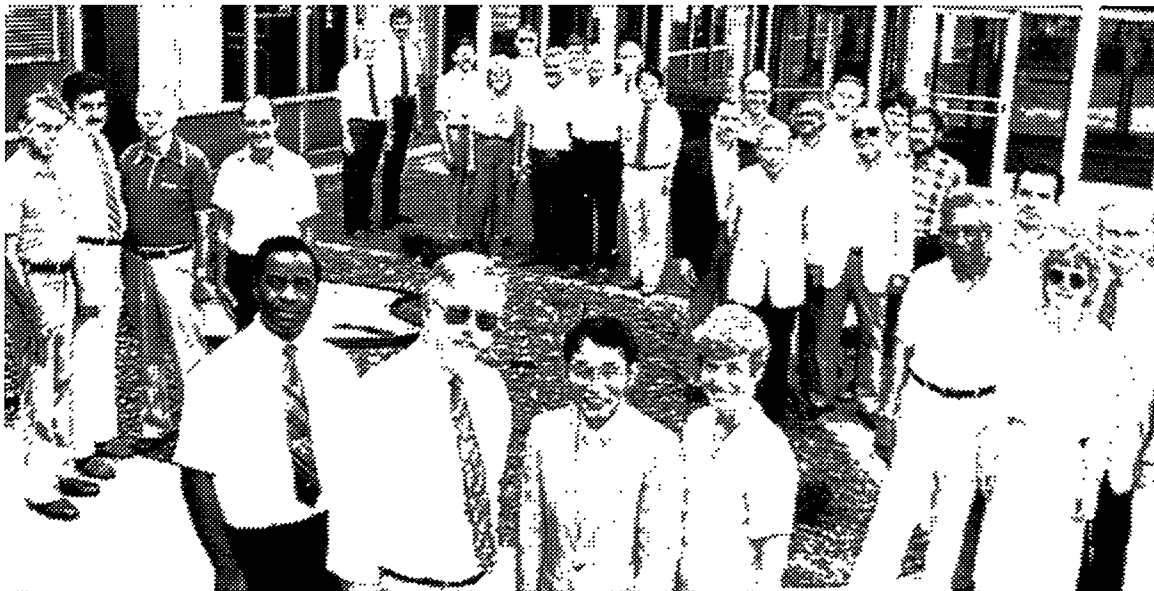


Fig. 13. Contributors to the conceptual design report for the Advanced Photon Source project.

Many people went off to other national labs, DOE, and other Federal agencies to do all sorts of interesting things. Free electron laser research at Los Alamos, SSC research and development, the AGS and NSLS programs at Brookhaven, biomagnetism at MIT, and the B Factory project at SLAC are just a few of the activities of the people whose names appear in Figure 14. A quick look at the Fermilab telephone directory netted 70 recognizable names, some of whom may actually be the sons or daughters of ZGS people.

Some people have started their own businesses, as shown in Fig. 15.

What about people who went further afield? Some of them changed their lives very dramatically. Stuart Marcowicz and Pam Ogor became physicians, and a surprising number became farmers. Telecommunication has become infinitely better since about 10 high-energy physicists from Argonne joined Bell Labs. High-tech companies like Amoco, Motorola, DEC, Boeing and Northrup; pharmaceutical firms like Abbott and Searle; and utilities such as Commonwealth Edison, the Metropolitan Sanitary District and the Metropolitan Water Reclamation District all have ZGS'ers aboard.

Others have entered the environmental sciences world, doing work on alternative energy sources, waste and energy management, solar energy, ocean thermal research, environmental impact studies and other things too numerous to mention. Human resources, social services, the academic world, and all levels of management have drawn ZGS people.

From the information above, and also from the "brief statements" many of you supplied with your registration information, it is easy to see that the ZGS alumni went on to bigger and better things, proving that there was indeed "life after the ZGS." But I think we will all agree that the ZGS days were special and hold a never-to-be-forgotten place in our lives.

DOE AND NATIONAL LABS

DEPARTMENT OF ENERGY

Sam Barish
Kostas Burba
Gordon Chariton
Greg Chartrand
Bob Diebold
John O'Fallon
Tom Romanowski
Stan Rudnick
Lou Voyvodic

LOS ALAMOS NATIONAL LAB

Fred Brandeberry
Roland Brewton
Eugene Colton
Tom Dombeck
Tom Hardek
Earl Hoffman
Larry Marek
Robert Mundis
Oscar Sander
David Schmitt
Harunori Takeda
Tom Wangler
Jerry Watson
Shirley Watson

OAK RIDGE NATIONAL LAB

John Murphy

NASA

John Campbell

SANDIA

Michael Mazarakis

SLAC

Fred Catania
Lowell Klaisner

BROOKHAVEN NATIONAL LAB

Richard Fernow
Steve Kramer
Venetios Polychronakos
Larry Ratner

LAWRENCE LIVERMORE LAB

Barbara Foreman
William LaFave

HANFORD

Frank Bacchi

NRC

Don Sreniawski

NAVAL WEAPONS CENTER

Rodney Ditzler

NAT'L BUREAU OF STANDARDS

Ken Martin

NATIONAL MAGNET LAB-MIT

David Cohen

CEBAF/SURA

C.L. McGuire
W.A. Wallenmeyer

LAWRENCE BERKELEY LAB

T.A. Mulera

Fig. 14. Some ZGS alumni who stayed within the government system.

ENTREPRENEURS

James Simanton & Carl Wegner - Telesonics Systems, Inc.

John Purcell - Advanced Cryomagnetics

Ronald Martin - Acctek Assoc.

Bert Wang - Wang NMR

James McDonnell - KMA Sales Co.

Ron Timm & Tony Valente - R.E. Timm & Assoc.

Robert Lari - Vector Fields, Inc.

W.C. Martin & J. Stevenson - Kinetic Systems, Inc.

Neil Ondracek - accounting and tax business

Fig. 15. Some ZGS alumni who didn't.

CONCLUDING REMARKS

Robert G. Sachs*

The University of Chicago

*Transcribed from tape and edited by M. Derrick and R. G. S.

It's really wonderful to be here again, to meet so many old friends and to reminisce about "the good old days". One of my principal comments whenever I change jobs [as you know, I get fired from one job after another] is that there is no institutional memory. What we have heard today from the ZGS alumni is that this is one place where there is indeed an institutional memory. The people I talked to today still think of the ZGS organization as a big family. It is an impressive thing to come back to -- and I have been away for quite a time.

When Alan Schriesheim introduced me this morning he said that he was not at ANL during the time of the ZGS. That was when there was all that controversy with Midwest universities, MURA, etc. and he said Bob Sachs can take the blame! I am pleased to take the blame for what came out of the ZGS; however, I must be careful not to take the credit. Whatever I accomplished here I owe first of all to people who were here when I arrived; in particular to Roger Hildebrand who was my predecessor as Associate Lab. Director for High Energy Physics. He is the one who set up high energy physics and the ZGS as a free standing management center within the Argonne Lab. The new HEP program was different in so many ways from what Argonne was then doing that it was necessary to have a fresh approach.

One of the consequences was that I had some control of the HEP budget at Argonne, and if you have worked in a National Lab. for very long you know how important that was.

Another group that I have to thank is the Users' Group. As Alan mentioned, the users were not exactly friendly to the Laboratory. I had come from the University of Wisconsin and had been closely associated with the user community. In that role I had been a participant, as cheerleader and discussor of physics, in meetings with MURA. To my surprise I found a certain chill come

over our relationship the minute I took the ANL job. I had no friends left!

Ned Goldwasser, as a representative of the users, and Roger Hildebrand, worked hard to plan a structure for user-ZGS cooperation that would eliminate this atmosphere of controversy. The result was a somewhat Byzantine system that was called the Users Group. When I arrived I was handed the rules and was told: "This is the way it will work." There was also a letter from President Lyndon Johnson telling the Laboratory that we had better make it work in such a way as to satisfy the community at large. This was the beginning of the end of the controversy. The Argonne Universities Association was created as a party to the AEC-U. of C. contract shortly after I arrived and its Board provided some help in overcoming these problems when I was running the office of the ALD for HEP. (In fact Marie Carroll was running the office.) Later when I was Lab. Director, we did have a number of problems arising from the dual-contractor arrangement.

All of that is now well behind us and a major reason is that the people in this audience made everything work. Our Users' Group, as conceived by Roger and Ned, became a model for organizing HEP programs world-wide.

Another thing that came out of the free association of physicists in the ZGS Users' Group was a reorganization of the American Physical Society. After the site for Fermilab had been chosen, Leon Lederman called some of us to a small meeting to discuss our views on the management of the proposed new accelerator. He was in favor of an AUI-type organization, which became, in the case of Fermilab, the Universities Research Association, and it continues to serve as the Fermilab contractor. However, at the time, it was important to find out what the HEP community thought of these issues. It happened that, for unrelated historical reasons, I was the Regional Secretary of the APS at that time and I suggested that all of the users nationwide be organized as a Division of the APS, which is what happened, although the APS constitution had to be changed in order to do it.

At a meeting of the APS Council Owen Chamberlain and I were asked to suggest a name of the new division. John Wheeler was APS president and he insisted that the word "fields" be used in the name to be sure that General Relativity would be included, so the division

became that of "Particles and Fields." Thus this change in the divisional structure of the APS was a direct outcome of the efforts to bring the HEP community together at the ZGS.

Another group I should mention in the credits are the physicists at the University of Wisconsin from whom I learned a little about experimental HEP so that, on coming to Argonne, I had some, but not much, preparation for the job. The success of the ZGS program should be credited to the wonderful Program Committees on whom I was completely dependent for making judgements about the experimental program. Working with the members of that Committee was a tremendous educational experience for me.

Now a few comments about the talks of the day. The main thing that comes out is that it was fun. The fun thread runs through all of the talks presented this morning. Another thread is the drive to exploit creative opportunities when they arise. That attitude goes back to the origin of ANL in 1946 and to Wally Zinn, the first Argonne Director, a superb physicist/engineer. The opportunities grasped and set-backs accepted as new challenges to go forward with something even better, characterized the early developments of nuclear reactors at ANL and was typical of the experience in the HEP program here. The Laboratory has had many very promising green apples throughout its history that were never allowed to ripen, and the immediate response has been to take on the next one. [A good relatively recent example from my days as Lab Director was Lowell Bollinger's response to rejection by the AEC of the proposal for a heavy ion accelerator. On the plane returning home from Washington he was drawing up plans for ATLAS.]

These observations bring to mind a quote from my favorite philosopher, Mike Ditka. When asked about his goals at the beginning of his last year as coach of the Chicago Bears he answered: "Don't forget that success is *not* a destination, it's a journey." The talks of this morning were about journeys.

When I came to the Lab as ALD, we had a contract with AVCO for the construction of a superconducting magnet for a 10" helium bubble chamber. This contract had been initiated by Tom Fields because, when he had seen the Phys. Rev. Letter from Bell Labs. about hard superconductors he immediately concluded that if one could use magnets made of hard superconductors in a working SYSTEM then superconductivity would become a marvelous new tool

for HEP research. The bubble chamber group, together with people from Carnegie Tech., set out to demonstrate that. At that early stage of the development everyone else was concentrating on small, toy solenoids, emphasizing the potential for producing higher magnetic fields..

That this effort was a success is exemplified by Gale Pewitt's remark in passing that "We decided to use a superconducting magnet for the 12 ft. bubble chamber." I could not believe he could say it so casually after what we went thorough in deciding whether to use a conventional or superconducting coil. The helium chamber had not even run when the plans for the 12 ft. chamber were laid out but the 12 ft. chamber was designed to use either a superconducting or a conventional magnet. In making a commitment to build a first of a kind device you stick your neck out in many directions and must believe that you can deliver. Well, our 12 ft. group had long necks, and they believed, and delivered. At the beginning it was not a casual decision, I assure you.

Gale also mentioned the Argonne involvement in the POPAE proposal. This was a colliding beam proposal that Bob Wilson had drawn up on the back of an envelope. He intended this to be a credible alternative to the ISABELLE proposal being prepared by BNL. Such a new facility at Brookhaven could present major scientific and financial competition for Fermilab. Wilson's back-of-the-envelope proposal was not accepted by HEPAP. As Director I volunteered the services of ANL to help Fermilab flesh out the proposal and Wilson agreed to go ahead with a joint Argonne/Fermilab study under the leadership of Bob Diebold. At a HEPAP meeting here at Argonne, Diebold described the project and got an enthusiastic response. However, Ned Goldwasser, who was representing Wilson at the meeting, said that Fermilab was not interested in continuing the study. They seemed to think that the money to continue the study -- about \$200K -- would come from their budget. We all know the outcome: many tens of millions of dollars were spent at BNL and then ISABELLE was canceled.

From the beginning of the ZGS project Aki Yokosawa had undertaken the design of a polarized target modelled after the one first used at the Bevatron by Owen Chamberlain and his group. A polarized target makes it possible to study the spin dependence of the scattering of protons from polarized nuclei, thereby measuring a new, important physical parameter. He was very successful in this work but, to complete the information on spin dependence, it was

recognized that the value of the measurements would be greatly enhanced if they were carried out with a polarized proton beam. That is where Alan Krisch got into the picture.

To put the story in perspective I note that one of our objectives at the ZGS was to encourage young people and get them started doing their own experiments. Alan Krisch was one of those. He came to the ZGS as a very young man and immediately had an impact both on the program and on the ALD. After doing some elegantly simple measurements of proton scattering cross sections he became interested in the possibility of accelerating a polarized proton beam in the ZGS.

This possibility had been emphasized by Albert Crewe when the ZGS was first proposed. Crewe was initially in charge of the ZGS construction and he had pointed out that, the zero gradient of the magnetic field in the ZGS should make it possible to maintain the polarization of the protons while accelerating them. The strong magnetic field gradients associated with the alternating gradient design, which was the design of choice at that time, made it a much less attractive possibility for producing polarized beams.

Krisch undertook the promotion of a polarized beam at the ZGS and, with the help of Larry Ratner and other members of the Accelerator Division, the resulting facility was a great success. Krisch and his associates produced so much good and unique physics with it that the ZGS was rescheduled to run for a couple of years beyond its original shutdown date. Afterwards, the "insurmountable" difficulties associated with the acceleration of polarized protons were tackled at the AGS, again under pressure from Alan, and these difficulties were overcome recently by the invention of the Siberian Snake. You have just heard Alan describe these recent developments at BNL: When Alan said that Nick Samios was polite to him even though these developments at the AGS were costing \$1M per week I found it (the politeness) hard to imagine!

After accepting the job but before returning to Argonne as Lab Director, I read a number of ANL reports. Among them was a report by Jack Carpenter on ZING, a joint Solid State/Accelerator Division proposal. I was captivated, partially because I had the good fortune to have been involved in one of the first experiments showing slow neutron diffraction from solids. This was in 1946 when I was helping with the design of a pile for producing nuclear power ("The Daniels Pile").

Bill Sturm had measured thermal neutron cross sections in polycrystalline beryllium and beryllium oxide, materials that were being considered as possible moderators. He used the new neutron monochromator developed by Zinn on the thermal (and epithermal) beam from CP3. The cross sections showed large up and down fluctuations as a function of energy. The reactor designers were using a thermal cross section obtained by taking the average of all the points. Kay Way, who was the physicist in charge of keeping the data books up-to-date, mentioned something about crystal effects and said: "Fermi knows all about that," so I went to see Fermi.

In his usual way, Fermi took down a notebook and there he had written a lecture (to himself) about the subject! The huge fluctuations in measured cross section resulted from the formation of Debye-Scherrer rings as a function of energy by elastic scattering from the randomly oriented microcrystals in the sample. It turned out that Mort Hammermesh had written a paper about this subject in 1941 and my learning about that led me to recruit him to Argonne in 1947 when, as director of the Theoretical Physics Division, I was trying to build a theory group.

This background of experience led me to be very positive about the pulsed neutron sources (ZING, now IPNS) that Jack Carpenter has just discussed. Carpenter played a decisive role in the conception and implementation of this project. So did the Accelerator Division (Ron Martin and Jim Simpson, I believe). IPNS has had its ups and downs but has always exceeded reasonable expectations. It is another sign of the special scientific character of this institution. This character was also particularly evident in the talk of Ron Martin. Ron has such remarkable creativity, motivation and energy he bowls you over.

The background to Earl Swallow's talk about the Winston collector involves what I believe to be an interesting story. It is another example of the outcome of my reading of Laboratory Reports when I had just come in as Director in early 1973. Task forces had been set up by the Laboratory to look at energy options other than the nuclear option. I read the report of the solar energy panel and was reminded by it that one of the problems in obtaining useful solar energy by means of a focusing detector is the need to track the sun. Another is that much of the light from the sky is diffuse, and this component is lost with a focusing device.

From my days as ALD for HEP I knew about Winston's work in high energy physics on Cerenkov detectors so I suggested that he look into applying his light collector to the collection of solar energy.

Within a few weeks he had a demonstration device working. We were funded by ERDA to further develop the concept. Government support for this kind of work in the U.S. has almost come to an end because, as Earl said: "The energy crisis went away."

Don't you believe it. I think it is essential to continue to have people at ANL thinking about energy issues on a continuing basis.

Many other memories have been awakened by listening to these stimulating talks but they must be left so that I'll have something to talk about on the 50th anniversary. Thanks to all of you for giving me the opportunity to revisit those fascinating days of the ZGS.

30th Anniversary of the Zero Gradient Synchrotron Participant List

1	Carl Akerlof	44	Phyllis Drabik Combs
2	Carl Albright	45	Arthur Cook
3	Ivars Ambats	46	Samuel L. Craig
4	Marcianne Ambats	47	Arthur Creer
5	Raymond G. Ammar	48	Edwin A. Crosbie
6	Charles O. Andrie	49	Walter S. Czyz
7	Joseph Asbury	50	Noreen Czyz
8	Elaine Aspel	51	Pam Dalman
9	David S. Ayres	52	Robert Dalman
10	Frank Bacci	53	James Davis
11	Leonard Balka	54	Joanne S. Day
12	Pete Bellinghausen	55	Malcolm Derrick
13	Edmond L. Berger	56	Anthony D. DeWitt
14	Ralph Bertermann	57	Richard Diaz
15	Paul Bertucci	58	John A. Dinkel
16	Leon Beverly	59	Joseph E. Dittrich
17	Armand Bianchi	60	Thomas Dombeck
18	Roger B. Blackman	61	Robert J. Ducar
19	Martin Block	62	Robert B. Duffield
20	Donald E. Bohringer	63	David DuPuis
21	Rudolph Bouie	64	Joseph Dvorak
22	Fred Brandeberry	65	Paul Eident
23	Ira Bresof	66	Richard Ely
24	Bruce Brown	67	Morton O. I. Erickson
25	Franklin R. Brumwell	68	Merle Faber
26	George W. Bryan	69	Donald Fearnley
27	Joyce Bryan	70	Robert Ferry
28	Kostas Burba	71	Thomas H. Fields
29	Ray A. Burnstein	72	John R. Forrestal
30	James Bywater	73	Jack Fry
31	Jack Carpenter	74	Raymond T. Fuja
32	Richard A. Carrigan	75	John Galayda
33	Neal M. Cason	76	Thomas Galvin
34	Linda Czimra Cason	77	Phillip Gavin
35	Fred Catania	78	Norman Gelfand
36	Chuck Catino	79	Lyle E. Genens
37	Gordon Charlton	80	Donald R. Getz
38	Yanglai Cho	81	John Gonczy
39	Clarence Clark	82	Andrew J. Gorka
40	David Cohen	83	Thomas H. Groves
41	Hans O. Cohn	84	Diana Grygiel
42	Emmett Collins	85	Gary R. Gunderson
43	Richard Combs	86	Jacque Habenicht

30th Anniversary of the Zero Gradient Synchrotron Participant List

87	William Haberichter	130	Gary L. Laurence
88	Vasken Hagopian	131	David Leach
89	Peggy Haldemann	132	Bernard Lepacek
90	Merle Haldemann	133	Ali M. T. Lin
91	Edward Heyn	134	Harry J. Lipkin
92	Roger H. Hildebrand	135	James S. Loos
93	Norman F. Hill	136	Richard Mahler
94	Ruth Hill	137	David S. Manson
95	David Hillis	138	Stewart Marcowitz
96	Gary Hodge	139	Gary J. Marmer
97	Earl Hoffman	140	Marvin Marshak
98	Roger L. Hogrefe	141	Ronald L. Martin
99	Ken Hostert	142	W. C. Martin
100	Richard L. Inskoop	143	John H. Martin
101	Michael James	144	Kenneth Martin
102	Shirley James	145	Beverly A. Marzec
103	Donald Jankowski	146	Dennis Marzec
104	Rosemary Johns	147	Edward N. May
105	James Joswick	148	James McDonnell
106	Alvin Kanofsky	149	Judith McGhee
107	Marshall Keig	150	Donald McGhee
108	Andrew L. Kelly	151	Al McKamey
109	V. Paul Kenney	152	Richard Meadowcroft
110	Raymond B. Kickert	153	William Mehler
111	Russ Klem	154	Kenneth Menefee
112	James Klen	155	James Metta
113	Sandy Klepec	156	Barbara Meurer
114	Carl M. Klindworth	157	Bruce Millar
115	Roy Kliss	158	Shelby A. Miller
116	Martin J. Knott	159	James R. Missig
117	Robert J. Kolar	160	Marvin J. Missig
118	Richard S. Konecny	161	John S. Moenich
119	Tom Kovarik	162	D. Read Moffett
120	Steven Kramer	163	Al Moretti
121	Charles I. Krieger	164	Michael Morgan
122	Alan D. Krisch	165	John Murphy
123	Frank Krzich	166	Brian Musgrave
124	E. C. Kulovitz	167	George L. Muszynski
125	Robert L. Kustom	168	Harry J. Myers
126	George LaForte	169	Wayne W. Nestander
127	Robert Laird	170	Arthur W. Neubauer
128	Robert J. Lari	171	Robert Nielsen
129	Sandra Marie Lauer	172	Ralph C. Niemann

30th Anniversary of the Zero Gradient Synchrotron Participant List

173	Lawrence J. Nodulman	216	John Rusnak
174	Dave Nordby	217	William Ruzicka
175	Elaine Novey	218	Jan Ryk
176	John R. O'Fallon	219	Robert G. Sachs
177	Pamela Ogor	220	Philip Schreiner
178	Joseph J. Ogor	221	Alan Schriesheim
179	Newt Okie	222	Peter Schultz
180	Neil Ondracek	223	Frank Schweingruber
181	Fred Onesto	224	C. W. Senders
182	Joseph G. Otavka	225	Gopal Shenoy
183	Carl B. Pallaver	226	Edward Shibata
184	Anthony R. Passi	227	James R. Simanton
185	Vincent Patrizi	228	James D. Simpson
186	Frank Pearsall	229	Richard A. Singer
187	E. Gale Pewitt	230	Dennis Sivers
188	James J. Phelan	231	Richard P. Smith
189	Donald J. Piatak	232	Roger Smith
190	Jack Picciolo	233	Gary A. Sprau
191	Irwin Pless	234	Don Sreniawski
192	John Pollock	235	Kenneth R. Stanfield
193	Judy Popik	236	Thomas Steelman
194	Walter F. Praeg	237	James Stevenson
195	Lawrence E. Price	238	Vernon F. Stipp
196	Richard J. Prien	239	Lou Strom
197	Stan Pruss	240	Dale E. Suddeth
198	Bob Pucci	241	William Sullivan
199	John Purcell	242	Earl C. Swallow
200	Cedric C. Putnam	243	David Swanson
201	Lazarus G. Ratner	244	Robert Taylor
202	Antanas V. Rauchas	245	Lee C. Teng
203	Don Reeder	246	Anthony Thomas
204	Kurt Reibel	247	Rosemary Thomas
205	Donald Reigle	248	Ron Timm
206	Stanley A. Reinke	249	Alice Townsend
207	Ronald R. Rezmer	250	Richard A. Trcka
208	D. E. Richied	251	Robert C. Trendler
209	Arthur Roberts	252	Larry Turner
210	Byron P. Roe	253	David G. Underwood
211	Richard D. Roman	254	Albert Upstrom
212	Thomas Romanowski	255	Jack L. Uretsky
213	Paul Roth	256	John Urish
214	Carmen Rotolo	257	Tony Valente
215	Keith Ruddick	258	Sandy Vasko

30th Anniversary of the Zero Gradient Synchrotron Participant List

- 259 Age T. Visser
- 260 Louis J. Voyvodic
- 261 Robert G. Wagner
- 262 Kameshwar C. Wali
- 263 William D. Walker
- 264 Edward J. Wallace
- 265 Al Wantroba
- 266 Charles Ward
- 267 Robert Ward
- 268 Jerry M. Watson
- 269 Albert Wattenberg
- 270 Robert B. Wehrle
- 271 William A. Welch
- 272 Marion White
- 273 William Williams
- 274 Penny Kobe Wills
- 275 Ronald L. Wilson
- 276 Douglas Wood
- 277 Robert M. Woods
- 278 Akihiko Yokosawa